Terms and Conditions of Use of Digitised Theses from Trinity College Library Dublin

Copyright statement

All material supplied by Trinity College Library is protected by copyright (under the Copyright and Related Rights Act, 2000 as amended) and other relevant Intellectual Property Rights. By accessing and using a Digitised Thesis from Trinity College Library you acknowledge that all Intellectual Property Rights in any Works supplied are the sole and exclusive property of the copyright and/or other IPR holder. Specific copyright holders may not be explicitly identified. Use of materials from other sources within a thesis should not be construed as a claim over them.

A non-exclusive, non-transferable licence is hereby granted to those using or reproducing, in whole or in part, the material for valid purposes, providing the copyright owners are acknowledged using the normal conventions. Where specific permission to use material is required, this is identified and such permission must be sought from the copyright holder or agency cited.

Liability statement

By using a Digitised Thesis, I accept that Trinity College Dublin bears no legal responsibility for the accuracy, legality or comprehensiveness of materials contained within the thesis, and that Trinity College Dublin accepts no liability for indirect, consequential, or incidental, damages or losses arising from use of the thesis for whatever reason. Information located in a thesis may be subject to specific use constraints, details of which may not be explicitly described. It is the responsibility of potential and actual users to be aware of such constraints and to abide by them. By making use of material from a digitised thesis, you accept these copyright and disclaimer provisions. Where it is brought to the attention of Trinity College Library that there may be a breach of copyright or other restraint, it is the policy to withdraw or take down access to a thesis while the issue is being resolved.

Access Agreement

By using a Digitised Thesis from Trinity College Library you are bound by the following Terms & Conditions. Please read them carefully.

I have read and I understand the following statement: All material supplied via a Digitised Thesis from Trinity College Library is protected by copyright and other intellectual property rights, and duplication or sale of all or part of any of a thesis is not permitted, except that material may be duplicated by you for your research use or for educational purposes in electronic or print form providing the copyright owners are acknowledged using the normal conventions. You must obtain permission for any other use. Electronic or print copies may not be offered, whether for sale or otherwise to anyone. This copy has been supplied on the understanding that it is copyright material and that no quotation from the thesis may be published without proper acknowledgement.

Immunomodulatory Properties of Endogenous Danger Signals

Graham A. Tynan

B.A (MOD) Biochemistry with Immunology

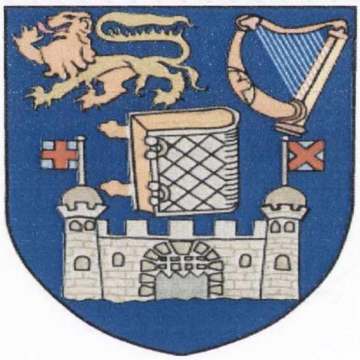

A thesis submitted to

Trinity College Dublin

For the Degree of
Doctor of Philosophy

Supervisor: Dr. E.C Lavelle

Adjuvant Research Group
School of Biochemistry and Immunology
Trinity College Dublin

2012

Declaration of Authorship

This thesis represents the sole work of the author except where stated and has not been submitted in whole or in part to this or any other university or institution for any other degree or qualification. The author gives permission for the library to lend or copy this work upon request.

Acknowledgements

First and foremost, I would like to express my sincerest thanks to Dr. Ed Lavelle for providing me with the opportunity to undertake this research project and for his invaluable support and encouragement throughout. Over the past four years, I have had some of the most fascinating discussions with Ed, whether it be how to approach a particular experiment, solve an immunological puzzle, how to approach science in general or even why Barcelona are such an amazing football team. These exchanges have helped tremendously not only in shaping my development as a research scientist but also my development as a person. I was extremely lucky to have such an inspirational supervisor whose enthusiasm for my project never waned. Indeed, Ed's door was always open and he went above and beyond to help in whatever way he could. Ed has been a truly inspirational figure in teaching me the scientific trade and for this I want to thank him sincerely.

I would also like to extend a heartfelt thanks to everybody in the Lavelle lab, both past and present; Fiona, Edel, Anne, Eimear, Jim, Andres, Ewa, Karen, Marie, Chris, Claire, Cliona, Corinna, Liz and Lorraine. The help and guidance that you have all provided me with has simply been invaluable. Everything I have learned in the lab I owe to those around me. Everybody was always such a great help on isolation days also and I was touched by the sense of togetherness and team spirit that exists in the lab. However, above all else I have made some great friends in the Lavelle lab. We have enjoyed so many fun times together and I hope that I can stay in touch with everybody. One memory that I will hold with me forever is the infamous '5-minute mile'.

I would also like to thank Prof. Seamus Martin for his advice and insight throughout this project. During the course of various meetings, Prof. Martin was instrumental in directing the proceedings of chapter 4. Indeed, chapter 4 was carried out as part of a very productive collaboration with Prof. Martin and his research laboratory. I would like to thank Prof. Martin for giving me the opportunity to be a part of this collaboration. I worked very closely with Dr. Inna Afonina who I would like to thank especially for her dedication and commitment to the cause. It was a pleasure to work with Inna and she was responsible for generating the *in vitro* data to support the *in vivo* data outlined in chapter 4. Thank you Inna. Thanks also to Dr. Takao Tsuji, Katrin Viikov and Dr. Eimear Lambe for supplying additional reagents.

Many thanks to Prof. Cliona O'Farrelly, Prof. Donal O'Shea, Dr. Ken Mok, Dr. Jean O'Connell, Dr. Lydia Lynch, Dr. Michelle Corrigan, Dr. Andrew Hogan, Dr. Conor Woods, Prof. Sean Callanan and Eamonn FitzPatrick who all contributed immensely to chapter 5 both in terms of advice and obtaining patient samples. Without the input of the above people, chapter 5 would not have been possible.

I would also like to convey my gratitude to all of the members of the Immunology Research Centre for their kind and insightful advice. I found the monthly meetings to be very beneficial and I was really humbled by the fact that such esteemed scientists took a keen interest and active role in my research. Undoubtedly, my work has benefitted greatly from their counsel.

I also want to thank Barry Moran for his extensive patience and expert advice on FACS. Barry is one of the most selfless people I have ever encountered, always generous with his time and extremely patient. I enjoyed drinking a pint with Barry as well; he's a great man for an interesting conversation. I still think it's odd that my one standout image of Barry is of me crossing the ball for him to volley home a magnificent goal in one of our hotly contested indoor football matches.

I would like to express my gratitude to the ladies in the office also; Mary-Pat and Miriam. I really enjoyed our chats and it was always a pleasure to call by. Often a good chat with the ladies in the office would help to reduce stress and bring about a smile. I have had the pleasure of knowing both Mary-Pat and Miriam since I first came to the School of Biochemistry and Immunology as an undergraduate over 6 years ago and they have always been great. I would also like to sincerely thank all of my friends within

the Department, particularly Lara, Sharee and Paddy with whom I hope to be friends with long after I leave here.

I want to give a special mention to Claire Hearnden for various reasons. She has been extremely patient and considerate for the past 6 months while I have tried to finish my experiments and write this thesis. Her constant support and understanding throughout this process have been amazing and it is something that I will never forget. Claire also proofread the entire thesis and was extremely meticulous in her efforts. Thank you Claire.

I also wish to express my heartfelt gratitude to my family for their constant understanding and support throughout. The only reason I am where I am today is because of you, there is no doubt about that. Thank you for helping me through the past 4 years.

Finally, I would like to thank Dr. Aisling Dunne and Dr. Kim Midwood for taking the time to read this thesis and to discuss different aspects of this work. In addition, I would like to thank Dr. Emma Creagh for chairing the *viva voce* examination.

Abstract

The 'danger model' proposes that dying cells release specific endogenous molecules into the extracellular milieu following loss of plasma membrane integrity. This model postulates that these endogenous molecules, referred to as 'danger signals', can induce robust immune responses. The overall aim of this project was to characterise the immunomodulatory properties of established danger signals and also to identify novel sources of danger signals.

Dendritic cell (DC) activation is commonly used as a measure of the immunomodulatory potential of candidate danger signals. However, residual lipopolysaccharide (LPS) contamination is a recurring theme. To address this, the antibiotic polymyxin B (PmB) is often used to neutralise contaminating LPS. However, the limited capacity of PmB to reverse these effects is neglected. Therefore, this study aimed to determine the minimum LPS concentration required to induce murine DC activation and to assess the ability of PmB to inhibit this process. LPS concentrations as low as 10pg/ml, 20pg/ml and 50pg/ml induced secretion of IL-6, TNF-α and IL-12p40 respectively. A higher threshold exists for IL-12p70 as an LPS concentration of 500pg/ml was required to induce its secretion. The efficacy of PmB varied substantially for different cytokines but it was particularly limited in its ability to inhibit LPS-induced secretion of IL-6 and TNF-α. Furthermore, an LPS concentration of only 50pg/ml was sufficient to promote DC expression of costimulatory molecules and PmB was limited in its capacity to reverse this effect when LPS concentrations of greater than 20ng/ml were used. Heat treatment attenuated the ability of low concentrations of LPS to induce cytokine secretion by DCs, thus suggesting that heat-inactivation is also an ineffective control for discounting potential LPS contamination. Finally, a concentration of 5pg/ml LPS alone was not sufficient to induce secretion of IL-6 but could still synergise with *E. coli* heat-labile enterotoxin to promote this effect. This suggests that some danger signals may elicit activity only as a result of synergy with low levels of residual LPS.

Exploring further the theme of endogenous danger signals, granzyme B (GzmB) can be secreted by a range of immune cells not associated with cell killing. Therefore, immune cells may secrete GzmB into the extracellular space with the ability to process molecules released from necrotic cells. Ultimately, it was hypothesised that GzmB processing of novel substrates may potentiate their inflammatory potential. This study found that GzmB processing of IL-1α (GzmB IL-1α) enhanced the ability of this cytokine to induce IL-17 production by splenocytes *ex vivo*. GzmB IL-1α also elicited increased adjuvanticity *in vivo*. Furthermore, GzmB can process IL-1α *in vivo* as a non-cleavable mutant form of IL-1α was a less potent adjuvant than full-length IL-1α.

This study also found that when injected with ovalbumin, the endogenous danger signals IL-1α and IL-33 induced qualitatively different T cell responses. IL-1α promoted a strong antigen-specific Th17 response in peritoneal exudate cells (PECs) which was not detected when IL-33 was used as an adjuvant. Thus, the consequences of necrosis on the adaptive immune system may be dependent on the repertoire of intracellular danger signals present.

Endogenous oils derived from white adipose tissue (WAT) adipocytes may also signal danger to the host. Obesity is characterised by chronic, low-grade inflammation associated with recruitment of neutrophils and proinflammatory macrophages into WAT. Adipocytes contain a single cytoplasmic lipid droplet which facilitates storage of endogenous oils. Some of the most powerful adjuvants are oil-based emulsions. Therefore, it was hypothesised that endogenous oils may act as adjuvants when released from necrotic adipocytes. This study demonstrated that endogenous oils elicit adjuvanticity *in vivo* which is comparable to incomplete Freund's adjuvant. Furthermore, endogenous oils induced IL-1R-dependent but TLR4-independent recruitment of neutrophils and macrophages into the peritoneum. In addition, injection of endogenous oils modulated the cytokine profile of PECs following *ex vivo* restimulation with PRR agonists. In particular, PECs isolated from mice injected with endogenous oils produced significantly more TNF-α and IL-12 which was dependent on the IL-1R, while also producing less IL-10. Thus, endogenous oils generate a cytokine profile in the peritoneum which reflects that found in inflamed WAT.

Overall, these studies offer new insights into Polly Matzinger's danger model.

Publications

Tynan GA, McNaughton A, Jarnicki, A, Tsuji T, Lavelle EC. (2012) Polymyxin B inadequately quenches the effects of contaminating lipopolysaccharide on murine dendritic cells. *PLoS One* 7(5): e37261.

Afonina IS, **Tynan GA**, Logue SE, Cullen SP, Bots M, Luthi AU, Reeves EP, McElvaney NG, Medema JP, Lavelle EC, Martin SJ. (2011) Granzyme B-dependent proteolysis acts as a switch to enhance the proinflammatory activity of IL-1α. *Molecular Cell*, Oct 21; 44 (2): 265-278.

Abbreviations

AGE	advanced glycated end-products
AHR	airway hyperresponsiveness
AIM	absent in melanoma
Alum	aluminium salts
AMPK	adenosine monophosphate-activated kinase
AP	activator protein
APC	antigen presenting cell
ASC	apoptosis-associated speck-like protein containing a CARD
Asn	asparagine
Asp	aspartic acid
ATP	adenosine triphosphate
B	bursa of Fabricius
BAT	brown adipose tissue
BCA	bicinchoninic acid
Bcl	B cell lymphoma
BCR	B cell receptor
BDCA2	blood DC antigen 2 protein
BIR	baculoviral inhibitory repeat
BMDC	bone marrow-derived DC
BMDM	bone marrow-derived macrophage
BMI	body mass index
BMMC	bone marrow-derived murine mast cell
BSA	bovine serum albumin
CARD	caspase activation and recruitment domain
CCL	CC chemokine ligand
CCR	CC chemokine receptor
cDC	classical DC
CDP	common DC precursor
CFA	complete Freund's adjuvant
CLEC9A	C-type lectin domain family 9 member A
CLP	cecal ligation and puncture
CLR	C-type lectin receptor
CLS	crown-like structure
CMP	common myeloid progenitor
CpG	cytidine-phosphate-guanosine
CPPD	calcium pyrophosphate dehydrate
CT	cholera toxin
CTL	cytotoxic T lymphocyte
CXCL	CXC chemokine ligand
CXCR	CXC chemokine receptor
DAI	DNA-dependent activator of IRF1
DAMP	damage-associated molecular pattern
DC	dendritic cell
DCIR	DC immunoreceptor
DC-SIGN	DC-specific intercellular adhesion molecule-3-grabbing non-integrin
DD	death domain

dectin	DC-associated C-type lectin
DIO	diet-induced obese
dl	decilitre
DMEM	Dulbecco's Modified Eagle Medium
DNA	deoxyribonucleic acid
dsRNA	double-stranded RNA
DTH	delayed-type hypersensitivity
dToll	Drosophila Toll
DTT	dithiothreitol
E. coli	*Escherichia coli*
EDTA	ethylenediaminetetraacetic acid
ELISA	enzyme-linked immunosorbent assay
ER	endoplasmic reticulum
ERK	extracellular signal-regulated kinase
EU	endotoxin unit
FACS	fluorescence-activated cell sorting
FADD	Fas-associated DD
FBG	fibrinogen-like globe
FCS	foetal calf serum
FDA	Food and Drug Administration
FIIND	function to find
FL HRF	full-length HRF
FL IL-1α	full-length IL-1α
Flt3L	fms-like tyrosine kinase 3 ligand
FN-EDA	extra domain A of fibronectin
Foxp3	forkhead box protein P3
GATA3	GATA-binding protein 3
GC	germinal center
GFI	growth factor independent
GI	gastrointestinal
GLUT	glucose transporter
GM-CSF	granulocyte-macrophage colony-stimulating factor
GMP	granulocyte-macrophage precursor
gp	glycoprotein
GPI	glycosylphosphatidylinositol
GzmA	granzyme A
GzmB	granzyme B
GzmB HRF	GzmB-processed HRF
GzmB IL-1α	GzmB-processed IL-1α
$GzmB^{SA}$	catalytically inactive GzmB mutant
$GzmB^{WT}$	wild-type GzmB
HA	hemagglutinin
HDL	high-density lipoprotein
H&E	haematoxylin and eosin
HI	heat-inactivated
HIV	Human Immunodeficiency Virus
HK	heat-killed
HMG	high mobility group

HMGB	high mobility group box
HPLC	high-performance liquid chromatography
HRF	histamine-releasing factor
HRP	horseradish-peroxidase
HSA	human serum albumin
HSC	hematopoietic stem cell
HSL	hormone-sensitive lipase
Hsp	heat shock protein
HTH	helix-turn-helix
ICAM	intercellular adhesion molecule
IFA	incomplete Freund's adjuvant
IFI	IFN-inducible protein
IFN	interferon
Ig	immunoglobulin
IKK	IκB kinase
IL	interleukin
IL-1α^{D103A}	GzmB non-cleavable mutant form of IL-1α
Ile	isoleucine
iNOS	inducible nitric oxide synthase
inter	intermediate
i.p.	intraperitoneal
IPS	IFN-β-promoter stimulator
IPTG	isospropylthio-b-D-galactosidase
IRF	IFN regulatory factor
IRS	insulin receptor substrate
ITAM	immunoreceptor tyrosine-based activation motif
ITIM	immunoreceptor tyrosine-based inhibitory motif
iTreg	inducible regulatory T
JNK	Jun N-terminal kinase
KC	keratinocyte-derived chemokine
kDa	kilodalton
KO	knockout
L	litre
LAL	limulus amoebocyte lysate chromogenic endpoint
LB	lysogeny broth
LBP	LPS-binding protein
Leu	leucine
LFA	leukocyte function-associated antigen
LGP	laboratory of genetics and physiology
LP	lymphoid precursor
lpDC	lamina propria DC
LPM	large peritoneal macrophage
LPS	lipopolysaccharide
LRR	leucine rich repeat
LT	heat-labile enterotoxin
Mø	macrophage
mA	milliampere
Mac	macrophage galactose-specific lectin

Mal	MyD88 adaptor-like
MALT	mucosa-associated lymphoid tissue
MAPK	mitogen-activated protein kinase
MCP	monocyte chemoattractant protein
MD	myeloid differentiated protein
MDA	melanoma differentiated-associated gene
MDP	macrophage/DC progenitor
MFI	median fluorescence intensity
mg	milligram
MGC	multinucleate giant cell
MHC	major histocompatibility complex
MHO	metabolically healthy obese
MICL	myeloid C-type lectin-like receptor
Mincle	macrophage-inducible C-type lectin
MIP	macrophage inflammatory protein
miR	microRNA
ml	millilitre
mM	millimolar
mmol	millimole
Mo	monocyte
MP	myeloid precursor
mRNA	messenger RNA
MS	multiple sclerosis
MSU	monosodium urate
MTOC	microtubule organising centre
MUO	metabolically unhealthy obese
MyD88	myeloid differentiation factor 88
NA	neuraminidase
NBNT	non-B non-T
NEMO	NF-κB essential modulator
NF-κB	nuclear factor-κB
ng	nanogram
NIK	NF-κB-inducing kinase
NK	natural killer
NLR	NOD-like receptor
nm	nanometre
nM	nanomolar
NO	nitric oxide
NOD	nucleotide-binding oligomerisation domain
NRS	nuclear retention sequence
nTreg	naturally occurring regulatory T
OD	optical density
OPD	0-phenylenediamine dihydrochloride
OVA	ovalbumin
Pam3	Pam3CSK4
PAMP	pathogen-associated molecular pattern
PAT	perilipin/ADRP/TIP47
PBMC	peripheral blood mononuclear cell

PBS	phosphate buffered saline
PCR	polymerase chain reaction
pDC	plasmacytoid DC
PEC	peritoneal exudate cell
Peril	perilipin
Phe	phenylalanine
PI	propidium iodide
PI3K	phosphoinositide 3-kinase
PLY	pneumolysin
PMA	phorbal myristate acetate
PmB	polymyxin B
Poly I:C	polyinosinic polycytidylic acid
PRR	pattern-recognition receptor
PS	polystyrene
ra	receptor antagonist
RA	rheumatoid arthritis
RAGE	receptor for advanced glycated end-products
rHMGB1	recombinant HMGB1
RIG	retinoic-acid-inducible gene
RIP	receptor-interacting protein
RLR	RIG-I-like receptor
RNA	ribonucleic acid
ROR	retinoid-related orphan receptor
ROS	reactive oxygen species
rpm	revolutions per minute
RPMI	Roswell Park Memorial Institute
Runx	runt-related transcription factor
SAP	spliceosome-associated protein
SARM	Sterile-alpha and Armadillo motif-containing protein
SDS	sodium dodecyl sulfate
SDS-PAGE	SDS- polyacrylamide gel electrophoresis
Ser	Serine
SFA	saturated fatty acid
SGT1	suppressor of G2 allele of Skp1
SHP	SH2-domain-containing protein tyrosine phosphatase
SLE	systemic lupus erythematosus
snRNP	small nuclear ribonucleoprotein
SPM	small peritoneal macrophage
SREBP	sterile regulatory element binding protein
ssRNA	single-stranded RNA
STAT	signal transducer and activator of transcription
SYK	spleen tyrosine kinase
T	thymus-derived
TAK	TGF-β-activated kinase
T-bet	T box transcription factor
Tc	T cytotoxic
TCD	Trinity College Dublin
TCR	T cell receptor

TEMED	tetramethylethylenediamine
Tfh	T follicular helper
TGF	transforming growth factor
Th	T helper
TIR	Toll/IL-1 receptor
TLR	Toll-like receptor
TM	transmembrane
T_N	naive $CD4^+$ T cell
TNF	tumour necrosis factor
TNFR	TNF receptor
Tr	T regulatory
TRADD	TNFR-associated DD protein
TRAF	TNFR-associated factor
TRAM	TRIF-related adaptor molecule
Treg	regulatory T
TRIF	TIR-related adaptor protein inducing IFN
TSLP	thymic stromal lymphopoietin
TXNIP	thioredoxin-interacting protein
UFA	unsaturated fatty acid
UPR	unfolded protein response
V	volt
WAT	white adipose tissue

Table of Contents

Chapter 1

Introduction

1.1 - Immunity: An Overview

The constant evolutionary battle between pathogens and their vertebrate hosts has undoubtedly played a hugely significant and important role in shaping the vertebrate immune system. These harmful microbes seek refuge in a resilient host in pursuit of optimal conditions for replication. However, this strong and persistent selective pressure has forced vertebrates to evolve a powerful and effective immune system capable of eliminating such infections.

The vertebrate immune system can essentially be divided into two distinct arms, the innate immune system and the adaptive immune system. Importantly, however, these systems are not mutually exclusive and thus function together in a complimentary fashion in order to prevent infection of the host.

The innate immune system is known to be evolutionarily older than the adaptive immune system and is found in all forms of plants and animals. Innate immunity, in combination with anatomical barriers, provides the first line of defence against infection and is triggered immediately following the host's exposure to a harmful pathogen. The effector functions of the innate immune response are dependent on several innate cells, including phagocytes such as neutrophils, macrophages and dendritic cells (DCs). This form of recognition triggers the activation of complex innate signalling pathways which lead to the induction of proinflammatory cytokines such as tumour necrosis factor (TNF)-α and interleukin (IL)-1, thus promoting the onset of inflammation.

The innate immune system is unable to generate immunological memory. However, it is intimately linked to the adaptive immune system by DCs, which are an important class of antigen presenting cell (APC) capable of activating naive T cells residing in the lymph nodes. Innate immunity is sufficient to eliminate many common infections without the aid of the adaptive immune response, which requires a priming period of approximately 4-5 days. However, some pathogens are not eliminated from the host by the innate immune system during this time, thus meaning that in this case innate immunity only serves to contain the infection until the adaptive response can be primed and unleashed on the invading pathogen. The adaptive immune system represents a vastly complex and advanced facet of immunity. This evolutionarily important system, present only in vertebrates, is mediated primarily by a group of highly specialised cells called lymphocytes which are capable of recognising antigens through unique antigenic receptors on their surface. These lymphocytes include B cells and T cells. Thus, the adaptive immune system possesses specificity for the infectious invader, a feature which is critical for the priming of an immune response specific for the pathogen.

The adaptive immune system can also generate 'memory' lymphocytes which is another distinct characteristic from the more ancient innate immune system. Indeed, this concept provides the fundamental basis of vaccination.

1.2 - Anatomical Barriers and Innate Immunity

Innate immunity is an evolutionarily ancient immune defence system utilised by all multicellular organisms. Microbes are initially encountered by a pre-existing innate immune system which serves to prevent the establishment of infection and oversee the removal of the infectious agent. Interestingly, it is only when the innate immune system is overwhelmed or successfully evaded by a pathogen that adaptive immunity is required. The importance of this age-old defensive stronghold is reflected in the fact that most organisms on the planet survive comfortably using only an innate immune system [1].

In many ways, the initial and most primitive component of the innate immune system is the presence of external and internal anatomical barriers. The protective layers of the skin provide a competent external physical barrier, while epithelial cells lining mucosal tubular structures such as the respiratory, gastrointestinal (GI) and urogenital tracts serve as efficient internal barriers against infection. Internal epithelia are referred to as mucosal epithelia as they secrete mucus which contains important glycoproteins called mucins. Microbes coated in mucus are prevented from adhering to mucosal epithelia and are effectively washed away in a tide of mucus driven by the beating of epithelial cilia. Peristalsis performs a similar role in the GI tract in maintaining the flow of both food and infectious agents through the body. A plethora of microbicidal substances can also be found at mucosal sites. For example, the upper GI tract contains bile salts, digestive enzymes, fatty acids and a low pH, all of which contribute to the demise of microbes. In the lower GI tract, Paneth cells secrete antibacterial and antifungal peptides known as α-defensins. The closely related β-defensins are synthesised by epithelia in the respiratory and urogenital tracts, while lysozyme and phospholipase A are found in tears and saliva. Furthermore, epithelial surfaces contain a resident microflora of non-infectious bacteria that compete with pathogens for nutrients and mucosal binding sites, thus contributing to the defence of the host [2-3].

Microbes that cause infection are referred to as pathogens and these infectious agents invade host tissues after successful evasion of the anatomical barriers described above. However, once access has

been gained into the subepithelial tissues, pathogens encounter a more vigorous and dynamic innate immune response. Phagocytic cells can recognise the presence of an invader through expression of receptors on their cell surface, some of which bind opsonins such as antibodies and complement proteins that coat the surface of the pathogen. This type of recognition results in the ingestion (i.e. phagocytosis) of the bound microbe in a membrane-bound vesicle called a phagosome. The phagosome later acquires a low pH, thus killing its microbial constituents. Furthermore, phagosomes also fuse with lysosomes containing antimicrobial enzymes and proteins to form a phagolysosome into which the lysosomal contents are released, leading to the termination of the infectious agent. Phagocytosis also induces the synthesis of a range of toxic products that facilitate the killing of the internalised pathogen, namely nitric oxide (NO), the superoxide anion (O_2^-) and hydrogen peroxide (H_2O_2) [4].

Pathogen recognition by innate sensor cells such as macrophages also induces secretion of a range of cytokines and chemokines resulting in a response termed inflammation [5]. The four cardinal signs of inflammation were described by Celsus over two thousand years ago as that of heat, redness, swelling and pain. The heat and redness are caused by an increase in vasculature diameter that results in enhanced local blood flow at a reduced velocity. Furthermore, endothelial cells lining the local blood vessels become activated and express adhesion molecules such as selectins and integrins. The combined effects of slowed blood flow and expression of adhesion molecules promotes binding of circulating leukocytes to endothelial cells and subsequent migration into the tissues in a process called extravasation [6]. Many of these physiological changes and their immunostimulatory consequences are initiated by cytokines and chemokines secreted primarily by tissue resident macrophages following pathogen recognition.

Among the first leukocytes recruited to sites of inflammation are neutrophils which are short-lived phagocytic cells present in significant numbers in the blood but not in normal healthy tissue. These cells are conscripted to inflamed tissue in response to CXC chemokine ligand (CXCL)8. Neutrophil infiltration is followed by monocyte recruitment from the bloodstream into the tissue in response to CC chemokine ligand (CCL)2, and these cells differentiate into effector tissue macrophages. During later stages of inflammation, further innate immune cells such as basophils and eosinophils also enter the infected site. On entering the site of infection, leukocytes proceed to phagocytose and destroy the invading pathogen and to propagate the inflammatory cascade. The symptoms of swelling and pain that accompany inflammation are induced by an increase in vascular permeability that leads to an efflux of soluble immune proteins from the blood and subsequent accretion in local tissue [7]. Thus,

inflammation mediated by cytokines and chemokines secreted by innate immune sentinel cells oversees the rapid delivery of both soluble and cellular immune components to sites of infection. Importantly, inflammation also induces local microvascular coagulation in order to prevent the spread of infection into the bloodstream, and promotes tissue repair when the insulting stimulus has been removed [8].

DCs are crucial innate sensors which are also recruited to sites of inflammation. However, these cells not only serve to amplify the inflammatory response and empower innate immune defence mechanisms, but are also professional APCs capable of migrating to secondary lymphoid organs and initiating adaptive immunity.

1.3 - DCs: Bridging the Divide between Innate and Adaptive Immunity

DCs are highly specialised APCs and represent a crucial link between innate and adaptive immunity. These innate sentinel cells are adherent mononuclear phagocytes first discovered by Steinman and Cohn in 1973. DCs were identified within adherent mononuclear cell preparations obtained from murine peripheral lymphoid organs based on their distinctive cytologic criteria and unique morphology [9]. In 1978, Steinman made another significant breakthrough when he discovered that DCs could induce T cell proliferation in mixed leukocyte reactions up to three hundred times more effectively than unfractionated splenocytes [10]. Furthermore, in 1980, Nussenzweig *et al.* demonstrated that DCs were approximately two orders of magnitude greater than other cells in antigen processing and presentation and subsequent activation of effector T cell responses [11].

Heterogeneous subpopulations of DCs exist in the body. Broadly speaking, these subpopulations comprise plasmacytoid DCs (pDCs) and classical DCs (cDCs). The cDC subpopulation can be further divided into $CD8\alpha^+$ cDCs and $CD8\alpha^-$ cDCs. pDCs are long-lived cells specialised for antiviral immunity as they secrete large amounts of interferon (IFN)-α in response to nucleic acid stimulation. pDCs are present in the bone marrow and all peripheral organs and can function efficiently as APCs to initiate adaptive immune responses [12]. cDCs are relatively short-lived cells with high phagocytic capacity as immature cells and significant cytokine-secreting ability as mature cells. Furthermore, cDCs are highly migratory and constantly travel between tissues and lymphoid organs. Thus, cDCs are highly specialised for antigen processing and presentation [13].

DCs originate from bone marrow-derived hematopoietic stem cells (HSCs). HSCs give rise to lymphoid precursors (LPs) and myeloid precursors (MPs). LPs can eventually differentiate into lymphocytes such as T cells, B cells or NK cells. MPs can differentiate into common myeloid progenitors (CMPs), granulocyte-macrophage precursors (GMPs) or macrophage/DC progenitors (MDPs), and it is primarily MDPs that give rise to DCs [14]. MDPs can differentiate into common DC precursors (CDPs) which are proliferating cells that give rise to pDCs and precursors for cDCs (pre-cDCs) in the bone marrow. These pre-cDCs are found in the bone marrow, blood and spleen. However, they proceed to enter lymphoid tissue where they exhibit a mature cDC phenotype and morphology, thus giving rise to $CD8\alpha^+$ and $CD8\alpha^-$ cDCs [15]. However, pre-cDCs can also enter non-lymphoid tissue where they give rise to lamina propria DCs (lpDCs) [16]. MDPs can also differentiate into two phenotypically and functionally distinct subsets of mature monocytes which can be found in the bone marrow, blood and spleen; Gr-1^+/Ly-$6C^+$ monocytes and Gr-1^-/Ly-$6C^-$ monocytes [17]. Importantly, Gr-1^+/Ly-$6C^+$ monocytes can give rise to inflammatory DCs known as Tip-DCs in response to infection with *Listeria monocytogenes* [18]. These Gr-1^+/Ly-$6C^+$ monocytes are also suspected to give rise to Langerhans cells and microglia, which can renew independently of the bone marrow [19-20].

There is no known cell surface receptor or marker that is expressed by all DCs. This is partly due to the existence of heterogeneous subpopulations of DCs. However, Meredith *et al.* have recently reported that the zinc finger transcription factor zDC, which is a negative regulator of cDC activation [21], is expressed exclusively by pre-cDCs and cDCs but not by pDCs, monocytes or other immune cell populations [22]. Thus, zDC appears to define the cDC lineage.

In vitro, highly purified DCs can be generated from murine bone marrow cells when cultured with granulocyte-macrophage colony-stimulating factor (GM-CSF) [23-24]. Murine bone marrow cells can also give rise to DCs *in vitro* in the presence of fms-like tyrosine kinase 3 ligand (Flt3L). Flt3L-derived DCs are more representative of DCs found in lymphoid tissue as these cultures include DC subsets eliciting features of pDCs and cDCs [25]. Interestingly, Flt3L is also crucial for the development of DC lineages *in vivo*. For example, Flt3L-deficient mice show impaired DC development [26] and administration of Flt3L in mice results in expansion of DC populations [27].

Upon recognition of an infectious agent, DCs initiate signal transduction cascades culminating in the synthesis and secretion of proinflammatory cytokines involved in promoting the onset of innate immunity [28].

Infectious agents can replicate in two distinct intracellular compartments. Viruses and intracellular bacteria tend to replicate in the cytosol of cells and are eliminated by effector $CD8^+$ T cells, also known as cytotoxic T lymphocytes (CTLs), which kill the infected cell by releasing toxic granules containing perforin and granzyme B (GzmB). However, most pathogenic bacteria and eukaryotic parasites replicate inside endosomes and lysosomes following internalisation into the vesicular system and are eliminated by $CD4^+$ T helper (Th) cells. These cells are specialised for the activation of additional effector cells capable of eliminating the invading microbe. Antigens internalised by phagocytosis (i.e. from extracellular bacteria and parasites) enter the major histocompatibility complex (MHC) class II pathway. These antigens are degraded in lysosomal vesicles by pH-dependent proteases and peptides derived from these antigens are loaded onto MHC class II molecules and transported to the surface of the cell [29]. Antigens synthesised in the cytosol of the cell (i.e. from intracellular bacteria and viruses) enter the MHC class I pathway and undergo proteasomal degradation. The resulting peptides are transported to the endoplasmic reticulum (ER) where they are loaded onto MHC class I molecules and transported to the cell surface [30].

Peptides derived from exogenous antigens can also enter the MHC class I pathway and be presented to CTLs [31-32]. This process is referred to as cross-presentation and is mediated by $CD8^+$ DCs *in vivo* [33]. Interestingly, the endocytic mechanism involved in antigen uptake may determine whether it is delivered to the MHC class II pathway or the MHC class I cross-presentation pathway [34].

Following antigen internalisation and processing, DCs alter their phenotype with regard to their chemokine receptor expression profile. Tissue-resident DCs express high levels of CC chemokine receptor (CCR)1, CCR5 and CCR6, which are receptors for chemokines synthesised and secreted by local tissue cells. However, upon DC activation, these receptors are downregulated and expression of CXC chemokine receptor (CXCR)4 and CCR7 is upregulated, thus facilitating DC homing to the regional lymph node via the afferent lymphatic vessels [35]. Within the lymph node, DCs present antigen to naive T cells. Interactions between surface molecules on DCs and T cells facilitates transient binding of these cells. For example, T cells express leukocyte function-associated antigen (LFA)-1, intercellular adhesion molecule (ICAM)-3 and CD2, which bind specifically to ICAM-1, DC-specific ICAM3-grabbing non-integrin (DC-SIGN) and CD58 respectively on the DC. This transient interaction provides sufficient time for T cells to sample MHC molecules on the surface of the DC for recognition of a specific peptide. Crucially, MHC class I molecules present peptides to CTLs while MHC class II molecules present peptides to $CD4^+$ Th cells [36].

Peptide recognition alone, however, is not sufficient to stimulate naive T cell activation, proliferation and subsequent adaptive immunity. This complex process also requires a second signal known as costimulation. Indeed, ligation of a T cell receptor (TCR) in the absence of costimulation induces T cell anergy which is characterised by a state of T cell non-responsiveness. Following ligation of pattern-recognition receptors (PRRs) (Section 1.7) by microbial products, DCs become activated and undergo a maturation process characterised by upregulation of MHC molecules as well as costimulatory molecules. These costimulatory molecules include CD80, CD86 and CD40. CD80 and CD86 bind CD28 on the surface of the T cell and thus provide the necessary costimulatory signals required for T cell activation following TCR peptide recognition. Subsequently, the T cell upregulates surface expression of CD40 ligand which binds to CD40 on the DC, and this interaction communicates activation signals to the T cell and further potentiates CD80 and CD86 expression on the surface of the activating DC [37]. T cell activation is succeeded by clonal expansion, differentiation and the onset of adaptive immunity (Figure 1.1).

Interestingly, the term 'mature' is commonly used to describe DCs expressing high surface levels of costimulatory and MHC molecules, but is also used to describe immunogenic DCs capable of initiating adaptive immunity to foreign antigens. The discovery that non-immunogenic or immature DCs can also express elevated surface costimulatory and MHC molecules has been the main focus of recent reports which have questioned the apparent simplicity and transposable use of this terminology [38].

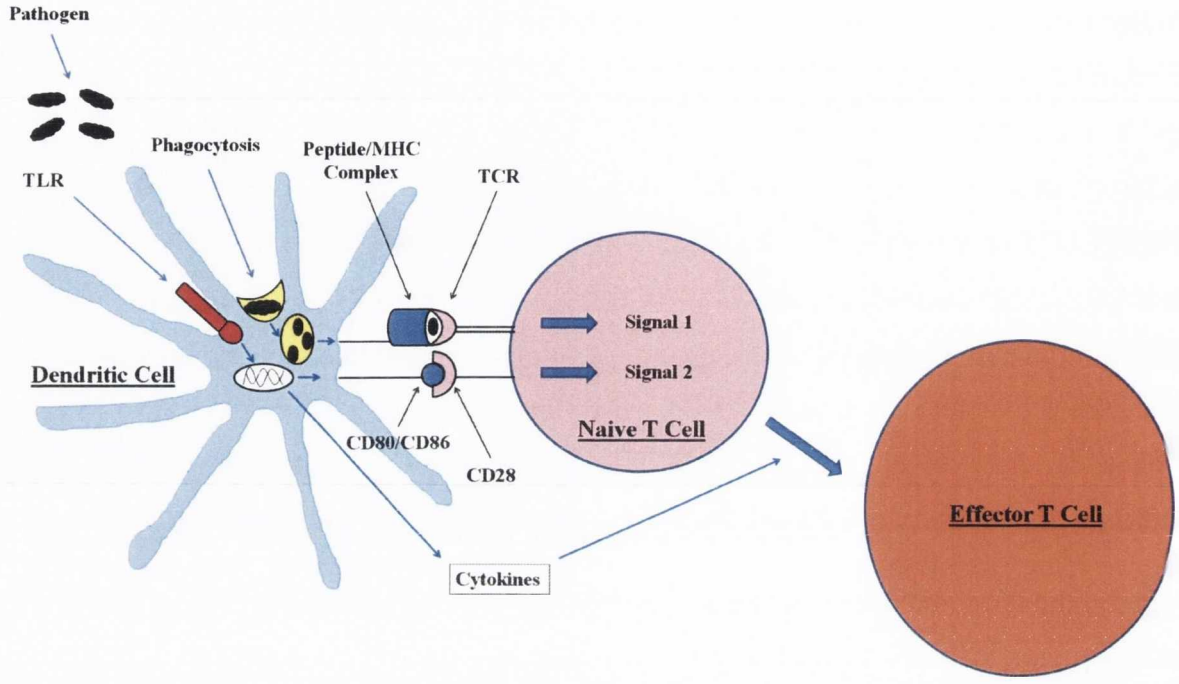

Figure 1.1 – DCs promote the onset of adaptive immunity. Following pathogen recognition in non-lymphoid tissues by cell surface PRRs such as members of the Toll-like receptor (TLR) family, an immature DC internalises the pathogen by phagocytosis and upregulates surface expression of costimulatory molecules such as CD80 and CD86. The antigen is processed into peptides, loaded onto MHC molecules and transported to the surface of the cell. The mature DC migrates to the regional lymph node where it presents peptide to naive T cells. Specific recognition of peptide by a naive T cell in the presence of costimulation promotes effector T cell responses and the subsequent onset of adaptive immunity. Importantly, DCs can also secrete cytokines that modulate the nature of the adaptive immune response.

1.4 - Adaptive Immunity

The adaptive immune system is present only in vertebrates and evolved approximately five hundred million years ago. This complex arm of immunity is fundamentally characterised by antigen specificity and is mediated principally by lymphocytes termed B and T cells. In 1960, Macfarlane Burnet first proposed the 'clonal selection' theory for which he later won a Nobel Prize in Physiology or Medicine. The clonal selection theory states that lymphocytes express many copies of a single surface receptor with specificity for a particular antigen. However, the specificity of this receptor on each lymphocyte is different, thus enabling the host to recognise a wide range of antigenic stimuli. Burnet's theory also explains that upon specific recognition of antigen by a lymphocyte receptor, the lymphocyte harbouring this receptor undergoes cell division and gives rise to identical progeny with surface receptor specificity identical to the parent lymphocyte. Indeed, the clonal selection theory was soon supported by convincing experimental evidence using single cells [39].

Following antigen receptor ligation in the presence of sufficient costimulation, B and T cells undergo clonal expansion and differentiate into effector cells capable of initiating powerful adaptive immunity directed against specific pathogens. The generation of effective adaptive immunity requires 4-5 days and is essential when an infectious stimulus successfully evades or overwhelms the innate immune system. Following the onset of adaptive immunity and the resolution of infectious disease, memory B and T cells are retained in the host and provide long-lasting protective immunity [40].

1.4.1 - B cells

B cells are the key cell type of the humoral immune response. In 1948, plasma cells were postulated as a source of antibody [41]. However, it was not until 1965 that Cooper and colleagues identified B cells. Interestingly, both T cells and B cells were discovered simultaneously during a series of landmark experiments. Cooper used surgical thymectomy and bursectomy in combination with sublethal irradiation techniques in chickens to distinguish antibody-producing bursa of Fabricius (B) cells from thymus-derived (T) cells. More specifically, footpad immunisation of control chickens with diphtheria toxoid resulted in a robust delayed-type hypersensitivity (DTH) response which was absent in thymectomized, irradiated chickens. Footpad immunisation of control chickens with the

pathogen *Brucella abortus* resulted in strong antibody responses, but these effects were absent in bursectomized, irradiated chickens [42-43]. Thus, Cooper had clearly shown that cells from the bursa of Fabricius are responsible for antibody production while cells from the thymus effectively mediate DTH responses. Subsequent murine transplant experiments demonstrated that antibody responses were mediated by bone marrow-derived cells [44-45]. Furthermore, a direct link between B cells and antibody production was later established when it was shown that surface immunoglobulin (Ig) expression could be used as a reliable marker for B cells [46-47].

The clonal surface receptor expressed by B cells is referred to as the B cell receptor (BCR). The BCR is composed of two heavy chains and two light chains, each of which consists of constant and variable regions [48-49]. Indeed, Tonegawa and colleagues proved that the specificity of BCRs is achieved through complex gene recombination of variable regions during B cell development in the bone marrow [50]. B cell development stages are characterised by the state of BCR expression. In the bone marrow, pluripotent HSCs give rise to pro-B cells that undergo genetic rearrangement at the BCR heavy chain locus. Pro-B cells differentiate into pre-B cells that express the BCR heavy chain at the cell surface in combination with a surrogate light chain to form the pre-BCR. Once gene rearrangements occur at the light chain locus, the newly synthesised light chain displaces the surrogate light chain at the cell surface and combines with the BCR heavy chain to form a complete BCR. B cells expressing a functional BCR are referred to as immature B cells. Immature B cells migrate from the bone marrow to peripheral lymphoid organs where they undergo natural selection for self-tolerance and become naive B cells [51-53].

Importantly, the BCR expressed on the surface of immature and naive B cells is in fact a complete IgM molecule. However, once activated, B cells can undergo isotype switching in order to change the antibody isotype expressed on the cell surface without altering the antigenic specificity of the receptor. Isotype switching in B cells is achieved by altering the constant region of the heavy chain of the BCR [54]. There are five different antibody isotypes which can potentially be expressed on the surface of B cells; IgM, IgD, IgG, IgA and IgE.

IgM can be expressed without isotype switching and is therefore the first antibody to be produced. In order to provide rapid host defence, IgM is produced before the occurrence of somatic hypermutation and consequently IgM monomers are of lower affinity for target antigens. However, IgM monomers form pentamers, whose ten antigen binding sites provide high avidity for antigen and somewhat compensate for the reduced affinity of this antibody. IgM pentamers are found primarily in the blood

where they serve to activate the complement system. IgD is co-expressed with IgM on the surface of mature B cells and its expression does not seem to require isotype switching. Circulating IgD can bind to myeloid cells such as basophils and subsequent cross-linking promotes release of antimicrobial, inflammatory and B cell-stimulating factors. Following B cell activation and somatic hypermutation, B cells can express IgA, IgG and IgE. IgA molecules are synthesised as monomers which can enter blood and extracellular fluids, but can also form dimers that are transported to mucosal sites such as the GI and respiratory tracts where they protect epithelial sites from pathogens. IgA antibodies are also constituents of breast milk, thus facilitating the transport of protective immunity from mother to child, and serve primarily as neutralising antibodies. IgG is monomeric and is the most abundant antibody isotype in the blood and extracellular fluid. Furthermore, maternal IgG is transported directly across the placenta and into the bloodstream of the foetus during pregnancy. IgG is an efficient neutralising antibody and activator of the complement system, but also serves as an effective opsonin for pathogens to be engulfed by phagocytes. IgE is present in only small amounts in the blood and extracellular fluid but functions predominantly in the sensitisation of mast cells. More specifically, IgE bound to antigen is recognised by Fc receptors on the surface of mast cells. This initiates mast cell degranulation and subsequent release of an array of inflammatory mediators [55-56].

Antigenic ligation of the BCR leads to internalisation of the antigen which is degraded and returned to the cell surface as peptides bound to MHC class II molecules. Importantly, the B cell co-receptor complex comprising CD19, CD21 and CD81 greatly potentiates the responsiveness of the BCR to antigen [57]. Peptides are recognised by $CD4^+$ Th cells which serve to deliver activating signals to the B cell in the form of costimulatory molecules and cytokines. Indeed, antigens that fail to activate B cells in the absence of T cell help are referred to as thymus-dependent antigens [58] (Figure 1.2).

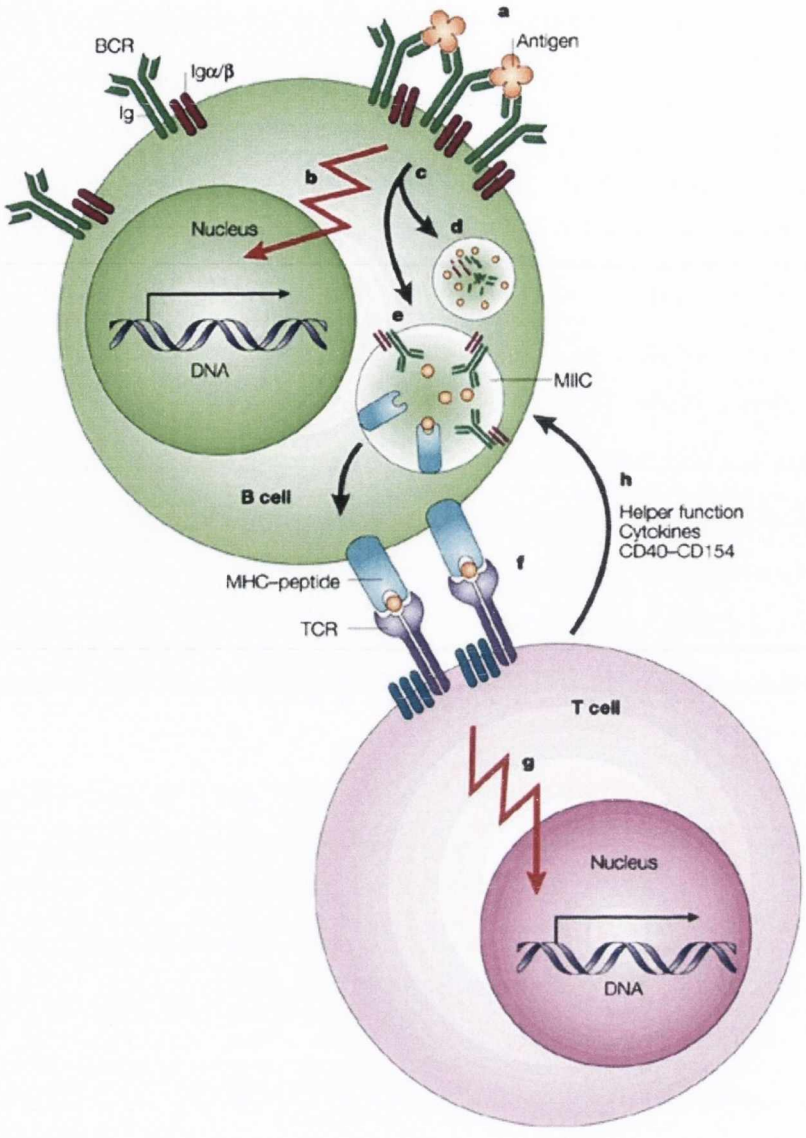

Figure 1.2 – T cell-dependent B cell activation. (a) Following antigen ligation, (b) the BCR initiates a signal transduction cascade resulting in transcription of a range of genes important for B cell activation. (c) The BCR is internalised and either (d) undergoes degradation or (e) is transported to an intracellular compartment where peptides derived from the antigen bound to the BCR are loaded onto MHC molecules. These MHC-peptide immune complexes are transported to the cell surface where (f) they are presented to naive T cells. (g) TCR cross-linking induces T cell activation. (h) The activated T cell facilitates B cell activation through secretion of cytokines and expression of surface molecules such as CD40L which interacts with CD40 on the surface of the B cell. Figure from [59].

The cytokines produced by armed $CD4^+$ Th cells influence the antibody isotype expressed by the activated B cell. For example, IL-4 promotes switching to IgG1 and IgE [60], transforming growth factor (TGF)-β and IL-10 induce switching to IgA and IgG2b [61], and IFN-γ stimulates switching to IgG2a and IgG3 [62]. Interestingly, recent evidence supports the idea that distinct B cell subsets can also influence helper T cell responses. For example, effector Be1 cells can secrete IFN-γ and IL-12, thus promoting Th1 cell differentiation, whereas effector Be2 cells produce IL-2, IL-4 and IL-13 which induce Th2 cell differentiation. Regulatory B cells, in marked contrast to effector B cells, secrete the anti-inflammatory cytokine IL-10 which suppresses $CD4^+$ T cell responses, alters the activity of DCs and induces the expansion of regulatory T (Treg) cells [63-65]. B cells can also be activated directly by certain bacterial antigens in the absence of T cell help, and these antigens are called thymus-independent antigens.

Following activation, B cells proliferate rapidly and form germinal centers (GCs) within lymphoid follicles of secondary lymphoid organs. These B cells undergo somatic hypermutation which alters the variable region of the BCR. Affinity maturation ensues and selects only for GC B cells expressing a mutated BCR with high affinity for antigen, as B cells expressing a low affinity BCR undergo apoptotic cell death. The selected high affinity B cells undergo isotype switching and differentiate into antibody-secreting plasma cells or long-lived memory B cells [66].

1.4.2 - $CD4^+$ T cells

$CD4^+$ T cells are known as T helper cells because of their ability to coordinate an appropriate immune response sufficient to combat a particular infection. Following activation, naive $CD4^+$ T cells in peripheral lymphoid organs can differentiate into one of a number of effector $CD4^+$ T cell subtypes capable of inducing the activation of distinct effector mechanisms to eliminate the invading microbe. The nature of the offending pathogen ultimately dictates the type of effector $CD4^+$ T cell response generated by the host. An initial Th1-Th2 paradigm was first proposed by Coffman and Mosmann in 1986 [67] (Figure 1.3). The predominant $CD4^+$ T cell subtypes are Th1, Th2, Th17 and Treg cells, although in recent years various other subtypes such as Th9, type 1 T regulatory (Tr)1 cells and T follicular helper (Tfh) cells have been proposed [68].

Naive $CD4^+$ T cells differentiate into Th1 cells in response to infection with intracellular pathogens [69]. Secretion of the cytokines IL-12 and IFN-γ from DCs and natural killer (NK) cells respectively,

together with TCR engagement and CD28 ligation on the naive T cell surface, induces differentiation of a naive T cell into a Th1 cell [70]. Th1 cells secrete IFN-γ, the signature cytokine of this particular subset which can further promote differentiation of Th1 cells in a positive feedback loop and suppress the development of other $CD4^+$ T cell subsets such as IL-4-producing Th2 cells. Th1 cells can also produce IL-2, IL-10, TNF-α and TNF-β [68]. The cytokine IL-18, which is produced by innate immune sentinel cells following PRR stimulation in conjunction with NLRP3 inflammasome activation, plays a synergistic role in Th1 cell differentiation [71]. IFN-γ can also orchestrate powerful cell-mediated immunity by recruiting and activating antiviral and antitumour CTLs as well as a host of innate immune effector cells including macrophages and neutrophils. The development of Th1 cells is dependent on IL-12-induced upregulation of signal transducer and activator of transcription (STAT)4 and also IFN-γ-mediated induction of STAT1 and the Th1 cell master transcription factor T box transcription factor (T-bet) [72].

Th2 cells promote antibody-mediated humoral immunity and are induced in response to parasitic infections. The cytokine IL-4 drives Th2 cell differentiation by upregulating sequential expression of the transcription factors STAT6 and GATA-binding protein 3 (GATA3) [73-74]. The Th2 master transcription factor GATA3 can inhibit the development of IFN-γ-producing Th1 cells. However, the source of this innate IL-4 is controversial. Traditionally, DCs have been thought to favour Th1 cell differentiation through secretion of IL-12, and indeed have not yet been shown to secrete IL-4 following PRR engagement. Therefore, one hypothesis for how DCs modulate Th2 cell responses proposes that in the absence of IL-12 or other T cell polarising cytokines, DC interaction with a naive T cell results in Th2 cell differentiation. Thus, in this context Th2 polarisation is essentially a default mechanism which occurs in the absence of signals instructing polarisation of a non-Th2 cell subset. However, recent studies have dismissed the role of DCs in Th2 polarisation and have shown that basophils are efficient APCs capable of secreting IL-4 and driving Th2 cell differentiation in mice and in humans [75-76]. Despite these revelations, it now appears that both DCs and basophils are important for promoting Th2 cell differentiation, but in different disease settings. For example, basophils function as the polarising APC in the papain allergen-induced model of Th2 cell differentiation, whereas DCs are not required in this particular model [77]. However, DCs are critically important as polarising APCs in the ovalbumin (OVA)-alum-induced Th2 cell responses *in vivo* [78]. Moreover, both basophils and DCs seem to be required for protective immunity against *Trichuris muris* [79]. Interestingly, STAT5 activation by IL-2, IL-7 and/or thymic stromal lymphopoietin (TSLP) also appears to play a significant role in Th2 cell differentiation [80].

Th2 cells secrete the signature cytokine IL-4 which strengthens the Th2 response through a positive feedback mechanism, as well as secreting IL-5, IL-9, IL-10, IL-13 and IL-25. IL-4 induces B cell class switching to IgE which in turn results in degranulation of various innate immune cells including basophils and mast cells, thus amplifying the inflammatory process. Amongst various other functions, IL-5 and IL-9 act on lung or intestinal tissues where they are involved in eosinophil and basophil recruitment respectively, IL-13 (in combination with IL-4) acts on epithelial cells and smooth muscle cells to induce mucus production and airway hyperresponsiveness (AHR) and IL-25 acts on so-called non-B non-T (NBNT) cells to further propagate the Th2 response [81].

Th17 cells are abundant at mucosal surfaces and generate protective immunity against extracellular bacteria and fungi [82]. This subset of $CD4^+$ T cells was only recently identified following the discovery that the p40 subunit of IL-12 and its receptor subunit, IL-12Rβ1, are shared by IL-23 and the IL-23 receptor respectively [83]. Subsequently, Th17 cells have been implicated in the pathogenesis of various autoimmune diseases including rheumatoid arthritis (RA) and multiple sclerosis (MS). The differentiation of Th17 cells requires IL-6, IL-21 and IL-1, and the stabilisation and proliferation of this subset is dependent on IL-23 [84]. Recent studies have demonstrated that engulfment of infected apoptotic dead cells by DCs results in secretion of cytokines (primarily TGF-β and IL-6) capable of initiating Th17 differentiation through upregulation of the transcription factors retinoid-related orphan receptor (ROR)γt and STAT3 [85-86]. Th17 cells secrete IL-17a (referred to as IL-17), IL-17f, IL-10, IL-21 and IL-22 [82].

Treg cells are immunosuppressive lymphocytes and are crucial in the implementation of peripheral tolerance as well as immune homeostasis. Indeed, dysfunction of Treg cells results in widespread autoimmune disease, immunopathology and allergy [87]. Treg cells are also believed to be involved in maintaining allograft tolerance as well as fetal-maternal tolerance during pregnancy [88]. However, the immunosuppressive nature of Treg cells can be detrimental in antitumour immunity as these cells favour tumour survival [89]. This subset of $CD4^+$ T cells express the forkhead box protein P3 (Foxp3) transcription factor [90] as well as STAT5 [91] and secrete the anti-inflammatory cytokines TGF-β, IL-10 and IL-35. Interestingly, Treg cells can be divided into two subtypes based on their development. Naturally occurring Treg (nTreg) cells develop in the thymus under the influence of the cytokines IL-2 and IL-7 [92]. However, inducible Treg (iTreg) cells differentiate from naive $CD4^+$ T cells in secondary lymphoid organs in the presence of TGF-β, IL-2 and retinoic acid. Thus, the differentiation of nTregs is intimately linked with Th17 cell development. Both

nTregs and iTregs seem to be important for maintaining peripheral tolerance and suppressing autoimmunity. However, their individual contributions have not yet been clearly defined.

Other $CD4^+$ T cell subtypes which have been proposed include Th9, Tr1 and Tfh cells. However, since these subtypes secrete signature cytokines also produced by at least one of the four established $CD4^+$ T cell subsets, there has been much debate about their existence as unique lineages distinct from Th1, Th2, Th17 and Treg lineages. The development of Th9 cells is mediated by TGF-β in combination with IL-4 [93]. However, IL-9 was initially characterised as a Th2 cytokine following the discovery that a GATA3 encoding retrovirus or a retrovirus encoding a constitutively active form of STAT5 could drive the induction of IL-9-producing cells [80]. Furthermore, Th17 and Treg cells have also been shown to secrete IL-9 [94-95] while a Th9-specific master transcription factor has yet to be identified. Tr1 cells are defined as a subset of Treg cells that lack expression of FOXP3 and are characterised by elevated expression of IL-10. Tr1 cells are believed to differentiate from naive $CD4^+$ T cells in an extracellular microenvironment containing TGF- β and IL-27 [96]. However, IL-10 was originally identified as a Th2 cytokine and has since been shown to be expressed by Th1 [97], Th17 [98] and Treg cells [99], while a Tr1-specific master transcription factor has yet to be identified.

IL-21-producing Tfh cells were identified in 2000 and are found in B cell follicles in secondary lymphoid organs where they provide B cell help and regulate antibody isotype class switching [100]. Thus, Tfh cells are crucial in mediating appropriate and effective B cell antibody responses and thereby antigen-specific humoral immunity. Tfh cells express CXCR5 which enables them to home to CCL13-rich B cell follicles [100]. These GC-resident cells develop under the influence of IL-6 and IL-21 through induction of the transcription factors STAT3 [101] and B cell lymphoma (Bcl)-6 [102], and have been shown to secrete IL-21 and IL-17 [101]. Interestingly, Tfh cells were initially characterised as a separate $CD4^+$ T cell lineage based on their failure to secrete Th1, Th2 or Th17 cell-associated cytokines. However, evidence is now accumulating in support of a model which proposes the existence of multiple Tfh subsets derived from established $CD4^+$ T cell lineages which adapt a Tfh cell development programme defined by downregulation of CCR7 expression and upregulation of CXCR5 expression, and also the presence of IL-6 and IL-21 in the local microenvironment. Thus, $CXCR5^+$ Th1 (Tfh1) cells would secrete IFN-γ, Tfh2 cells would secrete IL-4 and Tfh10 cells would secrete TGF-β and IL-10 [103]. Therefore, Tfh cells may simply represent a particular lineage state of Th1, Th2, Th17 and Treg cells rather than a separate lineage in itself.

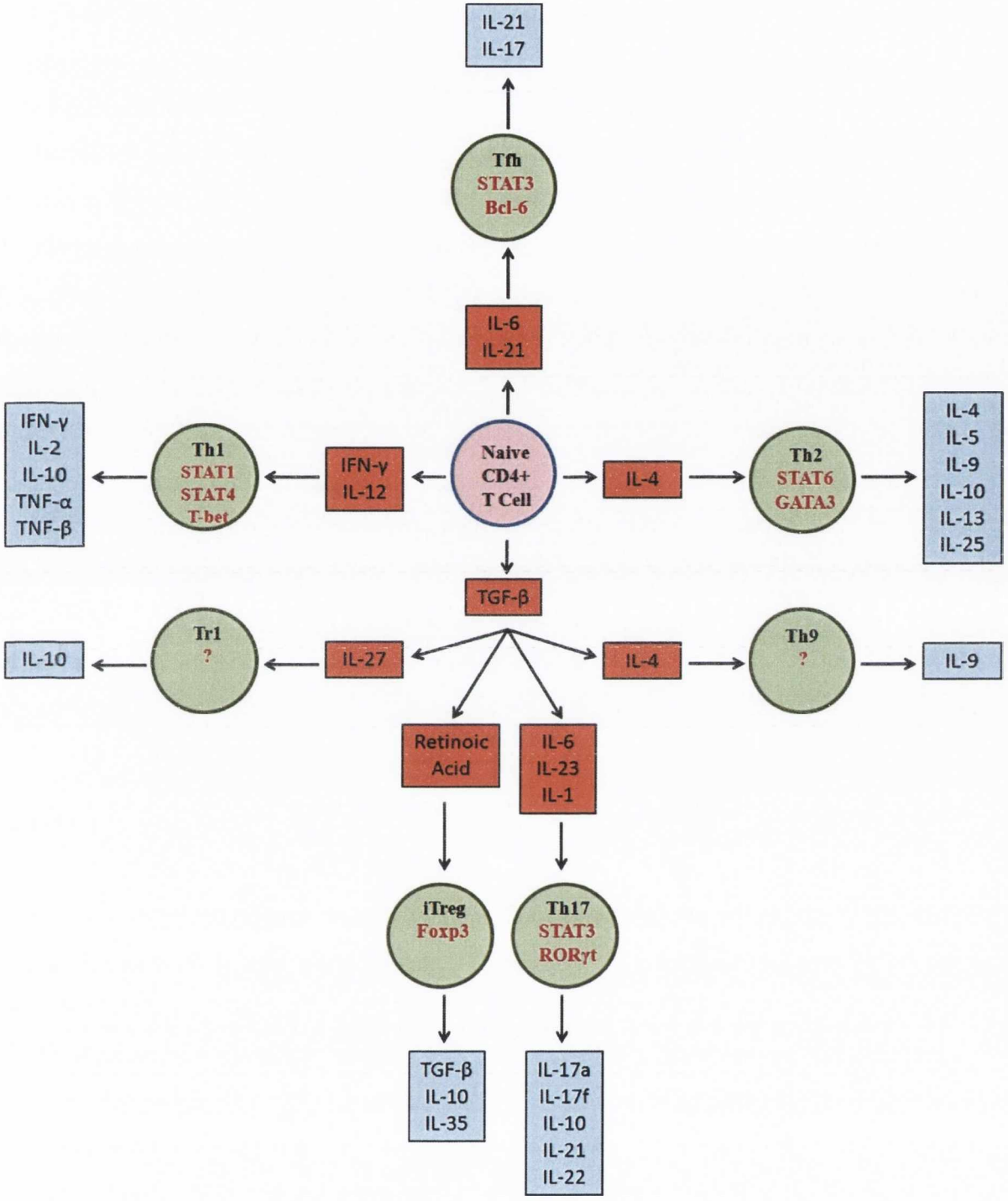

Figure 1.3 – Polarisation of CD4$^+$ T cell subsets. Following activation, naive CD4$^+$ T cells (T_N) can differentiate into a number of distinct lineages. The discrete phenotype obtained by T_N is dependent on the cytokines present in the local environment and subsequent expression of transcription factors (red). Each lineage secretes a range of cytokines characteristic of that particular lineage. Figure adapted from [104].

When Coffman and Mosmann originally proposed the Th1-Th2 paradigm of $CD4^+$ T cell differentiation, it was widely believed that these pathways of delineation were unidirectional. Therefore, once a naive $CD4^+$ T cell is polarised to become a Th1 or Th2 cell, this phenotype cannot be reversed. Indeed, this is still the case for Th1 and Th2 cells undergoing late stage differentiation. For example, IL-12Rβ2, which confers responsiveness to IL-12, is upregulated by T-bet activation and serves to promote Th1 cell differentiation [105]. However, IL-12Rβ2 expression is inhibited by the Th2 polarising cytokine IL-4, thus antagonising Th1 cell differentiation [106]. Similarly, IFN-γ activates T-bet which subsequently upregulates runt-related transcription factor (Runx)3 expression. Runx3 and T-bet serve to bind the *ifng* promoter and *il4* silencer respectively, thus promoting Th1 differentiation and inhibiting the corresponding Th2 process concomitantly [107]. Interestingly, Th1 and Th2 cells cannot be redirected to become Th17 or Treg cells [108]. T-bet negatively regulates IL-17 induction [109] whereas IL-4-induced growth factor independent (GFI)1 suppresses Th17 and iTreg cell differentiation [110]. Based on these observations, it is widely accepted that Th1 and Th2 cells represent two terminally differentiated lineages. However, this terminal differentiation state does not seem to apply to Th1 and Th2 cells undergoing early stage differentiation, as both phenotypes can be redirected to establish different $CD4^+$ T cell lineages. In fact, at early stages of differentiation, each lineage can be rerouted in any direction with relative ease [111].

There is abundant plasticity in the relationship between Th17 and iTreg cells which is perhaps not evident in the relationship between Th1 and Th2 cells. Indeed, characterisation of Th17 and iTreg cells has forced a rethink of the idea that lineage development is unidirectional. Naive $CD4^+$ T cells resident in a local microenvironment containing TGF-β upregulate both RORγt and Foxp3, the master transcription factors for Th17 and iTreg cells respectively. Thus, there exists a close link in the development of these respective $CD4^+$ T cell subsets. There is an interaction between RORγt and Foxp3, with Foxp3 antagonising RORγt-induced IL-17 expression [112-113]. Transduction of naive $CD4^+$ T cells with RORγt stimulates IL-17 expression but this process is suppressed by co-transduction with Foxp3. These RORγt and Foxp3 double-positive $CD4^+$ T cells can now differentiate into either Th17 or iTreg cells, depending on the constituents of the local microenvironment. In the presence of the pro-inflammatory cytokines IL-6, IL-21, IL-1 and IL-23, as well as low concentrations of TGF-β, Th17 cell development ensues while Foxp3 expression is inhibited and iTreg cell development is suppressed [114]. However, high concentrations of TGF-β in the presence of retinoic acid and IL-2 favours the development of iTreg cells [115-118].

When fully differentiated, Treg cells elicit considerable plasticity as they can be redirected to become Th17 cells. Thus, the developmental process of Tregs is not fixed and is in fact bidirectional. Thymus-derived Foxp3 expressing cells secrete IL-17 in response to IL-6 and TCR engagement [119]. However, it has been reported that iTregs are resistant to Th17 conversion by IL-6 [120]. Treg cell conversion into other $CD4^+$ T cell subsets has also been reported. For example, nTreg cells exposed to a Th1 polarising environment express T-bet and IFN-γ while maintaining Foxp3 expression [108]. Also, reduced expression of Foxp3 results in rapid acquisition of a Th2 phenotype [121]. In conditional Dicer-Foxp3-cre mice, genetic fate-mapping studies identified a significant number of IFN-γ and IL-4 producing cells which had previously expressed Foxp3 [122]. Differentiated Th17 cells also demonstrate significant plasticity. For example, Th17 cells can be converted into Th1 or Th2 cells following exposure to IL-12 and IL-4 respectively [123-124]. However, there is little evidence to support reciprocal conversion of Th17 cells into Treg cells. Some memory Th17 cells have been shown to be stable *in vivo*, thus suggesting that a number of Th17 subsets may become terminally differentiated [124].

1.4.3 - $CD8^+$ T cells

$CD8^+$ T cells are cytotoxic effectors of the adaptive immune system and serve primarily to kill tumour cells and virally infected cells. $CD8^+$ T cells, also known as CTLs, recognise specific peptides presented exclusively by surface MHC class I molecules and can induce apoptosis in target cells through a variety of mechanisms. However, perhaps the most prominent cytotoxic pathway utilised by $CD8^+$ T cells involves the controlled extracellular release of lethal granules (Figure 1.4). Within the cytoplasm of a $CD8^+$ T cell there are cytotoxic granules containing perforin and granzymes [125-126]. When the T cell is activated, the cytoskeleton and secretory apparatus are immediately rearranged. Within minutes, the golgi apparatus, microtubule organising centre (MTOC) and lethal intracellular granules are reorganised so that they are now orientated towards the target cell [127-128]. This enables the T cell to establish polarity with the target cell. Once this state of polarity is achieved, the cytotoxic granules move away from the MTOC and begin to fuse with the $CD8^+$ T cell plasma membrane. The granules then proceed to release their contents into the extracellular space existing between the T cell and the target cell [129]. The perforin protein punctures the plasma membrane of the target cell. Significantly, in the presence of perforin alone, the damage to the target cell membrane results in osmotic lysis and subsequent target cell death by

necrosis. However, in the presence of GzmB, the target cell is subjected to apoptosis [130-132]. This is due to the ability of granzymes to enter the cytoplasm of the target cell through membrane pores generated by perforin proteins, and to activate different caspases responsible for apoptosis [133].

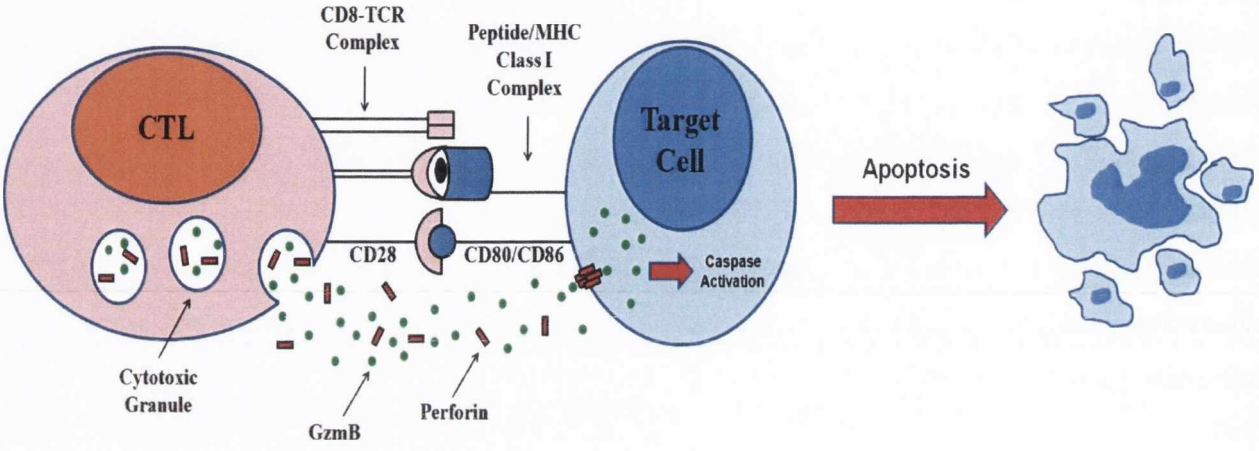

Figure 1.4 – CTL-mediated cytotoxicity. CTLs are activated following CD28-mediated costimulation and crosslinking of the CD8-TCR complex with peptide presented by MHC class I molecules. MHC class I molecules are expressed on the surface of virally infected or tumour target cells. CTL activation stimulates the extracellular release of perforin and GzmB from cytotoxic granules which function in a complimentary fashion to induce caspase activation and apoptosis in the target cell.

$CD8^+$ T cells can also secrete IFN-γ which is a particularly important regulatory cytokine for both innate and adaptive immunity. IFN-γ can regulate the innate response by inducing macrophage activation and subsequent phagocytosis of pathogens, amongst other functions. However, this particular cytokine can also regulate adaptive immunity by polarising Th1 cells and inhibiting the occurrence of a Th2 response [70].

For many years it was believed that $CD8^+$ T cells produced mainly IFN-γ and did not make discernable levels of Th2 cytokines [134]. In 1992, however, Seder *et al.* demonstrated that $CD8^+$ T cells can be classified into at least two functional subsets as murine $CD8^+$ T cells cultured in the presence of IL-2 and IL-4 secreted significant levels of IL-4 [135]. Furthermore, Salgame *et al.* identified IL-4-secreting $CD8^+$ T cells within the lesions of patients with lepromatous leprosy [136]. Thus, $CD8^+$ T cells can differentiate into two distinct subsets of cytotoxic effector cells: T cytotoxic (Tc)1 cells secrete the Th1 cytokines IL-2 and IFN-γ; and Tc2 cells produce the Th2 signature cytokines IL-4, IL-5 and IL-10. However, unlike Th2 cells, Tc2 cells retain their ability to produce IFN-γ, although at much lower concentrations than Tc1 cells [137]. The cytokines regulating the differentiation of naive $CD8^+$ T cells into Tc1 and Tc2 cells appear to be IL-12 and IL-4 respectively [136-137]. Both Tc1 and Tc2 cells show comparable toxicity and produce similar levels of perforin. However, Tc1 and Tc2 cells have opposing effects on the differentiation of naive $CD4^+$ T cells, inducing Th1 and Th2 responses respectively [138].

1.4.4 - Memory T cells

The development of memory $CD4^+$ and $CD8^+$ T cells is divided into three distinct phases. The first stage is referred to as the expansion phase and occurs in secondary lymphoid organs, where naive T cells encounter antigen and undergo clonal expansion and differentiation into effector T cells. Naive $CD4^+$ and $CD8^+$ T cells differentiate into Th cells and CTLs respectively, as discussed above. The second phase is known as the death phase or contraction phase and is initiated in the weeks following pathogen clearance. The contraction phase is responsible for killing the majority of effector T cells by apoptosis. T cells that survive the contraction phase enter the third and final phase, the memory phase. This phase stabilises the number of memory T cells and maintains these cells for long periods of time [139]. There is a greater understanding of memory $CD8^+$ T cell development than memory $CD4^+$ T cell development as memory $CD8^+$ T cells have been better characterised *in vivo*.

It is well-established that the recall response mediated by memory $CD4^+$ and $CD8^+$ T cells is more potent, rapid and aggressive than the initial primary response. Indeed, there are several explanations for this observation. Firstly, naive T cells differentiating into memory T cells undergo gene-expression profile reprogramming. For example, genes encoding IFN-γ, perforin and granzymes are not expressed in naive $CD8^+$ T cells, but are constitutively expressed in memory $CD8^+$ T cells [140-142]. Thus, memory $CD8^+$ T cells can secrete cytokines more rapidly and in larger quantities than

naive $CD8^+$ T cells and can also elicit cytotoxic activity almost immediately. Secondly, memory $CD8^+$ T cells express distinct surface proteins involved in adhesion and chemotaxis which are not expressed by naive $CD8^+$ T cells. This facilitates extravasation of memory $CD8^+$ T cells into non-lymphoid tissues and mucosal sites, locations where infectious disease is typically initiated. These memory $CD8^+$ T cells are referred to as 'effector' memory T cells, whereas those residing in secondary lymphoid organs are termed 'central' memory T cells. CD62L and CCR7 are essential for lymphocytes to traverse high endothelial venules and therefore to enter lymph nodes. Effector memory T cells are $CD62L^{low}$ $CCR7^-$ whereas central memory T cells are $CD62L^{high}$ $CCR7^+$ [143]. This difference therefore explains the distinct anatomical locations of these two memory $CD8^+$ T cell subsets. Finally, memory T cells undergo slow but steady homeostatic cell division in order to maintain these populations for a prolonged period of time [144]. Cytokines such as IL-15, IL-7 and IL-2 appear to play important roles in regulating memory T cell proliferation [145-147].

Ultimately, the memory phase of adaptive immunity and the retention of memory $CD4^+$ and $CD8^+$ T cells, as well as memory B cells, mediates host protection following secondary exposure to infectious agents and provides the immunological basis for vaccination.

1.5 - Vaccines and Adjuvants

Vaccination represents a hugely successful and incredibly important immunological application which has contributed immensely to public health for over 200 years. For example, vaccination has facilitated the successful worldwide elimination of smallpox which was famously announced by the World Health Organisation in 1980. Ultimately, vaccination has been hugely important in reducing mortality and morbidity caused by infectious diseases.

The story of vaccination began in 1796 with the work of Edward Jenner. During this time, smallpox was a very serious illness which was fatal in one third of all cases, and left those who survived badly disfigured. However, it was well known that milkmaids did not contract this disease. Noting this observation, Jenner proposed the idea that milkmaids were protected from smallpox by the pus in the blisters that they received from contracting cowpox, a similar but far less virulent disease than smallpox caused by infection with vaccinia (from vacca, Latin for cow). In order to test this hypothesis, Jenner inoculated a young boy (James Phipps) with pus from a blister on the hand of a milkmaid infected with cowpox. The young boy experienced fever but no life threatening or even

serious illness. Jenner subsequently injected the boy with smallpox but the infection failed to establish itself. Jenner had discovered that cowpox could provide protective immunity against smallpox in humans without risk of significant disease, and he named this process 'vaccination'. Louis Pasteur, who created vaccines against chicken cholera and human rabies, amongst others, later extended the term vaccination to include protection against other diseases.

The purpose of vaccination is to generate long-lasting protective immunity against disease by manipulating the memory potential of the adaptive immune system. Vaccination is induced by administering an antigen formulation that induces a natural, long-lasting protective immune response without causing disease. Therefore, upon exposure to the corresponding pathogen, the adaptive immune system will 'remember' the previous encounter and mount a more rapid and effective immune response, thus preventing infection and greatly reducing the symptoms of disease. Specialised cells such as memory T and B cells, as well as long-lived effector B cells (plasma cells) provide the foundation for immunological memory. Vaccines are comprised of attenuated organisms with reduced pathogenicity, killed organisms or more recently components of organisms which are referred to as subunit vaccines.

A successful vaccine must meet certain criteria. For example, it must be safe, cost-effective and generate long-lasting protective immunity in a high percentage of recipients. Also, an effective vaccine should generate herd immunity. This concept essentially implies that a vaccine should indirectly protect non-vaccinated members of a population from disease if the majority of the population have already been vaccinated. This is achieved by reducing the number of susceptible members of a population by vaccination, thus reducing the probability of transmission of disease to non-vaccinated members of the population.

In 1925, Ramon discovered that antitoxin responses were significantly augmented in horses when the toxin was administered with immunostimulatory substances including bread crumbs, tapioca, saponin and starch oil. Thus, Ramon had unearthed the concept of adjuvants (from the Latin verb 'adjuvare', meaning to help). In 1926, Alexander Glenny and colleagues first reported the adjuvant activity of aluminium salts (alum). Indeed, alum was the only Food and Drug Administration (FDA)-approved adjuvant for use in humans throughout the twentieth century. The purpose of an adjuvant is to potentiate the immunogenicity of a co-administered antigen and to enhance immunological memory. However, despite extensive research, the precise mechanism of action of most adjuvants remains unknown, and it is because of this that Charles Janeway once referred to adjuvants as 'the

dirty little secret of immunologists'. Adjuvants are quite diverse and comprise various different classes of compounds such as microbial products, mineral salts, emulsions, microparticles and liposomes.

Since 1926, alum has been incorporated into various human vaccines as particulate aluminium salts such as aluminium hydroxide ($AI(OH)_3$) and aluminium phosphate ($AIPO_4$). Alum is well known to promote strong humoral immunity as measured by increased antibody titres but is a poor inducer of cell-mediated immunity. Despite being administered as part of vaccine formulations for over 70 years, the mechanism of action of alum remains elusive. However, three credible theories have been proposed over time. The first hypothesis is that alum adsorbs antigen and serves as an antigen depot that facilitates the persistence of antigen at the injection site for a prolonged period of time, thus making the antigen available to sentinel phagocytic cells at high concentrations. In support of this hypothesis, alum has a very long half-life at sites of injection. For example, in a monkey model, alum can be detected in the muscle up to 6 months after intramuscular immunisation with a Diphtheria-Tetanus vaccine. Furthermore, the above study also suggests that the alum-adsorbed antigen can persist for longer than when administered in the absence of alum [148]. However, various studies have opposed this 'depot effect'. For example, it has been demonstrated that radioactively-labelled tetanus toxoid separates rapidly from alum at the injection site [149]. Also, excision of the diphtheria toxoid-alum injection site after subcutaneous immunisation fails to alter the immune response to the antigen [150].

The second hypothesis is that antigens adsorbed to alum are presented to APCs in a particulate multivalent form which is more immunogenic and enhances uptake by phagocytosis. In support of this idea, it has been shown that although DCs are capable of internalising soluble antigens by macropinocitosis, they are far more effective at taking up alum-adorbed antigen by phagocytosis in an aggregate size-dependent manner [151]. However, other studies have shown that alum does not enhance internalisation of fluorescently-labelled OVA by DCs [78].

Alum has also been suggested to function as an effective adjuvant by inducing inflammation and subsequent recruitment and activation of APCs that can internalise antigen. However, alum is not capable of directly activating DCs *in vitro* [152-153]. Despite this, alum can act directly on macrophages to induce their differentiation into DC-like cells with an increased capacity for antigen presentation. *In vivo*, intraperitoneal (i.p.) injection of alum promotes recruitment of a plethora of innate immune cells including neutrophils, eosinophils and in particular inflammatory monocytes

through a process dependent on keratinocyte-derived chemokine (KC), eotaxin and monocyte chemoattractant protein (MCP)-1. The inflammatory monocytes internalise antigen and migrate to the lymph nodes where they become monocyte-derived DCs and induce adaptive immunity [78].

Another mechanism by which alum promotes inflammation is through activation of the NLRP3 inflammasome. *In vitro*, it is universally accepted that alum activates caspase-1 through NLRP3 inflammasome assembly and synergises with TLR agonists to promote processing and secretion of the biologically active form of the proinflammatory cytokine IL-1β. However, the importance of NLRP3 in the adjuvanticity of alum is unclear. Initially, Eisenbarth *et al.* found that antibody responses to OVA or human serum albumin (HSA) co-administered with alum were abrogated in NLRP3-deficient mice [154]. However, in the same year, Nunez and colleagues published data contradicting these findings [155].

Alum adjuvanticity is at least partially dependent on the ability of this adjuvant to induce cell death at the injection site. Recently, Marichal *et al.* have shown that genomic DNA released by dying host cells mediates adjuvant activity *in vivo*, and the adjuvanticity of alum is partially attenuated when extracellular DNA is digested by treatment with DNase I [156]. Kool *et al.* previously described a role for uric acid released from dying host cells in mediating the immunostimulatory effects of alum. Recruitment of innate immune cells such as neutrophils and inflammatory monocytes, as well as T cell priming and humoral immunity, is abrogated in response to alum when uric acid is degraded by the enzyme uricase [78, 157].

There is currently very little known about the target cells, receptors and signalling pathways targeted by alum. However, a recent report has proposed that alum does not engage a specific cell surface receptor, but rather binds exclusively to plasma membrane lipids on the surface of DCs. Alum induces lipid sorting which subsequently activates a spleen tyrosine kinase (SYK) and phosphoinositide 3-kinase (PI3K)-mediated abortive phagocytic response, thus promoting antigen uptake. Interestingly, alum is not phagocytosed by DCs [158].

The oil-in-water emulsion MF59 was licensed for a flu vaccine formulation (Fluad) in Europe in 1997, 71 years after the discovery of the adjuvant properties of alum. Fluad combined MF59 with the two most prominent influenza antigens, hemagglutinin (HA) and neuraminidase (NA). Indeed, MF59 was only approved for use in humans after extensive clinical trials involving upwards of twenty thousand subjects. This adjuvant was developed by Chiron Corp which was acquired by Novartis in 2006. The oil component of MF59 is squalene which is derived from shark liver oil but is also

present in human sebum and is a naturally occurring precursor of cholesterol. Squalene droplets are stabilised in a thermodynamically unfavourable hydrophilic environment through addition of two non-ionic surfactants, Polysorbate 80 (Tween 80) and sorbitan triolate (Span 85). The squalene droplets exist at sizes ranging from 10-200 nanometres (nm). MF59 induces functional and protective humoral immunity, and can also mediate powerful T cell responses to several different types of antigens [159-163].

As in the case of alum, the mechanism of action of MF59 remains unclear. However, immunofluorescence studies have established that MF59 promotes antigen uptake by DCs following intramuscular injection. More specifically, antigen co-administered with MF59 localises to vesicular organelles more efficiently than antigen administered alone [164]. However, MF59 does not seem to promote a depot effect, as antigen localisation and clearance from the injection site are not altered by MF59. Indeed, 4 hours after intramuscular injection of fluorescently-labelled MF59 into mice, only 36% of the injected MF59 can be found in the muscle. Furthermore, antigen is cleared from the site of injection independently of MF59 [165].

Intramuscular administration of MF59 also promotes an influx of macrophages into the site of injection, and this process is partially dependent on CCR2 [166]. In support of this, MF59 has recently been shown to directly stimulate human macrophages, monocytes and granulocytes to secrete chemokines such as CCL2, CCL3, CCL4 and CXCL8. Interestingly, these chemokines further recruit macrophages and granulocytes which can phagocytose both antigen and adjuvant and transport them to the draining lymph nodes [167]. Consequently, the mechanism of action of MF59 has been postulated to involve chemokine-dependent immune cell recruitment into the injection site and subsequent chemokine release by these infiltrating cells, thus driving a positive feedback loop increasing the number of immune cells at the injection site. This increases the probability of an APC encountering antigen at the site of injection and therefore improves transport of antigen to secondary lymphoid organs, thereby enhancing T cell priming [168]. Moreover, MF59 also promotes the differentiation of human monocytes towards DCs as measured by downregulation of the monocytic marker CD14 [152]. Considering the role of DCs as professional APCs and key mediators of T cell priming, an increase in the number of these cells at the injection site may enhance the magnitude of the immune response to MF59.

The immunostimulatory effects of MF59 have been shown to be independent of the NLRP3 inflammasome. However, the TLR adaptor protein myeloid differentiation factor 88 (MyD88) and

the inflammasome adaptor protein apoptosis-associated speck-like protein containing a caspase activation and recruitment domain (ASC) are both crucial for MF59 adjuvanticity [169-170]. In addition to these findings, Hui *et al.* have demonstrated that both IL-4 and STAT-6, but not IFN-γ, are important for MF59 function [171], although further work is required to identify a specific receptor for this adjuvant.

Another emulsion with significant immunopotentiating ability is Freund's adjuvant which is the most commonly used adjuvant for experimental work. However, Freund's adjuvant is not used in clinical settings due to its unacceptable safety profile. The discovery of Freund's adjuvant was based on an observation by Jules Freund that the sera of pigs that had received heat-killed mycobacteria in paraffin oil contained high anti-mycobacterial antibody titres. Essentially, Freund had discovered that adding paraffin oil to heat-killed mycobacteria resulted in unprecedented immunostimulatory effects. When mixed with an aqueous solution, Freund's adjuvant forms a water-in-oil emulsion. The oil present in the preparation is paraffin oil and the surfactant used to stabilise water droplets in this thermodynamically unfavourable hydrophobic environment is mannide monoleate. Complete Freund's adjuvant (CFA) contains heat-killed mycobacteria, whereas incomplete Freund's adjuvant (IFA) lacks this component. CFA promotes a Th1 response primarily owing to recognition of mycobacterial components by PRRs present on the surface of APCs, thus resulting in APC activation and secretion of the Th1-polarising cytokine IL-12. However, IFA can initiate a Th2-skewing immune response. Despite being powerful adjuvants, the mechanism underlying the actions of CFA and IFA, similarly to alum and MF59, remain elusive.

Indeed, adjuvants have long been postulated to kick-start the immune system in response to co-administered antigen. However, this particular scenario brings attention to a long standing immunological puzzle. How exactly is an immune response initiated? More specifically, which stimuli are responsible? One crucial step in the initiation of innate and indeed adaptive immunity is recognition of dangerous situations. In order to combat infection, the host must first recognise the presence of an invader. However, exactly how do innate sentinel cells recognise harmful stimuli? For the past 18 years, the 'stranger model' and the 'danger model', two separate models of immune activation with very different principles, have competed in an attempt to resolve this important issue.

1.6 - The Stranger Model

It is widely believed that the immune system responds to 'foreignness'. The so-called stranger model is a theory essentially built upon major advances in immunology that provide it with solid foundations. The story began in 1959 with the initial 'self-nonself model' (clonal selection) proposed by Burnet. In this model, Burnet described the idea that each lymphocyte (B cell) expresses many copies of a single surface receptor specific for a foreign entity. In order to ensure that effector responses are directed only against non-self, Burnet incorporated Lederberg's theory that lymphocytes expressing self-reactive surface receptors are deleted early in ontogeny [172]. This model was supported by Medawar and colleagues who showed that adult mice would accept foreign skin grafts if they had been injected with donor cells when very young [173].

Burnet's original self-nonself model of immune activation was expanded in 1970 by Bretscher and Cohn. B cells had since been shown to hypermutate their surface receptor, thereby increasing antigen-specific receptor diversity. However, hypermutation could also generate potentially self-reactive lymphocytes. Bretscher and Cohn soon realised that the likelihood of developing autoimmune disease would be reduced considerably if immune activation required the contribution of two cells, and they subsequently proposed the 'associate recognition model' in which they describe the existence of a new helper cell (later identified as a T cell) and a new signal (help) provided by this cell. Bretscher and Cohn proposed that the B cell would die if it recognised antigen in the absence of help provided by a helper cell also activated by antigen [174]. This model was expanded further in 1975 by Lafferty and Cunningham who added another cell and another signal to the equation. These additions were a direct result of the discovery that T cells respond more vigorously to cells of their own species than to cells of another species. To address this issue, Lafferty and Cunningham proposed the idea that T cell activation is not achieved solely by recognition of antigen, but also requires a second signal (costimulation) provided by another cell (APC), and that this signal is species specific. Indeed, T cell activation in the absence of costimulation would lead to tolerance [175].

In 1989, Charles Janeway hypothesised that APCs possess their own unique form of self-nonself discrimination. He proposed that APCs express a family of receptors called PRRs that recognise evolutionarily conserved motifs called pathogen-associated molecular patterns (PAMPs) that are only present on microbes. Upon recognition of PAMPs, quiescent APCs become activated and begin to upregulate costimulatory molecules and process microbial antigens and present them to T cells in

secondary lymphoid organs, thus initiating adaptive immunity. Therefore, Janeway hypothesised that PAMP recognition by PRRs induces APC activation and thus enables discrimination between 'infectious-nonself' and 'noninfectious-self' [176]. Indeed, this 'infectious-nonself model' has long been referred to as the stranger model and has received much support since the discovery of PRRs [177].

1.7 - PRRs

PRRs sense a limited range of evolutionarily conserved motifs expressed by pathogens which are essential for the survival of the pathogen and thus cannot be mutated in an attempt to evade innate immune recognition. The conserved motifs recognised by PRRs are referred to as PAMPs and recognition of PAMPs by PRRs stimulates complex signalling cascades culminating in the onset of innate immunity. PRRs are expressed primarily by cells at the front line of the innate immune defence system, including monocytes, macrophages, DCs, neutrophils and epithelial cells. PRRs can currently be subdivided into four separate families depending on their cellular localisation and ligand recognition potential; TLRs, retinoic-acid-inducible gene (RIG)-I-like receptors (RLRs), C-type lectin receptors (CLRs) and nucleotide-binding oligomerisation domain (NOD)-like receptors (NLRs).

1.7.1 - TLRs

TLRs are the best characterised subset of PRRs and are crucial for optimal antimicrobial immune function. TLRs are characterised by the presence of N-terminal leucine rich repeats (LRRs) in the ectodomain and a transmembrane region followed by a C-terminal cytoplasmic Toll/interleukin-1 receptor (TIR) domain [178]. Currently, ten and twelve functional TLRs have been discovered in humans and mice respectively. TLR1-TLR9 are conserved between both species, TLR10 is non-functional in mice due to a retroviral insertion, while TLR11-TLR13 have been removed from the human genome.

Early studies of the pathogenesis of Gram-negative septic shock implicated both lipopolysaccharide (LPS)-binding protein (LBP) and CD14 in this disease. LBP was believed to function as an opsonin for LPS while CD14 could serve as an opsonic receptor for LBP-LPS complexes. However, further

studies concluded that CD14, despite the presence of multiple extracellular LRRs, failed to convey a transmembrane signal following ligand binding [179]. Thus, it was hypothesised that LBP-LPS/CD14 complexes could recruit a further receptor capable of communicating the ligand-binding activation signal across the membrane of the cell. The search for this elusive LPS-responsive receptor was relatively unsuccessful before the seminal discovery of human Toll.

The discovery of TLRs began with an important observation by Jules Hoffmann that Drosophila Toll (dToll), a Drosophila fruit fly protein involved in dorso-ventral polarity during embryogenesis, also plays a crucial role in anti-fungal defence in the adult Drosophila. Indeed, Drosophila expressing a mutated dToll are susceptible to infection by fungi [180]. Following on from this discovery, Charles Janeway and colleagues identified a human homologue of dToll, originally coined human Toll and subsequently termed TLR4 [181]. A constitutively active TLR4 mutant expressed in the THP-1 monocytic cell line induced expression of proinflammatory cytokines and chemokines involved in the modulation of innate immunity, as well as upregulation of costimulatory molecules required for adaptive immunity [181]. Soon afterwards, Bruce Beutler identified TLR4 as the receptor for LPS. Two particular mouse strains, C3H/HeJ and C57BL10/ScCr, were known to be hyporesponsive to LPS. Beutler and colleagues found mutations in the *Tlr4* gene in these strains. More specifically, a point mutation in the cytoplasmic portion of TLR4 in the C3H/HeJ strain resulted in an amino acid substitution from proline to histidine [182-183] which has since been shown to result in defective TLR4 signalling [184]. Furthermore, a chromosomal deletion in the TLR4 genomic locus of C57BL10/ScCr mice was discovered, thus rendering these mice TLR4 null [182-183]. In support of these findings, Shizuo Akira's group generated TLR4-deficient mice which were subsequently shown to be LPS hyporesponsive [184]. Indeed, the long sought after receptor capable of interacting with LBP/CD14 complexes and the more recently identified myeloid differentiation protein (MD)-2, which is a secreted protein that binds to the extracellular domain of TLR4 and increases LPS responsiveness, had been identified as the first member of the TLR family. Subsequent studies identified a series of receptors structurally related to TLR4 [185-188], thus giving rise to the TLR family.

The TLR family can recognise a limited range of evolutionarily conserved PAMPs, with each TLR recognising a specific PAMP or group of PAMPs. TLR2 recognises a range of components derived from bacteria, mycoplasma, fungi and viruses, particularly peptidoglycan-derived lipoproteins from Gram-positive and Gram-negative bacteria [189-191], lipoarabinomannan from mycobacteria [192] and zymosan from fungi [193]. TLR2 senses its ligands by forming a heterodimer with either TLR1

or TLR6, thus recognising distinct ligands in the form of triacyl or diacyl lipoproteins respectively [194]. TLR4 is, as discussed above, the receptor for LPS, while TLR5 recognises flagellin [195] which is a protein component of bacterial flagella. TLRs also serve as sensors for nucleic acids. TLR3 responds to double-stranded ribonucleic acid (dsRNA) generated during viral replication and is also involved in the recognition of polyinosinic polycytidylic acid (poly I:C), a synthetic analogue of dsRNA [196]. TLR7 recognises the synthetic imidazoquinoline-like molecules imiquimod (R-837) and resiquimod (R-848) [197], and also single-stranded ribonucleic acid (ssRNA) from RNA viruses [198]. TLR8 is very closely related to TLR7 and functional studies have shown that human, but not mouse, TLR8 also senses R-848 and ssRNA [198-199]. Unmethylated cytidine-phosphate-guanosine (CpG) motifs, which are rare in mammalian deoxyribonucleic acid (DNA) but abundant in bacterial DNA and DNA viruses, are sensed by TLR9 [187] (Figure 1.5).

TLRs can be divided into two subgroups based on their location in the cell. TLR1, TLR2, TLR4, TLR5 and TLR6 are expressed on the cell surface, whereas the nucleic acid sensing members of the family, namely TLR3, TLR7, TLR8 and TLR9, are located in endosomal and lysosomal compartments (Figure 1.5). This facilitates effective recognition of pathogen-derived nucleic acids following endocytosis and rupture of the pathogen and subsequent exposure of previously hidden DNA and RNA.

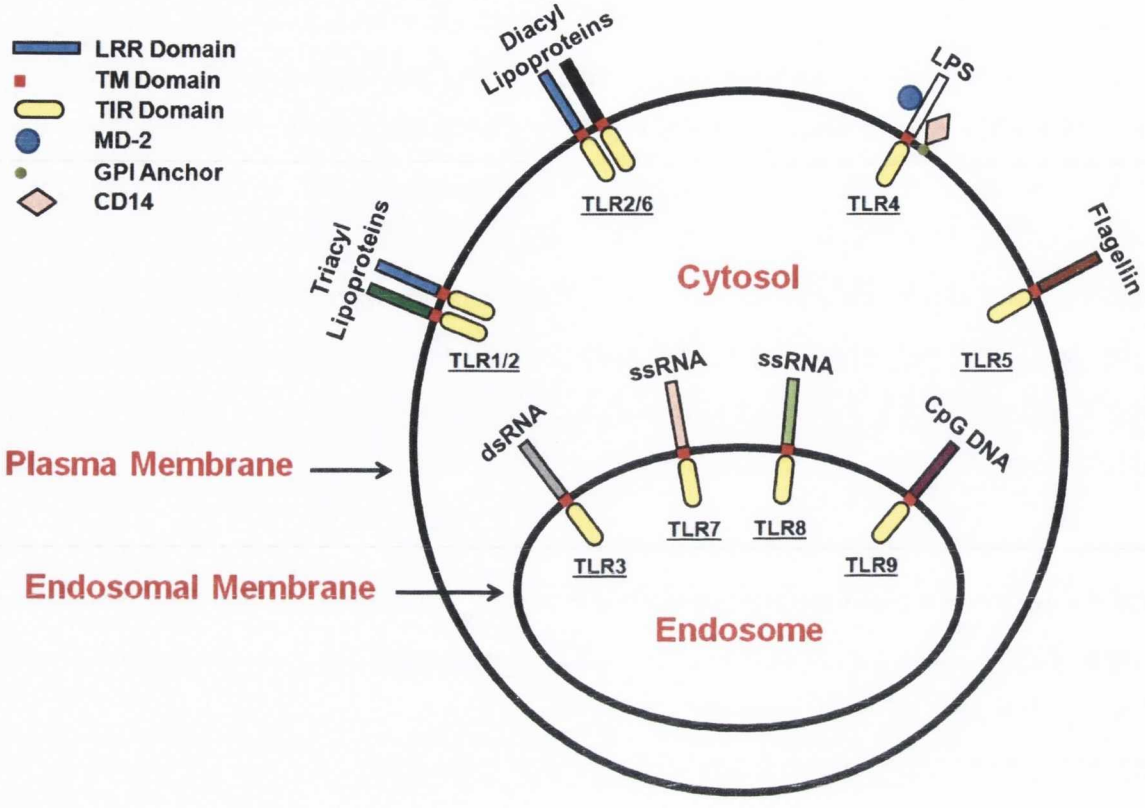

Figure 1.5 – Cellular distribution of TLRs and their respective ligands. TLRs can be expressed on the cell surface (TLR1, 2, 4, 5 and 6) or intracellularly on endosomal compartments (TLR3, 7, 8 and 9). TLR2 senses its ligands by forming a heterodimer with either TLR1 or TLR6, thus recognising triacyl or diacyl lipoproteins respectively. CD14 is glycosylphosphatidylinositol (GPI)-anchored to the plasma membrane and, in conjunction with MD-2, facilitates sensing of LPS by TLR4. TLR5 is the receptor for flagellin, whereas ssRNA is recognised by TLR7 and TLR8. TLR3 and TLR9 sense dsRNA and unmethylated CpG motifs respectively. TLRs each possess an N-terminal LRR domain and a transmembrane (TM) domain followed by a C-terminal cytoplasmic TIR domain.

Following recognition of a cognate ligand, different TLRs activate distinct TIR domain-dependent signalling cascades, thus inducing separate gene expression profiles. The ability of TLRs to drive unique signalling pathways is perhaps due to their respective ability to recruit different combinations of TIR domain-containing TLR adaptor molecules. There are five different adaptor molecules; MyD88, MyD88 adaptor-like (Mal), TIR-related adaptor protein inducing interferon (TRIF), TRIF-related adaptor molecule (TRAM) and Sterile-alpha and Armadillo motif-containing protein (SARM) [200] which was identified as the first TIR adaptor molecule to have an inhibitory role [201]. TLR signalling can be divided into two separate pathways, the MyD88-dependent pathway and the TRIF-dependent pathway.

The MyD88-dependent pathway is utilised by every member of the TLR family, with the exception of TLR3. MyD88 possesses a TIR domain and a death domain (DD), and TLRs recruit MyD88 through TIR domain interactions [202]. Interestingly, TLR2 and TLR4 require MAL for recruitment of MyD88 [203-204]. The MyD88-dependent pathway results in phosphorylation and activation of IκB kinase (IKK)-β and also the mitogen-activated protein kinase (MAPK) pathway. The IKK complex consists of IKK-α, IKK-β and nuclear factor-κB (NF-κB) essential modulator (NEMO), and this complex proceeds to phosphorylate the NF-κB inhibitory protein IκBα, thus leading to its subsequent degradation. This enables the transcription factor NF-κB to translocate into the nucleus where it regulates the expression of proinflammatory cytokines and chemokines such as IL-6, IL-1, TNF-α and IL-8. Activation of the MAPK pathway results in formation of the activator protein (AP)-1 complex which also modulates expression of proinflammatory genes in the nucleus [28].

The MyD88-independent pathway, or the TRIF-dependent pathway, was discovered following an important observation that MyD88-deficient cells retain activation of NF-κB and MAPK, although with delayed kinetics, and still upregulate costimulatory molecules in response to the TLR4 agonist LPS [205-206]. A similar MyD88-independent pathway has since been identified downstream of TLR3. Subsequent studies have shown that this pathway drives NF-κB, MAPK and IFN regulatory factor (IRF)3 activation. Following binding of their respective ligands, TLR3 and TLR4 recruit TRIF to the receptor complex [207]. TRIF recruitment by TLR4, but not TLR3, requires a second adaptor molecule TRAM [208]. Interestingly, LPS induces TLR4 transport to the endosome together with TRAM, whereas TLR3 is constitutively present in the endosome. TRIF has been shown to form part of a multiprotein signalling complex along with TNF receptor (TNFR)-associated factor (TRAF)6, TNFR-associated death domain protein (TRADD), the ubiquitin ligase Pellino-1 and receptor-interacting protein (RIP)-1. This complex switches on TGF-β-activated kinase (TAK)1 which

subsequently activates NF-κB and MAPK pathways [177]. TRIF also promotes IRF3 activation and this transcription factor can translocate to the nucleus, bind to DNA and promote expression of type I IFNs, particularly IFN-β, which is crucial for antiviral immunity [209].

1.7.2 - RLRs

As discussed above, TLRs recognise viruses in endosomal and lysosomal compartments, essentially sensing viruses that are present in the extracellular environment. However, most viruses replicate in the cytosol. This gave rise to a hypothesis outlining the existence of a family of PRRs capable of recognising cytoplasmic viruses. Indeed, this idea gained momentum when experiments revealed that fibroblasts lacking both MyD88 and TRIF maintained expression of IFN-inducible genes following RNA virus infection. Eventually, a family of RLRs were identified as cytoplasmic dsRNA sensors important for antiviral immunity.

The RLR family is composed of only three members; RIG-I, melanoma differentiated-associated gene (MDA)5 and laboratory of genetics and physiology (LGP)2. RIG-I and MDA5 contain two N-terminal caspase activation and recruitment domains (CARDs), a central DEAD box helicase/ATPase domain, and a C-terminal ligand binding regulatory domain. LGP2 lacks CARDs but possesses a helicase domain and a regulatory domain. RLR family members sense dsRNA which is generated by ssRNA viruses during replication and is also present in the genome of dsRNA viruses.

RIG-1 recognises short dsRNA (<1kb) [210] and is particularly important for host defence to a range of paramyxoviruses, including *Newcastle disease virus, Sendai virus, Vesicular stomatitis virus, Influenza virus and Japanese encephalitis virus* [211]. The potency of the antiviral response initiated by RIG-I is greatly enhanced by the presence of a 5' triphosphate end, although this feature is not essential [212]. MDA5 is a homologue of RIG-1 but instead recognises long dsRNA (>2kb) [211]. Indeed, poly I:C can be converted from an MDA5 ligand to a RIG-I ligand by shortening of its length by treatment with a dsRNA-specific nuclease. MDA5 senses a number of picornaviruses, including *Encephalomyocarditis virus, Theiler's virus and Mengo virus* [211]. Studies using mice with a loss of function point mutation in LGP2, as well as LGP2 knockout (KO) mice, have reported that LGP2 is a positive regulator of both RIG-I and MDA5 [213], although its precise mechanism of action is unclear.

RIG-I and MDA5 signal through a common CARD containing adaptor molecule, IFN-β-promoter stimulator (IPS)-1 [214], which is expressed on the surface of mitochondria. IPS-1 activates TRAF3 [215] which subsequently induces type I IFN gene expression. IPS-1 also activates TRADD which scaffolds with Fas-associated death domain (FADD) and caspase-8/-10 to drive NF-κB translocation into the nucleus [215].

1.7.3 - CLRs

CLRs are an important family of PRRs which contain at least one carbohydrate recognition domain that determines the carbohydrate specificity of the CLR [216]. CLRs predominantly sense mannose, fucose and glucan carbohydrate structures, thus facilitating recognition of a diverse range of pathogens. For example, viruses, fungi and mycobacteria can be recognised by mannose-specific CLRs, helminths and bacteria are sensed by fucose-specific CLRs, and glucan-specific receptors further recognise fungi and mycobacteria [217], thereby complementing other CLRs. Some CLRs are capable of modulating TLR-mediated gene expression but possess no independent gene expression capabilities of their own. Some good examples of these CLRs are DC-SIGN, blood DC antigen 2 protein (BDCA2), DC immunoreceptor (DCIR) and myeloid C-type lectin-like receptor (MICL) [218]. Other CLRs, including DC-associated C-type lectin (dectin) 1, dectin 2 and macrophage-inducible C-type lectin (Mincle) modulate gene expression independently of PRR signalling. Carbohydrate-mediated activation of CLRs seems to modulate the activity of NF-κB, but very little is known about the role of CLRs in AP-1 or IRF3/7 activation.

DC-SIGN senses a wide range of pathogens through mannose and fucose sensing, including *Mycobacterium tuberculosis* [219], *Helicobacter pylori* [220] and *human immunodeficiency virus (HIV)-1* [221]. Following mannose binding, DC-SIGN can modulate TLR-induced NF-κB activity [222]. BDCA2 senses a currently unidentified ligand but has been linked with suppression of TLR9 signalling in the endosome [223]. DCIR and MICL contain an immunoreceptor tyrosine-based inhibitory motif (ITIM) in their cytoplasmic tail and are known to recruit the phosphatases SH2-domain-containing protein tyrosine phosphatase (SHP)1 or SHP2 following activation by unknown ligands [224-225]. In the case of DCIR, recruitment of SHP1 or SHP2 leads to activation of a currently unknown signalling cascade resulting in the inhibition of TLR8-mediated IL-12 and TNF-α production in myeloid DCs and TLR9-mediated type I IFN secretion by pDCs [226-227].

Downstream of MICL, SHP1 or SHP2 can activate extracellular signal-regulated kinase (ERK) which leads to inhibition of TLR-induced IL-12 production by immune cells [228].

Dectin 1 is a prominent member of the CLR family and is capable of initiating its own signalling cascade with functional effects independent of TLRs. Dectin 1 recognises β-1,3-glucan structures expressed by a range of fungal pathogens including *Candida albicans* and *Aspergillus fumigatus* [229]. Ligation of dectin 1 initiates three distinct signalling pathways which are very closely related. The first pathway is characterised by the recruitment of SYK to a phosphorylated YxxL motif in the cytoplasmic tails of two dectin 1 molecules. SYK facilitates the assembly of a downstream signalling complex containing CARD9, BCL-10 and mucosa-associated lymphoid tissue (MALT)1 which subsequently drives canonical NF-κB activation (p65/RELA) [230]. However, dectin 1 activation also results in v-raf-1 murine leukemia viral oncogene homolog (RAF)1-mediated phosphorylation of NF-κB. Finally, SYK can induce activation of the non-canonical NF-κB (p52/RELB) pathway by sequential phosphorylation and activation of NF-κB-inducing kinase (NIK) and IKK-α.

Dectin 2 and Mincle are two additional receptors capable of signalling independently of TLRs. Dectin 2 binds high mannose on a wide range of pathogens [231] while Mincle senses α-mannose expressed by the fungus *Malassezia* [232]. Both dectin 2 and mincle complex with FcRγ and phosphorylation of the immunoreceptor tyrosine-based activation motif (ITAM) within this adaptor molecule leads to recruitment of SYK [231, 233].

1.7.4 - NLRs

There are twenty-three members of the NLR family in humans and there are at least thirty-four NLR-encoding genes in mice [234]. NLRs consist of a variable N-terminal domain which can be a pyrin domain, a baculoviral inhibitory repeat (BIR) domain or a CARD, as well as a central NOD and a C-terminal LRR domain. The LRR domain, in conjunction with the chaperones suppressor of G2 allele of Skp1 (SGT1) and heat shock protein (Hsp)90, is believed to fold back onto the NOD and retain the NLR in an autorepressed but signalling competent conformation [235]. NLRs are cytosolic sensors capable of recognising and responding to a range of pathogenic stimuli as well as endogenous 'self' molecules indicative of tissue injury.

Among the first members of the NLR family to be characterised were NOD1 and NOD2 which recognise the peptidoglycan components γ-D-glutamyl-meso-diaminopimelic acid and muramyl

dipeptide respectively [236-237]. NOD1 and NOD2 both express N-terminal CARDs (Figure 1.6) and receptor ligation induces oligomerisation and subsequent recruitment of RIP2 via CARD-CARD interactions. RIP2 can then promote activation of NF-κB and AP-1, thus leading to upregulation of proinflammatory gene expression.

Other NLR family members, principally NLRC4, NLRP1 and NLRP3, form crucial components of cytosolic caspase-1 activation platforms called inflammasomes. Inflammasome activation results in conversion of an inactive caspase-1 zymogen into a fully active caspase-1 tetramer composed of two p10 and two p20 subunits. The active form of the cysteine protease caspase-1 cleaves inactive pro-IL-1β and pro-IL-18 into their respective mature forms which possess functional activity important for both innate and adaptive immunity. The immature forms of IL-1β and IL-18 are upregulated by NF-κB and are efficiently synthesised as a result of TLR activation. Thus, both TLRs and NLRs act concomitantly to induce the synthesis, maturation and secretion of biologically active IL-1β and IL-18. In some cases, inflammasome activation can directly influence cell viability in either a positive or negative sense, depending on the stimulus. The NLR family member resident within a particular inflammasome complex gives rise to the name of the inflammasome complex itself [238].

The NLRP1 inflammasome was the first caspase-1 activation complex of this nature to be identified [239] and is known to sense *Bacillus anthracis*-derived lethal toxin [240]. NLRP1, like other NLRPs, possesses an N-terminal pyrin domain. However, NLRP1 also boasts a C-terminal extension which includes a function to find (FIIND) domain and a CARD (Figure 1.6), thus enabling NLRP1 to recruit caspase-1 directly via CARD-CARD interactions [241]. NLRs, including NLRP1, drive caspase-1 activation by oligomerising and thus facilitating the induced proximity of caspase-1 molecules which results in autoactivation. The N-terminal pyrin domain of NLRP1 can also recruit the adaptor protein ASC via pyrin domain interactions. ASC possesses a CARD which facilitates caspase-1 recruitment and autoactivation. However, not surprisingly, ASC is not essential for NLRP1-mediated IL-1β production but can augment this process significantly [241].

The NLRP3 inflammasome is probably the best characterised inflammasome and is composed of NLRP3, ASC and caspase-1 (Figure 1.6). NLRP3 recruits ASC via pyrin domain interactions and mediates caspase-1 activation and IL-1β secretion as described for NLRP1. Unlike the NLRP1 inflammasome, however, ASC is essential for this process [239]. NLRP3 senses a wide range of stimuli such as the fungi *Candida albicans* and *Saccharomyces cerevisiae* [242], bacteria including *Listeria monocytogenes* and *Staphylococcus aureus* [243], the bacterial pore-forming toxins

nigericin, maitotoxin and aerolysin [243], as well as crystalline structures such as silica, asbestos [244] and the commonly used adjuvant alum [245]. Furthermore, NLRP3 can also recognise a series of cell constituents released by injured tissues such as adenosine triphosphate (ATP) [243], monosodium urate (MSU) crystals and calcium pyrophosphate dihydrate (CPPD) crystals [246]. Interestingly, NLRP3 sensing of aerolysin leads to activation of sterile regulatory element binding proteins (SREBPs) which promote cell survival [247].

NLRC4 senses a number of Gram-negative bacteria with type III or type IV secretion systems, including *Salmonella typhimurium* [248], *Shigella flexneri* [249], *Legionella pneumophila* [250] and *Pseudomonas aeruginosa* [251]. NLRC4 activation results in pyroptosis, a caspase-1-dependent form of cell death which is characterised by cell lysis and secretion of IL-1β and IL-18 [252]. *Salmonella typhimurium* and *Pseudomonas aeruginosa* both use type III secretion systems to form pores in the cell membrane and deliver flagellin into the cytosol which is then sensed by NLRC4, while *Legionella pneumophila* achieves the same feat using a type IV secretion system. However, *Legionella pneumophila*-induced pyroptosis is also believed to require NAIP5, a separate NLR family member with an N-terminal BIR domain [253]. Interestingly, flagellin-deficient *Pseudomonas aeruginosa* is still capable of stimulating NLRC4 [254], while *Shigella flexneri*, which also uses a type III secretion system but is a nonflagellated bacterium, activates NLRC4 independently of flagellin. Thus, there exist further unidentified NLRC4 ligands awaiting discovery. NLRC4 contains an N-terminal CARD which enables direct interaction, recruitment and autoactivation of caspase-1 (Figure 1.6). The role of ASC in the NLRC4 inflammasome remains unclear. However, the current consensus is that ASC is dispensable for NLRC4-mediated caspase-1 activation in response to *Legionella pneumophila*, but maximal caspase-1 activation in response to *Salmonella typhimurium* [255], *Shigella flexneri* [249] and *Pseudomonas aeruginosa* [251] requires ASC.

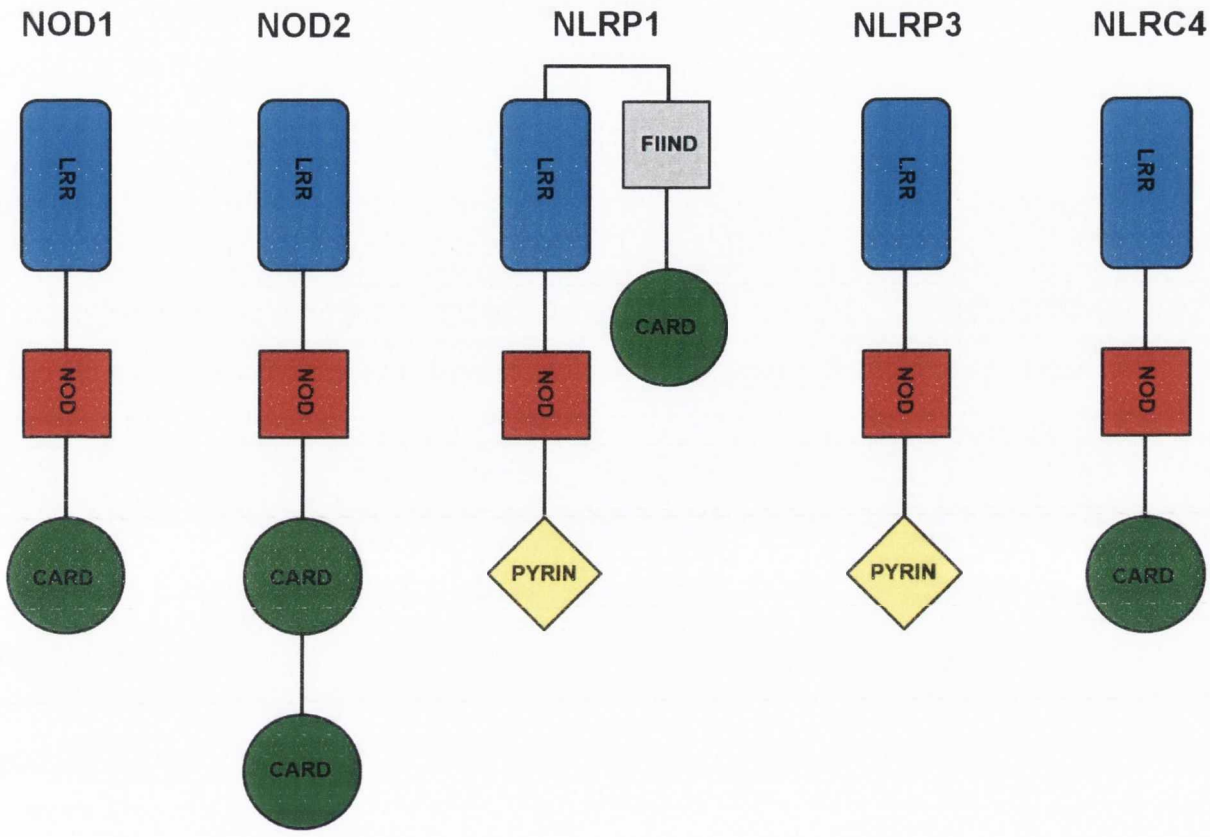

Figure 1.6 – Structure of prominent NLR family members. NLR family members all consist of a central NOD and a C-terminal LRR domain. NOD1 and NLRC4 both express a single N-terminal CARD, whereas NOD2 expresses two N-terminal CARDs. NLRP1 and NLRP3 both possess an N-terminal pyrin domain, but NLRP1 also expresses a C-terminal extension which includes a FIIND domain and a CARD.

The mechanism underlying inflammasome activation is unclear. NLRs, like TLRs, possess a C-terminal LRR domain and have been hypothesised to directly recognise cytosolic ligands using this domain [256]. However, inflammasome activators range from particulates to ATP and are hugely diverse in structure. Therefore, it is unlikely that inflammasomes sense such a broad spectrum of structurally distinct molecules using only a single recognition domain. However, it is conceivable that inflammasome activation is mediated by a single stimulus generated by all of these molecules.

NLRP3 inflammasome activation by particulates such as silica, asbestos, MSU, CPPD and alum requires uptake of these activators by phagocytosis [257]. Furthermore, this process also requires lysosomal disruption following uptake and release of cathepsin B which is believed to induce inflammasome activation [257]. However, pore-forming toxins do not require uptake into the cell to initiate inflammasome activation [258]. Moreover, phagocytosis is not required for ATP-mediated NLRP3 activation and instead involves ATP binding to the P2X7 receptor and triggering the assembly of a pannexin pore [256, 259]. One event that is required for inflammasome activation and is mediated by particulates, pore-forming toxins, ATP and all other known activators is potassium efflux, although its precise role has yet to be defined [242, 244, 260-263]. The production of reactive oxygen species (ROS) is another event common to many inflammasome activators and ROS have been shown to be important for inflammasome activation [244, 264-265], possibly through activation of the ROS-sensitive molecule thioredoxin-interacting protein (TXNIP) [266]. Despite these recent advances, the processes driving inflammasome activation remain a focal point of research interest.

1.8 - The Danger Model

There are a number of ambiguities, unanswered questions and perceived deficiencies associated with the concept that the immune system responds simply to 'foreigness'. For example, why do we not generate immunity against many antigens unless an adjuvant is co-administered? Why do we not respond to commensal bacteria or food antigens in the GI tract? Why does the immune system fail to eliminate tumours known to express tumour-specific antigens? Why are liver transplants rejected less vigorously than heart transplants? Why do we generate autoimmunity? Moreover, our bodies are constantly changing through puberty, pregnancy and ageing. Indeed, 'self' changes throughout life. Why do mammalian females not mount immune responses against their foetuses or the male sperm responsible for fertilisation? Moreover, why do these females fail to respond to newly lactating breasts that produce milk proteins not previously expressed?

Indeed, Janeway's stranger model and the concept that we respond only to infectious nonself rather than simply to anything that is foreign can account for some of these ambiguities. For example, foetuses, sperm, food and milk antigens, tumours and peripheral antigens associated with puberty and ageing are foreign entities not usually associated with microbes, and therefore the stranger model can provide an explanation for the failure of the immune system to generate responses against these entities. However, transplant rejection is characterised by a potent immune response against a foreign body in the apparent absence of microbes. The stranger model cannot account for this scenario. Furthermore, we generally fail to generate immunity against commensal bacteria, yet these bacteria are known to express PAMPs capable of stimulating activation of innate immune sentinel cells. Thus, in this setting we fail to respond to molecules that the stranger model defines as infectious. Finally, why do we develop autoimmunity in the absence of microbial infection?

In 1994, in order to address the ambiguities associated with the stranger model, Polly Matzinger proposed the danger model. This model postulates that the immune system responds specifically to molecules associated with dangerous situations rather than those simply recognised as infectious or foreign (Figure 1.7). More specifically, stressed, injured or dying cells associated with infection or mechanical stress such as trauma are hypothesised to release specific endogenous molecules into the extracellular milieu following loss of membrane integrity. These endogenous molecules, referred to as 'danger signals', 'alarmins' or 'damage-associated molecular patterns (DAMPs)', can activate APCs and induce robust innate and adaptive immune responses. Healthy cells retain membrane integrity and therefore do not release endogenous danger signals, thus failing to activate the immune system. Essentially, Matzinger proposes that the host tissue is in control of the immune system and functions as the master regulator of both innate and adaptive immunity. The danger model encompasses the idea that microbes that reside in mammalian host tissues but do not cause tissue destruction will be tolerated by the host, whereas microbes that induce tissue damage and release of danger signals will be rapidly eliminated [267].

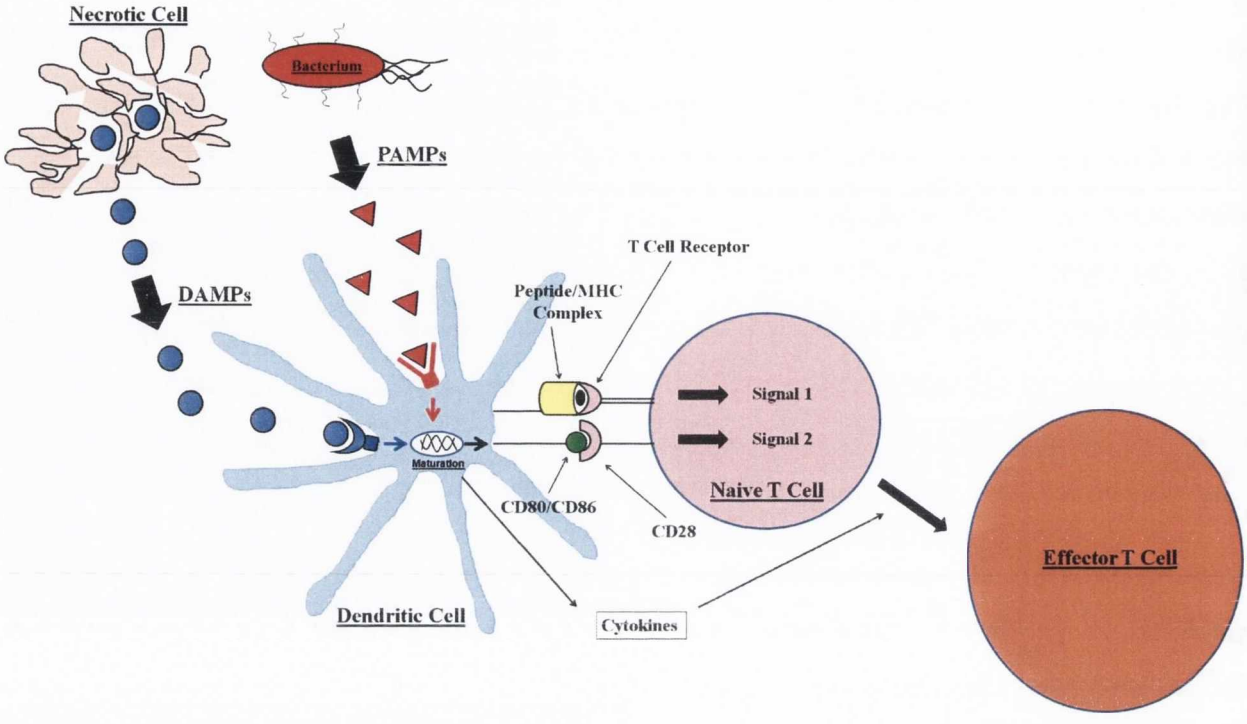

Figure 1.7 – The stranger model versus the danger model. The stranger model postulates that APCs express PRRs that recognise evolutionarily conserved PAMPs present on microbial invaders. In marked contrast to this, the danger model hypothesises that APCs sense potentially harmful situations through recognition of endogenous danger signals, or DAMPs, released into the extracellular milieu by damaged or necrotic cells following tissue injury. These molecules are recognised by DAMP receptors present on the surface of APCs such as DCs. Interestingly, the identity of some of these DAMP receptors may overlap with PRRs. Both the stranger and danger models of immune recognition postulate that following recognition of PAMPs or DAMPs, an immature DC upregulates surface expression of costimulatory molecules. The mature DC migrates to the regional lymph node where it presents MHC-bound peptide to naive T cells in the presence of costimulation, thus leading to the onset of adaptive immunity. Importantly, DCs can also secrete cytokines in response to PAMPs and DAMPs that can polarise the adaptive immune response.

The danger model can explain occurrances which contradict the stranger model. For example, Matzinger's model can account for transplant rejection in the absence of microbial stimuli. Transplants cannot be performed without surgical or ischemic damage, thus initiating release of endogenous danger signals which results in immune activation and destruction of the transplanted organ. Furthermore, commensal bacteria do not cause tissue damage and in fact share a symbiotic relationship with mammalian hosts, thereby explaining host tolerance to these bacteria. The danger model also proposes that autoimmunity occurs as a result of defective phagocytic clearance of dead cells. Thus, the immune system is functioning as normal by responding to danger signals, but in this case to the detriment of the host [268].

The danger model is now becoming more than just a hypothesis. Following initial scepticism, experimental evidence is now accumulating in support of this theory, thus making Matzinger's danger model a reality. The danger model can function either exclusively or in tandem with Janeway's stranger model. Some of the experimental evidence supporting the danger model includes the discovery of the immunogenic potential of dead cells and also the identification of a number of endogenous danger signals, including high mobility group box (HMGB)1 and uric acid.

1.8.1 - Necrotic cells

One of the earliest and most important reports demonstrating the immunostimulatory activity of dead cells was performed by Gallucci and Matzinger in 1999. This landmark study first investigated whether healthy syngeneic fibroblasts, or those rendered necrotic or apoptotic, could stimulate DC maturation. Interestingly, necrotic cells induced DC maturation while both apoptotic and healthy cells seemed to reduce the number of activated DCs below control levels. Gallucci and Matzinger speculated that this calming effect may have been achieved through secretion of anti-inflammatory cytokines by apoptotic and healthy fibroblasts, although this hypothesis was not tested any further. OVA was co-injected subcutaneously into mice at the base of the tail together with healthy, necrotic or apoptotic fibroblasts. One week later, these mice were challenged with OVA injected intradermally into the footpad and 48 hours later the DTH response was measured. In support of the *in vitro* data generated previously, necrotic cells were potent adjuvants, while apoptotic cells were particularly inefficient and the low levels of priming they did achieve was hypothesised to be a direct result of contaminating necrotic cells present in the preparation [269].

Necrotic cells undergo a non-programmed form of cell death which is characterised by loss of membrane integrity, thus facilitating the release of endogenous danger signals. However, apoptotic cells undergo a tightly regulated form of cell death in which membrane integrity is retained, thereby preventing the release of endogenous immunomodulators into the extracellular milieu (Figure 1.8). A subsequent study using co-injection of fluorescent microspheres and necrotic cells concluded that necrotic cells can also enhance migration of DCs into secondary lymphoid organs [270].

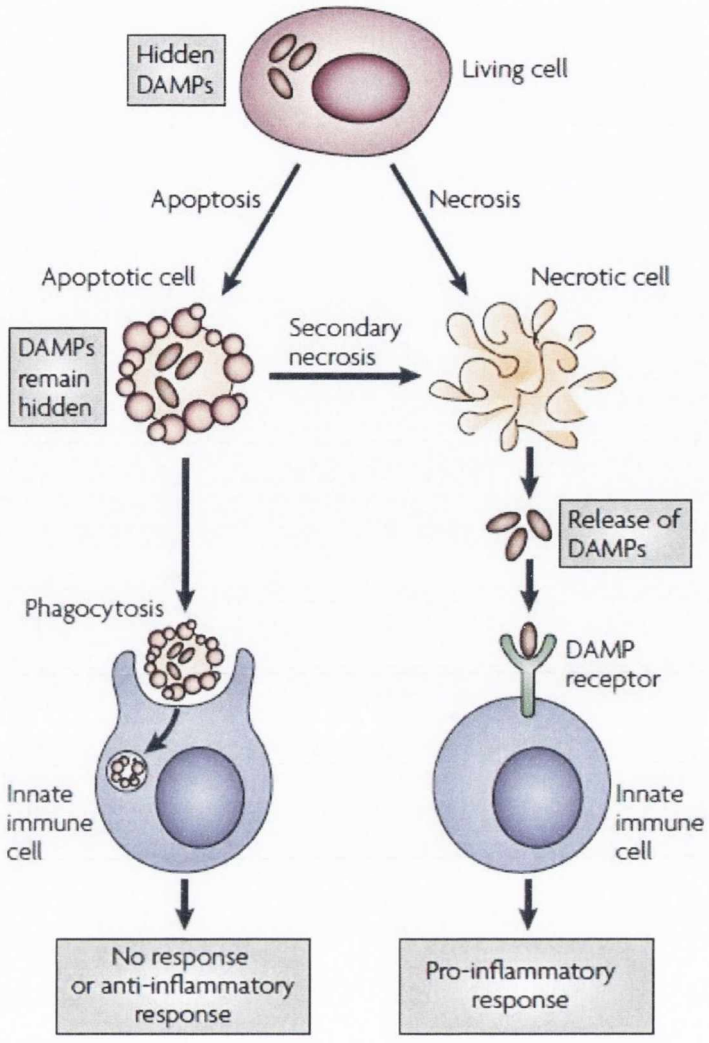

Figure 1.8 – The immunogenicity of necrotic and apoptotic cells. Viable cells contain endogenous DAMPs which are normally sequestered within the the cell. However, during necrosis, membrane integrity is lost and these endogenous immunomodulators are passively released into the extracellular environment where they are sensed by innate immune sentinels such as DCs. Following recognition of DAMPs, innate immune cells initiate a proinflammatory response characterised by expression of cytokines and chemokines. In contrast to necrosis, apoptotic cells retain membrane integrity and therefore fail to release intracellular DAMPs. Innate immune cells engulf apoptotic cells by phagocytosis and subsequently mediate an anti-inflammatory response. Importantly, apoptotic cells can undergo secondary necrosis if they are not efficiently phagocytosed. Secondary necrotic cells lose membrane integrity and drive similar proinflammatory responses to primary necrotic cells. Figure from [271].

Importantly, cells rendered instantly necrotic by freeze-thawing still induce robust inflammation [272] and possess adjuvant activity when injected *in vivo* [269]. This observation suggests that the alarmin properties of necrotic cells are derived from constitutively expressed pre-existing cellular molecules released by a process not requiring energy.

The receptors involved in mediating immune responses to necrotic cells have not yet been fully elucidated. Levy and collaborators reported a crucial role for TLR4 in the sterile inflammatory response to trauma in the context of bilateral femur fracture. More specifically, TLR4-defective C3H/HeJ mice demonstrate reduced systemic inflammation compared to wild-type mice as measured by serum levels of IL-6 and IL-10 [273]. These results were supported by work carried out by Chen *et al.* who showed that mice deficient in both TLR2 and TLR4 generated a weaker inflammatory response than wild-type mice when injected with dead cells. However, the author's noted that this reduction was very modest indeed. Furthermore, there was no significant reduction in the inflammatory response to necrotic cells in mice lacking any of the other TLRs tested. Interestingly, IL-1 was shown to be important for this inflammatory response, although mainly as a secondary mediator produced by $CD11b^{+}$ macrophages following initial recognition of necrotic cells by receptors not including the IL-1R [272, 274].

Apoptosis is a programmed and tightly regulated form of cell death characterised by chromatin condensation and plasma membrane blebbing. This well-established process of cellular suicide primarily occurs during physiological events such as elimination of cells during normal development processes, removal of trophic factors and central and peripheral deletion of T and B lymphocytes. Ultimately, apoptosis is usually associated with homeostatic events that do not represent a dangerous situation to the host [275-276]. Thus, in these situations, an inflammatory response to apoptosis is undesirable and does not usually occur. However, Torchinsky *et al.* have shown that innate immune recognition of apoptotic cells infected with the rodent pathogen *Citrobacter rodentium* directs Th17 differentiation [85]. Moreover, apoptosis can also occur in response to viral infection. CTLs and NK cells both recognise and respond to virally infected cells in a complimentary fashion. These immune cells induce apoptosis of the virally infected target cell by secreting lethal granules containing perforin and granzymes (Section 1.4.3) [126].

Granzymes are a family of serine proteases of which there are five members in humans (A, B, H, K and M) and ten members in mice (A, B, C, D, E, F, G, K, M and N) [277]. However, it is unclear why mice have so many granzymes relative to humans. Indeed, current understanding of the

functions relating to most of the granzymes is poor, although it is clear that they promote apoptosis through proteolysis of specific protein substrates within the target cell. The important physiological role of granzymes is best outlined in studies using perforin-deficient mice. Given the crucial role of perforin in trafficking granzymes into the cytosol of the target cell, perforin deficiency results in complete loss of granzyme activity. Importantly, perforin-deficient mice have an increased risk of tumour formation and experience severe defects in their immune response to viral infections [278]. Similar to other proteases, granzymes are initially synthesised as inactive zymogens. However, these serine proteases acquire activity within cytotoxic granules when their short N-terminal domain is excised following cleavage by another protease called dipeptidyl peptidase I [279].

GzmB is the best characterised member of the granzyme family and and is one of the most abundant granzymes present in cytotoxic granules [280]. This particular serine protease cleaves substrates after aspartic acid residues [281] and has been shown to promote rapid apoptosis of target cells. Indeed, GzmB-deficient CTLs exhibit significant defects in their abilty to induce caspase activation and DNA fragmentation in target cells [133, 282], whereas GzmB-deficient mice are more susceptible to mouse cytomegalovirus [283] and ectromelia virus [284] and have a reduced ability to clear tumours [285].

Importantly, in the context of viral infection, a proinflammatory response to apoptotic cell death may in fact be beneficial. Therefore, it can be hypothesised that during CTL/NK killing, processing of intracellular constituents by granzymes, in particular GzmB, within the target cell may potentiate the proinflammatory activity of these resident molecules and thus generate more powerful danger signals. This may exacerbate proinflammatory immune responses if these danger signals are released from secondary necrotic cells prior to clearance by phagocytes. It is also conceivable that CTLs and NK cells, as well as other immune cells, may secrete granzymes into the extracellular space with the ability to process molecules released from necrotic or secondary necrotic cells. In support of the above hypothesis, circulating levels of GzmB are elevated in patients with RA and melioidosis [286-287]. Moreover, GzmB has been shown to be expressed and secreted by a wide range of proinflammatory immune cells not associated with cell killing, including pDCs [288], macrophages [289], mast cells [290], basophils [291], B cells [292], platelets [293], keratinocytes [294], articular chondrocytes [295] and breast carcinoma cells [296]. In addition, GzmB has also been shown to elicit proinflammatory activity *in vivo* as GzmB-deficient mice are less susceptible to LPS-induced mortality [297]. Given the link between GzmB and inflammation, in addition to the ability of non-cytotoxic cells to secrete this particular serine protease, it is apparent that GzmB posseses

immunostimulatory activity which is independent of its contribution to apoptosis. Therefore, GzmB is a particularly attractive candidate protease for processing endogenous molecules and modulating their immune activation capacity in a similar fashion to caspase-1-mediated processing of IL-1β [298]. Ultimately, **one of the objectives of this thesis is to identify novel GzmB substrates and to assess their inflammatory potential as danger signals.**

Indeed, a number of danger signals released directly and exclusively from damaged or necrotic cells have already been proposed. These include HMGB1, uric acid, Hsps, extracellular matrix degradation products and the endogenous cytokines IL-1 and IL-33.

1.8.2 - HMGB1

The high mobility group (HMG) proteins were discovered in 1973 in an attempt to characterise specific modulators of gene expression. This group of non-histone, chromatin-associated nuclear proteins take their name from their high mobility in electrophoretic polyacrylamide gels [299]. HMG proteins can be subdivided into three families; HMGA, HMGB and HMGN. The HMGB family consists of three members; HMGB1, HMGB2 and HMGB3, which share 80% sequence similarity but are only partially redundant. HMGB1 is expressed by almost every cell type except those lacking a nucleus (e.g. erythrocytes) [300]. Structurally, HMGB1 consists of 215 amino acid residues constituting three separate domains; two DNA-binding domains referred to as 'HMG box' A (A box) and 'HMG box' B (B box) which share only 20% homology, followed by a negatively charged C-terminal tail [301-303] (Figure 1.10). Within the nucleus, HMGB1 binds non-specifically to the minor grooves of DNA and can induce bends in the helical structure, thereby facilitating interactions between several regulatory protein complexes and DNA [304-306]. Most cells express a high copy number of HMGB1 (approximately one million molecules per cell) which illustrates the importance of this protein. Indeed, HMGB1 functions are essential for life as HMGB1-deficient mice die shortly after birth with phenotypic features including small size, ruffled and disorganised fur, long hind paws and absence of fat [307]. HMGB1 is a highly conserved protein and shares 99% sequence similarity among all mammals. In fact there are only two residue substitutions between human and rodent HMGB1 [308-309]. HMGB2 and HMGB3 are also strongly conserved proteins and are widely expressed in embryos. However, this expression is downregulated during ontogenic development and adults show a far more restricted expression pattern for HMGB2 and HMGB3 (bone marrow, lymphoid tissues and testes) [310].

In 1999, Tracey and colleagues first identified a role for HMGB1 in the immune response. In an effort to broaden the therapeutic window for treatment of sepsis and endotoxemia, they searched for late mediators of these diseases. Macrophage-like RAW 264.7 cells secreted HMGB1 16 hours after LPS stimulation. This was much later than many of the classical proinflammatory cytokines; TNF-α and IL-1 secretion peaked after 2 hours and 6 hours respectively. Furthermore, stimulation of monocyte cultures with HMGB1 induced secretion of a range of proinflammatory mediators including TNF-α, IL-1β, IL-1α, IL-1 receptor antagonist (ra), IL-6, IL-8, macrophage inflammatory protein (MIP)-1α and MIP-1β. Immunisation of mice with LPS in an endotoxemia model resulted in an increase in serum HMGB1 16-32 hours later, and significant protection against lethality was achieved after passive immunisation with anti-HMGB1 antibodies [311]. HMGB1 is a leaderless protein and is therefore not secreted via the golgi/ER pathway. Instead, HMGB1 is secreted by a non-classical pathway, similar to IL-1. This involves acetylation of nuclear HMGB1 on many of its forty-three lysine residues following stimulation with an inflammatory signal such as LPS, TNF-α or IL-1. This acetylation process induces the accumulation of HMGB1 in the cytosol and inhibits re-entry into the nucleus. Cytosolic HMGB1 is packaged by endolysosomes which subsequently fuse with the plasma membrane and mediate HMGB1 secretion into the extracellular milieu by an ATP-dependent active process [312]. Further studies have determined that apart from monocytes and macrophages, HMGB1 is also actively secreted by pituicytes [313], enterocytes, [314], DCs, NK cells [315] and hepatocytes [316].

In 2002, Scaffidi and collaborators demonstrated that proinflammatory HMGB1 can also be passively released from necrotic cells. Cells rendered necrotic by repeated cycles of freeze-thawing released nuclear HMGB1 into the supernatant and promoted secretion of TNF-α from macrophage cultures. This was in stark contrast to apoptotic cells where HMGB1 remained irreversibly bound to DNA and failed to elicit proinflammaory responses [317]. Interestingly, apoptosis has been reported to drive caspase-dependent oxidation of cysteine 106 by mitochondrial ROS within the HMGB1 B box domain which attenuates the proinflammatory capability of this protein [318]. Scaffidi and co-workers demonstrated that necrotic wild-type fibroblasts induced much higher levels of TNF-α secretion from macrophage cultures than necrotic fibroblasts deficient in HMGB1 [317].

HMGB1 has since been shown to play important roles in both innate and adaptive immunity (Figure 1.9). HMGB1 stimulation of neutrophils induces NF-κB activation and secretion of proinflammatory cytokines and chemokines [319], and also increases the migratory and adhesive function of these cells [320]. Administration of low doses of HMGB1 in mice causes fever, weight loss and

piloerection, while injection of higher doses is lethal. Interestingly, these results are also evident in LPS-resistant mice, suggesting that the *in vivo* effects of HMGB1 are not mediated by TLR4 [311]. HMGB1 administered intratracheally promotes acute lung injury characterised by neutrophil recruitment, lung edema and increased synthesis of pulmonary cytokines. Moreover, treatment of mice with anti-HMGB1 antibodies following intratracheal LPS administration reverses the symptoms of lung injury [321]. Mice that undergo bilateral femur fracture after administration of anti-HMGB1 antibodies have lower serum levels of IL-6 and IL-10 than mice that receive a control antibody, thus supporting a role for HMGB1 in the robust inflammatory response to trauma [322]. HMGB1 levels are elevated in the serum of patients with sepsis [311] and hemorrhagic shock [323], and also in the synovial fluid of patients with RA [324]. Alarmingly, serum HMGB1 levels in patients with sepsis are higher in non-survivors than in survivors [311].

Various reports have suggested that HMGB1 is also capable of regulating the adaptive immune response. According to Messmer *et al.*, HMGB1 stimulates DC maturation and secretion of cytokines [325]. Furthermore, Yang *et al.* found that HMGB1 can switch DC chemokine sensitivity from CCL5 to CCL21, thus improving the ability of DCs to migrate to secondary lymphoid organs [326]. *In vivo*, HMGB1 increases IgG antibody titres directed against soluble antigens such as OVA and also generates protective immunity against a highly tumourigenic lymphoma [327].

HMGB1 can function as a chemoattractant for a vast number of different cell types, including all inflammatory cells as well as cells which are important for wound healing and repair (e.g. fibroblasts, endothelial and smooth muscle cells) [328] (Figure 1.9). Indeed, wound healing is an important phase of the inflammatory response and HMGB1 seems to be intimately involved in this process. Mesoangioblasts, which are essentially vessel-associated stem cells, proliferate in serum-free medium containing HMGB1. Moreover, when injected into the general circulation, mesoangioblasts migrate into healthy muscle tissues where HMGB1-releasing beads have been implanted [329]. Capogrossi and co-workers have also shown that HMGB1 can promote cardiac regeneration and recovery of function following myocardial infarction [330].

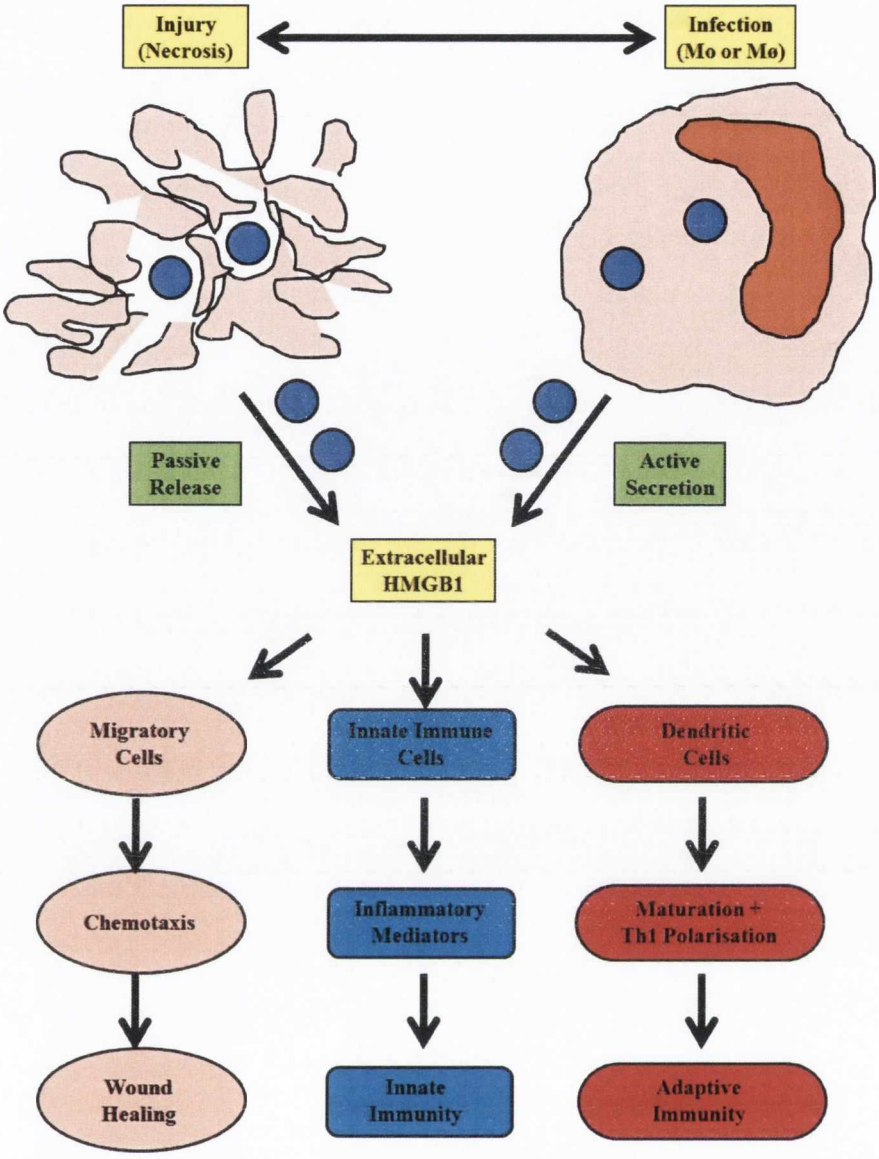

Figure 1.9 – HMGB1 mediates tissue repair and immunostimulatory functions. The nuclear protein HMGB1 can be actively secreted by immune cells such as monocytes (Mo) and macrophages (Mø) in response to stimulation with microbes or proinflammatory cytokines. However, HMGB1 can also be passively released from damaged or necrotic cells following tissue injury. Extracellular HMGB1 is involved in numerous processes, including tissue repair and immune defence. HMGB1 induces secretion of proinflammatory mediators from immune cells and can also promote DC maturation and Th1 polarisation.

Truncation studies have revealed that the B box domain is responsible for the immunomodulatory effects of HMGB1 (Figure 1.10). These observations are further supported by experiments using a chemically synthesised B box. The B box retains the TNF-α-stimulatory activity of HMGB1 in cultured monocytes and is lethal when injected into mice. Furthermore, injection of anti-B box antibodies protects against LPS-induced lethality in mice. In contrast, the A box seems to antagonise HMGB1 signalling. HMGB1-mediated TNF-α secretion by macrophage cultures is dose-dependently inhibited by the A box, and experiments showing that the A box displaces [^{125}I]-HMGB1 cell surface binding indicate that the A box competes directly with HMGB1 for binding to the HMGB1 receptor. Administration of the A box significantly increases survival in mice with cecal ligation and puncture (CLP)-induced sepsis and LPS-induced endotoxemia [331].

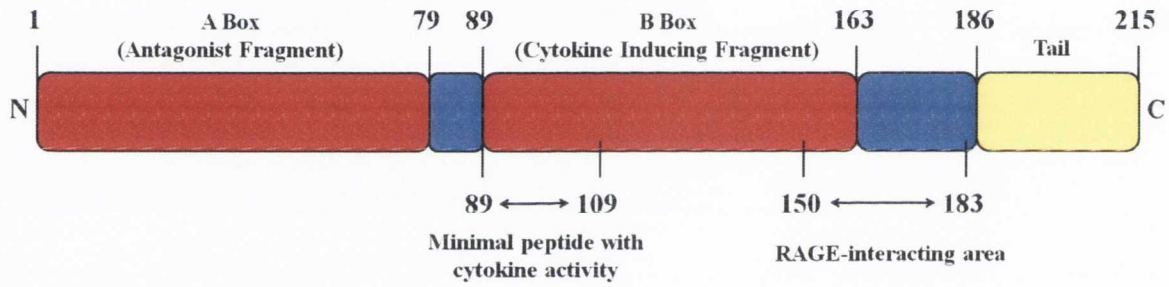

Figure 1.10 – Structure of HMGB1. HMGB1 consists of 215 amino acids comprising three separate domains; two respective DNA-binding domains (red) referred to as the A box and B box domains followed by a negatively charged C-terminal tail (green). The blue boxes do not encode functional domains. The receptor for advanced glycated end-products (RAGE)-interacting domain of HMGB1 is located between residues 150 and 183. The recombinant B box (90-176) is responsible for the immunomodulatory effects of HMGB1. The first twenty amino acids of the recombinant B box (89-109) represent the minimal peptide required for cytokine activity. In contrast, the recombinant A box (1-89) antagonises HMGB1 signalling. Figure adapted from [332].

RAGE binds HMGB1 and signals downstream to activate NF-κB and MAPK, thus inducing secretion of proinflammatory cytokines and chemokines [333-334]. RAGE is a member of the Ig superfamily which possesses three extracellular Ig domains, a transmembrane domain and a cytoplasmic segment with no homology to any other known signalling domain. RAGE is expressed at low levels by most cell types and is also known to function as a receptor for advanced glycated end-products (AGE) and S100 proteins [335]. However, ligand-binding studies have shown that HMGB1 binds RAGE with seven times greater affinity than S100 proteins or AGE [333]. Secretion of TNF-α and IL-6 following stimulation with HMGB1 was reduced in RAGE-deficient macrophages [336]. Furthermore, RAGE-deficient mice are less susceptible to sepsis [337].

Despite these observations, RAGE-blocking antibodies consistently fail to completely abrogate cellular activation in response to HMGB1 [336]. Therefore, it was hypothesised that receptors other than RAGE might be involved in responding to HMGB1. Ultimately, two members of the TLR family, TLR2 and TLR4, have been shown to play a role in HMGB1 signalling. Macrophage cell lines transfected with dominant negative constructs of TLR2 and TLR4 show decreased activation following stimulation with HMGB1 [338]. Thus, RAGE, TLR2 and TLR4 have all been implicated in HMGB1 signalling.

Recent studies have contradicted many of the above findings, however, demonstrating that a highly purified form of recombinant HMGB1 (rHMGB1) fails to induce cytokine secretion from murine or human macrophages. In contrast, rHMGB1 can still recruit cells in support of its function as a chemoattractant and can also promote tissue regeneration. Therefore, these studies propose that rHMGB1 can induce inflammation indirectly through recruitment of inflammatory cells [339]. Furthermore, the direct proinflammatory activity of HMGB1 reported previously and described above is likely to be a result of contamination with bacterial components as most of these studies were carried out using rHMGB1 derived from *Escherichia coli* (*E. coli)* expression systems. In support of this, Chen *et al.* have reported that there is no significant difference in the magnitude of the inflammatory response generated against necrotic $HMGB1^{-/-}$ cells and necrotic $HMGB1^{+/+}$ cells in a sterile peritonitis mouse model [272]. However, the conclusion that HMGB1 possesses minimal direct proinflammatory activity does not detract from other *in vivo* evidence pointing to its importance in inflammation. For example, administration of anti-HMGB1 antibodies protects against endotoxin-mediated lethality [311] as well as acute lung injury following intratracheal delivery of LPS in mice [312]. Furthermore, the inflammatory effects of trauma are partly mediated by HMGB1 [322]. *In vitro*, PAMP contamination of HMGB1 cannot account for the ability of necrotic wild-type

fibroblasts to promote higher levels of cytokine secretion from macrophage cultures than necrotic cells deficient in HMGB1 [317]. Based on these observations, many researchers now believe that HMGB1 is necessary but not sufficient to induce inflammation. In other words, HMGB1 may not function as a composer of inflammation but is an integral member of the inflammatory orchestra.

Recent reports state that the chemoattractant and proinflammatory cytokine functions of HMGB1 are in fact mutually exclusive and can be separated based on the redox state of the protein. Specifically, Venereau *et al.* demonstrate that the cytokine function of HMGB1 is dependent on three respective cysteine residues, C23 and C45 in the A box and C106 in the B box. For HMGB1 to function as a proinflammatory cytokine, C23 and C45 must form a disulfide bond whereas C106 must exist in a thiol state (disulfide-HMGB1). However, fully reduced HMGB1 containing all three cysteines in the thiol state (all-thiol-HMGB1) functions as a chemoattractant, whereas additional oxidation of cysteines to sulfonates by ROS attenuates both activities. This observation may help to explain some of the ambiguities and inconsistencies described above regarding the immunostimulatory potential of HMGB1. There is a very real possibility that different results may have been obtained by different research groups owing to the use of inconsistently defined forms of HMGB1 with regard to the oxidation state of the protein. In a cardiotoxin-induced model of muscle injury, all-thiol-HMGB1 is the dominant form of HMGB1 in the extracellular milieu immediately after necrosis, whereas disulfide-HMGB1 appears after approximately 6 hours. Venereau *et al.* therefore postulate that all-thiol-HMGB1 is released early by necrotic cells in order to promote leukocyte recruitment. Leukocytes then induce the production of disulfide-HMGB1 either directly through secretion or indirectly by oxidising extracellular HMGB1 through ROS. This is supported by the observation that THP-1 cells secrete disulfide-HMGB1 *in vitro*, whereas the form of HMGB1 found inside THP-1 cells is all-thiol-HMGB1. Finally, inflammation is resolved as HMGB1 undergoes terminal oxidation by ROS [340-341].

HMGB1 can also bind to PAMPs and other danger signals and synergise with these molecules to induce an inflammatory response greater than that generated against either component alone [342]. For example, HMGB1 specifically binds LPS by interacting with the lipid A moiety and can subsequently disaggregate LPS from bacterial membranes and deliver this PAMP to CD14 in a dose-dependent manner. Therefore, HMGB1 can act in a similar manner to LBP and can consequently increase the sensitivity of the TLR4-MD-2 complex to LPS. Indeed, monocytes stimulated with HMGB1 and LPS secrete higher levels of TNF-α than monocytes treated with LPS alone [343]. HMGB1 also forms complexes with IL-1β, IFN-γ and TNF-α which augments the

immunopotentiating capacity of these respective cytokines [344]. Furthermore, TLR9 activation is potentiated in the presence of HMGB1-DNA complexes as shown by increased production of IFN-α by bone marrow-derived pDCs in response to these complexes than either component alone [345]. Surprisingly, HMGB1 can also interact with TLR9 independently of DNA and may function as a nucleic acid sensor [346]. Interestingly, during apoptosis HMGB1 remains tightly bound to nucleosomes. However, some HMGB1 does in fact leak out of the apoptotic cell, particularly if the cell proceeds to secondary necrosis [347], and much of this released HMGB1 is complexed with nucleosomes. Recently, HMGB1-nucleosome complexes from secondary necrotic cells have been shown to activate macrophages and DCs [348]. Furthermore, mice immunised with HMGB1-nucleosome complexes develop anti-histone and anti-DNA autoantibodies, which are characteristic of the autoimmune disease systemic lupus erythematosus (SLE). RAGE-deficient mice still produce these autoantibodies, but mice lacking TLR2 or MyD88 do not [348].

A number of negative regulators of HMGB1 signalling have been identified. For example, Hsp72 overexpression in macrophages inhibits secretion of HMGB1 in response to inflammatory stimuli. This is believed to occur as a result of intranuclear interactions between Hsp72 and HMGB1 [349]. Chen and co-workers identified the CD24-Siglec pathway as another inhibitory mechanism regulating the function of HMGB1. CD24-deficient mice die rapidly in response to a sublethal dose of acetaminophen which induces liver necrosis. Proinflammatory cytokine levels (e.g. TNF-α, IL-6 and MCP-1) were elevated in the serum of these mice. Further biochemical studies proved that HMGB1 associates with CD24, and that administration of anti-HMGB1 antibodies ameliorates lethality in CD24-deficient mice. Thus, it has been proposed that HMGB1 recognition by CD24 suppresses the proinflammatory effects of the former protein. Siglec-G (Siglec-10 in humans) was also identified as a binding partner for CD24 in mice. Indeed, acetaminophen-induced inflammation was augmented in Siglec-G-deficient mice. Therefore, it is proposed that acetaminophen-induced liver necrosis results in HMGB1 release. HMGB1 subsequently promotes inflammation by initiating signalling cascades downstream of RAGE, TLR2 and TLR4, and this inflammatory process is dampened by HMGB1 interaction with CD24 and Siglec-G [350].

1.8.3 - Uric acid

Uric acid is generated from xanthine by the catabolism of purines by the enzyme xanthine oxidoreductase, and this reaction can be inhibited by the uric acid analogue allopurinol. Uric acid is

present at very high concentrations both in the cytosol of cells and in the extracellular milieu and was first identified as an endogenous danger signal by Shi *et al.* in 2003 following fractionation of the cytosol from a fibroblast cell line by high-performance liquid chromatography (HPLC). Each fraction was tested for its ability to potentiate $CD8^+$ T cell responses when co-injected with latex beads attached to the HIV protein gp120. Interestingly, both a low molecular weight fraction of less than 5 kilodaltons (kDa) and a high molecular weight fraction between 40-100kDa were shown to augment cytotoxic T cell responses to the gp120 antigen. Shi and colleagues focused exclusively on the low molecular weight fraction and quickly identified uric acid as the main component. Moreover, uric acid was shown beyond doubt to be the active component of the low molecular weight fraction when a highly purified preparation of this chemical was immunostimulatory, and uricase, an enzyme that degrades uric acid, reduced the adjuvant activity of the active fraction. The highly purified form of uric acid was also shown to promote $CD8^+$ T cell responses in TLR4-defective mice, thus ruling out the possibility of LPS contamination. *In vitro*, Shi *et al.* also reported that uric acid induced DC activation in both wild-type and TLR4-null murine bone marrow-derived DCs (BMDCs) as measured by upregulation of costimulatory molecules. Surprisingly, uric acid stimulated DC maturation even more potently than LPS. Interestingly, the active component of the high molecular weight fraction with adjuvant activity identified in this experiment remains unknown.

Shi and colleagues also showed that uric acid is biologically active only when it forms microcrystals called MSU crystals. This may seem surprising but is in fact an evolutionary masterstroke by the immune system. Uric acid is present in the extracellular fluid at near-saturating concentrations and if the immune system were to recognise this compound directly then it would constantly promote inappropriate responses, causing extensive collateral damage to the detriment of the host. However, the near-saturating levels of uric acid in the extracellular fluid become excessive and begin to crystallise when intracellular uric acid is released by necrotic cells and comes into contact with the high levels of free sodium in the extracellular milieu, thus leading to MSU crystal formation which alerts the immune system to a potentially dangerous situation [351].

Gout is an acute form of arthritis characterised by spontaneous periodic inflammation in joints and periarticular tissues of individuals with hyperuricemia. MSU crystals were first linked with gout over 200 years ago and were shown to contribute to the pathogenesis of this disease in 1899. However, it is only in recent years that the mechanisms underlying MSU crystal-induced gouty inflammation have been unravelled to some extent. In 2006, Martinon *et al.* demonstrated that MSU crystals can activate the NLRP3 inflammasome, thus promoting IL-1β secretion and subsequent inflammation

[246]. At the same time, Chen *et al.* were able to show that when injected into the peritoneal cavity of mice, the ability of MSU crystals to promote gouty inflammation was compromised in the absence of the IL-1R. Specifically, neutrophil recruitment was reduced by approximately 85% and this was accompanied by a decrease in neutrophil chemoattractants KC and MIP-2, as well as IL-1β. However, it was shown that MSU crystals do not signal directly through the IL-1R. Rather, these crystals stimulate $CD11b^+$ macrophages to produce IL-1 via an unknown mechanism, possibly NLRP3 inflammasome activation, although the IL-1R does not seem to be involved in this initial synthesis of IL-1. However, the IL-1R is important on non-hematopoietic cells which appear to bind IL-1 and respond by secreting a plethora of neutrophil chemoattractants. However, the identity of the key target cell of IL-1 remains elusive [274, 352].

MSU crystal-induced gouty inflammation is not reduced in the absence of TLRs [352]. Indeed, this study disproves earlier reports that uric acid stimulates robust inflammation through TLR2 and TLR4 [353]. Despite extensive research, an MSU-specific receptor has yet to be identified. However, Shi *et al.* have demonstrated that similarly to alum, MSU engages cholesterol in the plasma membrane of DCs and induces lipid sorting [354]. Another source of MSU-induced inflammation is through the activation of both the classical and alternative complement pathways to yield C3a and C5a, as well as membrane attack complexes [355-357].

Using Tg mice which have reduced intracellular and/or extracellular uric acid levels, Kono *et al.* have only recently confirmed that uric acid is indeed an important danger signal in promoting cell death-induced inflammatory responses *in vivo*. Acetaminophen-induced inflammation in the liver, as measured by myeloperoxidase activity, was markedly decreased in Tg mice compared to wild-type mice. Similar results were achieved following i.p. injection of recombinant uricase and also by blocking synthesis of uric acid using allopurinol [358].

In summary, uric acid appears to be a genuine endogenous danger signal with immunostimulatory activity *in vivo* completely independent of PAMP contamination.

1.8.4 - Hsps

Hsps are evolutionarily highly conserved chaperone molecules found in all prokaryotes and eukaryotes. Hsps facilitate folding of nascent polypeptides and are responsible for protein protection from denaturation or aggregation and transport through membrane channels. Hsps can be divided

into ten families, with each family consisting of between one and five closely related members which are either constitutively expressed or upregulated under stressful conditions. Structurally, Hsps are comprised of an adenine nucleotide-binding domain that binds and hydrolyses ATP, and a peptide-binding domain that binds hydrophobic residues exposed by target proteins.

Hsps have been postulated to be immunostimulatory for many years, both in cross-presentation of antigen and also directly as endogenous danger signals. Indeed, Hsps were the first large family of endogenous danger signals identified and are released by stressed, infected, necrotic and tumour cells, thus meaning that Hsps become accessible to innate immune sentinel cells in the extracellular environment during dangerous situations. However, as we will see below, the function of Hsps as alarmins acting directly on the immune system remains unclear owing to potential PAMP and more specifically endotoxin contamination.

In 1986, Srivistava and colleagues demonstrated the immunogenic potential of Hsps when they reported that immunisation of mice with tumour-derived glycoprotein (gp)96 resulted in specific antitumour immunity sufficient for tumour rejection [359]. Interestingly, various other Hsps including cytosolic Hsp70 and Hsp90 were also shown to have immunostimulatory potential. Furthermore, subsequent studies proved that Hsps were able to prime specific antitumour immunity because of their ability to bind tumour-derived antigenic peptides and target these peptides to APCs [360-361]. APCs have since been shown to internalise Hsp-peptide complexes by receptor-mediated endocytosis in a process dependent on CD91 [362-363]. This facilitates transport of the antigenic peptides into the MHC I presentation pathway, thus initiating CTL responses [360-361].

Hsps have also been shown to act directly on the immune system as danger signals independently of their ability to bind peptides. Hsp60, Hsp70, Hsp90 and gp96 have all been shown to possess immunostimulatory potential in a significant number of different studies. All of the aforementioned Hsps have been reported to stimulate DC activation as measured by maturation and secretion of proinflammatory cytokines such as IL-1, IL-6, IL-12 and TNF-α [364-367], and also to induce macrophage activation [366, 368-370]. Cohen-Sfady and colleagues claim that Hsp60 can promote B cell proliferation, upregulation of costimulatory molecules and also secretion of IL-6 and IL-10 [371], while Multhoff *et al.* have shown that Hsp70 can stimulate proliferation and cytolytic activity of NK cells [372]. The effects of Hsp60, Hsp70 and gp96 are mediated predominantly by TLR4, although a role for TLR2 has also been proposed [367, 373-374]. TLR4-defective APCs derived from C3H/HeJ mice fail to respond to Hsp60 [375], Hsp70 [376] or gp96 [367]. Interestingly, these

Hsps have been shown to activate NF-κB in a MyD88 and TRAF6-dependent manner [367, 373-374], similar to the signalling cascade initiated by recognition of LPS.

Interestingly, studies using Hsps purified from eukaryotic tissue also provide support for these molecular chaperones as danger signals. Hsp70, Hsp90 and gp96 purified from human liver stimulate DC and macrophage activation [365, 377]. Furthermore, Hsp60 can induce the secretion of IFN-α which is important for enhanced T cell activation [378-379].

The fact that Hsps and LPS share the same receptor and downstream signalling cascade in innate cells has been met with much scepticism, and it is becoming increasingly evident that the alarmin properties of Hsps are in fact mediated by endotoxin contamination. Many of the studies that propose immunostimulatory functions for these proteins use recombinant Hsps derived from *E. coli* expression systems which may have contained residual contaminating LPS. Moreover, control studies used to eliminate the possibility of LPS contamination in these samples have since been shown to be inefficient and unsuitable. These controls include use of the limulus amoebocyte lysate chromogenic endpoint (LAL) assay to determine contaminating LPS concentrations, use of the antibiotic polymyxin B (PmB) to sequester LPS and prevent interaction with TLR4, and the use of heating to inactivate proteins but not LPS. However, the LAL assay is rendered ineffective in the presence of molecules that bind LPS. For example, LBP completely inhibits the ability of LAL to detect LPS [380]. The LAL assay also fails to detect lipopeptide contaminants which is a serious concern since various studies have elucidated a role for TLR2 in response to Hsps. PmB fails to eliminate the possibility of LPS contamination as this antibiotic does not completely inhibit the signalling of LPS-contaminated Hsps [381], raising the possibility that molecules capable of binding to LPS significantly reduce the efficacy of LPS sequestration by PmB. This theory is supported by the observation that PmB fails to completely inhibit LPS signalling in the presence of soluble CD14 [382]. Finally, relying on the heat resistant properties of LPS to rule out contamination is also a fallible control resulting in hugely misleading conclusions. Indeed, for a long time researchers have boiled protein preparations assuming that the subsequent loss of immunostimulatory activity proved the absence of contaminating LPS as this PAMP was believed to be heat resistant. However, in 2003, Gao and colleagues demonstrated that LPS is in fact heat-sensitive [383].

DC activation is commonly used as a measure of the immunomodulatory potential of candidate exogenous and endogenous molecules. However, candidate danger signals are commonly purified from bacterial expression systems, particularly *E. coli*, and are frequently contaminated with

bacterial PAMPs, especially LPS. Residual LPS contamination is a recurring theme and the potency of LPS is not always fully appreciated. To address this, PmB is often used to neutralise contaminating LPS. However, the limited capacity of this antibiotic to successfully block these effects is neglected. **Therefore, the first objective of this work is to determine the minimum LPS concentration required to induce murine BMDC maturation and cytokine secretion and to assess the ability of PmB to inhibit these processes.**

In support of the scepticism surrounding Hsps and the controls used to address the issue of LPS contamination, Wallin and colleagues noted that highly purified murine liver Hsp70 failed to stimulate cytokine secretion from murine DCs even at concentrations as high as 300 micrograms per millilitre (μg/ml). In contrast, a Hsp70 preparation contaminated with tiny levels of LPS induced cytokine secretion at concentrations as low as 50 nanograms (ng)/ml, and these effects were not inhibited by PmB and were also heat-sensitive [384]. In recent years, many reports have been published which consistently outline the failure of highly purified Hsp molecules to stimulate immune responses in the absence of contaminating PAMPs. Following on from the work of Wallin *et al.* [384], Bausinger and colleagues demonstrated that highly purified recombinant human Hsp70 could not activate DCs [385], Gao *et al.* proved that the ability of commercially available recombinant human Hsp60 [381] and Hsp70 [383] to induce TNF-α production in macrophages was completely LPS-dependent, while Reed *et al.* reported that gp96-induced activation of NF-κB was also LPS-mediated [386]. Significantly, these reports all confirmed that the Hsp under investigation retained its molecular chaperone function following the rigorous purification procedures. Thus, the lack of immunostimulatory activity displayed by these molecules was not due to denaturation or loss of function.

Another layer of complexity in the Hsp story is added by the finding that Hsps can specifically bind LPS and augment LPS-induced responses *in vitro*. In 1999, Hsp70 and Hsp90 were shown to specifically bind LPS [387], and soon after human and murine Hsp60 were reported to do the same. Importantly, an Hsp60 epitope responsible for LPS binding was identified, and antibodies specific for this epitope disrupted binding of Hsp60 to LPS [388]. Soon after, a report emerged documenting that when purifying gp96, fractions containing gp96 always contained much higher levels of LPS than fractions lacking gp96, thus ascribing an LPS-binding role for gp96 which was later shown to be dependent on the N-terminal domain of the protein [389]. Hsp binding to LPS serves to augment LPS-mediated responses *in vitro*, thus potentiating the potency of this molecule. For example, LPS-induced secretion of TNF-α by macrophages is enhanced significantly in the presence of

recombinant Hsp60 and recombinant Hsp70 in a process entirely dependent on pre-incubation of Hsps with LPS, and thus complex formation [390]. Stimulation of DCs with LPS in the presence of gp96 also elicits synergistic effects as evidenced by an increase in costimulatory molecules as well as IL-6 and IL-12 secretion compared to LPS alone. This effect is dependent on the N-terminal LPS-binding domain of gp96 [389]. Based on these results, it is conceivable that Hsps may function in a similar manner to LBP and therefore increase the sensitivity of the immune system to Gram-negative bacterial infection by binding LPS and stimulating robust immune responses via TLR4. However, to date there are no reports of Hsps bound to LPS in the circulation.

In order to truly establish the importance of Hsps as endogenous danger signals, it will be necessary to test the effect of eliminating individual Hsps on the adjuvanticity and inflammatory potential of dead cells. However, this feat will be very difficult to achieve considering the large number of intracellular Hsps. Furthermore, given the crucial functions of these molecular chaperones, cells lacking particular Hsps may not be viable.

1.8.5 - Extracellular matrix constituents

There is evidence supporting an alarmin function for several extracellular matrix constituents. For example, fibronectin can promote chemotaxis for fibroblasts [391], endothelial cells [392], neutrophils and monocytes [393]. It has also been reported by Gondokaryono *et al.* that the extra domain A of fibronectin (FN-EDA) can stimulate bone marrow-derived murine mast cells (BMMCs) to secrete TNF-α, IL-6 and IL-1β in a TLR4-dependent manner and can also induce joint swelling *in vivo* [394]. Fibrinogen stimulates DC maturation [395] as well as cytokine and chemokine secretion by mononuclear cells [396-397], whereas biglycan promotes the release of TNF-α and MIP-2 from macrophages in a TLR2 and TLR4-dependent fashion. Elastin and collagen-derived peptides have both been linked with chemotaxis for neutrophils and monocytes [398-400], and elastin-derived peptides can stimulate DC maturation [401]. However, the glycosaminoglycans heparin sulfate and hyaluronic acid as well as the gp tenascin-C are the most well-established and best characterised danger signals within the extracellular matrix.

1.8.5.1 – Heparan sulfate and hyaluronic acid

Heparan sulfate and hyaluronic acid are glycosaminoglycans that form part of the extracellular matrix. Heparan sulfate is a polysaccharide which occurs as a proteoglycan and is ubiquitously distributed on cell surfaces and extracellular matrices. Hyaluronic acid is a polysaccharide not found as a proteoglycan but is distributed extensively in connective, epithelial and neural tissues. The degradation products of both heparan sulfate and hyaluronic acid have been shown to function as danger signals.

Injection of mice with heparan sulfate breakdown products results in robust systemic inflammation [402]. *In vitro*, Kodaira have reported that heparan sulfate degradation products stimulate DC activation as characterised by phenotypic maturation, reducted antigen uptake, increased allostimulatory capacity and secretion of IL-1, TNF-α and IL-6 [403]. These immunostimulatory effects are mediated by TLR4 [404]. Hyaluronic acid fragments induce activation of DCs and endothelial cells *in vitro* [403, 405] and stimulate chemokine expression when injected *in vivo*, particularly MIP-2 and KC [405]. Furthermore, small breakdown products of hyaluronic acid also possess adjuvant activity as shown by their ability to augment OVA-specific T cell responses *in vivo* [406]. Recently, Campo *et al.* demonstrated that these fragments also synergise with LPS to potentiate cytokine secretion by murine chondrocyte cultures [407]. Hyaluronic acid is known to bind to CD44 but this receptor does not seem to be important for the immunostimulatory activity of hyaluronic acid breakdown fragments as these responses are intact in CD44-deficient mice [408]. Consequently, many studies have reported a role for TLR4 [405, 409] and to a lesser extent TLR2 [406] in regulating the alarmin activity of these fragments. Despite these encouraging studies describing alarmin activity for degradation products of heparan sulfate and hyaluronic acid, caution must be warranted given that these molecules signal through TLR4, a receptor notorious for signalling in response to LPS contamination. These concerns are heightened by the finding that highly purified pharmacological-grade hyaluronic acid fragments fail to induce NF-κB activation or cytokine secretion in murine macrophages [410].

1.8.5.2 – Tenascin-C

Tenascin-C (encoded by Tnc) is an extracellular matrix gp with alarmin properties. This gp consists of an oligomerisation domain, epidermal growth factor-like repeats, fibronectin type III-like repeats

and a fibrinogen-like globe (FBG) [411]. In most healthy adult tissues, very little tenascin-C is expressed. However, expression of this glycoprotein is transiently upregulated during acute inflammation and is persistently elevated in chronic inflammation [412]. In 2009, it was demonstrated that tenascin-C is capable of sustaining inflammation in arthritic joint disease. Using a methylated bovine serum albumin (BSA)-induced mouse model of erosive arthritis similar to human RA, Midwood *et al.* reported no significant difference in cell infiltration or synovial thickening between wild-type and $Tnc^{-/-}$ mice after 24 hours. However, $Tnc^{-/-}$ mice were protected from sustained inflammation and joint destruction over the course of 7 days. Thus, tenascin-C does not appear to initiate joint inflammation but does seem to play a crucial role in maintaining this process. Midwood *et al* have also reported that the immunostimulatory activity of tenascin-C is restricted to the FBG domain and is mediated by TLR4. FBG is capable of inducing proinflammatory cytokine release from synovial membrane cultures from patients with RA, and can also upregulate secretion of IL-6, IL-8 and TNF-α by primary human macrophages and IL-6 synthesis in synovial fibroblasts. In addition, intra-articular injection of wild-type mice with FBG promotes joint inflammation. Interestingly, FBG and LPS have different co-receptor requirements as FBG-mediated cytokine production is independent of both CD14 and MD-2 [413]. However, Kanayama *et al.* have also reported a role for α_9-integrin in the activation of myeloid cells by the third fibronectin type III-like repeat of tenascin-C [414].

Using an experimental sepsis model, Piccinini *et al.* have shown that tenascin-C also plays a key role in regulating the inflammatory response to LPS *in vivo*. Circulating levels of tenascin-C were elevated in wild-type mice following injection with LPS, peaking after 90 minutes. Moreover, septic $Tnc^{-/-}$ mice exhibited lower levels of circulating TNF-α compared to wild-type mice. However, this effect was reversed following allogeneic transplantation of bone marrow from wild-type mice. Interestingly, $Tnc^{-/-}$ mice failed to produce HMGB1 in response to LPS, thus suggesting that tenascin-C modulates LPS-induced TLR4 signalling upstream of both TNF-α and HMGB1. Following stimulation with LPS, $Tnc^{-/-}$ bone marrow-derived macrophages (BMDMs) secreted supoptimal levels of TNF-α and significantly increased levels of IL-10 compared to wild-type BMDMs, thereby exhibiting an anti-inflammatory phenotype. However, there was no significant difference in the expression of TNF-α or IL-6 mRNA between wild-type and $Tnc^{-/-}$ BMDMs, thus suggesting that tenascin-C regulates LPS-induced cytokine synthesis at a posttranscriptional level. Importantly, LPS potently induced microRNA (miR)-155 expression in wild-type BMDMs, an effect which was inhibited in $Tnc^{-/-}$ BMDMs. There was also a positive correlation between expression of

miR-155 and secretion of TNF-α, with LPS-stimulated $Tnc^{-/-}$ BMDMs expressing low levels of miR-155 and secreting suboptimal levels of TNF-α. Moreover, TNF-α secretion by LPS-stimulated $Tnc^{-/-}$ BMDMs was restored by overexpressing miR-155, thereby confirming that tenascin-C modulates LPS-induced secretion of TNF-α by upregulating expression of miR-155. However, it is not yet known how tenascin-C modulates miR-155 expression [415].

According to Ruhmann *et al.*, tenascin-C also has an important function in polarising the adaptive immune response. BMDCs derived from wild-type and $Tnc^{-/-}$ mice were stimulated with LPS and co-cultured with $CD4^+$ T cells isolated from the spleen and lymph nodes of wild-type mice. Interestingly, wild-type and $Tnc^{-/-}$ BMDCs induced similar levels of IFN-γ, IL-5 and IL-10 secretion by $CD4^+$ T cells, but $Tnc^{-/-}$ BMDCs were less effective in their abilty to promote IL-17 synthesis. Furthermore, in a methylated BSA-induced mouse model of erosive arthritis, wild-type mice exhibited a significant increase in IL-17 in the knee joint which was absent in $Tnc^{-/-}$ mice. This trend was also evident when measuring levels of the Th17 polarising cytokines IL-6 and IL-23 [416]. Ultimately, tenascin-C seems to play a crucial role in polarising Th17 responses which have been shown to contribute significantly to the pathogenesis of RA [417].

Tenascin-C is an example of a model danger signal which is beyond repute. There is convincing and robust *in vitro* and *in vivo* data to support its claim of being a bona fide alarmin capable of mediating both innate and adaptive immunity and modulating the inflammatory profile of various pathogenic conditions. However, as mentioned previously this is not always the case with endogenous danger signals, which ultimately raises an important point. Many of these novel immunostimulatory molecules, including the flagship danger signal HMGB1, tell contradicting stories and are never far from the issue of TLR4 dependency and thus LPS contamination. It seems fair to conclude that contamination is a serious concern with regard to reports in the literature ascribing immunostimulatory activity to danger signals *in vitro*. However, LPS contamination certainly cannot account for the immune activation capacity of many of these molecules *in vivo*. Indeed, *in vivo* data supporting a number of danger signals is very strong and certainly confirms the existence of these endogenous immunomodulators. It is also important to note that the TLR4 dependency of various danger signals *in vivo* is not necessarily a major concern as TLR4 is likely to have numerous functions and ligands *in vivo* which are distinct from its ability to recognise and respond to LPS. Ultimately, it is important to note that although much scepticism surrounds the immunostimulatory activity of danger signals *in vitro,* there is little doubt that these endogenous molecules have significant credibility *in vivo*.

1.8.6 - IL-1 and IL-33

The IL-1 superfamily consists of eleven members: IL-1α, IL-1β, IL-1ra, IL-18, IL-33, IL-36α, IL-36β, IL-36γ, IL-36ra, IL-37 and IL-38 [418]. Each of the respective IL-1 family members share a conserved C-terminal IL-1-like cytokine domain that facilitates folding of the protein into a 12-stranded β-barrel conformation [419] (Figure 1.11). IL-1α, IL-1β, IL-18, IL-33, IL-36α, IL-36β and IL-36γ have all been reported to be proinflammatory, whereas IL-1ra, IL-36ra and IL-37 elicit anti-inflammatory effects on the immune system [420]. The function of IL-38 remains unknown, although it shares homology with IL-1ra and IL-36ra and has been shown to bind to the IL-1R [421]. Interestingly, only IL-1ra possesses a classical signal peptide and is secreted via the ER/Golgi pathway. The mechanism of secretion for all other members of the IL-1 family remains unclear.

It has been proposed that the potent proinflammatory cytokines IL-33 and IL-1α can be considered as endogenous danger signals. IL-1 is a classic example of an inducible danger signal produced during early stages of infection or sterile injury. IL-1 is produced in two different forms, IL-1α and IL-1β, which bind and signal through the same IL-1R complex [422]. IL-1β is mainly produced by monocytes and macrophages whereas IL-1α production is more diverse and is expressed by immune cells as well as resident tissue cells such as keratinocytes and endothelial cells [423]. Both IL-1α and IL-1β lack classical leader peptide sequences and are therefore not secreted by the ER and Golgi apparatus [298, 424]. IL-1β is synthesised as a 31kDa precursor molecule (pro-IL-1β) that cannot bind the IL-1R and is therefore biologically inactive [298, 424]. However, as discussed in Section 1.7.4, pro-IL-1β acquires biological activity following processing into a 17kDa mature form by caspase-1 [298], thus eliciting a wide range of immunostimulatory effects such as fever [425]. Specifically, caspase-1 processes human IL-1β at aspartic acid (Asp)116 [426] (Figure 1.11).

IL-1α is also synthesised as a 31kDa precursor molecule. However, in contrast to pro-IL-1β, full-length IL-1α can bind the IL-1R and is biologically active [298, 424]. IL-1α is predominantly cell-associated and a portion of this cytokine localises to the plasma membrane [427]. However, IL-1α also contains an N-terminal nuclear retention sequence (NRS) and possesses transcriptional transactivating activity which can modulate gene expression and promote cell survival [428]. Full-length IL-1α is susceptible to cleavage by calpain which is a membrane-bound cysteine protease that requires calcium. Calpain processes human IL-1α at phenylalanine (Phe)118 and yields an 18kDa processed form of this proinflammatory cytokine (Figure 1.11). However, in marked contrast to IL-1β, processing of full-length IL-1α reportedly has minimal effects on the biological activity of this

cytokine [429-430]. Interestingly, it has recently been shown that all inflammasome activators induce secretion of an 18kDa form of IL-1α. However, depending on the type of inflammasome activator, secretion of IL-1α can be NLRP3 and caspase-1-dependent or –independent. Secretion of IL-1α in response to ATP and nigericin is entirely dependent on NLRP3 and caspase-1, whereas particulate stimuli such as MSU and silica induce secretion of IL-1α in a NLRP3 and caspase-1-independent manner. In both cases, IL-1α is processed by intracellular calpain-like proteases [431].

IL-1α is typically released into the extracellular milieu by damaged or dying cells where it has a wide range of immunostimulatory effects. Interestingly, serum IL-1α levels are elevated in patients with inflammatory conditions such as RA. Furthermore, a recent study has shown that IL-1α is released from necrotic cells but is retained in the nucleus of cells undergoing apoptosis [432]. In 2007, the crucial role of IL-1α in the inflammatory response to necrotic cells was outlined in a simple experiment performed by Chen and colleagues. In wild-type mice, i.p. injection of necrotic cells promoted neutrophil recruitment into the peritoneal cavity. However, this effect was abolished in IL-1R mutant mice, thus suggesting an important role for IL-1 in the inflammatory response to necrotic cells. Chen *et al.* determined the active species of IL-1 in this model using neutralising monoclonal antibodies specific for IL-1α or IL-1β. Notably, antibodies to IL-1α suppressed neutrophil recruitment in response to necrotic cells, whereas antibodies to IL-1β had no effect on this response. Furthermore, caspase-1-deficient mice elicited normal recruitment of neutrophils, thus supporting the idea that IL-1β is not important in the inflammatory response to dead cells. Necrotic cells were also shown to induce secretion of IL-1α from macrophages *in vitro*. Ultimately, these experiments proved that IL-1α, and not IL-1β, is the key active cytokine in response to necrotic cell death [272]. In contrast to IL-1β, IL-1α is considered an endogenous danger signal owing to the the fact that it is widely and constitutively expressed, active in its uncleaved form and passively released from necrotic cells.

IL-33 binds to ST2 [433]. Following ligation, the IL-33-ST2 complex recruits the IL-1R accessory protein to initiate signal transduction [434]. Unlike other IL-1 family members, IL-33 is not typically expressed by hematopoietic cells but is abundantly expressed in many tissues [433]. In addition, IL-33 contains an N-terminal helix-turn-helix (HTH)-like motif in its prodomain that is crucial for nuclear localisation of the protein [435] (Figure 1.11). In 2005, Schmitz *et al.* showed that an artificially truncated form of IL-33 ($IL\text{-}33^{112\text{-}270}$) could augment the production of the Th2 signature cytokines IL-5 and IL-13 from *in vitro*-polarised Th2 cells and could also inhibit Th1 cytokine production. Furthermore, i.p. injection of mice with the same artificially truncated form of IL-33

induced splenomegaly, peripheral blood eosinophila and lymphocytosis, as well as an increase in circulating IL-5, IL-13, IgE and IgA. IL-33 also promoted tissue lesions in the lung and epithelial hyperplasia in the GI tract [433]. Subsequent studies identified IL-33 as a potent activator of eosinophils, basophils and mast cells, and also an important cytokine capable of promoting mast cell differentiation from bone marrow precursors [436-437].

Initially, Schmitz *et al.* showed that full-length human IL-33 was processed by caspase-1 after serine (Ser)111 *in vitro*, thus yielding a more potent form of this cytokine [433]. However, it was subsequently demonstrated that IL-33 is in fact inactivated following processing by caspase-1 at Asp178 [438]. Recently, Luthi *et al.* reported that human IL-33 is processed exclusively by apoptotic caspases (caspase-3 and caspase-7), but not by inflammatory caspases (caspase-1, caspase-4 and caspase-5). In addition, the site of apoptotic caspase-mediated proteolysis of IL-33 was also located at Asp178 [439] (Figure 1.11). Proteolysis of IL-33 by apoptotic caspases attenuated its biological activity both *in vitro* and *in vivo*, generating a cytokine with significantly reduced proinflammatory potential. These observations suggest that caspase-mediated proteolysis of full-length IL-33 in cells undergoing apoptosis serves to inactivate this cytokine and dampen immune responses to apoptotic cell death. However, apoptotic caspases remain inactivated during necrosis and thus cannot process intracellular IL-33. Therefore, the biologically more potent full-length form of IL-33 is likely to be released from necrotic cells following loss of membrane integrity and may function to promote powerful immunostimulatory effects in response to necrotic cell death. Interestingly, Luthi *et al.* also proved that IL-33 is readily cleaved in apoptotic cells but fails to undergo proteolytic processing in necrotic cells [439-440]. In support of these observations, IL-33, similarly to IL-1α and IL-1β, lacks a classical secretory sequence and is therefore not released via the ER-Golgi secretory pathway [433]. Thus, it is likely that IL-33 is primarily released as a direct consequence of necrosis. Indeed, this hypothesis coincides with findings that necrosis, but not apoptosis, is associated with inflammation [441].

Interestingly, human IL-33 is also processed by neutrophil serine proteases cathepsin G and elastase. Lefrancais *et al.* recently demonstrated that cathepsin G processing of IL-33 generates two major cleavage products of 21kDa and 18kDa and these cleavage sites were mapped at Phe94 and leucine (Leu)108 respectively. In addition, an elastase cleavage site at isoleucine (Ile)98 was identified which generates a single 20kDa cleavage product (Figure 1.11). Unlike processing of IL-33 by apoptotic caspases however, the bioactivity of IL-33 is enhanced following processing by these neutrophil proteases [442].

As described above, the cytokines IL-33 and IL-1α can be considered as endogenous danger signals. During necrosis, cellular integrity is compromised, leading to the release of endogenous cytokines into the extracellular milieu. Previous work in this lab has helped to show that full-length IL-33 is a potent inducer of innate immunity [439]. **The next objective of this work is to assess the adjuvant properties of IL-33 and IL-1α as measured by their ability to drive antigen-specific cellular and humoral immunity and also to compare the nature of the responses induced.** It is hypothesised that the impact of cell death in specific tissues on adaptive immunity may reflect the nature of the alarmins present inside necrotic cells. Ultimately, distinct tissues may possess distinct alarmins and therefore promote distinct immune responses.

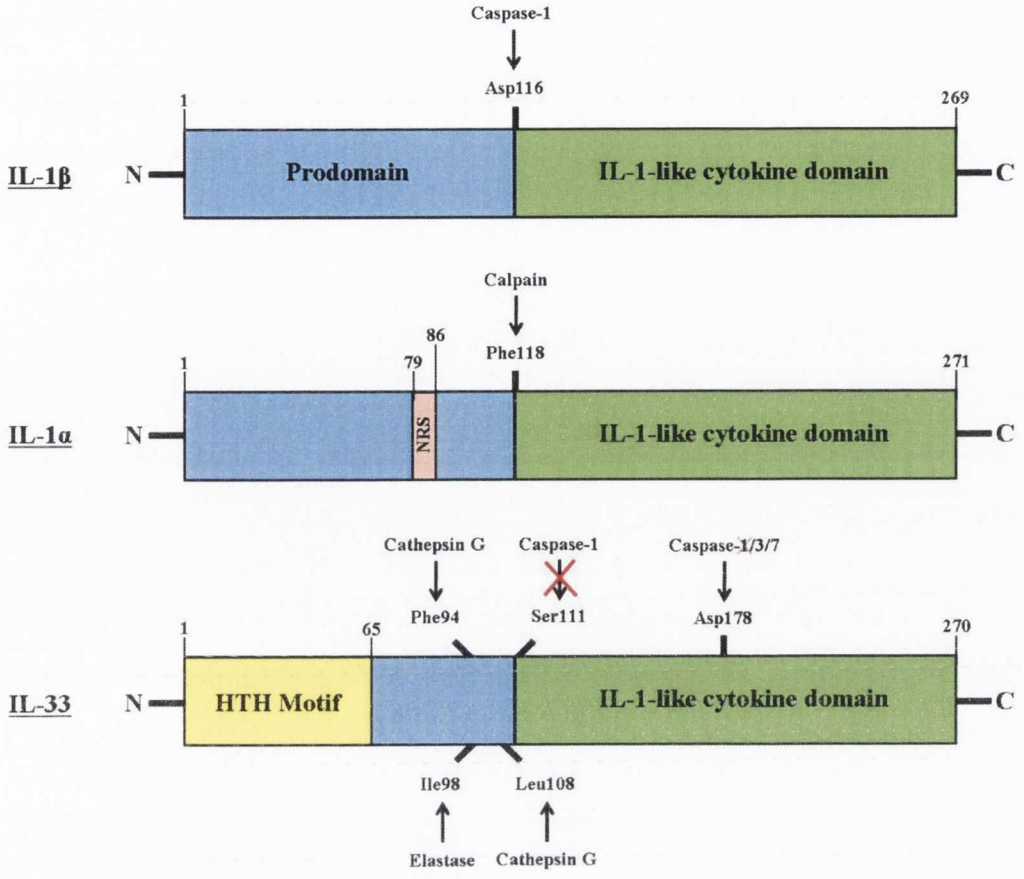

Figure 1.11 – Cleavage sites in human IL-1β, IL-1α and IL-33. IL-1β, IL-1α and IL-33 are members of the IL-1 family that are synthesised as precursor proteins containing an N-terminal prodomain and a C-terminal IL-1-like cytokine domain that is important for folding of the protein into a 12-stranded β-barrel conformation. The precursor form of human IL-1β contains 269 amino acid residues and is processed by the cysteine protease caspase-1 at Asp116, thus yielding a biologically active form of IL-1β. The precursor form of human IL-1α consists of 271 amino acid residues and contains a NRS in the prodomain. This sequence is lost following cleavage of the precursor form of IL-1α at Phe118 by the calcium-dependent cysteine protease calpain. Human IL-33 is comprised of 270 amino acid residues and is retained in the nucleus by a HTH motif in the prodomain of the cytokine. The neutrophil serine protease cathepsin G processes IL-33 at Phe94 and also at Leu108, whereas an elastase cleavage site has been identified at Ile98. Processing of IL-33 by cathepsin G and elastase is believed to potentiate the bioactivity of this cytokine, whereas processing of IL-33 at Asp178 by caspase-3 and caspase-7 has been shown to reduce its immunostimulatory activity. Although caspase-1 was originally shown to process IL-33 at Ser111 and also at Asp178, this is no longer believed to be true.

1.8.7 - Other danger signals

Some of the most prominent and well-characterised danger signals discovered to date have been discussed above. However, other danger signals have also been proposed, including RNA, mammalian genomic and mitochondrial DNA, ATP, nonmuscle myosin heavy chains and the spliceosome-associated protein (SAP)130.

Studies have shown that messenger RNA (mRNA) prepared *in vitro* can stimulate DC maturation and secretion of proinflammatory cytokines, and also induce downregulation of CCR5 and CCR6 and upregulation of CXCR4, which facilitatates DC migration to secondary lymphoid organs [443]. Also, heterologous RNA released from necrotic cells promotes IFN-α production by DCs. The effects of both *in vitro* transcribed mRNA and heterologous RNA released by necrotic cells are dependent on TLR3 [444]. However, the credibility of RNA as an alarmin remains questionable due to the inherent instability of these nucleic acids and also the ubiquitous presence of RNases in the extracellular environment.

DNA is another nucleic acid with immunostimulatory potential. Prokaryotic DNA is a well-known PAMP that signals through TLR9 and cytosolic DNA sensors such as DNA-dependent activator of IRF1 (DAI) [445], absent in melanoma (AIM)2 [446] and IFN-inducible protein (IFI)16 [447], thus facilitating immune recognition of viruses and bacteria. TLR9 recognition of prokaryotic DNA is dependent on unmethylated CpG motifs. Mammalian DNA also contains these motifs, although at a much lower frequency [448]. Murine genomic dsDNA released from necrotic cells stimulates phenotypical and functional DC maturation *in vitro*, and can serve as an effective adjuvant *in vivo* as measured by its ability to augment antigen-specific cellular and humoral immunity. Interestingly, unmethylated CpG motifs are not required for the immunostimulatory activity of murine dsDNA. Specifically, polynucleotides lacking C or G nucleotides are stimulatory, and methylation fails to inhibit the immunomodulatory effects of dsDNA, thus indicating that TLR9 recognition of unmethylated CpG motifs is not responsible for these effects [449]. However, Zhang and colleagues recently discovered that severe trauma in humans is accompanied by release of mitochondrial DNA into the circulation, and that this mitochondrial DNA is capable of activating p38 MAPK in neutrophils in a process dependent on TLR9 recognition of unmethylated CpG motifs [450]. Host genomic DNA released from dying cells has also been reported to mediate the adjuvanticity of alum *in vivo* [156].

ATP has also been reported to induce activation of human DCs as measured by upregulation of costimulatory molecules, secretion of IL-12 and improved stimulatory capacity for allogeneic T cells. These responses are augmented in the presence of TNF-α and are mediated by the P2Y11 receptor [451-452]. ATP can be chemotactic for immature DCs [453] and neutrophils [454], and as discussed previously can also induce NLRP3 inflammasome activation and synthesis of the biologically active form of IL-1β [243].

Nonmuscle myosin heavy chains are released in the aftermath of ischemia-reperfusion injury of the intestine, myocardium and skeletal muscle. Independently, these myosin molecules do not possess any intrinsic proinflammatory activity. However, circulating natural IgM autoantibodies bind the myosin chains following their release from damaged tissue. Thus, nonmuscle myosin heavy chains and IgM autoantibodies form immune complexes. Importantly, these immune complexes can activate the complement pathway, a cascade characterised by the generation of immunostimulatory complement fragments and subsequent robust inflammation [455]. Immunodeficient mice lacking antibodies fail to generate inflammation after ischemia-reperfusion injury in the bowel [456], heart [457] and skeletal muscle [458]. However, injection of a monoclonal myosin-heavy-chain-specific antibody into these mice is sufficient to induce inflammation at sites of ischemia-reperfusion injury [459]. Furthermore, infusion of myosin peptide into wild-type mice to block the circulating myosin-specific antibodies serves to reduce the inflammatory response to ischemia-reperfusion injury [455].

As discussed previously, Mincle is a member of the CLR family. While searching for ligands of Mincle, Yamasaki and colleagues identified endogenous SAP130 which is a component of the U2 small nuclear ribonucleoprotein (snRNP). Indeed, ligation of Mincle by SAP130 on macrophages induced secretion of proinflammatory cytokines and chemokines such as IL-6, TNF-α, KC and MIP-2 via an FcRγ and CARD9-dependent signalling cascade. This study also investigated the importance of SAP130 in modulating immune responses to cell death *in vivo*. Yamasaki *et al.* induced thymocyte necrosis by irradiating mice and observed that infiltration of neutrophils into the thymus was suppressed in the presence of neutralising anti-Mincle antibodies. Furthermore, co-injection of these antibodies with necrotic cells into the peritoneal cavity of mice resulted in reduced levels of MIP-2 accompanied by decreased neutrophil recruitment [233].

C-type lectin domain family 9 member A (CLEC9A) is another CLR family member capable of recognising endogenous danger signals. Sancho and collaborators initially demonstrated that DCs utilise CLEC9A to recognise a preformed signal exposed on necrotic cells. More specifically, loss of

CLEC9A reduces cross-presentation of antigens derived from necrotic cells *in vitro* and decreases the immunostimulatory activity of necrotic cells *in vivo* [460]. The CLEC9A ligand has only recently been identified as the F-actin component of the cytoskeleton [461].

In challenging Janeway's well-established stranger model, Matzinger's theory experienced a slow start. However, experimental evidence is now rapidly accumulating in support of the danger model and in particular on its emphasis on the host tissues being the master regulator of the immune system. Indeed, one particular tissue that has caught our attention as a potentially rich source of endogenous immunomodulators is that of white adipose tissue (WAT).

1.9 - The Adipose Organ

1.9.1 – WAT and the lipid droplet

The adipose organ is the largest endocrine organ in the body and consists of both brown adipose tissue (BAT) and WAT which can form either subcutaneous or visceral fat [462]. BAT is characterised by the presence of brown adipocytes which are multilocular cells highly specialised for heat production by non-shivering thermogenesis. However, here the focus will specifically be on WAT. The predominant constituents of WAT are white adipocytes which are unilocular cells that serve as a long term energy depot for the animal by storing fatty acids in the form of triglycerides. A triglyceride comprises three fatty acids attached to a single glycerol molecule by specialised enzymes located in the ER membrane. When cells require lipids for membrane synthesis or energy, lipolysis is activated and triglycerides are catabolised as fatty acyl chains are sequentially cleaved from the glycerol backbone and released into the circulation. Indeed, WAT is the dominant energy reservoir in the body, mainly because of the high caloric value of lipid compared to carbohydrates but also because, unlike carbohydrates, hydrophobic lipids can be stored with few associated water molecules, thus enabling over 85% of adipocyte mass to consist entirely of lipid.

In order to store dietary lipids, white adipocytes contain a single intracellular lipid droplet which can occupy a huge volume of the cytoplasm, often forcing other organelles to the periphery of the cell. Lipid droplets are characterised by a phospholipid monolayer containing significant amounts of phosphatidylcholine and abundant neutral lipids, but also free cholesterol. Numerous proteins, including adipocyte-specific perilipin/ADRP/TIP47 (PAT) family member proteins involved in lipid droplet homeostasis, are also embedded in the membrane. This phospholipid monolayer surrounds a

core of neutral lipids predominantly comprising triglycerides but also diglycerides and sterol esters (Figure 1.12).

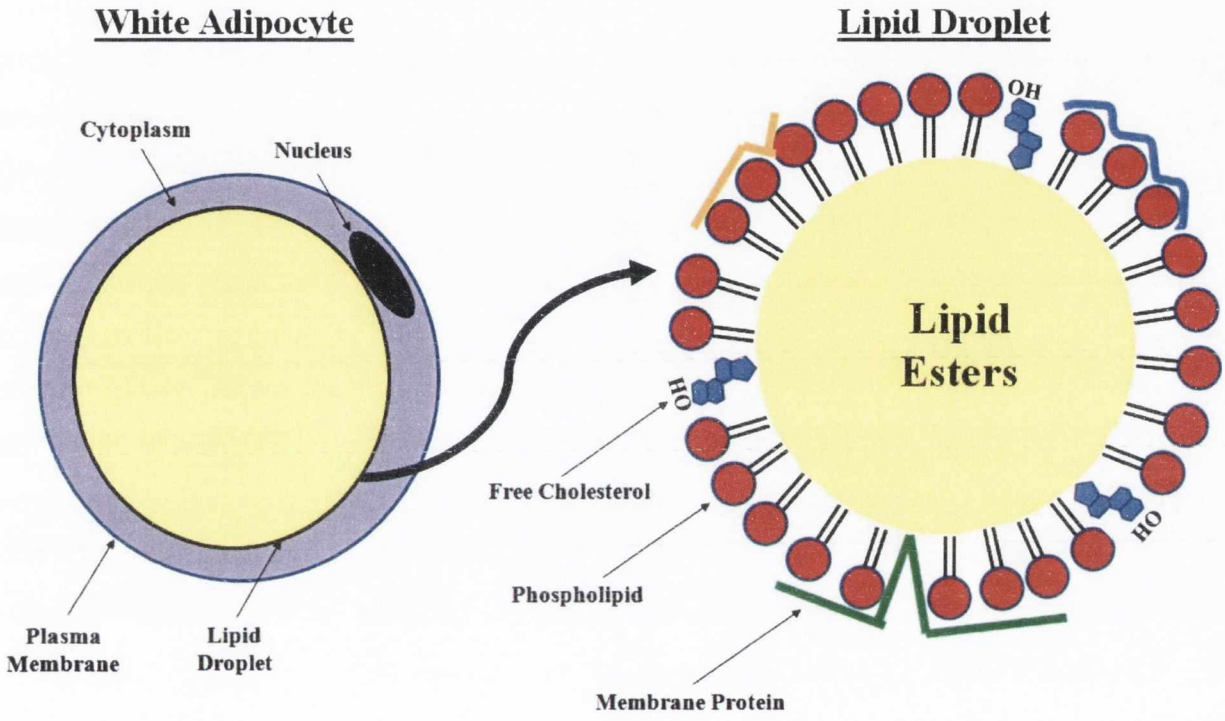

Figure 1.12 – Lipid droplet structure. The lipid droplet consists of a phospholipid monolayer surrounding a lipid ester core. The monolayer itself contains free cholesterol and also a range of adipocyte-specific proteins crucial for maintenance of lipid droplet homeostasis.

Importantly, WAT is made up not only of adipocytes but also a stromal vascular fraction containing stem cells, fibroblasts, preadipocytes, endothelial cells, lymphocytes and macrophages. Moreover, adipose tissue is not simply an inert site of passive fuel storage, but is a well-established endocrine organ capable of synthesising many different adipokines with local and systemic effects. Generally,

an adipokine is referred to as any protein that can be synthesised and secreted by adipocytes. These include cytokines, chemokines, fatty acids, prostaglandins, steroids and hormones.

1.9.2 – Obesity, inflammation and insulin resistance

Obesity is an issue concerning energy balance, regardless of any social, cultural, behavioural or genetic contributions. More specifically, obesity occurs when energy intake and triglyceride storage exceed the rate of lipolysis in adipocytes. This condition is a direct result of lipid accumulation which is characterised by an increase in both adipocyte size (hypertrophy) and adipocyte number (hyperplasia). Obesity is linked with insulin resistance and the onset of type 2 diabetes. Insulin resistance is characterised by decreased sensitivity to insulin by its main target organs; adipose tissue, liver and muscle. Insulin decreases lipolysis in adipocytes, thus reducing circulating free fatty acid levels; in liver, insulin suppresses gluconeogenesis, and in skeletal muscle, insulin promotes glucose uptake by promoting the translocation of glucose transporter (GLUT)4 to the plasma membrane of the cell. Ultimately, insulin regulates circulating free fatty acid and glucose levels. Insulin resistance results in increased lipolysis and elevated levels of circulating free fatty acids, augmented gluconeogenesis and subsequent glucose production in the liver, and impaired glucose uptake in skeletal muscle. Visceral fat is more pathogenic than subcutaneous fat with regard to developing insulin resistance and type 2 diabetes. For example, people who undergo liposuction, which is predominantly the removal of subcutaneous fat, show no increase in insulin sensitivity. In contrast, loss of visceral fat simply by using conventional dieting techniques is associated with a significant improvement in insulin sensitivity.

The link between inflammation and type 2 diabetes was first discovered more than a century ago when Ebstein reported that high doses of sodium salicylate could reduce glycosuria in patients with type 2 diabetes. Moreover, it was concluded that sodium salicylate could completely abrogate the symptoms of this disease. This effect was indirectly rediscovered in 1957 when a patient with type 2 diabetes was prescribed aspirin for treatment of arthritis associated with rheumatic fever. While taking aspirin, this patient no longer required daily insulin injections as fasting and postchallenge glucose levels were almost normal. Moreover, when the aspirin treatment was discontinued in this patient following resolution of joint symptoms, a repeat glucose tolerance test was completely abnormal and indicative of insulin resistance. Reid and colleagues confirmed the therapeutic potential of high-dose aspirin treatment in resolution of the symptoms of type 2 diabetes in a number

of other patients, with average blood glucose levels falling from 190 milligrams per decilitre (mg/dl) to 92mg/dl [463].

Obesity is characterised by chronic, low-grade inflammation that promotes insulin resistance and type 2 diabetes. The proinflammatory cytokine TNF-α is overexpressed in WAT in various different animal models of obesity. In 1993, Hotamisligil and colleagues first demonstrated the potential of proinflammatory cytokines in driving insulin resistance when they reported that neutralisation of TNF-α in genetically obese rats improved insulin sensitivity [464]. Subsequently, it was shown that genetic or diet-induced obese (DIO) mice deficient in TNF-α are protected from insulin resistance [465]. IL-6 is another proinflammatory cytokine whose production by WAT is significantly enhanced in obesity [466]. In fact, adipose tissue-derived IL-6 is believed to account for up to 30% of total circulating levels of IL-6 in obese individuals in the absence of acute inflammation [467].

1.9.3 – Adipose tissue macrophages

In support of the low-grade inflammatory state associated with obesity, gene expression studies using microarray approaches have shown that in rodent models of genetic obesity, adipose tissue expression of inflammatory genes is significantly distorted [468]. Surprisingly, however, subsequent studies proved that these alterations in gene expression were directly associated with a large infiltration of macrophages into the adipose tissue of obese mice [469] (Figure 1.13). Indeed, these infiltrating macrophages are the predominant cell type responsible for TNF-α production in adipose tissue, and are also a major player in the expression of other proinflammatory mediators including IL-6 and inducible nitric oxide synthase (iNOS) [469].

Like other tissues, adipose tissue contains resident macrophages. However, these resident macrophages have an anti-inflammatory profile with an 'alternatively activated' phenotype and are referred to as M2 macrophages, although their precise function in adipose tissue remains unclear [470]. Importantly, obesity induces a phenotypic shift in adipose tissue macrophages from M2 macrophages to M1 macrophages with a proinflammatory profile and a 'classically activated' phenotype [470]. Furthermore, there is a significant increase in the number of these proinflammatory macrophages in adipose tissue from obese mice compared with lean mice [471]. Despite suggestions that macrophages present within WAT may be derived from preadipocytes due to the phagocytic capability of both cell types [472], it is now widely accepted that these macrophages in fact originate

from bone marrow precursors [469]. Clinical studies have confirmed a strong positive correlation between body mass index (BMI) and adipose tissue macrophage numbers in humans, particularly in the more pathogenic visceral fat [473]. However, whether these infiltrating macrophages represent either the cause or consequence of the low-grade inflammation associated with obesity is unknown.

Neutrophils have also been implicated in the chronic inflammation associated with obesity. In 2008, Elgazar-Carmon *et al.* demonstrated that neutrophils transiently infiltrate intra-abdominal tissue during the early stages of high-fat feeding and interact directly with adipocytes (Figure 1.13). Neutrophil recruitment into the adipose tissue peaks after 3-7 days of high-fat feeding and precedes macrophage infiltration by approximately 2 weeks [474]. Moreover, neutrophils mediate tissue inflammation and insulin resistance in DIO mice through secretion of neutrophil elastase [475], a protease which is proinflammatory in several disease models [476] and has been shown to promote degradation of insulin receptor substrate (IRS)-1 [477]. Ultimately, neutrophils may secrete chemokines and cytokines in WAT, thereby facilitating macrophage infiltration and promoting the onset of the inflammatory cascade associated with insulin resistance.

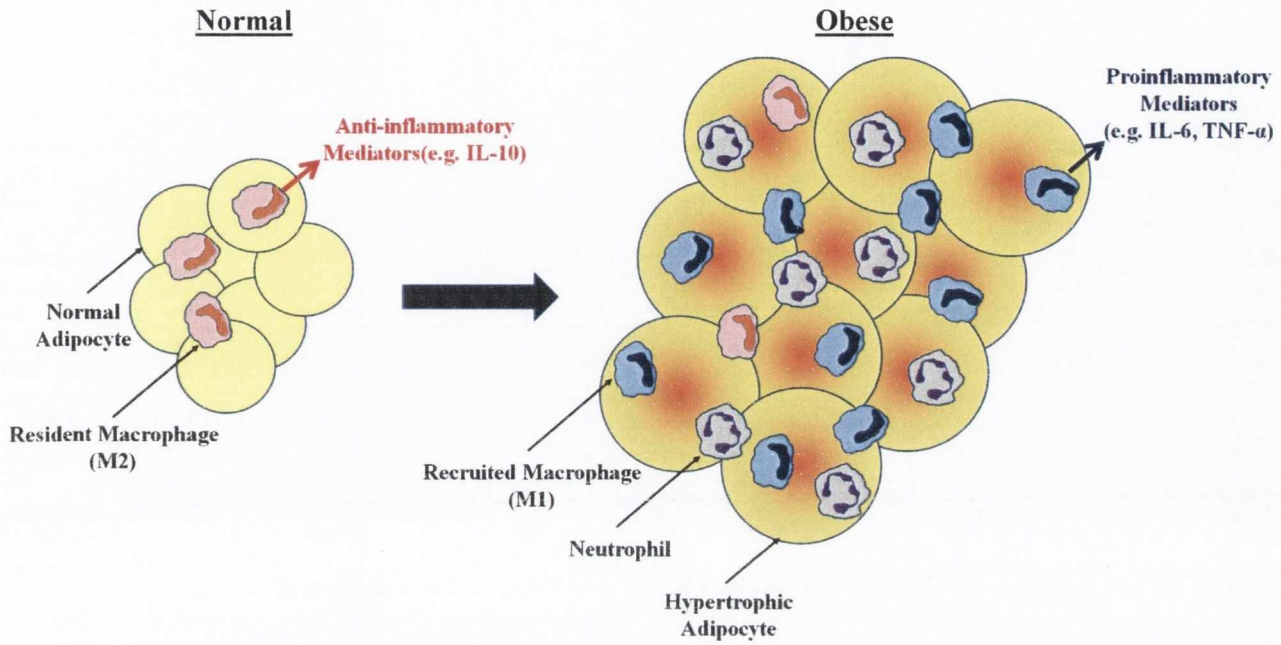

Figure 1.13 – Adipose tissue macrophages and inflammatory gene expression. Under normal conditions, WAT contains small adipocytes and a modest number of M2 alternatively activated resident macrophages. These resident macrophages are anti-inflammatory and serve to dampen immune responses in WAT. In obese conditions, however, adipocytes accumulate increased lipid and become enlarged. Furthermore, WAT recruits a huge number of neutrophils and M1 classically activated macrophages. M1 macrophages secrete proinflammatory mediators which can activate the adipocytes in WAT and can also act at distant sites in the body. Adipocyte activation further propagates this inflammatory cascade. Figure adapted from [478].

1.9.4 – NLRP3 in obesity

The role of the proinflammatory cytokine IL-1β has long been established in the pathogenesis of type 2 diabetes. For example, IL-1β mediates pancreatic β cell deterioration and dysfunction [479]. Furthermore, IL-1β inhibits insulin signalling pathways by reducing IRS-1 gene expression levels and also tyrosine phosphorylation of IRS-1, thus promoting insulin resistance [480]. In DIO mice, the absence of IL-1β or the IL-1R protects against adipose tissue inflammation and insulin resistance [481-482], whereas there is a positive correlation in humans between circulating IL-1β levels and type 2 diabetes [483]. Subcutaneous injection of anakinra (a recombinant human IL-1ra) into patients with type 2 diabetes improves glycemia and β cell secretory function and reduces markers of systemic inflammation [484], while blockade of IL-1β signalling using neutralising antibodies has also been reported to diminish insulin resistance. As discussed in Section 1.7.4, the NLRP3 inflammasome regulates processing of IL-1β through the cysteine protease caspase-1. The pathogenic role of IL-1β in adipose tissue inflammation and insulin resistance has in turn focused attention on the role of the NLRP3 inflammasome in mediating these processes.

Stienstra *et al.* first demonstrated that caspase-1 and IL-1β activity is elevated in the adipose tissue of DIO and genetically obese mice. Caspase-1 deficient mice were more insulin sensitive than wild-type mice and treatment of obese mice with a caspase-1 inhibitor improved insulin sensitivity [485]. Vandanmagsar *et al.* have also shown that calorie restriction and exercise-induced weight loss in obese individuals with type 2 diabetes correlates with a reduction in adipose tissue expression of NLRP3, decreased inflammation and an improvement in insulin sensitivity. Moreover, DIO mice deficient in NLRP3 exhibit enhanced insulin signalling [486]. Further studies have reported that mice deficient in caspase-1, NLRP3 or ASC are resistant to the development of diet-induced obesity and are protected from obesity-induced insulin resistance. These mice also exhibit decreased adipocte hypertrophy. Macrophage infiltration into WAT is reduced in caspase-1 deficient DIO mice and this correlates with reduced levels of MCP-1 in adipose tissue [487].

Much work has been done in trying to identify physiological activators of NLRP3 in WAT. As mentioned in Section 1.7.4, activation of NLRP3 and secretion of IL-1β requires 2 signals. The first signal is typically provided by PAMPs or DAMPs that engage members of the TLR family and prime the cell for NLRP3 activation by upregulating transcription of pro-IL-1β and NLRP3, whereas the second signal promotes NLRP3 activation through a mechanism involving potassium efflux.

In the past 10 years, various metabolic activators of IL-1β in WAT have been proposed. In 2001, saturated fatty acids (SFAs) were first shown to bind to TLR4 and induce NF-κB activation and cyclooxygenase-2 expression in macrophages *in vitro*, whereas unsaturated fatty acids (UFAs) inhibited this process [488]. Shi *et al.* have also reported that the SFA palmitate upregulates IL-6 and TNF-α mRNA expression in macrophages and adipocytes in a TLR4-dependent manner. Furthermore, mice deficient in TLR4 are protected from high-fat diet-induced insulin resistance [489]. Interestingly, palmitate has also been shown to upregulate IL-1β mRNA levels in human THP-1 cells [490]. Indeed, it is entirely possible that palmitate may engage TLR4 and serve as a priming signal for IL-1β activation in WAT of obese individuals, particularly in light of the fact that elevated circulating levels of free fatty acids are characteristic of type 2 diabetes. Surprisingly, palmitate has also been reported to directly activate NLRP3 and thus supply the second signal required for caspase-1 activation and IL-1β secretion. Palmitate reduces adenosine monophosphate-activated kinase (AMPK) phosphorylation which leads to defective autophagy and failure to eliminate dysfunctional mitochondria. Wen *et al* hypothesise that an accumulation of mitochondrial-derived ROS as a result of these events promotes NLRP3 activation [481]. An alternative pathway for palmitate-induced NLRP3 activation is through intracellular accumulation of ceramides. Exposure of cells to palmitate results in increased ceramide biosynthesis, and ceramides have recently been shown to induce NLRP3 activation in macrophages [486].

Hyperglycemia is a hallmark feature of type 2 diabetes and glucose is capable of providing both the priming and activating signal for IL-1β production. This metabolic danger signal can activate NF-κB in monocytes and induce the expression of a range of proinflammatory cytokines and chemokines including IL-1β, TNF-α and MCP-1 [491]. Recent reports have also claimed that high-glucose levels are capable of activating NLRP3 in a TXNIP-dependent manner [266]. Interestingly, TXNIP levels are elevated in patients with type 2 diabetes [492] and the expression of this thioredoxin inhibitor is upregulated by glucose [493].

Uric acid has also been linked with the metabolic syndrome and obese individuals often have hyperuricemia. Since insulin reduces renal secretion of uric acid, it is believed that the onset of hyperuricemia is caused by hyperinsulinemia. As discussed in Section 1.7.4, uric acid promotes NLRP3 activation and subsequent IL-1β secretion. Indeed, insulin sensitivity in fructose-fed rats is improved by reducing circulating uric acid levels using allopurinol [494].

1.9.5 – Mechanisms of obesity-induced insulin resiatance

As mentioned previously, obesity-induced inflammation promotes insulin resistance and type 2 diabetes. So how exactly does inflammation drive insulin resistance? More specifically, what are the mechanisms underlying this process? Earlier work reporting the ability of sodium salicylate to improve insulin sensitivity and reverse the symptoms of type 2 diabetes eventually focused attention on IKK-β and NF-κB. Adiposity increases activation of both IKK-β and Jun N-terminal kinase (JNK) [495-496]. Proinflammatory cytokines, free fatty acids, cellular stresses such as ROS and ER stress, all of which are significantly elevated in obesity, can induce activation of these kinases. Phosphorylation of activatory tyrosine residues on IRS-1, a substrate downstream of the insulin receptor, is crucial for efficient insulin signalling. However, phosphorylation of inhibitory serine residues on IRS-1, particularly Ser307, makes IRS-1 a poor substrate for the insulin receptor and results in impaired insulin signalling [497].

JNK is a stress kinase normally responsible for phosphorylation of c-Jun and subsequent activation of the AP-1 transcription factor. However, JNK has also been shown to directly phosphorylate inhibitory Ser307 in IRS-1, thus impairing insulin signalling. In contrast to JNK, IKK-β does not phosphorylate IRS-1 directly. However, IKK-β-mediated degradation of Iκβ and subsequent translocation of NF-κB into the nucleus results in transcription of a range of proinflammatory cytokines that further activate JNK and IKK-β in a positive feedback loop [498]. Myeloid-specific deletion of IKK-β in obese mice protects against insulin resistance [499], thus implementing myeloid cells once more in the low-grade inflammation associated with obesity and type 2 diabetes.

The cellular and molecular mechanisms responsible for macrophage infiltration into adipose tissue and the inflammatory response associated with obesity remain largely unknown. However, MCP-1 is a chemoattractant for circulating monocytes that is believed to play an important role in obesity-mediated macrophage recruitment. MCP-1 synthesis and secretion by adipocytes is amplified proportionally with increasing adiposity [500] and this chemokine is overexpressed in obesity [501]. Adipose tissue macrophage numbers and inflammatory gene expression are significantly reduced in MCP-1-deficient obese mice, and consequently these mice are partly protected from insulin resistance [502]. In support of these findings, MCP-1 overexpression in adipose tissue promotes macrophage recruitment and insulin resistance. Not surprisingly, similar results have been reported in CCR2-deficient mice fed a high fat diet [471].

Although MCP-1 may be important for initiating the recruitment of inflammatory macrophages, elevated production of this cytokine does not solve the age old question of how exactly increased adiposity initially kickstarts a proinflammatory cascade resulting in production of immune mediators such as MCP-1, IL-1β, TNF-α and IL-6 by adipose tissue. In other words, the initial stimulus responsible for promoting inflammation in adipose tissue is ambiguous. In recent years however, a strong and convincing case has been made for ER stress in this spontaneous inflammatory response. The ER is primarily involved in protein synthesis and along with the Golgi apparatus it facilitates the transport and secretion of correctly folded proteins from the cell [503]. Moreover, the ER is the site of triglyceride-containing lipid droplet formation [504]. Under conditions of cellular stress, ER function can be compromised which leads to impaired protein folding resulting in the accumulation of misfolded proteins in the lumen of the ER [505]. In response to these conditions, the ER can activate the unfolded protein response (UPR) pathway which oversees the initiation of a proinflammatory signalling cascade.

Some of the cellular stresses that can promote the onset of the UPR include increased protein synthesis, imbalance of ER calcium levels, viral infections and toxins, and nutrient deficiency. The answer to the question of which stimulus activates adipocyte ER stress in obesity remains unknown, but there are several possibilities. Lipid accumulation can activate the UPR, and obesity is associated with this form of nutrient excess. In particular, lipid accumulation may lead to an increased demand for protein synthesis and consequently induce ER stress. Furthermore, the UPR may also be activated by the excess nutrients themselves in the form of free fatty acids. Indeed, serum free fatty acid levels are increased in obesity and these nutrients have been shown to activate the UPR in hepatocytes, cardiomyoblasts, pancreatic β-cells and macrophages [506-509]. Glucose deprivation has also been shown to activate the UPR in adipocytes [510] and this process may occur as a direct result of impairment of insulin signalling and reduced glucose uptake by adipocytes. Murine adipose tissue has also been shown to elicit signs of hypoxia in obesity [511], and this process is known to activate the UPR. Finally, although the ability of the UPR to mediate inflammatory responses is well documented, it is possible that proinflammatory cytokines present in adipose tissue can also initiate UPR activation. For example, TNF-α has been shown to activate the UPR in murine fibrosarcoma cells, and this process was dependent on ROS which is known to activate the UPR [512]. Indeed, obesity can potentially induce the UPR and subsequent inflammatory cascades in various different ways, although the importance and relative contribution of each of these processes has yet to be fully elucidated.

Another explanation for the rapid infiltration of phagocytic macrophages into WAT in obesity is the occurrence of adipocyte necrosis. Indeed, work carried out by Cinti *et al.* provides a detailed insight into this particular scenario as the frequency and distribution of mature macrophages in WAT of lean and genetically obese mice was assessed. It was discovered that macrophages are non-randomly distributed in WAT of lean and obese mice and form highly organised crown-like structures (CLS) which contain up to fifteen macrophages surrounding a single adipocyte. Some of these macrophages even form multinucleate giant cells (MGCs), indicating that individual adipocytes surrounded by CLS act as chronic sites of macrophage activation. Importantly, the frequency of CLS is approximately thirty times greater in obese mice than in lean mice (Figure 1.14).

Cinti *et al.* examined the ultrastructural features of the adipocytes that were surrounded by CLS. Surprisingly, it was found that these CLS are specifically localised to dead adipocytes (Figure 1.14). These adipocytes do not exhibit morphological features of apoptosis such as chromatin condensation, plasma membrane blebbing or membrane-bound apoptotic bodies containing nuclear fragments. However, many features of necrosis are evident, including loss of plasma membrane integrity, dilated ER and cell debris in the extracellular space.

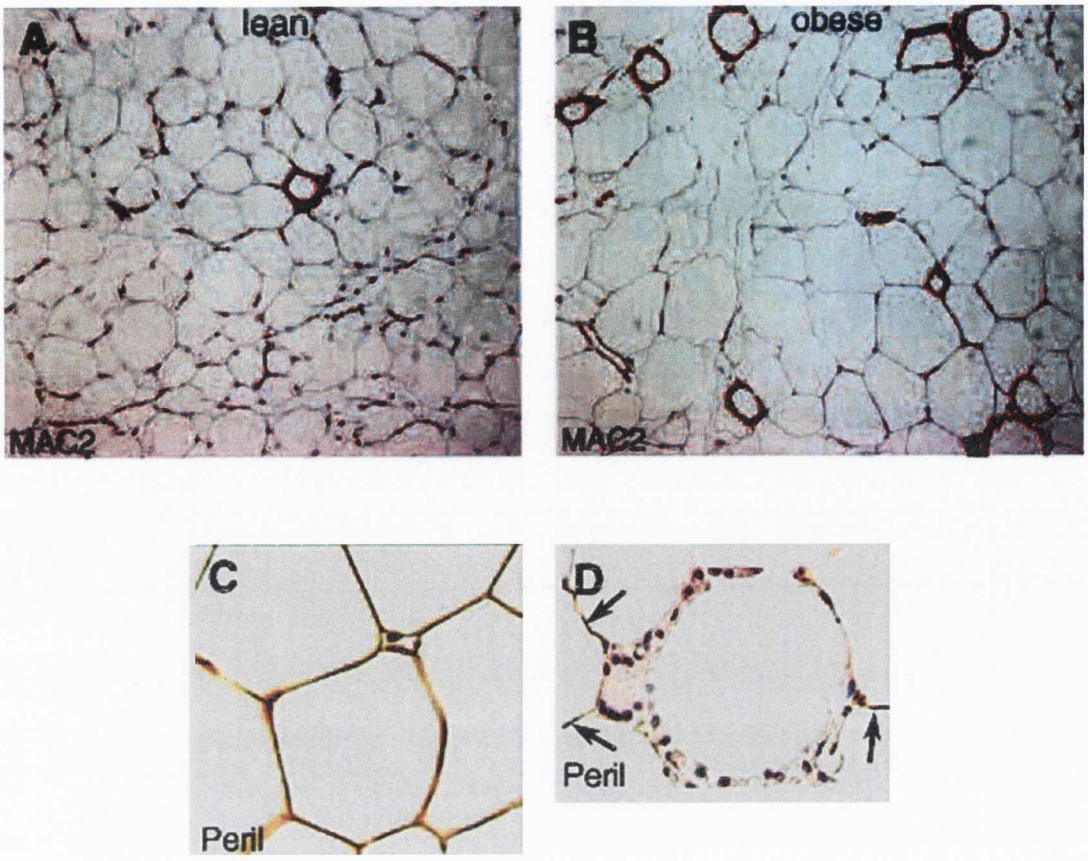

Figure 1.14 – WAT macrophages localise to CLS surrounding dead adipocytes which increase in frequency in obesity. (A) Light microscopy of visceral WAT from lean and (B) obese mice stained for the macrophage surface marker macrophage galactose-specific lectin (MAC)-2 (brown). MAC-2 immunoreactive macrophages aggregate to form CLS surrounding individual adipocytes. These CLS are rare in lean WAT but are numerous in obese WAT. (C) Light microscopy of visceral WAT from lean and (B) obese mice stained for the essential lipid droplet-associated protein perilipin (Peril) (brown). Adipocytes from lean mice are Peril immunoreactive, whereas adipocytes surrounded by CLS in obese mice are not Peril immunoreactive. Figure from [513].

The findings discussed above were also evident in humans as CLS macrophages localised around necrotic adipocytes. Furthermore, there was a strong positive correlation between adipocyte death and obesity and also between adipocyte death and mean adipocyte size, which increases significantly in obesity. Interestingly, adipocyte death was evident in a lean individual with large adipocytes, whereas adipocyte death could not be detected in an obese individual with small adipocytes. The positive correlation of adipocyte death with adipocyte size suggested that adipocyte hypertrophy could potentially mediate cell death. Indeed, this hypothesis was tested using hormone-sensitive lipase (HSL)-deficient mice. HSL-deficiency results in increased adipocyte lipid accumulation and ultimately hypertrophy. Hypertrophy in HSL-deficient mice was shown to elicit increased macrophage recruitment into WAT, inflammation and a fifteen-fold increase in adipocyte death compared to wild-type mice, events which are identical to those in obese mice and humans [513].

The underlying mechanism by which hypertrophy induces adipocyte death is unclear. However, cellular stress, as discussed above, is believed to be involved. Importantly, the above study also recognised the appearance of small lipid droplets in the cytoplasm of necrotic adipocytes which is indicative of breakdown of the large unilocular lipid droplet. These suspicions regarding lipid droplet degeneration were later confirmed by immunohistochemistry [513]. Indeed, it appears that CLS macrophages persist at sites of adipocyte necrosis in order to scavenge lipids released from these adipocytes which are now exposed in the interstitium. Furthermore, the persistence of CLS macrophages and MGCs around free lipid droplets of dead adipocytes suggests that these lipid droplets act as sites of chronic macrophage activation. Crucially, however, it remains unknown whether or how scavenging of free lipid by adipose tissue macrophages influences proinflammatory gene expression by these macrophages. Since a number of the most effective vaccine adjuvants in clinical and experimental use are lipid-based emulsions (e.g. MF59 and Freund's adjuvant), and indeed one of the earliest adjuvants discovered was starch oil, **the final objective of this work is to investigate the immunomodulatory potential of endogenous oils derived from the human omentum.** It is hypothesised that endogenous oils released from the droplet core of hypertrophic adipocytes following necrosis may represent a novel source of potent danger signals and provide the missing link between obesity and inflammation.

1.10 - Hypothesis

There are many studies in the literature accrediting immunostimulatory activity to endogenous danger signals when in fact contaminating LPS is responsible for mediating the observed effects. We hypothesise that low levels of LPS often considered to be residual in bacterial expression systems are in fact sufficient to promote immune activation, and that experimental controls used to reverse these effects are exceedingly limited in their ability to do so.

Exploring further the theme of endogenous danger signals, GzmB has been reported to elicit proinflammatory activity and can be expressed and secreted by a wide range of immune cells not associated with cell killing. Therefore, immune cells may secrete GzmB into the extracellular space with the ability to process molecules released from necrotic or secondary necrotic cells. Ultimately, it is hypothesised that GzmB processing of novel substrates may potentiate their inflammatory potential and yield a fresh source of endogenous danger signals.

It is further hypothesised that the impact of cell death on adaptive immunity may reflect the nature of the alarmins present inside necrotic cells. Specific danger signals, including novel GzmB substrates, within different tissues may promote distinct immune responses.

Endogenous oils derived from WAT adipocytes may also signal danger to the host. Lipid-based emulsions such as MF59 and Freund's adjuvant are some of the most effective vaccine adjuvants in clinical and experimental use and up to 85% of adipocyte mass consists entirely of lipid. Therefore, it is hypothesised that endogenous oils released from necrotic adipocytes may represent a novel source of potent danger signals and supply a key link between obesity and inflammation.

1.11 - Aims and Objectives

- To determine the minimum LPS concentration required to induce DC maturation and cytokine secretion, and to assess the ability of PmB to inhibit these processes.
- To investigate the immunomodulatory activity of novel GzmB substrates.
- To compare the adjuvant properties of IL-1α with another endogenous danger signal, IL-33.
- To investigate the immunomodulatory potential of endogenous oils derived from the human omentum.

Chapter 2

Materials and Methods

2.1 – Materials

All materials are from Sigma-Aldrich unless otherwise stated.

2.1.1 – General cell culture materials

Complete RPMI 1640 medium

Roswell Park Memorial Institute (RPMI) 1640 medium (Biosera) was supplemented with 2 millimolar (mM) L-Glutamine (Gibco), 50units/ml penicillin (Gibco), 50µg/ml streptomycin (Gibco) and 8% (v/v) heat-inactivated (56°C for 30 minutes) and filter sterilised foetal calf serum (FCS) (Biosera).

Complete DMEM-F12

Dulbecco's Modified Eagle Medium (DMEM): Nutrient Mixture-F12 (Biosera) was supplemented with 2mM L-Glutamine, 50units/ml penicillin, 50µg/ml streptomycin and 8% (v/v) heat-inactivated (56°C for 30 minutes) and filter sterilised FCS.

0.88% Ammonium chloride (NH_4Cl) red blood cell lysis solution

8.8g ammonium chloride

1 litre (L) endotoxin-free water (Baxter)

Filter sterilised with 0.22µm syringe-driven filter (Millipore)

2.1.2 – Treatments for cell culture and animal studies

PRR agonists (Table 2.1)

Table 2.1 – Identity and source of TLR and NLRP3 agonists used in cell culture experiments.

TLR Agonist	Source	NLRP3 Agonist	Source
***E. coli* LPS, Serotype R515 (TLR4)**	Enzo Life Sciences	**MSU crystals**	Enzo Life Sciences
Pam3CSK4 (Pam3) (TLR2)	InvivoGen	**Alum (Alhydrogel)**	Brenntag Biosector, Frederikssund, Denmark
CpG (TLR9)	Oligos Etc. Inc.	**ATP**	Sigma-Aldrich
Poly I:C (TLR3)	InvivoGen		
Heat-killed (HK) BL21 strain *E. coli* (Various)	N/A		

Recombinant mouse IL-23 (R&D)

Phorbal myristate acetate (PMA)

Purified hamster anti-mouse CD3e monoclonal antibody (BD Pharmingen)

Polymyxin B

A range of concentrations of sonicated LPS from *E. coli,* Serotype R515, TLRgrade (Enzo Life Sciences) were incubated on a rotator for 2 hours at 37°C with 100μg/ml of PmB. These treatments were then used to stimulate BMDCs.

Ovalbumin (albumin from chicken egg white), Grade V, 98% (agarose gel electrophoresis)

Human serum albumin (Novozymes Biopharma UK Ltd)

Complete Freund's adjuvant

Incomplete Freund's adjuvant

HK *E. coli*

This work was performed by Dr. Eimear Lambe of the Adjuvant Research Group in the School of Biochemistry and Immunology, Trinity College Dublin (TCD). An agar plate containing lysogeny broth (LB) was streaked with BL21 strain *E. coli*. The bacteria were left to grow overnight at 37°C in 10ml of LB. The culture was then transferred into 100ml of LB and was incubated shaking for 2 hours at 37°C. Serial dilutions of the culture were made and a known volume of each of these dilutions was spread onto LB agar plates and incubated overnight at 37°C. The number of colonies were counted and then multiplied by the dilution factor to determine the number of cells/ml in the original culture. The number of bacteria in the culture was confirmed further using a spectrophotometer to measure the optical density (OD) value of a sample at 600nm. The *E. coli* were killed by heating at 70°C for 15 minutes and were then plated onto LB agar to ensure that no growth occurred. The cells were pelleted by centrifugation and resuspended in phosphate buffered saline (PBS) (Biosera) to a final concentration of 1 x 10^9 cells/ml.

***E. coli* heat-labile enterotoxin**

E. coli heat-labile enterotoxin (LT) was kindly provided by Dr. Takao Tsuji (Department of Microbiology, School of Medicine, Fujita Health University, Aichi, Japan) and was subsequently passed through three separate endotoxin removal columns (Pierce) three times each. Endotoxin level was subsequently measured using the LAL assay (Pierce) and was determined to be 0.049pg of endotoxin per μg of *E. coli* LT.

Histamine-releasing factor (HRF)

This work was performed by Katrin Viikov of the Molecular Cell Biology Laboratory in the Department of Genetics, TCD. A bacterial expression plasmid encoding N-terminally polyhistidine-tagged human HRF (pET15b.HRF) was generated by polymerase chain reaction (PCR) using the plasmid pGEX-2T-HRF as a template [514]. Freshly transformed BL21 strain *E. coli* containing the required expression plasmid were grown overnight at 37°C. The following day this culture was used to seed a larger culture and the bacteria were allowed to grow until an OD600 of 0.1-0.2 was reached. 500 micromolar (μM) isospropylthio-b-D-galactosidase (IPTG) was added to induce expression of recombinant HRF. The bacteria were grown for a further 2-3 hours before pelleting at 3500g. The supernatant was decanted and the cells were resuspended in buffer. The cells were then sonicated with 30-second pulses in order to rupture the outer membrane. Insoluble material was

pelleted at 15000g. The supernatant containing the induced HRF was then incubated with a 50% slurry of NiTA beads and rotated at 40^0C for 4 hours to capture the protein. Elution of HRF was facilitated by addition of Imidazole elution buffer (100μM) at 40^oC at twice the volume of NiTA beads. This was followed by three separate 30 minute elutions. The eluted HRF was then concentrated in Vivaspin 0.5 ml concentrators (Sartorius).

Prior to use in BMDC experiments, eluted HRF was depleted of LPS by three successive incubations in PmB-agarose or TritonX-100. Proteins were then washed extensively in endotoxin-free PBS and concentrated by centrifugation in microconcentrator filters or by dialysis. Full-length HRF was incubated for 3 hours at 37^oC with 200 nanomolar (nM) active or heat-inactivated GzmB. GzmB was heat-inactivated by incubating at 95^0C for 20 minutes.

Human GzmB

This work was performed by Dr. Inna Afonina of the Molecular Cell Biology Laboratory in the Department of Genetics, TCD. *Pichia Pastoris* yeast clones stably harboring a human GzmB expression plasmid were provided by W. Wels (Chemotherapeutisches Forschungsinstitut Georg-Speyer-Haus, Frankfurt, Germany). Yeast clones expressing human GzmB were grown in 1L cultures for 3 days at 25°C. GzmB was purified from culture supernatants using nickel affinity chromatography followed by extensive washing in buffer supplemented with 5mM imidazole. Purified GzmB was eluted with 500mM imidazole and washed extensively in PBS, followed by concentration in microconcentrator units.

The catalytically inactive GzmB mutant ($GzmB^{SA}$) was expressed and purified in the same yeast system that was used to generate wild-type GzmB.

IL-1α and IL-33

This work was performed by Dr. Inna Afonina of the Molecular Cell Biology Laboratory in the Department of Genetics, TCD. Full-length polyhistidine-tagged IL-1α was generated by cloning the human IL-1α coding sequence in frame with the polyhistidine tag sequence in the bacterial expression vector pET45b (Novagen, U.K.). Protein was expressed by addition of 600μM IPTG to exponentially growing cultures of BL21 strain *E. coli* followed by incubation for 3 hours at 37°C. Sodium sarcosyl was added to the bacterial pellet to a final volume of 0.25%. Bacteria were lysed by sonication, sarcosyl was sequestered by addition of TritonX-100 to a final volume of 0.5% and polyhistidine tagged IL-1α was captured using nickel-NTA agarose (Qiagen, UK), followed by

elution into PBS, pH 7.2, in the presence of 100mM imidazole. Full-length IL-1α was incubated for 3 hours at 37°C with 200nM active or heat-inactivated GzmB. GzmB was heat-inactivated by incubating at 95°C for 20 minutes. IL-1α^{D103A} mutant was expressed and purified in the same way.

Truncated IL-1$\alpha^{104-271}$ and IL-33$^{112-270}$ were expressed in BL21 strain *E. coli* for 3 hours at room temperature, and purified using nickel-NTA agarose.

Endotoxin-free OVA

OVA (albumin from chicken egg white), Grade V, 98% (agarose gel electrophoresis), lyophilized powder was resuspended in sterile PBS at a concentration of 100mg/ml. Three endotoxin removal columns were regenerated by washing with five resin-bed volumes (5 x 1ml) of sodium deoxycholate followed by five resin-bed volumes of endotoxin-free water to remove the detergent. The columns were then equilibrated with five additional resin-bed volumes of endotoxin-free water. The OVA solution was filter sterilised before being applied to the columns. The OVA was passed through each of the three endotoxin removing columns on three separate occasions. The final OVA concentration following endotoxin removal was determined using a bicinchoninic acid (BCA) protein assay kit (Thermo Fisher Scientific).

Human omental and subcutaneous oils

Omental and subcutaneous adipose tissue biopsies were obtained from obese patients undergoing bariatric surgery at St. Vincent's University Hospital (Elm Park, Dublin 4, Ireland). The St. Vincent's University Hospital Ethics and Medical Research Committee approved the use of these patient samples to investigate the immunomodulatory potential of endogenous oils derived from human adipocytes. The metabolic profile of the patients was determined, as detailed in Section 2.2.9.

Fresh samples of adipose tissue were incubated in complete DMEM-F12 medium supplemented with collagenase type II (1mg/ml) for 1 hour at 37°C in a metabolic shaker (80 strokes per minute). The cell suspension was filtered through a 250μm Nitex mesh and washed three times in complete DMEM-F12 medium. The infranatant was removed using a syringe and 18G needle and the adipocytes were resuspended in fresh medium, inverting several times to ensure an even suspension. The above work was performed by Dr. Michelle Corrigan of the Obesity Group, St. Vincent's University Hospital. The adipocytes were ruptured by centrifugation, thus facilitating the release of intracellular lipids. The infranatant was removed and the remaining lipid and fatty acid mixture was subsequently collected. This mixture was first centrifuged to eliminate cellular debris and other

insoluble components, then solubilised and fractionated in methanol-chloroform solvent layers. The aqueous and organic layers were then separately rotary evaporated under vacuum. The aqueous components were resuspended in endotoxin-free water, while the organic components were utilised as a pure lipid preparation. The lipid extraction procedure was carried out by Dr. Ken Mok of the Protein Folding and Biomolecular and NMR Spectroscopy Group, TCD.

2.1.3 – Fluorescence-activated cell sorting (FACS) materials

FACS buffer

1X PBS was supplemented with 0.1% sodium azide and 2% heat-inactivated and filter sterilised FCS.

Cell death stains (Table 2.2)

Table 2.2 – Cell death stains

Stain	Source	Concentration
Propidium Iodide (PI) Staining Solution	BD Pharmingen	1μg/ml (0.1μg) (3.75×10^5 cells in 100μl volume)
LIVE/DEAD Fixable AQUA Dead Cell Stain	Invitrogen	0.5μl stain for 0.5×10^6 cells in 250μl volume

FACS Antibodies (Tables 2.3 and 2.4)

Table 2.3 – Fluorescent antibodies used to assess DC maturation by FACS.

Antibody	Fluorochrome	Source	Concentration (3.75×10^5 cells in 100µl volume)
CD11c	PerCP-Cy5.5	BD Pharmingen	**0.3µg/ml (0.03µg)**
CD80	FITC	BD Pharmingen	**1µg/ml (0.1µg)**
CD40	APC	BD Pharmingen	**0.3µg/ml (0.03µg)**
MHC Class II	APC-eFluor 780	BD Pharmingen	**0.6µg/ml (0.06µg)**
CD16/CD32 Fc Block	N/A	BD Pharmingen	**2.5µg/ml (0.25µg)**

Table 2.4 – Fluorescent antibodies used to characterise peritoneal exudate cells (PECs) by FACS.

Antibody	Fluorochrome	Source	Concentration (0.5×10^5 cells in 100µl volume)
CD11b	PE-Cy7	BD Pharmingen	**0.05µg/ml (0.005µg)**
Gr-1	APC-Cy7	BD Pharmingen	**0.4µg/ml (0.04µg)**
Gr1	PE	BD Pharmingen	**0.4µg/ml (0.04µg)**
F4/80	PerCP-Cy5.5	eBioscience	**1µg/ml (0.1µg)**
ckit	PE-Cy7	BD Pharmingen	**1µg/ml (0.1µg)**
ckit	FITC	BD Pharmingen	**0.5µg/ml (0.05µg)**
CCR3	A647	BD Pharmingen	**1µg/ml (0.1µg)**
SiglecF	PE	BD Pharmingen	**0.2µg/ml (0.02µg)**
CD16/CD32	N/A	BD Pharmingen	**2.5µg/ml (0.25µg)**

2.1.4 – Enzyme-linked immunosorbent assay (ELISA) materials

10X PBS

400g NaCl

58g Na_2HPO_4

10g KH_2PO_4

10g KCl

Made up to a final volume of 5L with distilled water (dH_2O) and brought to pH 7.2.

1X PBS

100ml 10x PBS

900ml dH_2O

1% BSA

10g BSA

1L dH_2O

3% BSA

30g BSA

1L dH_2O

10% Milk

100g Marvel dried milk (Fluka Analytical)

1L dH_2O

Carbonate buffer

8.4g $NaHCO_3$

3.56g Na_2CO_3

Made up to a final volume of 5L with dH_2O and brought to pH 9.5.

Phosphate citrate buffer

10.19g $C_6H_8O_7$

14.6g Na_2HPO_4

Made up to a final volume of 1L with dH_2O and brought to pH 5.0.

0.05% PBS-Tween

8995ml dH_2O

1000ml 10x PBS

5ml Tween 20

ELISA antibodies (Tables 2.5 and Table 2.6)

Table 2.5 – Antibodies used to measure cytokine concentrations by ELISA.

Antibody	Source	Concentration	Blocking Solution	Top Working Standard
TNF-α	R&D Systems	Capture – 0.8μg/ml Detection – 0.4μg/ml	1% BSA	2000pg/ml
IL-1β	R&D Systems	Capture – 4μg/ml Detection – 1μg/ml	1% BSA	1000pg/ml
IL-1α	R&D Systems	Capture – 2μg/ml Detection – 0.1μg/ml	1% BSA	1000pg/ml
IL-10	R&D Systems	Capture – 4μg/ml Detection – 0.3μg/ml	1% BSA	2000pg/ml
IL-17	R&D Systems	Capture – 2μg/ml Detection – 0.4μg/ml	1% BSA	1000pg/ml
GM-CSF	R&D Systems	Capture – 2μg/ml Detection – 0.05μg/ml	1% BSA	1000pg/ml
IL-12p70	R&D Systems	Capture – 4μg/ml Detection – 0.4μg/ml	1% BSA	2500pg/ml
IL-6	BD Pharmingen	Capture – 1μg/ml Detection – 1μg/ml	3% BSA	5000pg/ml
IL-12p40	BD Pharmingen	Capture – 0.5μg/ml Detection – 1μg/ml	10% Milk	5000pg/ml
IL-4	BD Pharmingen	Capture – 0.5μg/ml Detection – 1μg/ml	10% Milk	2500pg/ml
IL-5	BD Pharmingen	Capture – 1μg/ml Detection – 1μg/ml	10% Milk	2500pg/ml
IFN-γ	BD Pharmingen	Capture – 1μg/ml Detection – 1μg/ml	10% Milk	10ng/ml

Table 2.6 – Antibodies used to measure serum Ig titres by ELISA.

Antibody	Source	Concentration
IgG	Sigma-Aldrich	3μg/ml
IgG1	BD Pharmingen	0.1μg/ml
IgG2a	BD Pharmingen	0.1μg/ml
IgG2b	BD Pharmingen	0.1μg/ml
IgG2c	BD Pharmingen	0.1μg/ml
IgA	BD Pharmingen	0.5μg/ml

2.1.5 – Western blot materials

1M Tris-HCl pH 6.8

12.11g Tris base

80ml dH_2O

Made up to a final volume of 100ml with dH_2O and brought to pH 6.8.

8x Resolving gel buffer

0.8g sodium dodecyl sulfate (SDS)

36.3g Tris base (3M)

Made up to a final volume of 100ml with dH_2O and brought to pH 8.8.

4x Stacking gel buffer

0.4g SDS

6.05g Tris base (0.5M)

Made up to a final volume of 100ml with dH_2O and brought to pH 6.8

Stopping buffer

680µl Milli-Q H_2O

130µl 1M Tris-HCl (pH 6.8)

10µl 10% SDS

175µl 30% Acrylamide, 10.8% Bis-acrylamide solution

12µl Ammonium persulfate

2µl Tetramethylethylenediamine (TEMED)

10x Running buffer

10g SDS (1%)

30.3g Tris base (0.25M)

144g Glycine (1.9M)

Made up to a final volume of 1L with dH_2O and brought to pH 8.3.

Transfer buffer

0.15g SDS

0.19g Tris base

4.32g Glycine (0.19M)

60ml Methanol (MeOH)

240ml dH_2O

Blocking buffer

5g Marvel dried milk

100ml dH_2O

SDS-polyacrylamide gel electrophoresis (SDS-PAGE) sample buffer

62.5mM Tris-HCl (pH 6.8)

2% (w/v) SDS

10% (v/v) Glycerol

0.1% (w/v) Bromophenol blue

50mM DL-Dithiothreitol (DTT)

0.1% PBS-Tween

899ml dH_2O

100ml 10x PBS

1ml Tween 20

Table 2.7 – Composition of resolving and stacking gels.

	Volume (15% Acrylamide Resolving Gel)	**Volume (5% Acrylamide Stacking Gel)**
dH_2O	3.71ml	1.16ml
30% Acrylamide, 10.8% Bis-acrylamide solution	5ml	333µl
8x Resolving gel buffer	1.25ml	-
10% Ammonium persulfate	33µl	5.4µl
TEMED	7µl	2µl
4x Stacking gel buffer	-	500µl

Table 2.8 – Antibodies for western blot analysis

Antibody	Source	Dilution	Diluent
Rat anti-mouse IL-1β (Primary)	R&D Systems	1/1000	3% BSA
Goat anti-rat IgG, peroxidise conjugate (Secondary)	Sigma-Aldrich	1/5000	0.1% PBS-Tween

2.2 – Methods

2.2.1 – Animals

Female BALB/c and C57BL/6 mice were obtained from Harlan Olac (Bicester, United Kingdom) and were used at 9-16 weeks old. C3H/HeN and C3H/HeJ mice were obtained from Harlan Olac and bred in the TCD Bioresources Unit. IL-1R KO mice were obtained from Jackson Laboratories (Maine, United States of America) and bred in the TCD Bioresources Unit. NLRP3 KO breeding pairs were provided by the late Prof. Jurg Tschopp (Department of Biochemistry, University of Lausanne, Switzerland) and bred in the TCD Bioresources Unit. ASC KO mice were obtained from Genentech (California, United States of America) and bred in the Smurfit Institute of Genetics in TCD. Animals were maintained according to the regulations of the European Union and the Irish Department of Health. Animal studies were approved by the TCD Animal Research Ethics Committee (Ethical Approval Number 091210) and were performed under the appropriate licence (Licence Number B100/3321).

2.2.2 – Cell culture

Cells were cultured at 37°C with an atmosphere maintained at 95% humidity and 5% CO_2.

2.2.2.1 – Cell viability and counting

Cell viability was determined using a trypan blue exclusion method. 10µl of the cell suspension was added to 90µl of trypan blue and 10µl of this solution was loaded onto a KOVA Glasstic cell counter slide with grids (Hycor Biomedical Inc.). Cells were viewed under a light microscope and cell viability was assessed by dye exclusion. The number of cells/ml was ascertained using the following formula:

$$\text{number of cells/ml} = \text{cell number} \times 10^4 \text{ cells/ml} \times \text{dilution factor}$$

2.2.2.2 – Culture of J558 GM-CSF-expressing cell line

The murine gene for GM-CSF was cloned into a mammalian expression vector and transfected into the plasmacytoma line X63-AgS. These cells were grown for two passages in tissue culture flasks containing complete RPMI supplemented with the antibiotic Geneticin (Gibco, final concentration of

1mg/ml Geneticin) and were incubated at 37°C in a humidified environment (5% CO_2). Following the completion of the second passage, the cells were washed with complete RPMI and re-seeded at 1 x 10^6 cells/ml in the absence of Geneticin. The cells were cultured to a medium density for the first passage without Geneticin and were re-seeded at lower concentrations (2.5 x 10^5 cells/ml) for subsequent passages. The supernatant was collected from each passage up until passage nine. The supernatants were pooled and the concentration of GM-CSF was determined by ELISA (Section 2.2.4).

2.2.2.3 – Isolation and culture of murine BMDCs

Murine BMDCs were prepared using protocols adapted from Lutz *et al.* [23]. Female mice (BALB/c, C3H/HeN, C3H/HeJ and C57BL/6 strains) were euthanized by cervical dislocation and their femurs and tibia were dissected from the surrounding muscle tissue. Using a 27G needle, the bone marrow was flushed aseptically from the femurs and tibia with complete RPMI. Aggregates of bone marrow cells were dispersed using a 19G needle and the cell suspension was pelleted by centrifugation at 1200 revolutions per minute (rpm) for 5 minutes at 4°C. The supernatant was decanted and the cell pellet was resuspended in 1ml of NH_4Cl (0.88%) for 2 minutes before washing with complete RPMI. The cell suspension was pelleted once again by centrifugation (1200rpm for 5 minutes at 4°C). The supernatant was decanted and the cell pellet was resuspended in 10ml of complete RPMI. Cell numbers were determined as described in Section 2.2.2.1. Bone marrow cells were seeded at 1 x 10^6 cells/ml (BALB/c, C3H/HeN and C3H/HeJ) or 4 x 10^5 cells/ml (C57BL/6) in tissue culture flasks (Greiner BioOne) containing 30ml of complete RPMI supplemented with supernatant obtained from a GM-CSF-expressing J558 cell line (final concentration of 20ng/ml GM-CSF unless otherwise stated). The culture of this J558 cell line is described in Section 2.2.2.2. The flasks were incubated at 37°C in a humidified atmosphere (5% CO_2).

After 3 days of incubation, an additional 30ml of complete RPMI supplemented with GM-CSF was added to each of the tissue culture flasks. On day 6, the supernatant from each flask was discarded in order to remove any non-adherent cells from the culture. 30ml of sterile PBS, preheated at 37°C, was added to each flask. The cells were removed from the surface of the flask by repeated pipetting. The PBS was collected from each flask and added to a 50ml falcon tube (Greiner BioOne) containing 10ml of complete RPMI. 30ml of sterile 0.02% Ethylenediaminetetraacetic Acid (EDTA) solution, preheated at 37°C, was added to each flask. The flasks were incubated for 10 minutes at 37°C before

the cells were removed by repeated pipetting. The EDTA solution was removed from each flask and subsequently added to a 50ml falcon tube containing 10ml of complete RPMI. The cells in each of the 50ml falcon tubes were pelleted by centrifugation (1200rpm for 5 minutes at 4°C). The cell pellets were resuspended and pooled in 10ml of complete RPMI, counted as described in Section 2.2.2.1 and seeded at 7 x 10^5 cells/ml (BALB/c, C3H/HeN and C3H/HeJ) or 4.2 x 10^5 cells/ml (C57BL/6) in complete RPMI supplemented with GM-CSF.

On day 7, an additional 30ml of complete RPMI supplemented with GM-CSF was added to each of the tissue culture flasks. On day 10, loosely adherent cells were harvested by gentle repeat pipetting. The cells were pelleted by centrifugation (1200rpm for 5 minutes at 4°C) and resuspended in 10ml of complete RPMI. Cell numbers were determined as described in Section 2.2.2.1 and the cells were plated at 6.25 x 10^5 cells/ml (BALB/c, C3H/HeN, C3H/HeJ and C57BL/6) in 200µl complete RPMI supplemented with GM-CSF (final concentration of 10ng/ml GM-CSF) in 96-well round bottom tissue culture plates (Greiner BioOne).

On day 11, the cells were stimulated with the appropriate treatments. The specific treatments and conditions for stimulation of BMDCs are outlined in each experimental figure legend. Supernatants were collected 24 hours later for analysis of cytokine levels by ELISA. Following the removal of supernatants, the cells were harvested and assessed for maturation by flow cytometry.

2.2.2.4 – Isolation and culture of splenocytes

Female mice (BALB/c and C57BL/6) were euthanized by cervical dislocation and their spleens were isolated. The spleens were homogenised and passed through a 70µm cell strainer (BD) to obtain a single cell suspension. The cell suspension was pelleted by centrifugation (1200rpm for 5 minutes at 4°C). The supernatant was decanted and the cells were resuspended in 1ml of NH_4Cl (0.88%) for 2 minutes before washing with complete RPMI. The cell suspension was pelleted once again by centrifugation (1200rpm for 5 minutes at 4°C). The supernatant was decanted and the splenocytes were resuspended in 5ml of complete RPMI. Cell numbers were determined as described in Section 2.2.2.1. Splenocytes were plated at 2 x 10^6 cells/ml in 200µl complete RPMI in 96-well round bottom tissue culture plates. Splenocytes were restimulated *ex vivo* with the appropriate treatments. The specific treatments and conditions for restimulation of splenocytes are outlined in each experimental

figure legend. The tissue culture plates were incubated at 37°C in a humidified atmosphere (5% CO_2). Supernatants were collected 72 hours later for analysis of cytokine levels by ELISA.

2.2.2.5 – Isolation and culture of lymph node cells

Female mice (BALB/c and C57BL/6) were euthanized by cervical dislocation and the appropriate lymph nodes were isolated. The lymph nodes were homogenised and passed through a 70µm cell strainer to obtain a single cell suspension. The cell suspension was pelleted by centrifugation (1200rpm for 5 minutes at 4°C). The supernatant was decanted and the lymph node cells were resuspended in 1ml of complete RPMI. Cell numbers were determined as described in Section 2.2.2.1. Lymph node cells were plated at 1 x 10^6 cells/ml in 200µl complete RPMI in 96-well round bottom tissue culture plates. Lymph node cells were restimulated *ex vivo* with the appropriate treatments. The specific treatments and conditions for restimulation of lymph node cells are outlined in each experimental figure legend. The tissue culture plates were incubated at 37°C in a humidified atmosphere (5% CO_2). Supernatants were collected 72 hours later for analysis of cytokine levels by ELISA.

2.2.2.6 – Isolation and culture of PECs

Female mice (BALB/c, C57BL/6, C3H/HeN, C3H/HeJ, NLRP3 KO, IL-1R KO and ASC KO) were euthanized by cervical dislocation. The peritoneal cavity was washed with 5ml of ice-cold PBS. The wash volume was collected and the PECs were pelleted by centrifugation (1200rpm for 5 minutes at 4°C). The supernatant was collected and the PECs were resuspended in 1ml of complete RPMI. PEC numbers were determined as described in Section 2.2.2.1. PECs were plated at 1 x 10^6 cells/ml in 200µl complete RPMI in 96-well round bottom tissue culture plates. PECs were restimulated *ex vivo* with the appropriate treatments. The specific treatments and conditions for restimulation of PECs are outlined in each experimental figure legend. The tissue culture plates were incubated at 37°C in a humidified atmosphere (5% CO_2). Supernatants were collected either 24 or 72 hours later (indicated in figure legend) for analysis of cytokine levels by ELISA.

2.2.3 – Flow cytometry

2.2.3.1 – BMDCs

Following the removal of supernatants from 96-well tissue culture plates, BMDCs were resuspended in 200µl FACS buffer and transferred into separate FACS tubes (BD Falcon). The cells were pelleted by centrifugation (1200rpm for 5 minutes at 4°C). The supernatant was decanted and the cells were resuspended in 100µl of FACS buffer supplemented with anti-mouse CD16/CD32 monoclonal antibody (dilution outlined in Table 2.3). The cells were subsequently incubated at 4°C for 10 minutes. Fluorochrome-labelled anti-CD11c and antibodies specific for the DC maturation markers CD80, CD40 and MHC class II were then added to the cells (dilutions outlined in Table 2.3). The cells were incubated with the above antibodies for 30 minutes on ice in the dark and were then washed with 2ml of FACS buffer. The cells were centrifuged (1200rpm for 5 minutes at 4°C) and resuspended in 300µl of FACS buffer before being analysed for immunofluorescence. Necrotic cells were identified by adding PI staining solution (dilution outlined in Table 2.2) directly to the samples immediately prior to their acquisition on the flow cytometer. Samples were acquired using summit software (Dako, Colorado) and the data was analysed using Flowjo™ software (Treestar, Oregon).

2.2.3.2 – PECs

PECs were plated at 1 x 10^6 cells/ml in a 250µl volume of PBS in a 96-well round bottom tissue culture plate and were pelleted by centrifugation (1200rpm for 5 minutes at 4°C). The supernatant was decanted and the cell pellet was resuspended in an additional 250µl volume of PECs at a concentration of 1 x 10^6 cells/ml. This yielded a total of 5 x 10^5 cells per well. The cell suspension was pelleted by centrifugation (1200rpm for 5 minutes at 4°C). The supernatant was decanted and the cells were resuspended in 250µl of PBS supplemented with LIVE/DEAD fixable AQUA dead cell stain (dilution outlined in Table 2.2). The cells were subsequently incubated at 4°C for 30 minutes. The cell suspension was pelleted by centrifugation (1200rpm for 5 minutes at 4°C). The supernatant was decanted and the cells were resuspended in 200µl PBS. The cell suspension was pelleted by centrifugation (1200rpm for 5 minutes at 4°C). The supernatant was decanted and the cells were resuspended in 100µl FACS buffer supplemented with anti-mouse CD16/CD32 monoclonal antibody (dilution outlined in Table 2.4). The cells were subsequently incubated at 4°C for 10 minutes. PECs were then incubated with the relevant fluorochrome-labelled antibodies for 30 minutes on ice in the

dark (dilutions outlined in Table 2.4). After 30 minutes, the cell suspension was pelleted by centrifugation (1200rpm for 5 minutes at 4°C). The supernatant was decanted and the cell pellet was resuspended in 200µl FACS buffer. PECs were centrifuged (1200rpm for 5 minutes at 4°C) and the supernatant was decanted before the cells were resuspended in 200µl FACS buffer for analysis of immunofluorescence. Samples were acquired using summit software (Dako, Colorado) and the data was analysed using Flowjo™ software (Treestar, Oregon).

2.2.4 – Measurement of cytokine secretion by ELISA

Concentrations of the cytokines TNF-α, IL-1β, IL-1α, IL-10, IL-17, IL-12p70 and GM-CSF were measured using ELISA kits obtained from R&D systems. 96-well high binding ELISA plates (Greiner Bio-one) were coated with 40µl per well of rat anti-mouse capture antibody diluted in PBS (dilutions outlined in Table 2.5) and were incubated overnight at 4°C. The ELISA plates were washed with 0.05% PBS-Tween and incubated with 100µl per well of blocking solution (see Table 2.5) for 2 hours at room temperature. The blocking solution was washed from the ELISA plates with 0.05% PBS-Tween before samples and standards (recombinant cytokines of known concentration) were diluted in 1% BSA and added to the plates (top working standards outlined in Table 2.5). The ELISA plates were incubated overnight at 4°C and were subsequently washed in 0.05% PBS-Tween. 40µl per well of biotinylated goat anti-mouse detection antibody diluted in 1% BSA (dilutions outlined in Table 2.5) was added to the plates which were incubated for 2 hours at room temperature in the dark. The ELISA plates were then washed with 0.05% PBS-Tween and incubated with 40µl per well of horseradish-peroxidase (HRP)-conjugated streptavidin (1/200 dilution of stock, R&D) diluted in 1% BSA for 20 minutes at room temperature in the dark. Following this incubation step, the ELISA plates were once again washed with 0.05% PBS-Tween. 0-phenylenediamine dihydrochloride (OPD) substrate was dissolved in phosphate citrate buffer (0.4mg/ml OPD) and hydrogen peroxide (0.7µl hydrogen peroxide per 1mg of OPD) was added to the solution. 40µl per well of this solution was added to the ELISA plates which were allowed to develop for the required time in the dark. The enzyme reaction was halted by addition of 20µl per well of sulfuric acid (1M). The OD values were measured at 492nm using a Versa Max Microplate Reader. A standard curve was generated and this was then used to determine the cytokine concentration of the unknown replicates.

Concentrations of the cytokines IL-6, IL-12p40, IL-4, IL-5 and IFN-γ were measured using ELISA kits obtained from BD Pharmingen. 96-well high binding ELISA plates were coated with 40µl per well of rat anti-mouse capture antibody diluted in PBS (dilutions outlined in Table 2.5) and incubated overnight at 4°C. The ELISA plates were washed with 0.05% PBS-Tween and blocked with 100µl per well of blocking solution (see Table 2.5) for 2 hours at room temperature. The blocking solution was washed from the ELISA plates with 0.05% PBS-Tween before samples and standards (recombinant cytokines of known concentration) were diluted in PBS and added to the plates (top working solutions outlined in Table 2.5). The ELISA plates were incubated overnight at 4°C and were subsequently washed with 0.05% PBS-Tween. 40µl per well of biotinylated goat anti-mouse detection antibody diluted in PBS (dilutions outlined in Table 2.5) was added to the plates which were incubated in the dark for 1 hour at room temperature. The ELISA plates were then washed with 0.05% PBS-Tween and incubated with 40µl per well of HRP-conjugated streptavidin (700ng/ml, Sigma-Aldrich) diluted in PBS for 20 minutes at room temperature in the dark. Following this incubation step, the ELISA plates were once again washed with 0.05% PBS-Tween. OPD substrate was dissolved in phosphate citrate buffer (0.4mg/ml OPD) and hydrogen peroxide (0.7µl hydrogen peroxide per 1mg of OPD) was added to the solution. 40µl per well of this solution was added to the ELISA plates which were allowed to develop for the required time in the dark. The enzyme reaction was halted following the addition of 20µl per well of sulfuric acid (1M). The OD values were measured at 492nm using a Versa Max Microplate Reader. A standard curve was generated and this was then used to determine the cytokine concentration of the unknown replicates.

2.2.5 - Measurement of antigen-specific serum antibodies by ELISA

Serum concentrations of antigen-specific total IgA and IgG as well as the IgG subtypes IgG1, IgG2a, IgG2b and IgG2c were determined using commercially available antibodies obtained from BD Pharmingen. 96-well medium binding ELISA plates (Greiner Bio-one) were coated with 50µl per well of OVA (50µg/ml) diluted in carbonate buffer and incubated overnight at 4°C. The ELISA plates were washed with 0.05% PBS-Tween and blocked with 100µl per well of 10% marvel dried milk. The blocking solution was washed from the ELISA plates with 0.05% PBS-Tween before the serum samples were diluted in PBS and added to the plates. The samples were serially diluted across the plate and incubated overnight at 4°C. 50µl per well of biotinylated anti-mouse detection antibody diluted in PBS (dilutions outlined in Table 2.6) was added to the plates which were incubated in the

dark for 1 hour at 37°C. The ELISA plates were then washed with 0.05% PBS-Tween and incubated with 50µl per well of HRP-conjugated streptavidin (700ng/ml) diluted in PBS for 20 minutes at room temperature in the dark. Following this incubation step, the ELISA plates were once again washed with 0.05% PBS-Tween. OPD substrate was dissolved in phosphate citrate buffer (0.4mg/ml OPD) and hydrogen peroxide (0.7µl hydrogen peroxide per 1mg of OPD) was added to the solution. 50µl per well of this solution was added to the ELISA plates which were allowed to develop for the required time in the dark. The enzyme reaction was halted following the addition of 25µl per well of sulfuric acid (1M). The OD values were obtained using a Versa Max Microplate Reader measuring absorbance at 492nm. Antibody concentrations were expressed as endpoint titres calculated by regression of a curve of OD values versus reciprocal serum levels to a cut off point of 2 standard deviations.

Alternatively, 96-well medium binding ELISA plates were coated with 50µl per well of HSA (50µg/ml) diluted in carbonate buffer and incubated overnight at 4°C. Measurement of HSA-specific serum antibody titres was then performed in an identical fashion to that described above for measurement of OVA-specific serum antibody titres.

2.2.6 – Western blot analysis

2.2.6.1 – Protein extraction from supernatants

BMDCs (derived from female C57BL/6 mice) were plated at 6.25 x 10^5 cells/ml in 1ml of complete RPMI supplemented with GM-CSF (final concentration of 10ng/ml GM-CSF) in a 12-well round bottom tissue culture plate (Greiner BioOne). The cells were pelleted by centrifugation (1200rpm for 5 minutes at 4°C) 24 hours after the appropriate stimulation. Supernatants were collected and 500µl of this volume was mixed with 500µl of methanol and 100µl of chloroform. The resulting solution was centrifuged at 13000 rpm for 5 minutes and the supernatant was removed. An additional 500µl of methanol was added to the remaining solution which was then centrifuged at 13000rpm for 5 minutes. The supernatant was removed and the protein pellet was air dried for 1 hour. The protein pellet was resuspended in 50µl of SDS-PAGE sample buffer and heated at 99°C for 5 minutes.

2.2.6.2 – SDS-PAGE

The stop buffer was poured and allowed to set for 30 minutes before the resolving and stacking gels were poured respectively (Table 2.7). Once the resolving gel was set, 20µl of sample was loaded into each well in addition to 8µl of a protein molecular weight ladder (Biorad Dual Colour 5-75kDa). Once the samples were loaded, the gel was run at 120 volts (V) for 90 minutes in running buffer.

2.2.6.3 – Transfer of proteins onto nitrocellulose membrane

The transfer of proteins onto a nitrocellulose membrane was performed using a semi-dry blotter (Cleaver Scientific Ltd). The gel was removed from the glass plates and placed onto a sheet of filter paper that had been soaked in transfer buffer. The nitrocellulose membrane was also soaked in transfer buffer and placed carefully over the gel. An additional sheet of moist filter paper was placed on top of the nitrocellulose membrane. Great care was taken to ensure that there were no air bubbles in the system and the proteins were transferred for 1 hour at 300 milliamperes (mA).

2.2.6.4 – Immunodetection of proteins

All steps encompassed in the detection stage of western blotting were carried out on a rocker. The membrane was washed in 0.1% PBS-Tween for 5 minutes and blocked for 1 hour with 20ml of 5% milk in 0.1% PBS-Tween. The membrane was washed six times for 5 minutes in 0.1% PBS-Tween and was then probed with 5ml of primary antibody (dilution outlined in Table 2.8) for 1 hour at room temperature. The membrane was washed three times in 0.1% PBS-Tween and probed with HRP-conjugated secondary antibody (dilution outlined in Table 2.8) for 1 hour at room temperature. The membrane was then washed three times in 0.1% PBS-Tween and developed with freshly prepared luminol-based detection solution.

2.2.7 – Protein concentration assay

The BCA protein assay kit was used to measure protein concentration. The procedure was performed according to the manufacturer's protocol as described below. BSA protein standards ranging from 0-2000µg/ml were prepared and 25µl of each standard and unknown replicate were pipetted in

triplicate onto a 96-well flat bottom tissue culture plate (Greiner BioOne). The BCA assay working reagent was next prepared by mixing 50 parts of BCA reagent A (containing sodium bicarbonate, bicinchoninic acid and sodium tartrate in 0.1M sodium hydroxide) with 1 part of BCA reagent B (containing 4% cupric sulphate). 200µl of the working reagent was added to each well and the plate was incubated for 30 minutes at 37°C. The plate was cooled to room temperature for 10 minutes and the absorbance values were measured at 562nm using a Versa Max Microplate Reader. The average 562nm absorbance measurement of the blank standard replicates was subtracted from the 562nm measurements of all other individual standard and unknown sample replicates. A standard curve was prepared and this was then used to determine the protein concentration of each unknown sample.

2.2.8 – Defining metabolic profile of obese individuals

Metabolically healthy obese (MHO) patients had no history of cardiovascular, respiratory or metabolic diseases. They were not on any lipid-lowering, anti-hypertensive or hypoglycaemic agents. Clinical examination was unremarkable and thyroid status was normal. Fasting glucose level was <5.6 millimoles (mmol)/L, blood pressure was <135/85, and triglyceride/high-density lipoprotein (HDL) cholesterol ratio was <1.65 (men) or <1.32 (women). These cut-off points were adapted from the International Diabetes Federation worldwide consensus definition of the metabolic syndrome, 2006. The plasma triglyceride/HDL cholesterol concentration ratio was used as this has been shown to provide a simple means of identifying insulin-resistant, dyslipidemic individuals who are likely to be at increased risk of cardiovascular disease. Metabolically unhealthy obese (MUO) patients were defined by failure to meet at least one of the criteria above.

2.2.9 – Histology

The histology work in this project was carried out in collaboration with Dr. Jean O'Connell (Obesity Group, St. Vincent's University Hospital, Elm Park, Dublin 4, Ireland) and Prof. Sean Callanan (School of Agriculture, Food Science and Veterinary Medicine, University College Dublin, Belfield, Dublin 4, Ireland). The embedding and sectioning was carried out by Dr. Jean O'Connell and the haematoxylin and eosin (H&E) staining was performed by Prof. Sean Callanan. This work was approved by the St Vincent's University Hospital Ethics and Medical Research Committee.

Approximately 10-30 grams of omental adipose tissue was obtained at the time of bariatric surgery. A piece of this tissue was immediately fixed in formalin, prior to paraffin mounting and preparation of H&E slides.

Adipocyte size was determined using Image Pro Plus 7 Software. The mean diameter of a range of adipocytes from 5 MHO individuals and 5 MUO individuals was calculated from 10 separate photographs of randomised areas of the same section.

2.2.10 - Animal studies

2.2.10.1 - Intraperitoneal injection with full-length and GzmB-processed HRF for 4 consecutive days

Female BALB/c mice were injected i.p. for 4 consecutive days with PBS or 1μg of either full-length HRF or GzmB-processed HRF (200μl volume). On day 5, the mice were sacrificed by cervical dislocation and splenocytes as well as mesenteric and mediastinal lymph nodes were isolated and cultured as described previously (Section 2.2.2.4 and Section 2.2.2.5).

2.2.10.2 - Intraperitoneal injection with full-length and GzmB-processed IL-1α for 4 consecutive days

Female BALB/c mice were immunised i.p. for 4 consecutive days with PBS or 1μg of either full-length IL-1α or GzmB-processed IL-1α (200μl volume). On day 5, the mice were sacrificed by cervical dislocation and splenocytes, mesenteric and mediastinal lymph nodes and PECs were isolated and cultured as described previously (Section 2.2.2.4, Section 2.2.2.5 and Section 2.2.2.6). PECs were also analysed by flow cytometry.

2.2.10.3 - Adjuvant model

Female mice (BALB/c and C57BL/6) were injected i.p. on day 0 with PBS as a control or a model antigen (nature and concentration of antigen indicated in each experimental figure legend) either alone or mixed with specific treatments (outlined in each experimental figure legend) (200μl volume). Where indicated in the figure legend, a blood sample was collected from the tail of the

mice on day 13. The serum was separated by density gradient centrifugation, and antigen-specific antibody titres were determined by ELISA (Section 2.2.5). The mice were boosted i.p. with these same treatments on day 14 and were sacrificed by cervical dislocation on day 21. Blood was recovered and antigen-specific antibody titres in the serum were determined by ELISA (Section 2.2.5). Any additional tissues isolated from the mice for each of the adjuvant studies are outlined in the respective figure legends and were isolated and cultured as described previously (Section 2.2.2.4, Section 2.2.2.5 and Section 2.2.2.6).

2.2.10.4 - Peritonitis model

Female mice (C57BL/6, C3H/HeN, C3H/HeJ, NLRP3 KO, IL-1R KO and ASC KO) were injected i.p. with the specific treatments and volumes outlined in each experimental figure legend. The mice were euthanized by cervical dislocation at the time points indicated in each experimental figure legend. The peritoneal cavity was washed with 5ml of ice-cold PBS. The wash volume was collected and the PECs were harvested for FACS analysis and/or *ex vivo* restimulation (See Section 2.2.3.2 and 2.2.2.6). Where indicated, PEC supernatants and serum were also collected and cytokine levels were measured by ELISA.

2.2.11 – Statistical analysis

Statistical analysis was performed using Graphpad Prism 5 software. The means for three or more groups were compared by one-way ANOVA. Where significant differences were found, the Tukey-Kramer multiple comparisons test was used to identify differences between individual groups. The means for two groups were compared using an unpaired Student's t test.

Chapter 3

An Evaluation of the Dose Response of Murine Dendritic Cell Activation by LPS, and the Capacity of Polymyxin B to Reverse this Effect

3.1 - Introduction

LPS is a major component of the outer membrane of Gram-negative bacteria. This pyrogen is essential in maintaining the structural integrity of bacteria and repelling antimicrobial responses. LPS is a potent endotoxin comprised of a repetitive glycan polymer referred to as the O-antigen, which is connected to the core polysaccharide. The core domain is directly attached to Lipid A which is a phosphorylated glucosamine disaccharide containing multiple fatty acids which serve to secure the LPS molecule to the bacterial membrane (Figure 3.1). LPS is a PAMP known to signal through the CD14/TLR4/MD-2 receptor complex, thereby promoting innate immune responses characterised by rapid secretion of proinflammatory cytokines and chemokines [179, 181-183]. Importantly, the Lipid A moiety is mainly responsible for these immunostimulatory effects [515-516].

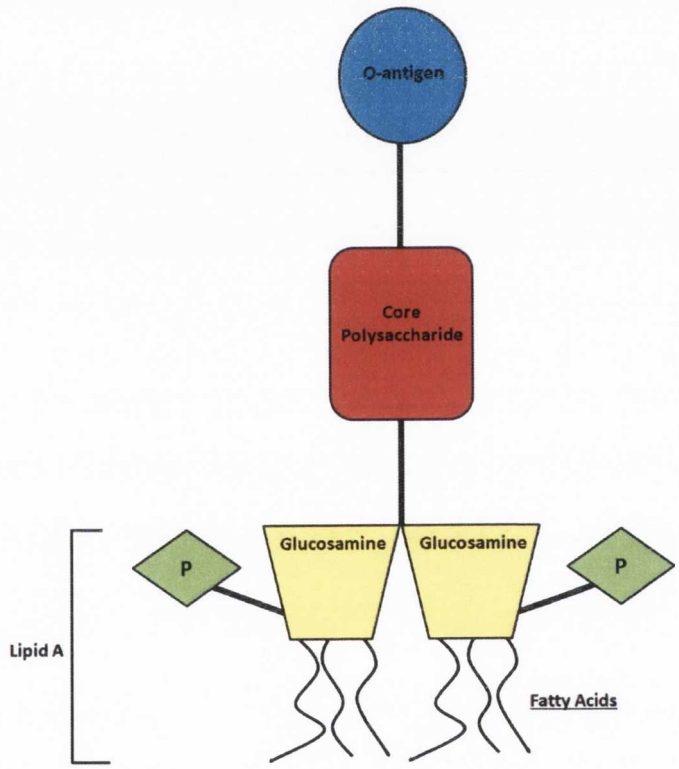

Figure 3.1 – LPS structure. LPS contains Lipid A, a phosphorylated (P) glucosamine disaccharide containing multiple fatty acids, attached directly to a polysaccharide tail which comprises a core polysaccharide chain linked with the O-antigen.

In studies assessing the effects of candidate microbial and endogenous immunomodulators, LPS contamination of sample preparations has proven to be a hugely significant problem, often resulting in misleading and inaccurate conclusions. For example, one need look no further than the ambiguities associated with many of the more established endogenous danger signals identified thus far in order to gauge the magnitude of the problem concerning residual LPS contamination [517].

In 1999, an immunomodulatory role for HMGB1 was proposed; stimulation of monocyte cultures with HMGB1 induced secretion of a range of proinflammatory mediators including TNF-α, IL-1β, IL-1α, IL-1ra, IL-6, IL-8, MIP-1α and MIP-1β. HMGB1 has since been shown to play important roles in both innate and adaptive immunity [319-320, 325-327]. However, recent studies have contradicted many of the above findings, demonstrating that a highly purified form of recombinant HMGB1 fails to induce cytokine secretion from mouse or human macrophages [339]. Furthermore, the direct proinflammatory activity of HMGB1 reported previously and described above is likely to be a result of contamination with bacterial components as most of these studies were performed using recombinant HMGB1 derived from *E. coli* expression systems. Hsp60, Hsp70, Hsp90 and gp96 have all been reported to stimulate DC [364-367] and macrophage activation [366, 368-370]. However, Wallin and colleagues noted that highly purified murine liver Hsp70 failed to stimulate cytokine secretion from murine DCs. In contrast, an Hsp70 preparation contaminated with low levels of LPS induced cytokine secretion at concentrations as low as 50ng/ml, and these effects were not inhibited by PmB and were also heat-sensitive [384]. In recent years many reports have been published which consistently outline the failure of highly purified Hsp molecules to stimulate immune responses in the absence of contaminating PAMPs [381, 383-384, 386].

In vitro, heparan sulfate degradation products and hyaluronic acid fragments stimulate activation of DCs and endothelial cells [403, 405]. However, many studies have reported a role for TLR4 [405, 409], and to a lesser extent TLR2 [406], in regulating the alarmin function of these fragments. Despite these encouraging studies, caution must be warranted given that these fragments signal through TLR4. These concerns are heightened by the finding that highly purified pharmacological-grade hyaluronic acid fragments fail to induce NF-κB activation or cytokine secretion in murine macrophages [410].

DC activation, as measured by cytokine secretion and increased expression of costimulatory and MHC molecules, is commonly used as a measure of the potency of candidate immunomodulators, particularly endogenous danger signals. However, it is important to note that many recombinant

protein preparations are derived from bacterial expression systems. Thus, residual LPS contamination is a significant issue and the potency of LPS is not always fully appreciated. To address this, PmB is often used to neutralise contaminating LPS. However, the limited capacity of this antibiotic to successfully block these effects is neglected. Therefore, in order to characterise the immunomodulatory effects of candidate molecules with confidence, it is crucial to address this key issue. This study aimed to determine the minimum LPS concentration required to induce DC maturation and cytokine secretion, and to assess the ability of PmB to inhibit these processes.

3.2 - Results

3.2.1 - Different thresholds exist for secretion of specific cytokines by DCs in response to LPS

In order to assess proinflammatory cytokine secretion by DCs in response to LPS, murine BMDCs were stimulated with concentrations from 1pg/ml to 1μg/ml *E. coli* LPS. LPS concentrations as low as 10pg/ml and 20pg/ml were sufficient to induce secretion of IL-6 (Figure 3.2A) and TNF-α (Figure 3.2B) respectively, while maximal secretion of these cytokines was evident when a concentration of 500pg/ml LPS was added (Figure 3.2A, 3.2B).

LPS concentrations of 50pg/ml and 500pg/ml were required to promote detectable secretion of IL-12p40 (Figure 3.2C) and IL-12p70 (Figure 3.2D) respectively, while maximal secretion of both of these cytokines was reached following stimulation with 50ng/ml LPS (Figure 3.2C, 3.2D).

3.2.2 - A concentration of 50pg/ml LPS is sufficient to increase DC surface expression of costimulatory and MHC class II molecules

DC activation is also characterised by increased expression of surface markers, including CD80, CD40 and MHC class II, in a process referred to as maturation. In order to evaluate the dose response of DC maturation by LPS, murine BMDCs were stimulated with concentrations from 1pg/ml to 1μg/ml LPS. A concentration as low as 50pg/ml LPS was sufficient to upregulate surface expression of CD80, CD40 and MHC class II (Figure 3.3). Furthermore, maximal BMDC maturation was achieved when an LPS concentration of 1ng/ml was used (Figure 3.3).

3.2.3 - 10μg/ml PmB is the optimal concentration for inhibiting LPS-induced DC activation

PmB is often used to neutralise contaminating LPS in sample preparations and therefore to eliminate the possibility that residual LPS may be responsible for any immunostimulatory effects observed. In order to determine the optimal PmB concentration for treating murine BMDCs without eliciting toxicity or maturation, these cells were stimulated with concentrations from 0.01μg/ml to 500μg/ml PmB. Notably, concentrations of 100μg/ml PmB and higher were toxic to BMDCs (Figure 3.4A) and a concentration of 50μg/ml PmB was sufficient to enhance expression of CD80, CD40 and MHC II

(Figure 3.4B). Therefore, 10μg/ml PmB was determined to be the optimal concentration for inhibiting LPS-induced DC activation without having any direct effect on the cells.

3.2.4 - The ability of PmB to reverse secretion of proinflammatory cytokines by DCs in response to LPS is cytokine-dependent

In order to assess the ability of PmB to inhibit proinflammatory cytokine secretion by DCs in response to LPS, murine BMDCs were stimulated with concentrations from 1pg/ml to 1μg/ml LPS, which were pre-incubated alone or in the presence of 100μg/ml PmB for 2 hours at 37^0C. Following pre-incubation of LPS with PmB, the final concentration of PmB added to the cells was 10μg/ml.

The efficacy of PmB in suppressing secretion of proinflammatory cytokines was cytokine-dependent. When measuring IL-6, the inhibitory properties of PmB began to subside when LPS concentrations greater than 0.5ng/ml were used. Furthermore, the ability of PmB to inhibit IL-6 secretion continued to decrease proportionally with increasing LPS concentrations until it was completely ineffective at concentrations greater than 50ng/ml (Figure 3.5A). The capacity of PmB to inhibit LPS-induced TNF-α production was limited at LPS concentrations higher than 1ng/ml. Moreover, following a steady decline in efficacy coinciding with increased concentrations of LPS, PmB was rendered entirely redundant when concentrations greater than 200ng/ml LPS were used (Figure 3.5B). In contrast, the inhibitory properties of PmB on IL-12p40 were almost completely preserved until an LPS concentration of 20ng/ml (Figure 3.5C) was used, whereas PmB was very effective at inhibiting BMDC secretion of IL-12p70 at all concentrations of LPS tested (Figure 3.5D).

3.2.5 - PmB is limited in its capacity to inhibit DC maturation in response to LPS

In order to assess the ability of PmB to inhibit DC maturation in response to LPS, murine BMDCs were stimulated with concentrations from 1pg/ml to 1μg/ml LPS, which was pre-incubated alone or in the presence of 100μg/ml PmB for 2 hours at 37^0C. Again, the final concentration of PmB added to the cells was 10μg/ml. Importantly, LPS-driven BMDC maturation was no longer completely inhibited by PmB at concentrations greater than 20ng/ml (Figure 3.6A). Furthermore, the efficacy of PmB in suppressing this effect decreased proportionally with increasing concentrations of LPS (Figure 3.6B).

3.2.6 - Following heat treatment, low concentrations of LPS fail to promote secretion of the proinflammatory cytokines IL-6 and IL-12p40 by DCs

A second strategy used to determine if contaminating LPS is responsible for immunomodulatory effects is heat-inactivation of the protein [518-520]. Following heating to high temperatures, a protein is presumed to become unstable and thus inactivated, whereas any LPS present in the preparation remains stable and intact. It can therefore be inferred that if the immunostimulatory response persists after heat-inactivation, it is a direct result of LPS contamination. Conversely, if the response is no longer observed after heat-inactivation then the protein is deemed to mediate the response rather than any contaminating LPS. However, Gao and colleagues have previously shown that following heat treatment, low concentrations of LPS fail to promote secretion of TNF-α by murine macrophages [381, 383].

As mentioned above, secretion of proinflammatory cytokines by DCs, particularly IL-6 and IL-12p40, is often used as a means to assess the immunomodulatory potential of candidate microbial and endogenous immunomodulators. In order to determine the effect of heat treatment on the ability of low concentrations of LPS to promote secretion of IL-6 and IL-12p40 by murine BMDCs, these primary cells were stimulated with LPS or heat-inactivated LPS (100°C or 60°C). A concentration of 50pg/ml LPS induced secretion of IL-6 and IL-12p40 by BMDCs, but this response was attenuated when heat-inactivated LPS was used (Figure 3.7).

3.2.7 - 5pg/ml LPS is sufficient to promote secretion of the proinflammatory cytokine IL-6 in the presence of *E. coli* heat-labile enterotoxin

Some of the more established endogenous danger signals, such as HMGB1, Hsps and small breakdown products of hyaluronic acid, have been reported to synergise with TLR agonists to promote a more potent inflammatory response than that generated against either component alone [342, 388-389, 407]. Furthermore, bacterial toxins including cholera toxin (CT), pneumolysin (PLY) and *E. coli* heat-labile enterotoxin (LT) can also elicit synergistic effects when used in combination with TLR agonists, in particular enhancing BMDC secretion of IL-6 [521-522]. This suggests that contaminating LPS concentrations which are incapable of promoting BMDC secretion of proinflammatory cytokines independently may synergise with candidate immunomodulators to

enhance this effect, thus reducing even further the minimal LPS concentration required for BMDC activation.

In order to establish if concentrations of LPS that are incapable of promoting cytokine secretion by BMDCs independently can synergise with a bacterial toxin to potentiate cytokine secretion, murine BMDCs were stimulated with suboptimal concentrations of LPS, either alone or in the presence of *E. coli* LT. Subsequently, BMDC secretion of IL-6 was measured. The presence of *E. coli* LT significantly augmented IL-6 secretion from BMDCs in response to as little as 5pg/ml LPS, which did not activate BMDCs in the absence of *E. coli* LT (Figure 3.8).

3.3 - Discussion

DCs are professional APCs capable of linking innate and adaptive immunity. Following recognition of an activating stimulus, DCs initiate signal transduction cascades culminating in the synthesis and secretion of cytokines involved in promoting the onset of innate immunity and modulating subsequent effector T cell responses. Importantly, DCs have been classified into two discrete functional states, with each expressing a distinct phenotype. Immature DCs are highly efficient at antigen capture and processing, while mature DCs are potent APCs specialised for subsequent interactions with naive T cells [523-524]. DC activation is characterised by elevated surface expression of costimulatory molecules, including CD80 and CD40 as well as MHC molecules [38] in a process referred to as maturation. Interestingly, the term 'mature' is commonly used to describe DCs expressing high surface levels of costimulatory and MHC molecules, but is also used to describe immunogenic DCs capable of initiating adaptive immunity to foreign antigens. The discovery that non-immunogenic or immature DCs can also express elevated surface costimulatory and MHC molecules has been the main focus of recent reports which have questioned the apparent simplicity and transposable use of this terminology [38]. However, for the purpose of this study the term 'maturation' was used exclusively to define elevated expression of costimulatory and MHC molecules on the surface of BMDCs.

DC activation is often used as a means of determining the immunomodulatory properties of both PAMPs and host-derived danger signals. However, candidate danger signals are commonly purified from bacterial expression systems, particularly *E. coli*, and are frequently contaminated with bacterial PAMPs, especially LPS. Despite this problematic issue, many studies have failed to appreciate the potency of LPS and the profound ability of residual LPS contamination to induce DC activation.

In order to raise awareness of the potency of residual LPS, this study evaluated the dose response of DC activation by this PAMP. LPS concentrations as low as 10pg/ml and 20pg/ml were sufficient to induce BMDC secretion of the proinflammatory cytokines IL-6 and TNF-α respectively. Furthermore, a concentration of 50pg/ml LPS was adequate to enhance expression of costimulatory and MHC II molecules. The magnitude of both costimulatory molecule expression and cytokine secretion increased dramatically with elevated concentrations of LPS. However, with regard to LPS-induced secretion of IL-6 and TNF-α, maximal activation was achieved by relatively low concentrations of LPS, more specifically concentrations upwards of 500pg/ml. Therefore, when

using these readouts to assess potential immune activation properties of candidate molecules, particularly endogenous danger signals, it is essential to almost completely eliminate all of the LPS in the preparation in order to circumvent artificial and misleading conclusions.

Interestingly, this study also found that secretion of IL-12p40 and particularly IL-12p70 by BMDCs is less sensitive to LPS than secretion of IL-6 and TNF-α or surface expression of costimulatory and MHC molecules. More specifically, LPS concentrations of 50pg/ml and 500pg/ml were required to promote minimal secretion of IL-12p40 and IL-12p70 respectively, while maximal secretion of these cytokines was achieved by stimulating BMDCs with 50ng/ml LPS. Therefore, there are different thresholds for secretion of specific cytokines by DCs in response to LPS. Ultimately, it is important for researchers to be vigilant of this when assessing the immune activation properties of candidate molecules.

The molecular weight of LPS can vary a great deal due to the heterogeneity within the acyl chains and differential phosphorylation. In order to address this problem, the FDA has developed endotoxin units (EU) as an alternative to units of weight. EU describes the biological activity of LPS and a single EU is equal to approximately 100pg of *E. coli* LPS, the amount present in 1 x 10^5 bacteria. Many research laboratories use EU values to determine contaminating LPS concentrations in sample preparations, particularly when using LAL testing. It is important to note that 10pg/ml LPS is equivalent to as little as 0.1EU/ml.

The literature contains many studies reporting novel immunostimulatory properties for endogenous molecules, many of which signal through TLR4. However, many of these reports fail to use effective controls for residual LPS contamination.

Perhaps the most common control used to eliminate LPS contamination is the *Bacillus polymyxa*-derived antibiotic PmB. PmB possesses a very high binding affinity for the lipid A moiety of LPS, thus serving to neutralise this PAMP and prevent interaction with TLR4 [525]. However, the limitations of PmB in reversing the effects of DC activation are often neglected. This study has shown that the assumption that the presence of PmB eliminates LPS-mediated effects on DCs is inaccurate, and its effects are dependent on both the concentration of LPS present and the particular cytokines under investigation.

Many studies reporting immunomodulatory activity for endogenous danger signals routinely use a concentration of 10μg/ml PmB to antagonise residual LPS contamination [338, 397, 409, 526-528].

Indeed, higher concentrations of PmB are not normally used to inhibit LPS-mediated DC activation due to concerns over toxicity. By performing a dose response determination, this study has shown that 10μg/ml PmB is an appropriate concentration for inhibiting LPS-induced BMDC activation without eliciting any adverse effects on the cells. 50μg/ml PmB induced partial upregulation of CD80, CD40 and MHC II, whereas 100μg/ml PmB was toxic. Importantly, in this study, LPS was pre-incubated with 100μg/ml PmB for 2 hours at 37^0C, thereby exposing LPS to PmB concentrations ten-fold greater than the optimal 10μg/ml concentration determined here and also used in other studies. However, once added to the DCs, the final concentration of PmB was 10μg/ml which is non-toxic and does not enhance expression of costimulatory or MHC II molecules.

The efficacy of PmB varied for different cytokines and PmB was ineffective for LPS concentrations greater than 10ng/ml in the case of IL-6 and TNF-α. Therefore, not only can extremely low concentrations of LPS induce secretion of IL-6 and TNF-α, but PmB is also exceedingly limited in its capacity to successfully reverse these effects. However, for IL-12p40 the inhibitory properties of PmB were preserved until an LPS concentration of 0.5μg/ml was reached, whereas PmB-mediated inhibition of IL-12p70 secretion was evident at all concentrations of LPS tested. Despite this, LPS-driven BMDC maturation was no longer completely inhibited by PmB at LPS concentrations greater than 20ng/ml, thereby further emphasising the inadequacies of this control.

The common perception that LPS is heat resistant dates back to the nineteenth century when it was demonstrated by Richard Pfeifer that heat-inactivated *Vibrio cholera* retained their ability to induce shock in experimental animals. This led to a widely used method of boiling protein preparations for at least 30 minutes to rule out LPS contamination as the cause of the observed effects [520]. However, this study has shown that secretion of IL-6 and IL-12p40 by BMDCs in response to low concentrations of LPS is reduced by heating at 60°C or 100°C.

These results support other studies which have shown that low concentrations of heat treated *E. coli* LPS fail to promote TNF-α secretion by murine macrophages [381, 383]. Importantly, Gao and colleagues outline that many studies use very high concentrations of LPS, approximately 10-500ng/ml, to test for heat sensitivity. Since only minute concentrations of LPS are required to fully activate an APC, Gao *et al.* propose that even if practically all of the LPS is inactivated by heat treatment, the active residual LPS is sufficient to activate an APC, thus leading to the incorrect conclusion that LPS is heat resistant. In support of this idea, this study found that a concentration of 50pg/ml LPS was sufficient to induce BMDC maturation and robust secretion of a number of

proinflammatory cytokines. Therefore, LPS is capable of promoting DC activation at concentrations approximately two hundred times less than the minimal concentrations being used to test for heat sensitivity.

Many studies have reported that TLR agonists can synergise with microbial and endogenous immunomodulators to enhance BMDC secretion of specific proinflammatory cytokines, in particular IL-6 [342, 388-389, 407, 521-522]. This study hypothesised that extremely low concentrations of LPS that are incapable of promoting cytokine secretion independently can synergise with candidate molecules to promote this effect. This ultimately generates the incorrect conclusion that the candidate molecule can induce cytokine secretion independently of LPS. Interestingly, this study shows that a concentration as low as 5pg/ml LPS alone is not sufficient to induce secretion of IL-6 but can still synergise with *E. coli* LT to promote this effect. Crucially, *E. coli* LT alone was unable to induce IL-6 secretion, thus raising the possibility that many proposed exogenous and endogenous immunomodulators elicit activity only as a direct result of synergy with low levels of contaminating LPS. Furthermore, the effects of contaminating LPS are also likely to result in misleading conclusions when using other APCs, including macrophages.

In conclusion, this study has revealed that extremely low concentrations of LPS can promote DC activation and that different thresholds exist for secretion of specific cytokines in response to this potent bacterial PAMP. Furthermore, PmB is limited in its capacity to reverse the effects of residual LPS contamination and is therefore an inadequate and unreliable control. In light of both the potency of LPS and the inability of PmB to efficiently neutralise this PAMP, it is necessary to completely remove LPS from candidate immunostimulatory molecules before using murine BMDC activation to test for potential activity. However, the complete removal of LPS from preparations is exceedingly difficult to accomplish, particularly for proteins such as HMGB1 and certain Hsps that bind specifically to this PAMP [343, 387-388]. Therefore, in cases where removal of LPS is not feasible we propose that the only definitive way to eliminate the possibility of residual LPS contamination is to use TLR4-deficient DCs or immortalised cell lines which do not express TLR4. However, the obvious drawback to this method is that genuine TLR4 agonists may evade discovery.

It is imperative that the potency of LPS in promoting DC activation is fully appreciated and the limitations of many of the controls for residual LPS contamination are not neglected. In order to reliably identify novel endogenous danger signals using DC models, these key issues must be addressed appropriately.

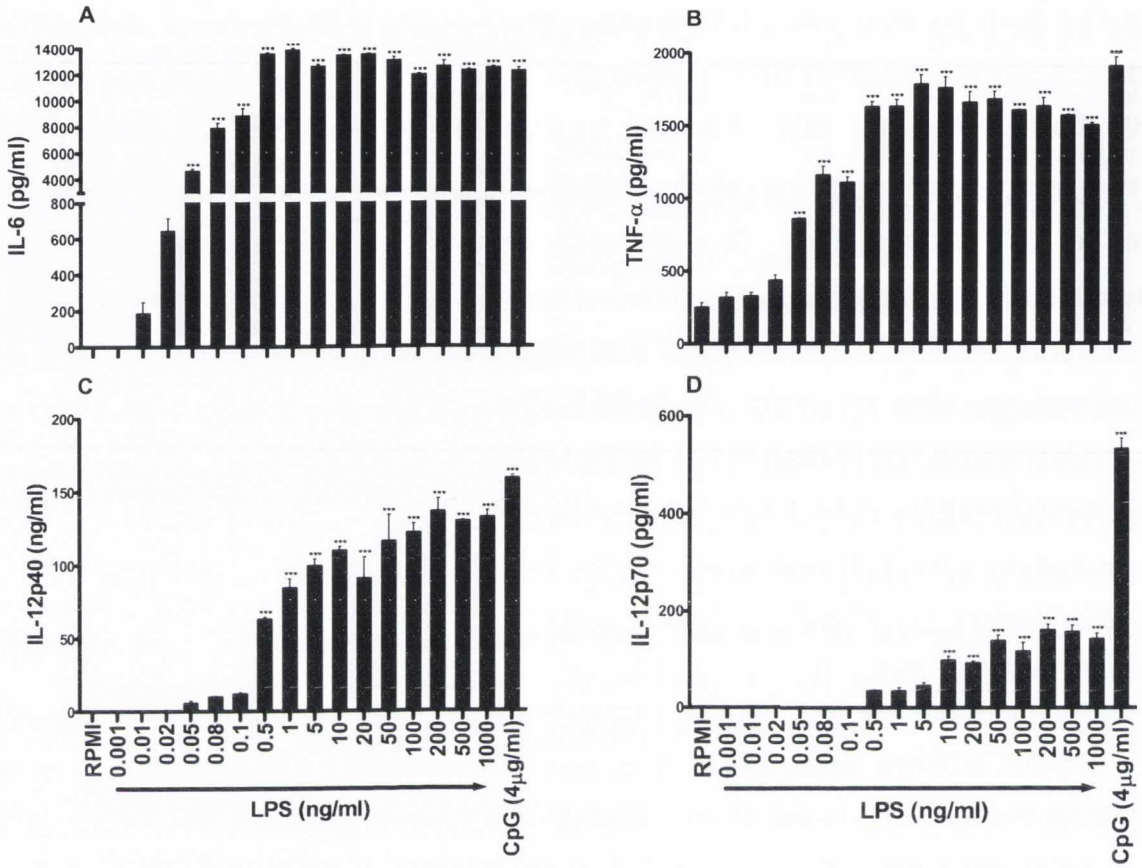

Figure 3.2 – LPS concentrations as low as 10pg/ml induce secretion of proinflammatory cytokines by BMDCs. BMDCs (6.25 x 10^5 cells/ml) from BALB/c mice were stimulated with RPMI, CpG (4μg/ml) or concentrations from 1pg/ml to 1μg/ml LPS. Supernatants were collected 24 hours later and tested for IL-6 (A), TNF-α (B), IL-12p40 (C) and IL-12p70 (D) by ELISA. Results are mean cytokine concentrations (+ SEM) for triplicate samples. Versus RPMI alone, *** $p<0.001$. Data are representative of three independent experiments.

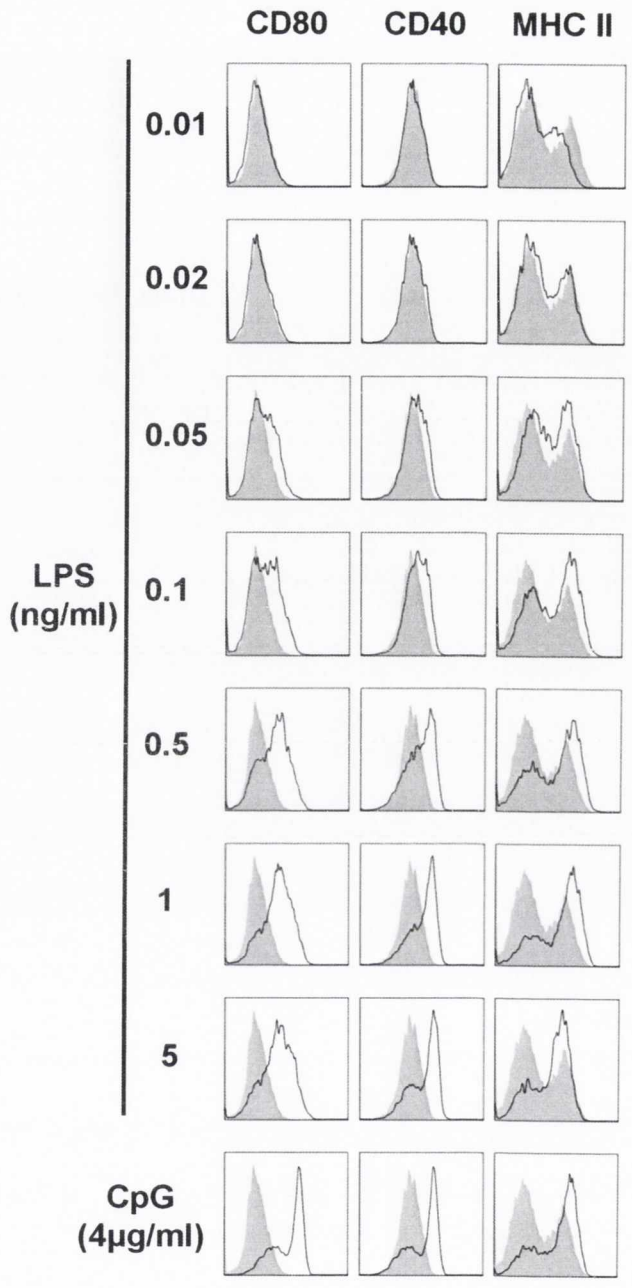

Figure 3.3 – LPS concentrations as low as 50pg/ml increase expression of CD80, CD40 and MHC II on BMDCs. BMDCs (6.25 x 10^5 cells/ml) from BALB/c mice were stimulated for 24 hours with RPMI or the indicated concentrations of LPS and CpG. $CD11c^+$ BMDCs were analysed for expression of CD80, CD40 and MHC II by flow cytometry. Immunofluorescence is shown for LPS- or CpG-treated BMDCs (black line) compared to untreated cells (grey histograms). Data are representative of three independent experiments.

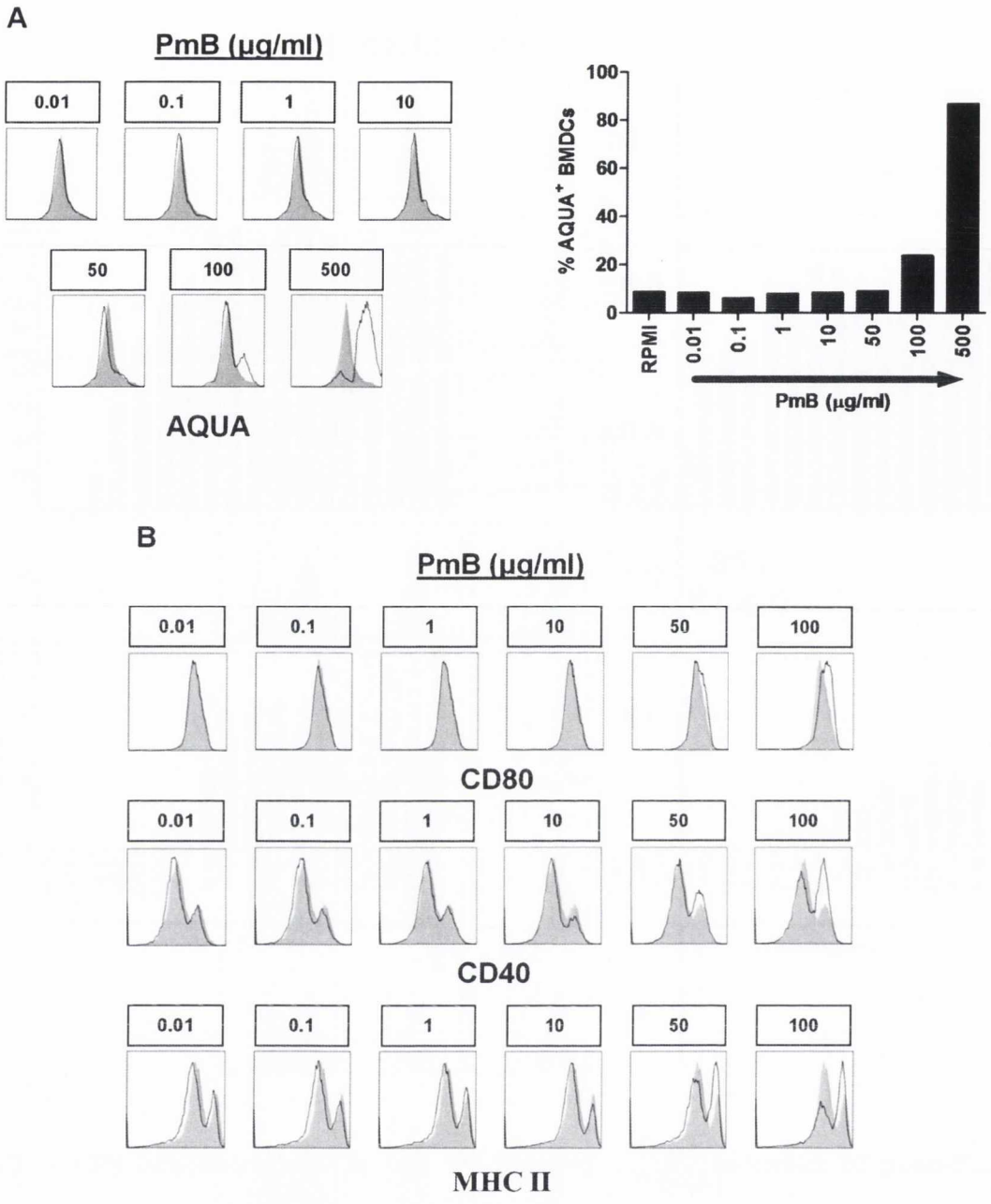

Figure 3.4 – PmB concentrations greater than 10µg/ml are toxic and increase expression of costimulatory molecules on BMDCs. BMDCs (6.25 x 10^5 cells/ml) from BALB/c mice were stimulated for 24 hours with RPMI or the indicated concentrations of PmB. (A) BMDCs were stained with AQUA reactive dye and an antibody specific for CD11c and were analysed by flow cytometry. (B) $CD11c^+$ BMDCs were also analysed for expression of CD80, CD40 and MHC II by flow cytometry. Immunofluorescence is shown for PmB-treated BMDCs (black line) compared to untreated cells (grey histograms). Data are representative of five independent experiments.

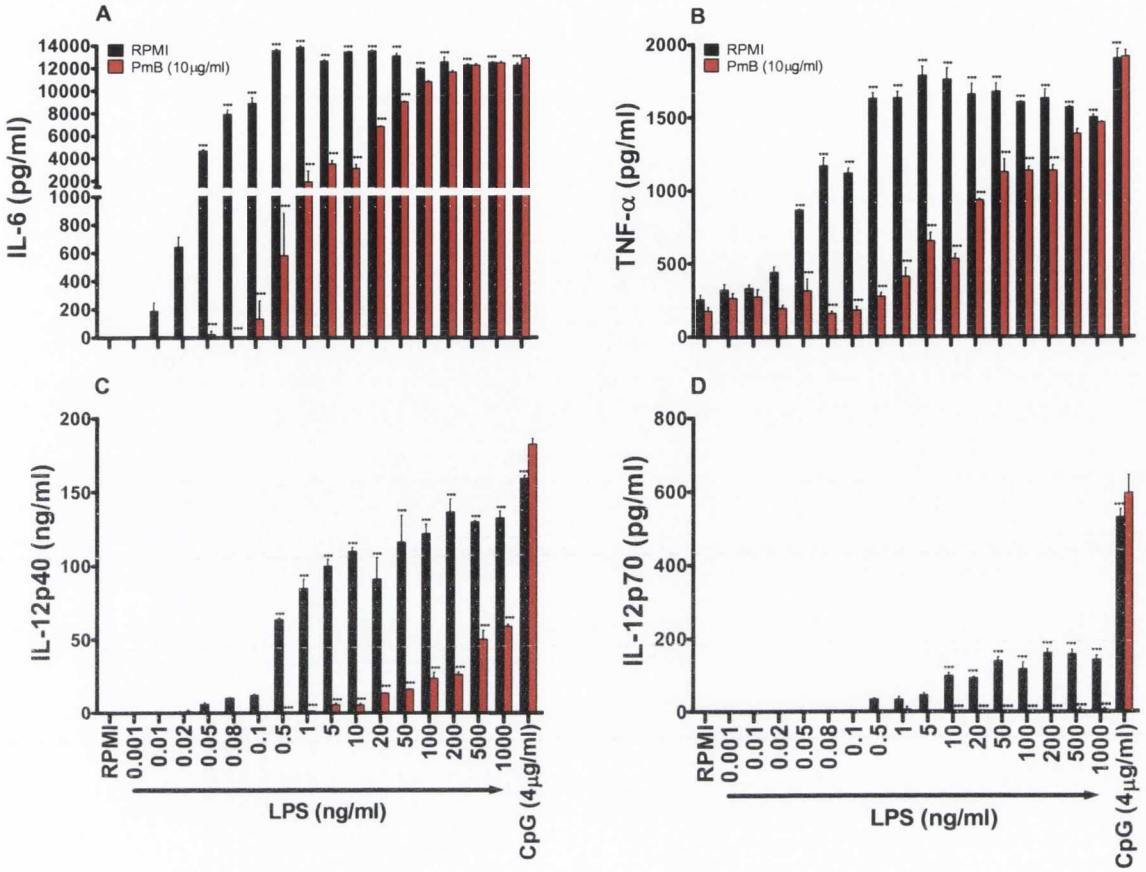

Figure 3.5 – PmB exhibits a limited capacity to inhibit LPS-induced secretion of proinflammatory cytokines from BMDCs. BMDCs (6.25 x 10^5 cells/ml) from BALB/c mice were stimulated with RPMI, CpG (4µg/ml) or concentrations from 1pg/ml to 1µg/ml LPS, which were pre-incubated alone or in the presence of PmB (100µg/ml) for 2 hours at 37^0C. Supernatants were collected 24 hours later and tested for IL-6 (A), TNF-α (B), IL-12p40 (C) and IL-12p70 (D) by ELISA. Results are mean cytokine concentrations (+ SEM) for triplicate samples. LPS + PmB versus corresponding concentration of LPS alone, ••• $p<0.001$. Data are representative of three independent experiments.

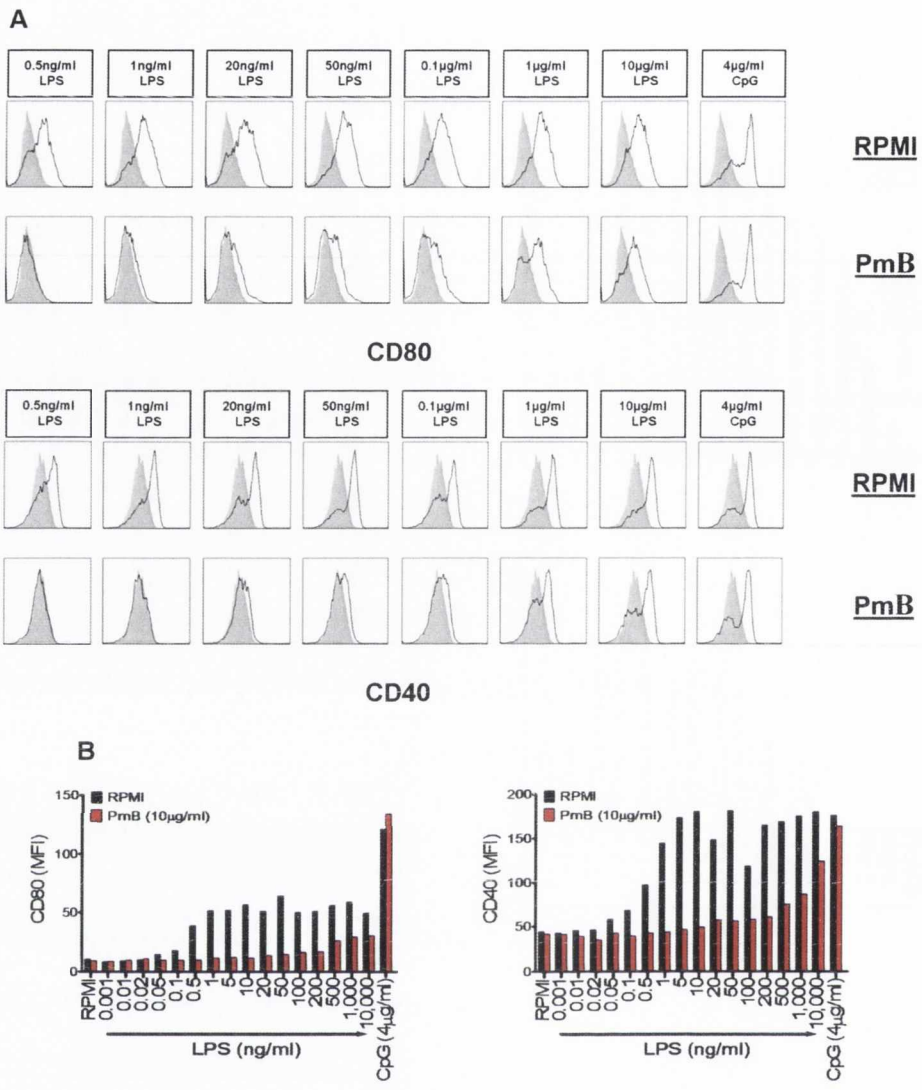

Figure 3.6 – LPS-induced expression of CD80 and CD40 is no longer completely inhibited by PmB at a concentration of 20ng/ml.

(A) BMDCs (6.25 x 10^5 cells/ml) from BALB/c mice were stimulated with RPMI or the indicated concentrations of LPS and CpG, which were pre-incubated alone or in the presence of PmB (100µg/ml) for 2 hours at 37^0C. BMDCs were harvested 24 hours later and $CD11c^+$ cells were analysed for expression of CD80 and CD40 by flow cytometry. Immunofluorescence is shown for LPS- or CpG-treated BMDCs (black line) compared to untreated cells incubated with RPMI (grey histograms). (B) BMDCs (6.25 x 10^5 cells/ml) from BALB/c mice were stimulated as described in Figure 3.6A. BMDCs were harvested 24 hours later and $CD11c^+$ cells were analysed for expression of the maturation markers CD80 and CD40 by flow cytometry. Data are represented as median fluorescence intensity (MFI) and are representative of three independent experiments.

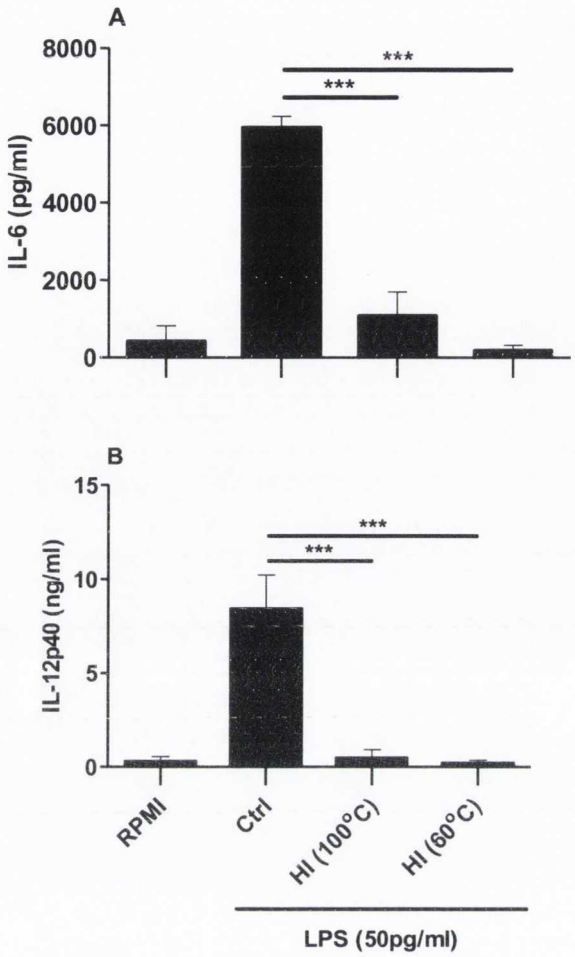

Figure 3.7 - Heating low concentrations of LPS negates its ability to modulate BMDC secretion of IL-6 and IL-12p40. BMDCs (6.25 x10^5 cells/ml) from BALB/c mice were stimulated with RPMI, control LPS (50 pg/ml) (Ctrl) or heat-inactivated (HI) LPS (100°C or 60°C for 1 hour). Supernatants were collected 24 hours later and tested for IL-6 and IL-12p40 by ELISA. Results are mean cytokine concentrations (+ SEM) for triplicate samples. Versus RPMI alone, *** $p<0.001$. Data are representative of four independent experiments. This work was performed by Dr. Anne McNaughton of the Adjuvant Research Group, TCD.

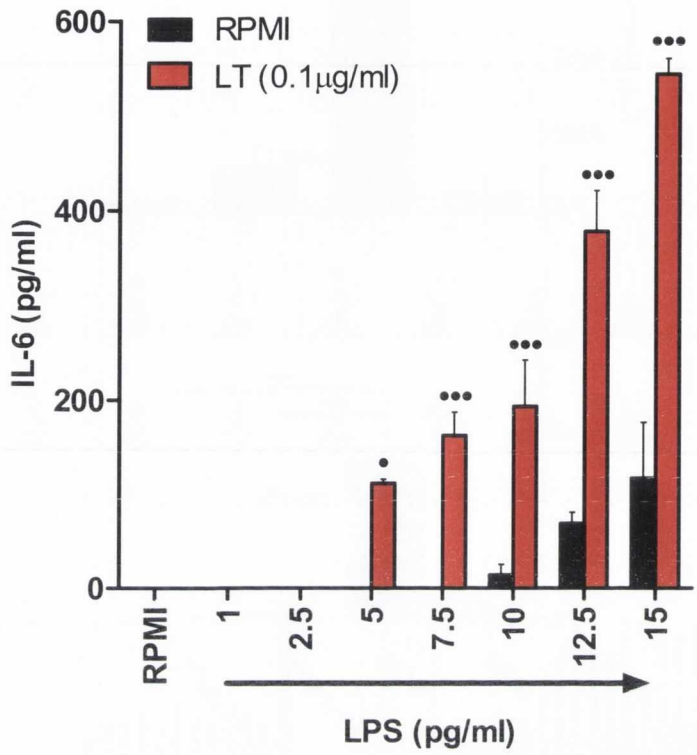

Figure 3.8 – LPS concentrations as low as 5pg/ml induce secretion of IL-6 by BMDCs in the presence of *E. coli* LT. BMDCs (6.25 x 10^5 cells/ml) from BALB/c mice were stimulated with RPMI or concentrations from 1pg/ml to 15pg/ml LPS, either alone or in the presence of *E. coli* LT (0.1μg/ml). Supernatants were collected 24 hours later and tested for IL-6 by ELISA. Results are mean cytokine concentrations (+ SEM) for triplicate samples. LPS + *E. coli* LT versus corresponding concentration of LPS alone, * $p<0.05$ *** $p<0.001$. Data are representative of five independent experiments.

Chapter 4

An Investigation of the Immunostimulatory Activity of the Granzyme B Substrate IL-1α

4.1 – Introduction

CTLs and NK cells mediate rapid elimination of transformed and virally infected cells. This feat is primarily accomplished by inducing apoptosis in the target cell. Indeed, one particularly important apoptotic pathway involved in this process is the cytotoxic granule-dependent pathway. Within the cytoplasm of CTLs and NK cells there are cytotoxic granules containing a battery of destructive proteins, including the pore-forming protein perforin, a number of serine proteases called granzymes, and the GzmB-chaperone known as serglycin. CTL/NK cell activation promotes exocytosis of these cytotoxic granules in close proximity to the target cell, thus resulting in apoptosis [126].

GzmB is an aspartic acid-specific protease and is one of the most abundant granzymes present in cytotoxic granules [280]. Relatively few GzmB substrates have been identified thus far. However, most of these substrates constitute crucial components of the cytotoxic granule-dependent apoptotic pathway, including various members of a cysteine protease family known as caspases [529]. Indeed, the importance of GzmB in CTL/NK cell-mediated immunity is outlined by the observation that GzmB null mice elicit pronounced defects in their ability to clear certain viruses [133].

CTL/NK cell-mediated apoptosis is a rather unorthodox form of programmed cell death as target cells usually contain viruses or display aberrant proteins. Unlike most other scenarios encompassing apoptosis, where involvement of the immune system is undesirable, a proinflammatory response may be beneficial to the host in this case in order to ensure efficient removal of a harmful pathogen. Therefore, on the basis of Matzinger's danger model, it is proposed that during CTL/NK cell-mediated apoptosis, GzmB may cleave distinct substrates within the target cell with consequences other than programmed cell death. More specifically, it is hypothesised that GzmB processing of intracellular targets may generate immunostimulatory danger signals, or may enhance the immune activation capacity of pre-existing danger signals. Following GzmB processing, these active danger signals may be released from secondary necrotic cells prior to clearance by phagocytosis and thus potentiate the ensuing inflammatory response.

Perhaps even more interesting is a second scenario in which GzmB may encounter extracellular substrates. CTLs and NK cells, as well as other immune cells, may secrete granzymes into the extracellular space with the ability to process molecules released from either primary or secondary necrotic cells, thus generating potent danger signals. In support of this hypothesis, circulating levels of GzmB are elevated in patients with RA and melioidosis [286-287]. Moreover, GzmB has been shown to be secreted by a wide range of immune cells under conditions not associated with toxicity

(Section 1.8.1). GzmB has also been reported to elicit proinflammatory activity *in vivo* as GzmB-deficient mice are less susceptible to LPS-induced mortality [297]. Indeed, given the link between GzmB and inflammation, in addition to the ability of non-cytotoxic cells to secrete this particular serine protease, it is apparent that GzmB posseses immunostimulatory activity which is independent of its contribution to apoptosis. Therefore, GzmB is a particularly attractive candidate protease for processing endogenous molecules and modulating their immune activation capacity

Using a proteome-wide screening approach, both histamine-releasing factor (HRF) and IL-1α were identified as novel GzmB substrates by Dr. Inna Afonina of the Molecular Cell Biology Laboratory in the Department of Genetics, TCD. HRF and IL-1α are cleaved at asparagine (Asn)51 and aspartic acid (Asp)103 respectively by GzmB. HRF has pleitropic effects on immune cells, promoting basophil degranulation and histamine release [530-531], eosinophil activation [532], B cell proliferation [533] and inhibition of cytokine transcription in T cells [514]. However, despite an established extracellular biological role, HRF does not possess a classical secretory sequence and does not share sequence homology with known cytokines. In collaboration with the Molecular Cell Biology Laboratory in the Department of Genetics, TCD, the immunostimulatory activity of both full-length HRF (FL HRF) and GzmB-processed HRF (GzmB HRF) as well as full-length IL-1α (FL IL-1α) and GzmB-processed IL-1α (GzmB IL-1α) was assessed.

Importantly, preparations of FL HRF and FL IL-1α contained these respective proteins in combination with heat-inactivated GzmB (HI GzmB), whereas preparations of GzmB IL-1α and GzmB HRF consisted of the same proteins mixed with active GzmB. Heating GzmB may have eliminated co-purifying GzmB contaminants present within preparations of FL HRF and FL IL-1α. However, preparations of GzmB HRF and GzmB IL-1α contained GzmB which had not been heat treated, thus raising the possibility that these preparations may have contained co-purifying GzmB contaminants which were absent in FL HRF and FL IL-1α. In order to control for this issue in the case of IL-1α, a catalytically inactive GzmB mutant was generated in the same yeast system used to produce active GzmB, thus meaning that any co-purifying microbial contaminants would be present in both preparations. Subsequently, both active GzmB and the catalytically inactive GzmB mutant were mixed with IL-1α. In addition, the issue of residual GzmB activity was controlled for by testing both active GzmB and HI GzmB independently for immunostimulatory activity.

In addition to constituting a novel GzmB substrate, IL-1α has been proposed to function as an endogenous danger signal. During necrosis, cellular integrity is compromised, leading to the release

of endogenous cytokines, including IL-1α and IL-33, into the extracellular milieu [534]. Interestingly, IL-1α lacks a classical leader peptide sequence and is therefore not secreted by the ER and Golgi apparatus. Rather, IL-1α is reported to be typically released into the extracellular milieu by damaged or dying cells where it elicits a plethora of immunostimulatory effects. This concept is supported by a recent study showing that IL-1α is readily released from cells undergoing necrosis, but is retained in the nucleus of apoptotic cells [432]. IL-33 also lacks a classical secretory sequence but can be rapidly released from necrotic cells into the extracellular milieu where it serves to augment immune responses. In support of this hypothesis, Luthi *et al.* recently reported that IL-33 is processed exclusively by apoptotic caspases, but not by inflammatory caspases. More specifically, proteolysis by apoptotic caspases attenuated the biological activity of IL-33 both *in vitro* and *in vivo*, thus generating a cytokine with significantly reduced proinflammatory activity [439]. However, apoptotic caspases remain inactive during necrosis, thus meaning that the biologically more potent full-length form of IL-33 is likely to be released from necrotic cells following loss of membrane integrity. Full-length IL-33 may subsequently promote powerful immunostimulatory effects in response to necrotic cell death.

The second objective of this work, therefore, was to assess the adjuvant properties of IL-33 and IL-1α as measured by their ability to drive antigen-specific cellular and humoral immunity and also to compare the nature of the responses induced. It is hypothesised that the impact of cell death on adaptive immunity may reflect the nature of the alarmins present inside necrotic cells. Ultimately, different tissues may possess discrete alarmins and therefore promote distinct immune responses. Truncated IL-$33^{112\text{-}270}$ and truncated IL-$1\alpha^{104\text{-}271}$ were used in this experiment in order to facilitate the recovery of a higher protein yield following purification. Importantly, the truncated cytokines represent the most active forms of IL-33 and IL-1α, with IL-$33^{112\text{-}270}$ and IL-$1\alpha^{104\text{-}271}$ mimicking full-length IL-33 and GzmB IL-1α respectively.

4.2 – Aims

- To investigate the immunomodulatory activity of novel GzmB substrates, paying particular attention to the issues of microbial contamination and residual GzmB activity.
- To compare the adjuvant properties of IL-1α with another endogenous danger signal, IL-33.

4.3 – Results

4.3.1 – Both FL HRF and GzmB HRF promote secretion of proinflammatory cytokines from BALB/c BMDCs

The first question addressed was whether FL HRF or GzmB HRF could potentiate secretion of proinflammatory cytokines by BMDCs. Furthermore, if any immunostimulatory activity was identified, it was important to establish whether there were any significant differences between FL HRF and GzmB HRF. Importantly, HRF preparations were depleted of LPS by three successive incubations in TritonX-100. BALB/c BMDCs were stimulated with both forms of HRF and IL-6 and TNF-α secretion was measured. Both FL HRF and GzmB HRF potently induced secretion of IL-6 and TNF-α and were comparable to LPS in their ability to promote these effects. However, there was no significant difference in the cytokine response to FL HRF and GzmB HRF (Figure 4.1).

4.3.2 – Both FL HRF and GzmB HRF fail to induce IL-6 secretion from TLR4-defective C3H/HeJ BMDCs

The next question addressed was whether LPS contamination was responsible for the immunostimulatory activity of both forms of HRF. Therefore, wild-type C3H/HeN and TLR4-defective C3H/HeJ BMDCs were stimulated with FL HRF and GzmB HRF, as well as LPS, CpG and Pam3CSK4 which are potent agonists for TLR4, TLR9 and TLR2 respectively. IL-6 and TNF-α secretion was subsequently measured in response to these stimuli. Both FL HRF and GzmB HRF potently induced secretion of IL-6 and TNF-α in C3H/HeN BMDCs and were comparable to LPS, CpG and Pam3CSK4 in their ability to promote this effect. However, similarly to LPS, both forms of HRF failed to induce IL-6 or TNF-α secretion from TLR4-defective C3H/HeJ BMDCs (Figure 4.2), thus suggesting that they were either novel TLR4 agonists or contaminated with residual LPS.

4.3.3 – FL HRF and GzmB HRF fail to induce secretion of proinflammatory cytokines from BALB/c BMDCs in the presence of PmB

In order to determine whether HRF was simply contaminated with LPS or was instead a novel TLR4 agonist, BALB/c BMDCs were stimulated with both FL HRF and GzmB HRF, as well as LPS, CpG and Pam3CSK4, which were pre-incubated alone or in the presence of PmB. Subsequently, secretion

of the proinflammatory cytokines IL-6 and TNF-α was measured. Both FL HRF and GzmB HRF potently induced secretion of IL-6 and TNF-α in the absence of PmB and were comparable to LPS, CpG and Pam3CSK4 in their ability to promote this effect. However, similarly to LPS, both forms of HRF failed to induce secretion of IL-6 or TNF-α from BALB/c BMDCs in the presence of PmB (Figure 4.3), thus suggesting that the immunostimulatory effects described in Section 4.3.1 for both forms of HRF were a direct result of LPS contamination.

4.3.4 – FL HRF depleted of LPS by successive incubations in PmB-agarose does not induce BMDC maturation or secretion of proinflammatory cytokines

Despite the fact that GzmB processing of HRF failed to potentiate the immunostimulatory activity of this protein, the potential discovery of even FL HRF as a danger signal in itself would be extremely novel. Therefore, it was important to confirm beyond doubt that the immune activation capacity of FL HRF was in fact mediated exclusively by LPS. The HRF preparations tested previously were depleted of LPS by three successive incubations in the detergent TritonX-100. Therefore, a new batch of FL HRF was instead LPS-purified through three successive incubations in PmB-agarose. Wild-type C3H/HeN and TLR4-defective C3H/HeJ BMDCs were stimulated with PmB-agarose purified FL HRF, as well as LPS, CpG and Pam3CSK4, and IL-6 and TNF-α secretion was measured. However, FL HRF failed to induce cytokine secretion or maturation of C3H/HeN or C3H/HeJ BMDCs (Figure 4.4).

4.3.5 – HRF does not synergise with TLR agonists to potentiate proinflammatory cytokine secretion from BALB/c BMDCs

Some of the more established endogenous danger signals, such as HMGB1, Hsps and small breakdown products of hyaluronic acid, synergise with TLR agonists to promote an inflammatory response greater than that generated against either component alone [342, 388-389, 407]. In order to establish if HRF synergises with TLR agonists to potentiate immune activation, BALB/c BMDCs were stimulated with a range of suboptimal concentrations of LPS, Poly I:C and Pam3CSK, which were pre-incubated alone or in the presence of PmB-agarose purified FL HRF, previously shown to have no effect on BMDCs (Section 4.3.4). Subsequently, BMDC secretion of IL-6 and TNF-α was

measured. The presence of HRF failed to augment proinflammatory cytokine secretion from BMDCs in response to suboptimal concentrations of any of the TLR agonists tested (Figure 4.5).

4.3.6 – HRF fails to elicit biological activity *in vivo*

BMDC cultures essentially comprise a uniform population of cells. One significant problem associated with using BMDCs in testing for immunomodulatory properties of candidate molecules is that these molecules may have a different target cell *in vivo*. In order to tackle this issue, and possibly discover immunomodulatory activity for HRF or even consequences of GzmB processing of this protein, female BALB/c mice were immunised i.p. for 4 consecutive days with PBS, FL HRF or GzmB HRF. This ensured that the mice were chronically exposed to these respective molecules. Importantly, both forms of HRF were LPS-purified through three successive incubations in PmB-agarose. On day 5, the mice were sacrificed and peritoneal exudates cells (PECs), splenocytes, mesenteric and mediastinal lymph node cells were recovered. Splenocytes, mesenteric and mediastinal lymph node cells were restimulated *ex vivo* with RPMI, anti-CD3 or anti-CD3 in combination with phorbal myristate acetate (PMA). After 72 hours, T cell cytokine profiles were measured in the supernatant by ELISA. In addition, PECs were analysed by flow cytometry.

Following restimulation with anti-CD3, splenocytes recovered from mice immunised with either FL HRF or GzmB HRF did not elicit an altered cytokine profile in comparison with splenocytes isolated from control mice immunised with PBS (Figure 4.6). These results were also evident in the mesenteric and mediastinal lymph node cells, while HRF also failed to induce granulocyte recruitment into the peritoneum (data not shown).

4.3.7 – GzmB IL-1α potentiates IL-17 production by splenocytes in the absence of TCR engagement

Inna Afonina of the Molecular Cell Biology Laboratory in the Department of Genetics, TCD, had previously shown that GzmB-mediated proteolysis of IL-1α at Asp103 potentiates the activity of this cytokine several-fold *in vitro*. In particular, both HeLa cells and primary HUVECs were more responsive to GzmB IL-1α than FL IL-1α, as measured by secretion of IL-6 and IL-8 (Figure 4.7). In collaboration, the biological potency of FL IL-1α and GzmB-processed IL-1α was compared *in vivo*.

Sutton *et al.* have previously shown that IL-1 and IL-23 induce IL-17 production by spleen-derived γδ T cells in the absence of TCR engagement (anti-CD3 stimulation) [535]. Adapting this model, the bioactivity of FL IL-1α and GzmB IL-1α was compared. Splenocytes were stimulated with FL IL-1α or GzmB IL-1α with and without IL-23 and plate-bound anti-CD3. Subsequently, secretion of IL-17 was measured in response to these stimuli. In the presence of IL-23, both forms of IL-1α induced IL-17 production by splenocytes without anti-CD3 stimulation. However, GzmB IL-1α was significantly more potent than FL IL-1α in its ability to promote this effect. In the absence of IL-23, IL-17 was not detectable in response to either form of IL-1α without anti-CD3 stimulation (Figure 4.8). Following stimulation with anti-CD3, secretion of IL-17 by splenocytes was evident but was not modulated by FL IL-1α or GzmB IL-1α either in the presence or absence of IL-23 (Figure 4.8).

4.3.8 – GzmB IL-1α mediates enhanced granulocyte recruitment *in vivo*

In order to compare the effects of GzmB-mediated proteolysis of IL-1α with the full-length cytokine following chronic exposure to these molecules *in vivo*, female BALB/c mice were immunised i.p. for 4 consecutive days with either PBS, FL IL-1α or the GzmB-processed form of this cytokine. On day 5, the mice were sacrificed and PECs, splenocytes, mesenteric and mediastinal lymph node cells were recovered. Splenocytes, mesenteric and mediastinal lymph node cells were restimulated *ex vivo* with RPMI, anti-CD3 or anti-CD3 in combination with PMA. After 72 hours, T cell cytokine profiles were measured in the supernatant by ELISA and PECs were analysed by flow cytometry.

Following restimulation with anti-CD3, splenocytes recovered from mice immunised with either FL IL-1α or GzmB IL-1α did not elicit an altered cytokine profile in comparison with splenocytes isolated from control mice immunised with PBS (Figure 4.9). These results were also evident in the mediastinal lymph nodes (Figure 4.10). In contrast, data obtained following restimulation of the mesenteric lymph node cells revealed that GzmB IL-1α had increased biological activity compared to FL IL-1α. FL IL-1α promoted enhanced secretion of the cytokines IL-4, IL-5 and IFN-γ in comparison with PBS. However, GzmB IL-1α was more potent than its full-length counterpart as it induced considerably higher levels of secretion of these respective cytokines, in addition to IL-17 (Figure 4.11).

IL-1α is a well-known granulocyte chemoattractant [272]. Therefore, the ability of both FL IL-1α and GzmB IL-1α to recruit granulocytes into the site of injection (i.e. peritoneum) was compared.

PECs were recovered and analysed by flow cytometry. Granulocytes were identified on the basis of their high SSC/FSC profile. As shown in Figure 4.12, both forms of IL-1α enhanced granulocyte recruitment. However, GzmB IL-1α exhibited significantly greater potency in this regard, thus reinforcing the idea that GzmB processing of IL-1α potentiates the activity of this proinflammatory cytokine *in vivo*.

4.3.9 – GzmB IL-1α exhibits increased adjuvanticity *in vivo*

The adjuvanticity of FL IL-1α versus GzmB IL-1α was next compared using OVA as a model antigen. Female BALB/c mice were immunised i.p. on day 0 with PBS as a control or OVA either alone or mixed with FL IL-1α or GzmB IL-1α. Blood samples were recovered on day 13. The mice were boosted i.p. with these same treatments on day 14 and were sacrificed on day 21. Spleens, PECs and blood were recovered.

Antigen-specific secretion of IL-4, IL-5 and IL-10 from PECs was elevated in mice that received OVA alone. OVA administered in combination with FL IL-1α was no more effective than OVA alone at promoting secretion of these cytokines. However, injection of OVA with FL IL-1α also enhanced antigen-specific IL-17 from PECs. Injection of OVA mixed with GzmB IL-1α resulted in antigen-specific IL-4, IL-5, IL-10 and IL-17 secretion from PECs, but was more potent in this induction than either OVA alone or OVA in combination with FL IL-1α. Although IFN-γ from PECs was elevated in mice that received OVA mixed with GzmB IL-1α, this response was clearly not antigen-specific as a response of similar magnitude was also evident following restimulation with RPMI (Figure 4.13).

Enhanced OVA-specific IL-4, IL-5, IL-10 and IFN-γ was also evident in splenocytes from mice that received OVA alone. As with the response from PECs, OVA injected with FL IL-1α also enhanced production of these respective cytokines by splenocytes but was no more effective than OVA alone. One exception to this, however, was that OVA mixed with FL IL-1α more potently enhanced IFN-γ production by splenocytes. Injection of OVA mixed with GzmB IL-1α enhanced antigen-specific IL-4, IL-5 and IL-10 secretion from splenocytes more effectively than either OVA alone or in combination with FL IL-1α (Figure 4.14). However, while the above observations were indicative of a robust trend towards more potent OVA-specific responses, the differences were not statistically significant.

Restimulation with anti-CD3 also revealed enhanced secretion of IL-4, IL-5 and IL-10 from PECs collected from mice that had received OVA alone. Mice that had received OVA mixed with FL IL-1α also exhibited enhanced production of these respective cytokines, but only IL-4 secretion was more effectively induced than with OVA alone. However, injection of mice with OVA in combination with GzmB IL-1α dramatically increased production of the cytokines IL-4, IL-5 and IL-10 by PECs in comparison to mice that received either OVA alone or OVA mixed with FL IL-1α. These responses were particularly robust and were found to be statistically significant (Figure 4.15). However, restimulation with anti-CD3 failed to induce more potent responses in splenocytes from the same mice (Figure 4.16), suggesting that these modulatory effects were principally at the site of cytokine injection.

Overall, the cytokines IL-4, IL-5 and IL-10 were elevated in mice that received OVA mixed with GzmB IL-1α in comparison to those that received either OVA alone or in combination with FL IL-1α. These cytokines are characteristic of a Th2 response, thus suggesting that GzmB IL-1α may polarise the immune response in this particular direction.

Serum levels of antigen-specific IgG as well as the IgG subtypes IgG1, IgG2a and IgG2b were also determined. Co-injection of GzmB IL-1α augmented OVA-specific IgG and IgG1 titres prior to boosting, exhibiting a greater potency than FL IL-1α in this regard (Figure 4.17). Moreover, these observations were even more pronounced after boosting, with GzmB IL-1α driving significantly higher IgG and IgG1 titres than FL IL-1α, but also greater IgG2a and IgG2b titres (Figure 4.18).

4.3.10 – The enhanced adjuvanticity of GzmB IL-1α is not mediated by co-purifying microbial contaminants within GzmB preparations

In order to eliminate the possibility that co-purifying microbial contaminants are responsible for mediating the enhanced adjuvanticity of GzmB IL-1α *in vivo*, a catalytically inactive GzmB mutant ($GzmB^{SA}$) was expressed and purified in the same yeast system as that used to produce wild-type GzmB ($GzmB^{WT}$). $GzmB^{SA}$, $GzmB^{WT}$ and HI GzmB were incubated with IL-1α to generate preparations of $GzmB^{SA}$ IL-1α, $GzmB^{WT}$ IL-1α and FL IL-1α respectively. Female BALB/c mice were immunised i.p. on day 0 with PBS as a control or OVA either alone or mixed with FL IL-1α, $GzmB^{WT}$ IL-1α or $GzmB^{SA}$ IL-1α. Blood samples were recovered on day 13. The mice were boosted i.p. with these same treatments on day 14 and were sacrificed on day 21 before blood was recovered.

Antigen-specific IgG and IgG1 titres were determined in pre-boost serum samples and antigen-specific IgG, IgG1, IgG2a and IgG2b titres were determined in post-boost serum samples.

GzmB^{SA} IL-1α failed to elicit the same adjuvanticity displayed by GzmB^{WT} IL-1α. More specifically, GzmB^{WT} IL-1α induced significantly higher IgG and IgG1 titres compared with GzmB^{SA} IL-1α in both pre-boost (Figure 4.19) and post-boost serum samples and also significantly higher IgG2a and IgG2b titres in post-boost serum samples (Figure 4.20). Furthermore, serum antibody titres following co-injection of GzmB^{SA} IL-1α were comparable to those induced by FL IL-1α.

4.3.11 – Residual GzmB activity is not responsible for potentiating GzmB IL-1α adjuvanticity

In order to eliminate the possibility that residual GzmB activity within the IL-1α preparations is responsible for mediating the immunostimulatory effects of IL-1α *in vivo*, the adjuvanticity of both active GzmB and HI GzmB was assessed. Female BALB/c mice were immunised i.p. with PBS or OVA either alone or in combination with active GzmB or HI GzmB. Blood samples were recovered on day 13. The mice were boosted with these same treatments on day 14 and were sacrificed on day 21 before blood samples were recovered. OVA-specific antibody titres (IgG, IgG1, IgG2a, IgG2b) in the serum were measured in both pre-boost and post-boost samples.

Both active and HI GzmB failed to increase antigen-specific antibody titres in the serum for any of the IgG subtypes tested and this was evident in both pre-boost (Figure 4.21) and post-boost (Figure 4.22) blood samples.

4.3.12 – GzmB contributes to IL-1α processing *in vivo*

The next question addressed was whether GzmB can mediate IL-1α processing *in vivo*. In order to answer this question, a GzmB non-cleavable mutant form of IL-1α (IL-1α^{D103A}) was generated. It was necessary to determine whether IL-1α^{D103A} elicited reduced activity *in vivo* compared to wild-type FL IL-1α. Female BALB/c mice were immunised i.p. on day 0 with PBS as a control or OVA either alone or mixed with FL IL-1α or the GzmB non-cleavable IL-1α^{D103A}. Blood samples were recovered on day 13. The mice were boosted i.p. with these same treatments on day 14 and were sacrificed on day 21 before blood was recovered. Antigen-specific IgG and IgG1 titres were

determined in pre-boost serum samples and antigen-specific IgG, IgG1, IgG2a and IgG2b titres were determined in post-boost serum samples.

FL IL-1α induced much higher antibody titres than the GzmB resistant IL-1α^{D103A} mutant. This was evident in both pre-boost (Figure 4.23) and post-boost (Figure 4.24) serum samples.

4.3.13 – IL-1α and IL-33 are potent immunomodulatory alarmins that induce qualitatively different T cell responses

IL-1α, in addition to its role as a GzmB substrate, has also been postulated to function as an endogenous danger signal. During necrosis, plasma membrane integrity is compromised, leading to the release of endogenous cytokines, including IL-1α and another IL-1 family member IL-33, into the extracellular environment [534]. The impact of cell death on adaptive immunity may reflect the specific alarmins present inside necrotic cells. Ultimately, different tissues may possess discrete alarmins and therefore promote distinct immune responses.

In order to address this hypothesis, the adjuvanticity of truncated IL-33$^{112-270}$ was compared against truncated IL-1α$^{104-271}$ using OVA as a model antigen. These truncated forms of the respective cytokines were used in order to address protein solubility issues and this approach facilitated the recovery of a higher protein yield following purification. Importantly, the truncated cytokines represent the most active forms of IL-33 and IL-1α, with IL-33$^{112-270}$ and IL-1α$^{104-271}$ mimicking full-length IL-33 and GzmB IL-1α respectively. Female BALB/c mice were immunised i.p. on day 0 with PBS as a control or OVA either alone or mixed with IL-33$^{112-270}$ or IL-1α$^{104-271}$. Blood samples were recovered on day 13. The mice were boosted i.p. with these same treatments on day 14 and were sacrificed on day 21. Spleens, PECs and blood were recovered.

Both IL-33$^{112-270}$ and IL-1α$^{104-271}$ functioned as potent adjuvants, enhancing OVA-specific T cell responses in the spleen and PECs. Following *ex vivo* restimulation with OVA, higher concentrations of the cytokines IL-4 and IL-10 were secreted by splenocytes collected from mice that were immunised with OVA in combination with IL-33$^{112-270}$ or IL-1α$^{104-271}$ than splenocytes collected from mice injected with OVA alone. IL-33$^{112-270}$, unlike IL-1α$^{104-271}$, also promoted strong induction of OVA-specific IL-5 by splenocytes, in accordance with previous studies [439]. However, more robust OVA-specific IL-17 production was evident in splenocytes from mice immunised with IL-1α$^{104-271}$ (Figure 4.25).

Both IL-33$^{112-270}$ and IL-1α$^{104-271}$ induced Th2 signature cytokines from PECs, in particular IL-4 and IL-5. Notably, IL-1α$^{104-271}$ more potently induced IL-4 production by PECs in comparison with IL-33$^{112-270}$. Furthermore, the type of T cell response induced by IL-1α$^{104-271}$ and IL-33$^{112-270}$ was qualitatively different. In particular, IL-1α$^{104-271}$ promoted a strong antigen-specific Th17 response in PECs, while a Th17 response was not detected when IL-33$^{112-270}$ was used as an adjuvant (Figure 4.26).

PECs were also restimulated *ex vivo* with anti-CD3 alone or in combination with PMA. As with the antigen-specific responses, restimulation with anti-CD3 revealed robust secretion of IL-4 and IL-10 by splenocytes from mice injected with IL-33$^{112-270}$ or IL-1α$^{104-271}$. Again, IL-33$^{112-270}$ and IL-1α$^{104-271}$ were more potent in their respective induction of IL-5 and IL-17 by splenocytes (Figure 4.27). Both IL-33$^{112-270}$ and IL-1α$^{104-271}$ induced secretion of the Th2 signature cytokine IL-5 from PECs. However, IL-1α$^{104-271}$ more potently stimulated production of IL-4 and IL-10 in comparison with IL-33$^{112-270}$. Furthermore, the qualitatively different type of T cell response induced by IL-1α$^{104-271}$ and IL-33$^{112-270}$ in PECs when restimulated with OVA was also evident here. Following restimulation with anti-CD3, IL-1α$^{104-271}$ significantly potentiated IL-17 secretion by PECs, while this effect was absent in PECs obtained from mice immunised with IL-33$^{112-270}$. In fact, IL-33$^{112-270}$ appeared to actively suppress Th17 responses (Figure 4.28).

IL-33$^{112-270}$ and IL-1α$^{104-271}$ also promoted strong OVA-specific antibody titres in the serum. Specifically, IL-33$^{112-270}$ and IL-1α$^{104-271}$ elevated serum levels of antigen-specific IgA and IgG as well as the IgG subtypes IgG1, IgG2a and IgG2b. However, there were no significant differences in the magnitude of the response or the antibody isotypes elicited in either pre-boost (Figure 4.28) or post-boost (Figure 4.29) serum samples.

4.4 – Discussion

GzmB IL-1α exhibits enhanced biological activity *in vivo*. Proteolytic processing of this proinflammatory cytokine at Asp103 by GzmB potentiates its stimulatory effects on both cellular and humoral immunity. This suggests that GzmB may promote potent proinflammatory responses *in vivo* in certain situations through cleavage of IL-1α. Furthermore, the data indicate that contrary to popular belief, the biological activity of IL-1α is indeed regulated by proteolytic processing.

The capacity of both FL IL-1α and its GzmB-processed counterpart to recruit granulocytes into the peritoneum was compared. Indeed, both forms of IL-1α enhanced granulocyte recruitment. However, GzmB IL-1α exhibited considerably greater potency in this regard. When employed in an adjuvant model using OVA as an antigen, GzmB IL-1α displayed greater biological potency than the full-length form of this cytokine. In particular, both forms of IL-1α enhanced OVA-specific antibody titres in the serum, but GzmB IL-1α was more potent than the full-length form in this regard. Furthermore, GzmB IL-1α was also more potent than FL IL-1α in its ability to induce strong antigen-specific secretion of the cytokines IL-4, IL-5 and IL-10 from PECs. Enhanced OVA-specific IL-4, IL-5 and IL-10 responses were also evident in splenocytes from the same mice. Restimulation of PECs with anti-CD3 revealed a dramatic increase in secretion of IL-4, IL-5 and IL-10 in mice that had received GzmB IL-1α. Indeed, these responses are indicative of a Th2-biased immune response.

HeLa cells are very sensitive to IL-1α but fail to respond to a wide range of PAMPs including LPS. This confirms that residual LPS contamination is not responsible for mediating the immunostimulatory effects of this cytokine *in vitro*. However, the possibility that the enhanced immunogenicity of GzmB IL-1α *in vivo* may have been owing to microbial contaminants present within the GzmB preparations was also explored. Importantly, preparations of FL IL-1α contained IL-1α in combination with HI GzmB, whereas preparations of GzmB IL-1α consisted of IL-1α which was exposed to active GzmB (Section 2.1.2). Heating GzmB may have eliminated co-purifying GzmB contaminants within FL IL-1α preparations, but GzmB IL-1α preparations contained GzmB which had not been heat-inactivated. Therefore, it was conceivable that residual contaminants present in active GzmB preparations were responsible for potentiating the immunostimulatory effects attributable to GzmB IL-1α *in vivo*. To address this issue, a catalytically inactive GzmB mutant ($GzmB^{SA}$) was generated in the same yeast system used to produce active GzmB ($GzmB^{WT}$), thus meaning that any co-purifying microbial contaminants present within $GzmB^{WT}$ preparations would also be present within $GzmB^{SA}$ preparations. Importantly, $GzmB^{SA}$ IL-1α failed to elicit the same

adjuvanticity as $GzmB^{WT}$ IL-1α, as measured by OVA-specific antibody titres in the serum. Furthermore, antibody titres in response to $GzmB^{SA}$ IL-1α were comparable to those induced by FL IL-1α. This confirms that the catalytic activity of GzmB is necessary for potentiating IL-1α bioactivity *in vivo* and that co-purifying microbial contaminants present within the respective GzmB preparations are not responsible for this effect. Interestingly, it was also confirmed that residual GzmB activity is not responsible for potentiating GzmB IL-1α adjuvanticity as neither $GzmB^{WT}$ nor HI GzmB elicited adjuvant activity independently when using OVA as a model antigen.

Perhaps most interesting is the finding that IL-1α is in fact processed by GzmB *in vivo*. More specifically, a non-cleavable mutant form of IL-1α ($IL\text{-}1\alpha^{D103A}$) is a less potent adjuvant than FL IL-1α. Indeed, there are a number of physiological scenarios where GzmB may encounter IL-1α. Firstly, immune cells such as CTLs and NK cells actively secrete GzmB in order to eliminate virally infected and transformed cells [126]. If the target cell expresses IL-1α, this cytokine may be processed by GzmB, thereby enhancing the inflammatory response upon subsequent release of the processed form of IL-1α into the extracellular milieu from secondary necrotic cells. Secondly, a number of studies have reported that CTLs and NK cells, as well as various other immune cells, may express and actively secrete GzmB into the extracellular milieu (Section 1.8.1). In this particular scenario, IL-1α released from primary or secondary necrotic cells as a result of injury or infection may be processed by circulating GzmB. Interestingly, patients with RA and melioidosis have been reported to express elevated levels of circulating GzmB [286-287], thus further suggesting that this particular granzyme may possess alternative, non-cytotoxic functions.

The precise mechanism through which GzmB processing of IL-1α enhances the biological activity of this classical proinflammatory cytokine *in vivo* remains ambiguous. However, it is hypothesised that proteolytic processing of IL-1α by GzmB may induce conformational changes in this cytokine that enhance its affinity for the IL-1R complex, thereby increasing its biological potency. It is also possible that the N-terminus of the cytokine may partially conceal the receptor binding domain, therefore preventing a stable interaction with the IL-1R complex. Ultimately, removal of this domain may reverse this effect and potentiate the affinity of IL-1α for the IL-1R complex. Interestingly, Hazuda *et al.* have reported that IL-1α undergoes a profound conformational change following proteinase K-mediated proteolytic removal of the N-terminus [536], thus supporting this hypothesis.

Processing of IL-1α by GzmB may also interfere with the nuclear localisation of this cytokine. Cohen *et al.* have previously shown that IL-1α is passively released from necrotic cells, but is

retained in the nucleus of cells undergoing apoptosis [432]. Importantly, the nuclear localisation of IL-1α is facilitated by a nuclear retention sequence present within the N-terminus of the protein, the region that is discarded from the molecule following processing by GzmB. Thus, in addition to enhancing the biological potency of IL-1α by increasing its affinity for the IL-1R complex, GzmB-mediated proteolysis of IL-1α may also facilitate the release of this molecule by disrupting nuclear retention mechanisms successfully employed during apoptosis.

Thus, based on these findings, in addition to directly facilitating CTL/NK-mediated apoptosis in virally infected and transformed cells, GzmB may also promote robust inflammation through restricted proteolysis of IL-1α, perhaps assisting the release of this pluripotent cytokine and facilitating a more stable interaction with the IL-1R complex.

Interestingly, HRF was also identified as a novel GzmB substrate and is cleaved at Asn51. Initially, data was generated which suggested that both FL HRF and GzmB HRF were capable of inducing secretion of proinflammatory cytokines from BMDCs. However, after rigorous investigation involving the use of PmB, TLR4-defective C3H/HeJ BMDCs and an alternative protein purification protocol, the immunostimulatory effects of both forms of HRF were found to be a direct result of LPS contamination. Indeed, once entirely depleted of LPS, these molecules were incapable of activating BMDCs. Furthermore, neither FL HRF nor its GzmB-processed counterpart exhibited enhanced biological activity *in vivo* after chronic exposure to these molecules. This suggests that HRF does not have a different target cell *in vivo*. These findings, although time-consuming, further highlight the importance of addressing LPS contamination in a meticulous and thorough manner and should also serve to raise awareness of the potency of residual LPS even after the application of recommended LPS-depletion assays. Indeed, these findings prove the merits and credibility of the previous chapter of this thesis.

In addition to constituting a novel GzmB substrate, IL-1α as well as another IL-1 family member IL-33, have been proposed as endogenous danger signals. Indeed, during necrosis, cellular integrity is compromised leading to the release of endogenous cytokines into the extracellular milieu [534].

Previous work in this laboratory has demonstrated that full-length IL-33 is a potent inducer of innate immunity [439]. The next objective of this work was to assess the adjuvant properties of IL-33 and IL-1α as measured by their ability to drive antigen-specific cellular and humoral immunity and also to compare the nature of the responses induced. In order to address protein solubility issues and to facilitate a higher protein yield following purification, truncated forms of both IL-33 (IL-$33^{112\text{-}270}$)

and IL-1α (IL-1α$^{104-271}$) were used. Both IL-33$^{112-270}$ and IL-1α$^{104-271}$ induced potent OVA-specific T cell responses in the spleen and PECs. Furthermore, the type of T cell response induced by IL-1α$^{104-271}$ and IL-33$^{112-270}$ was qualitatively different. In particular, IL-1α$^{104-271}$ promoted a strong antigen-specific Th17 response in PECs whereas a Th17 response was not detectable when IL-33$^{112-270}$ was used as an adjuvant. Both IL-33$^{112-270}$ and IL-1α$^{104-271}$ induced Th2 signature cytokines from splenocytes and PECs, particularly IL-4 and IL-5. IL-33$^{112-270}$ and IL-1α$^{104-271}$ also promoted strong OVA-specific antibody responses in the serum but there was no significant difference in the magnitude of the response or the antibody isotypes elicited.

Similar results were found regarding cytokine secretion profiles following restimulation of splenocytes and PECs with anti-CD3. Importantly, the qualitatively different type of T cell response induced by IL-1α$^{104-271}$ and IL-33$^{112-270}$ in PECs when restimulated with OVA was also evident following restimulation with anti-CD3. IL-1α$^{104-271}$ significantly potentiated IL-17 secretion by PECs, but this effect was absent in PECs obtained from mice immunised with IL-33$^{112-270}$. In fact, IL-33$^{112-270}$ appeared to actively suppress Th17 responses in PECs compared to responses from mice immunised with OVA alone. This finding supports the hypothesis that different endogenous danger signals may promote distinct immune responses and that the impact of cell death on adaptive immunity may reflect the nature of the alarmins present inside necrotic cells. Ultimately, different tissues may possess discrete alarmins and therefore promote dissimilar immune responses. This discovery supports Matzinger's hypothesis that the tissues directly modulate the immune response by releasing immunostimulatory signals that initiate immunity and influence the choice of effector class [537].

Having demonstrated that both IL-33$^{112-270}$ and IL-1α$^{104-271}$ possess powerful adjuvant properties but induce qualitatively different T cell responses, it will be important to compare the innate immune responses induced following injection of these cytokines. This should be accomplished by characterising cell recruitment into the injection site and also peripheral blood at various time points following i.p. injection of mice with these danger signals. Serum cytokines as well as IgA and IgE levels should also be measured. Furthermore, modulation of cytokine response profiles in the spleen, lymph nodes and PECs should be assessed. It will be interesting to establish whether IL-33$^{112-270}$ and IL-1α$^{104-271}$ can also modulate distinct acute responses at these early time points and particularly whether they reflect the qualitatively different responses found in the adjuvant model.

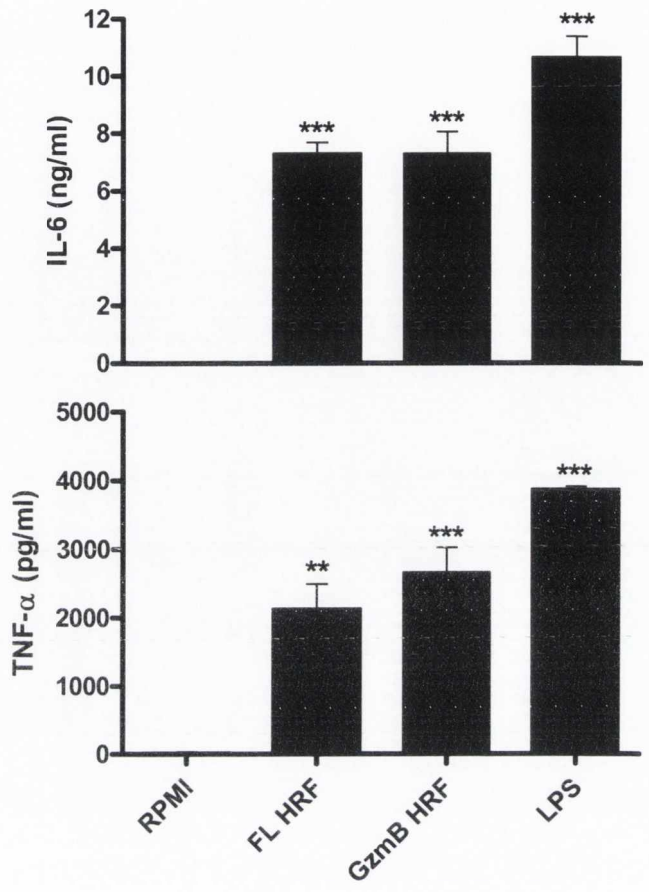

Figure 4.1 – Both FL and GzmB HRF potently induce proinflammatory cytokine secretion from BALB/c BMDCs. BMDCs (6.25 x 10^5 cells/ml) from BALB/c mice were stimulated with RPMI, LPS (0.01μg/ml), FL HRF (1μg/ml) or GzmB HRF (1μg/ml). Supernatants were collected 24 hours later and tested for the cytokines IL-6 and TNF-α by ELISA. Results are mean cytokine concentrations (+ SEM) for triplicate samples. Versus RPMI, **p<0.01, *** p<0.001.

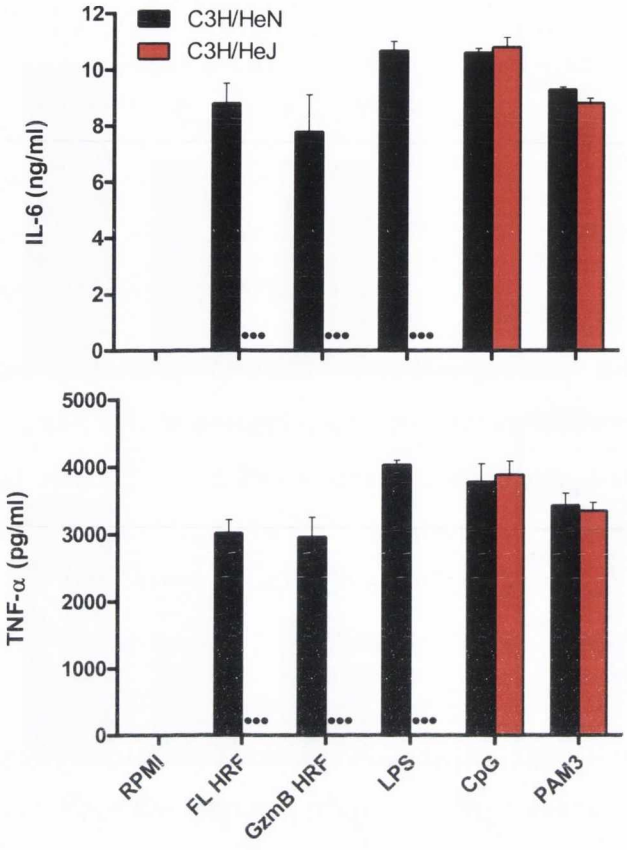

Figure 4.2 – Both FL and GzmB HRF fail to induce proinflammatory cytokine secretion from TLR4-defective C3H/HeJ BMDCs. BMDCs (6.25 x 10^5 cells/ml) from C3H/HeN and C3H/HeJ mice were stimulated with RPMI, LPS (0.01μg/ml), FL HRF (1μg/ml), GzmB HRF (1μg/ml), CpG (4μg/ml) or Pam3CSK4 (4μg/ml). Supernatants were collected 24 hours later and tested for the cytokines IL-6 and TNF-α by ELISA. Results are mean cytokine concentrations (+ SEM) for triplicate samples. Treatment of C3H/HeN BMDCs versus corresponding treatment of C3H/HeJ BMDCs, ••• $p<0.001$.

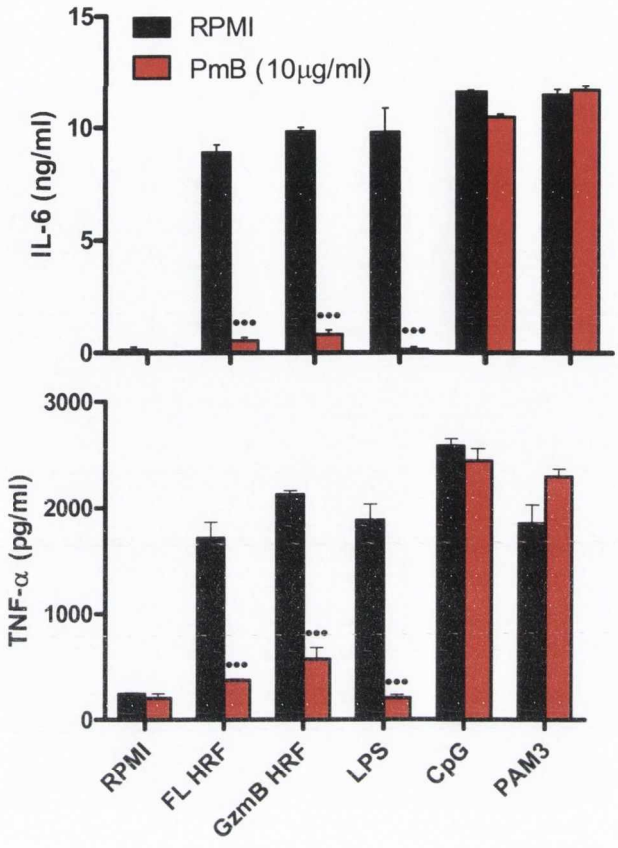

Figure 4.3 – The ability of both FL and GzmB HRF to induce cytokine secretion from BALB/c BMDCs is inhibited in the presence of PmB. BMDCs (6.25 x 10^5 cells/ml) from BALB/c mice were stimulated with RPMI, LPS (0.01μg/ml), FL HRF (1μg/ml), GzmB HRF (1μg/ml), CpG (4μg/ml) or Pam3CSK4 (4μg/ml), which were pre-incubated alone or in the presence of PmB (100μg/ml) for 2 hours at 37^0C. Supernatants were collected 24 hours later and tested for the cytokines IL-6 and TNF-α by ELISA. Results are mean cytokine concentrations (+ SEM) for triplicate samples. Treatment + PmB versus corresponding treatment alone, ••• $p<0.001$.

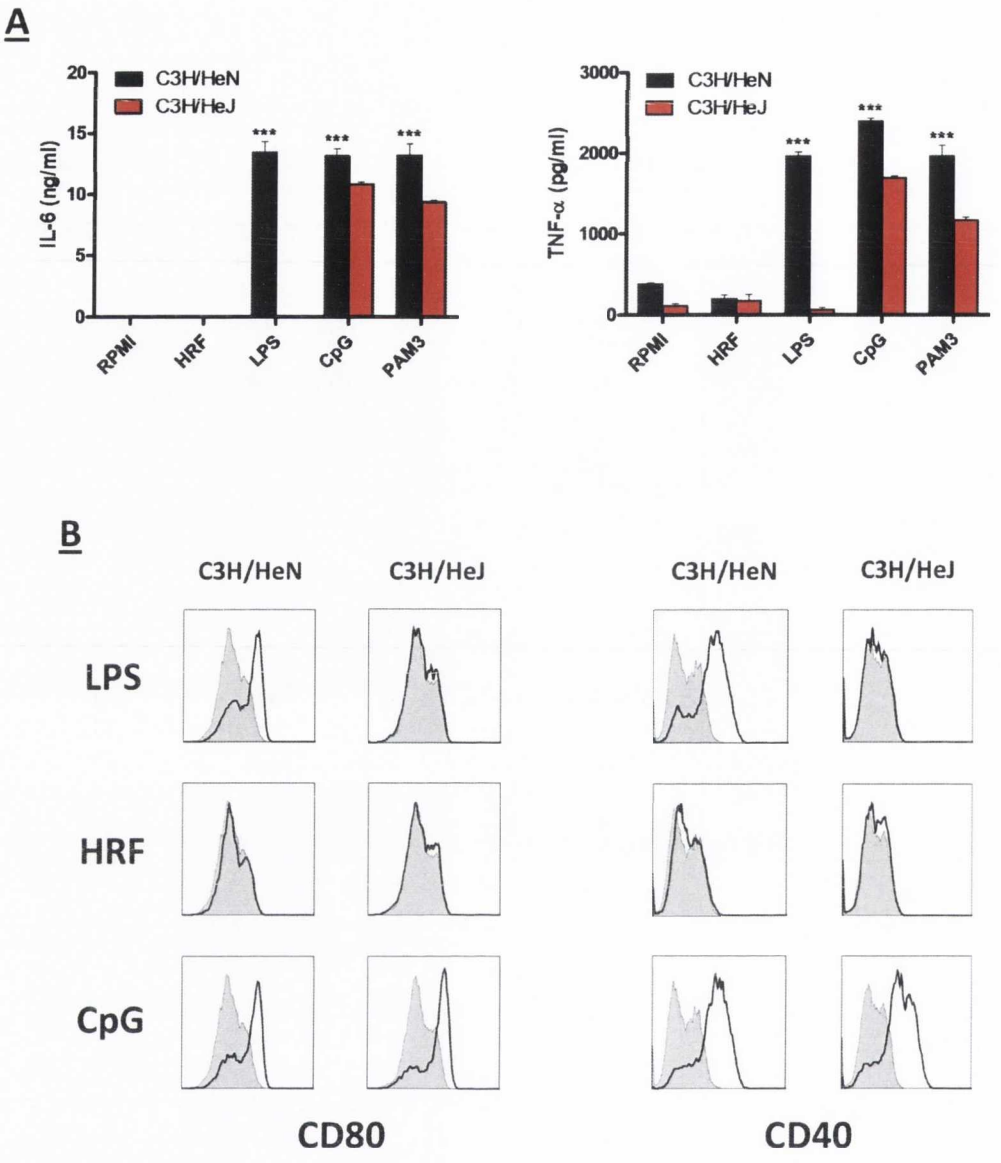

Figure 4.4 – PmB-agarose purified FL HRF does not induce proinflammatory cytokine secretion from C3H/HeN or C3H/HeJ BMDCs. BMDCs (6.25 x 10^5 cells/ml) from C3H/HeN and C3H/HeJ mice were stimulated with RPMI, LPS (0.01μg/ml), PmB-agarose purified FL HRF (HRF, 1μg/ml), CpG (4μg/ml) or Pam3CSK4 (4μg/ml). (A) Supernatants were collected 24 hours later and tested for the cytokines IL-6 and TNF-α by ELISA. Results are mean cytokine concentrations (+ SEM) for triplicate samples. Versus RPMI C3H/HeN, *** $p<0.001$. (B) $CD11c^+$ BMDCs were analysed for expression of the maturation markers CD80 and CD40 by flow cytometry. Immunofluorescence is shown for LPS-, HRF- or CpG-treated BMDCs (black line) compared to untreated cells incubated with RPMI (grey histograms).

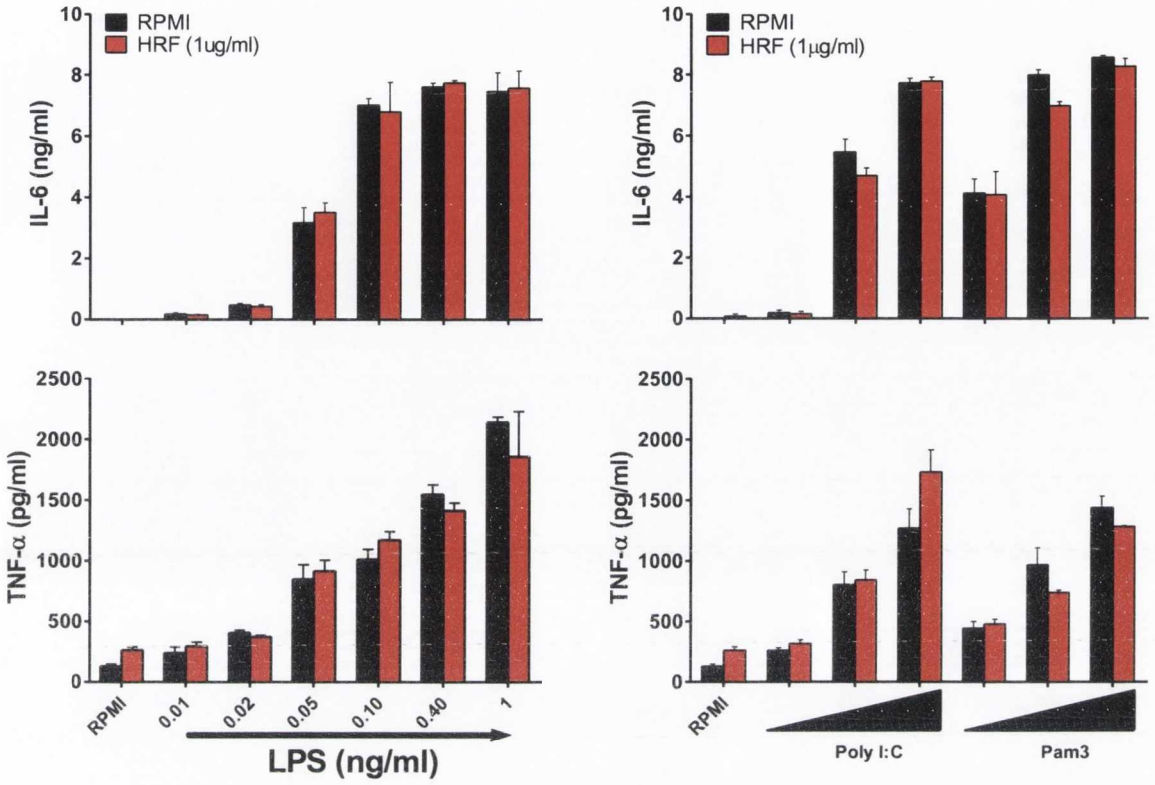

Figure 4.5 – FL HRF fails to synergise with TLR agonists to promote cytokine secretion. BMDCs (6.25 x 10^5 cells/ml) from BALB/c mice were stimulated with RPMI or the indicated concentrations of LPS as well as Poly I:C (1μg/ml, 5μg/ml and 10μg/ml) and Pam3CSK4 (1ng/ml, 5ng/ml and 10ng/ml), which were pre-incubated alone or in the presence of PmB-agarose purified FL HRF (HRF, 1μg/ml) for 2 hours at 37^0C. Supernatants were collected 24 hours later and tested for the cytokines IL-6 and TNF-α by ELISA. Results are mean cytokine concentrations (+ SEM) for triplicate samples.

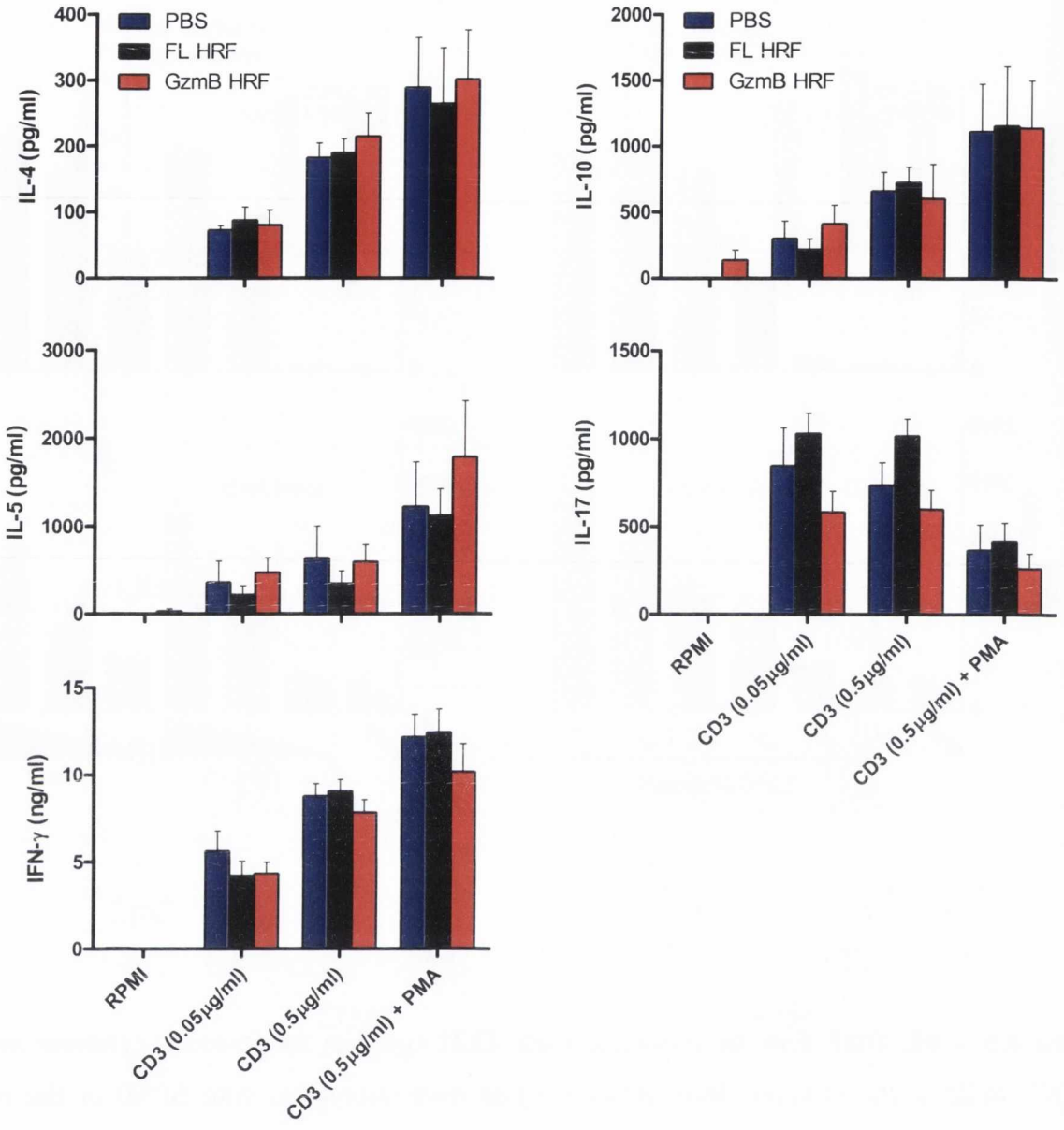

Figure 4.6 – Anti-CD3 restimulation of splenocytes from mice immunised for 4 consecutive days with PBS or 1µg of FL HRF or GzmB HRF. Female BALB/c mice were immunised i.p. for 4 consecutive days with PBS or 1µg of either FL HRF or GzmB HRF. The mice were sacrificed on day 5. Spleens were recovered and restimulated *ex vivo* with RPMI, anti-CD3 (0.05µg/ml and 0.5µg/ml) or anti-CD3 (0.5µg/ml) in combination with PMA (25ng/ml). After 72 hours, supernatants were collected and analysed for the cytokines IL-4, IL-5, IFN-γ, IL-10 and IL-17 by ELISA. Results are mean cytokine concentrations (+ SEM) for 4 mice per experimental group tested individually in triplicate.

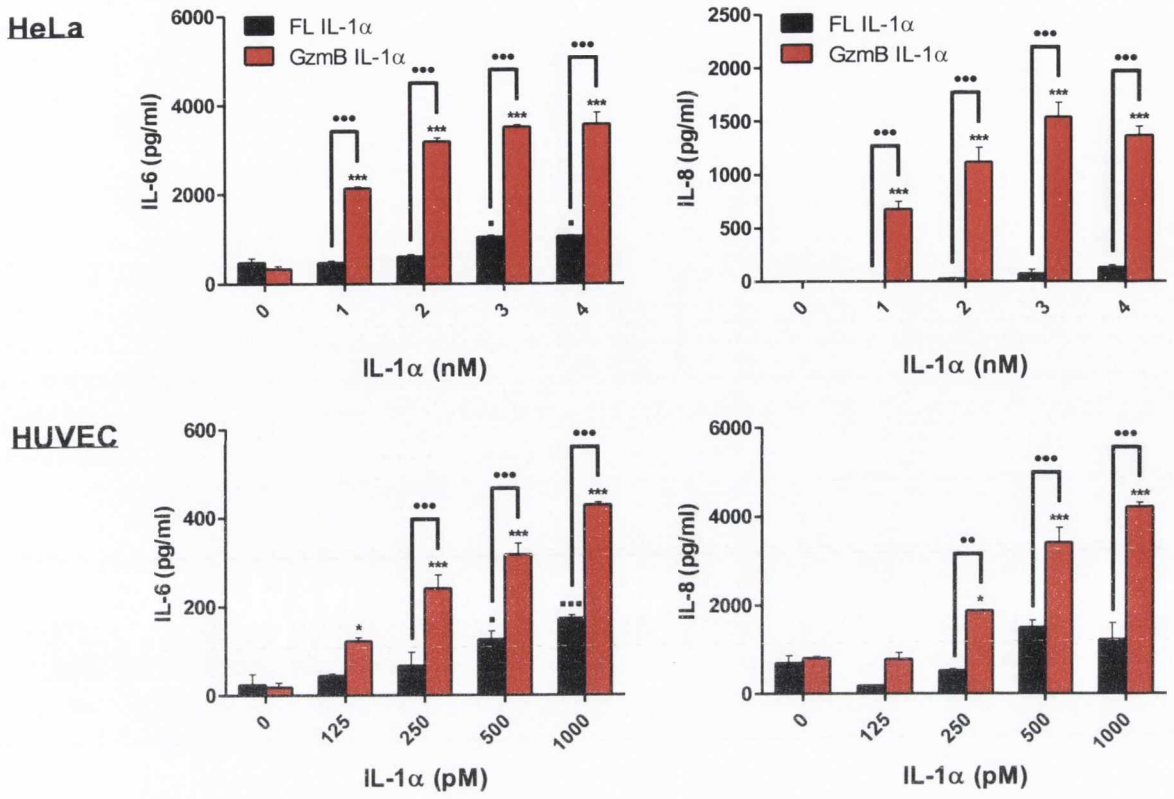

Figure 4.7 – GzmB-dependent proteolysis of IL-1α enhances cytokine bioactivity *in vitro*. HeLa or HUVEC cells were incubated with the indicated concentrations of FL IL-1α or GzmB IL-1α. Supernatants were collected 18 hours (HeLa) or 8 hours (HUVEC) later and were tested for the cytokines IL-6 and TNF-α by ELISA. Results are mean cytokine concentrations (+ SEM) for triplicate samples. Versus GzmB IL-1α (0pM), * $p<0.05$, ** $p<0.01$, *** $p<0.001$. Versus FL IL-1α (0pM), ▪ $p<0.05$, ▪▪ $p<0.01$, ▪▪▪ $p<0.001$. GzmB IL-1α versus corresponding concentration of FL IL-1α, •• $p<0.01$, ••• $p<0.001$. This experiment was performed by Dr. Inna Afonina of the Molecular Cell Biology Laboratory in the Department of Genetics, TCD.

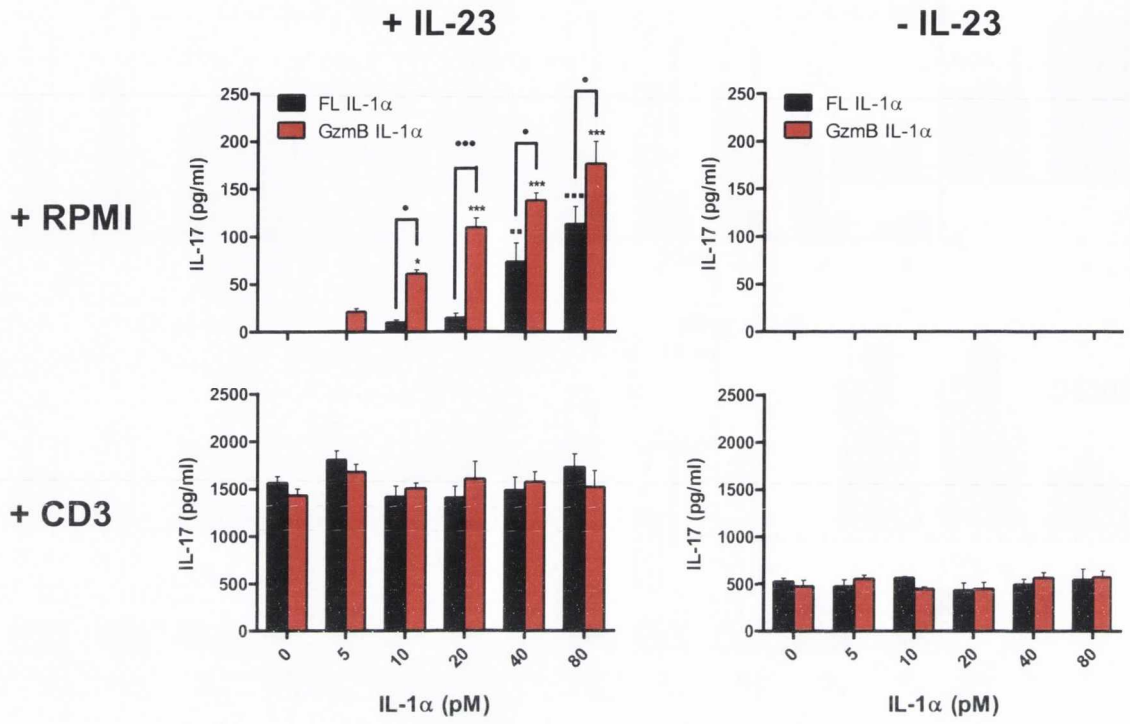

Figure 4.8 – GzmB-dependent proteolysis of IL-1α enhances IL-17 secretion by splenocytes in the presence of IL-23. Splenocytes (2 x 10^6 cells/ml) from BALB/c mice were stimulated with the indicated concentrations of FL IL-1α or GzmB IL-1α with and without IL-23 (10ng/ml) and plate-bound anti-CD3 (0.5μg/ml). Supernatants were collected 72 hours later and tested for the cytokine IL-17 by ELISA. Results are mean cytokine concentrations (+ SEM) for triplicate samples. Versus GzmB IL-1α (0pM), * $p<0.05$, *** $p<0.001$. Versus FL IL-1α (0pM), ▪▪ $p<0.01$, ▪▪▪ $p<0.001$. GzmB IL-1α versus corresponding concentration of FL IL-1α, • $p<0.05$, ••• $p<0.001$.

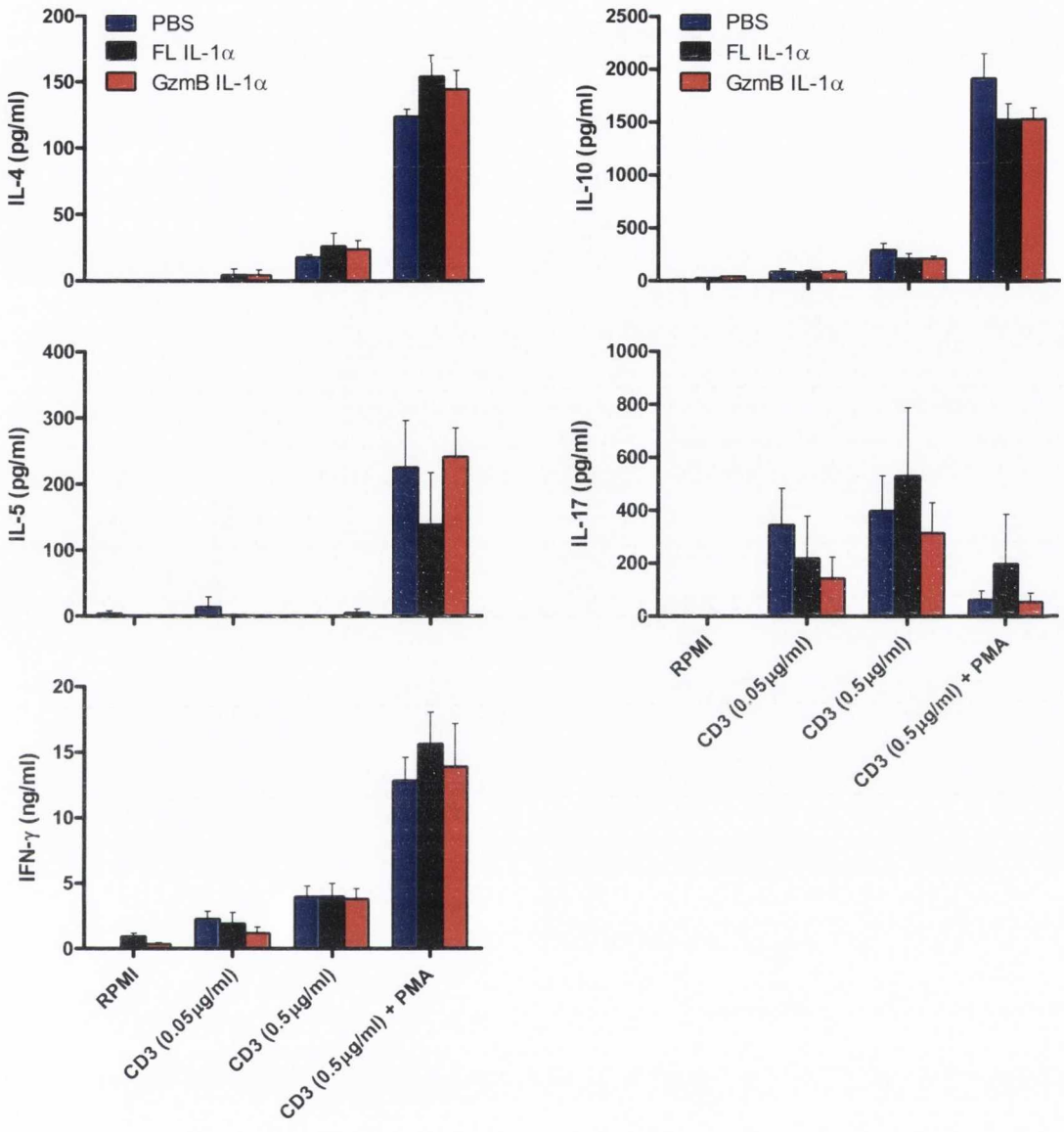

Figure 4.9 – Anti-CD3 restimulation of splenocytes from mice immunised for 4 consecutive days with PBS or 1µg of FL IL-1α or GzmB IL-1α. Female BALB/c mice were immunised i.p. for 4 consecutive days with PBS or 1µg of either FL IL-1α or GzmB IL-1α. The mice were sacrificed on day 5. Spleens were recovered and restimulated *ex vivo* with RPMI, anti-CD3 (0.05µg/ml and 0.5µg/ml) or anti-CD3 (0.5µg/ml) in combination with PMA (25ng/ml). After 72 hours, supernatants were collected and analysed for the cytokines IL-4, IL-5, IFN-γ, IL-10 and IL-17 by ELISA. Results are mean cytokine concentrations (+ SEM) for 4 mice per experimental group tested individually in triplicate.

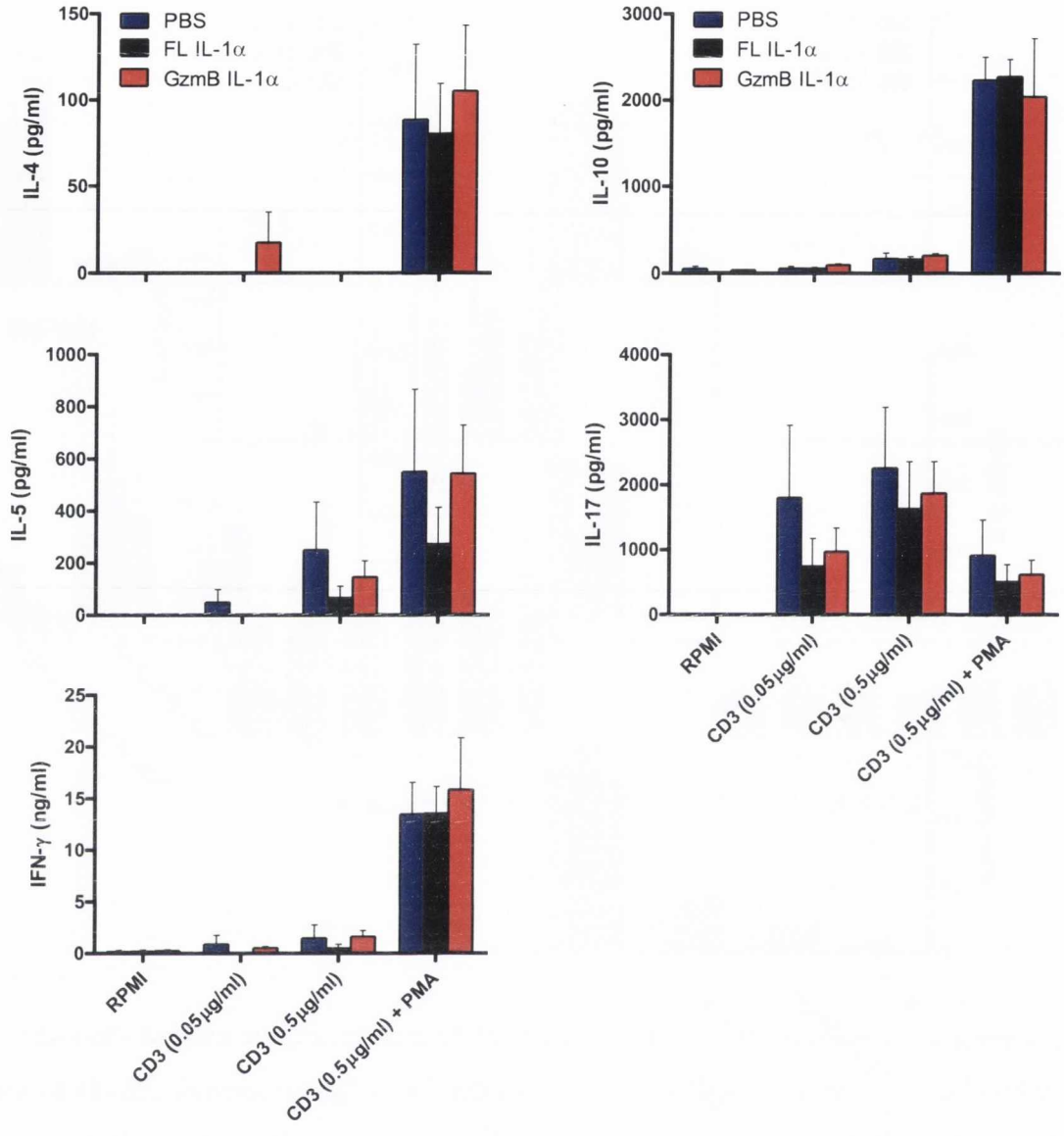

Figure 4.10 – Anti-CD3 restimulation of mediastinal lymph node cells from mice immunised for 4 consecutive days with PBS or 1µg of FL IL-1α or GzmB IL-1α. Female BALB/c mice were immunised as described in Figure 4.9. Mediastinal lymph nodes were recovered and restimulated *ex vivo* as described in Figure 4.9. After 72 hours, supernatants were collected and analysed for the cytokines IL-4, IL-5, IFN-γ, IL-10 and IL-17 by ELISA. Results are mean cytokine concentrations (+ SEM) for 4 mice per experimental group tested individually in triplicate.

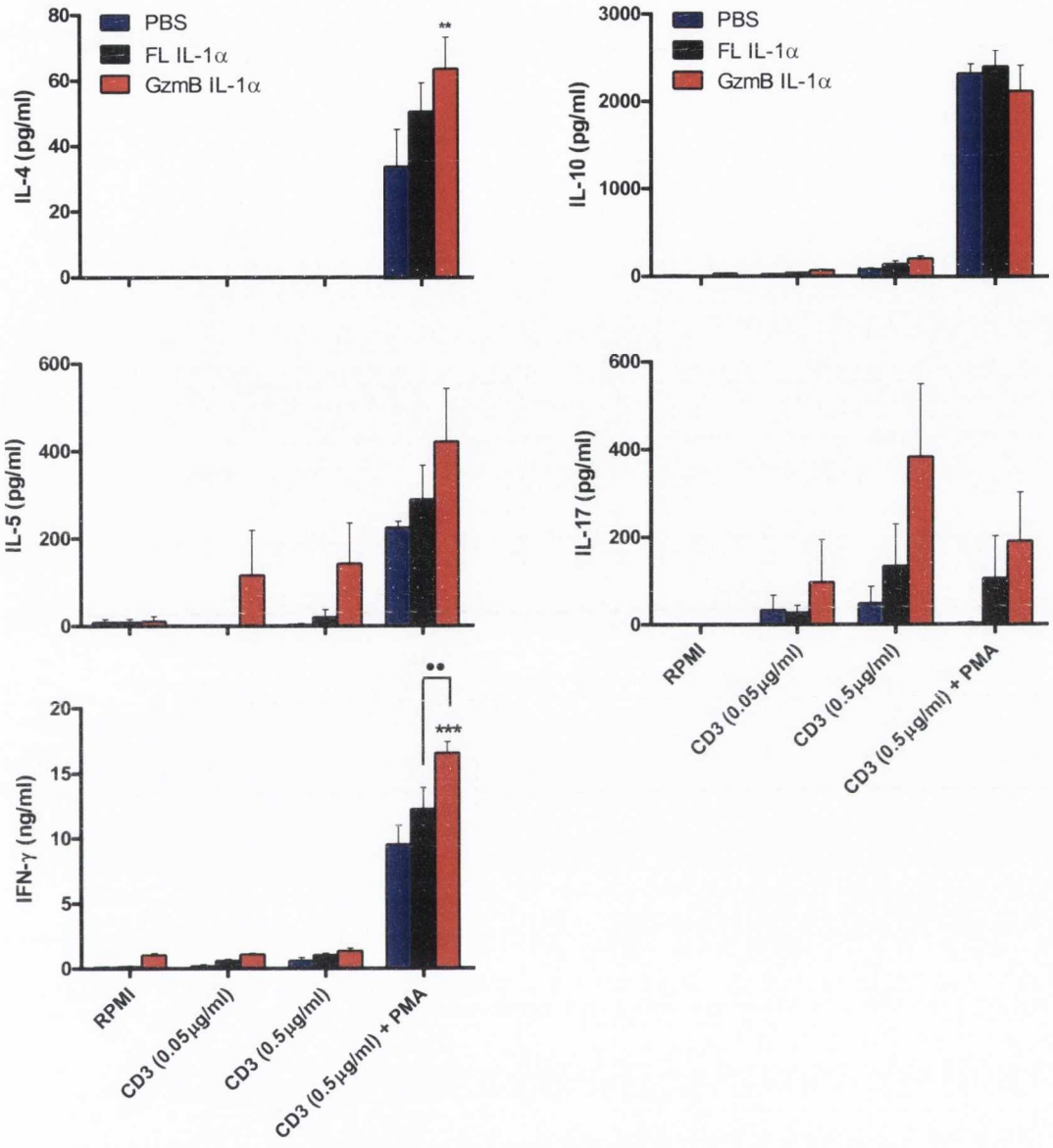

Figure 4.11 – Injection of GzmB IL-1α potentiates cytokine secretion by mesenteric lymph node cells following restimulation with anti-CD3. Female BALB/c mice were immunised as described in Figure 4.9. Mesenteric lymph nodes were recovered and restimulated *ex vivo* as described in Figure 4.9. After 72 hours, supernatants were collected and analysed for the cytokines IL-4, IL-5, IFN-γ, IL-10 and IL-17 by ELISA. Results are mean cytokine concentrations (+ SEM) for 4 mice per experimental group tested individually in triplicate. Versus PBS at corresponding concentration of stimulus, ** $p<0.01$, *** $p<0.001$. GzmB IL-1α versus FL IL-1α at corresponding concentration of stimulus, •• $p<0.01$.

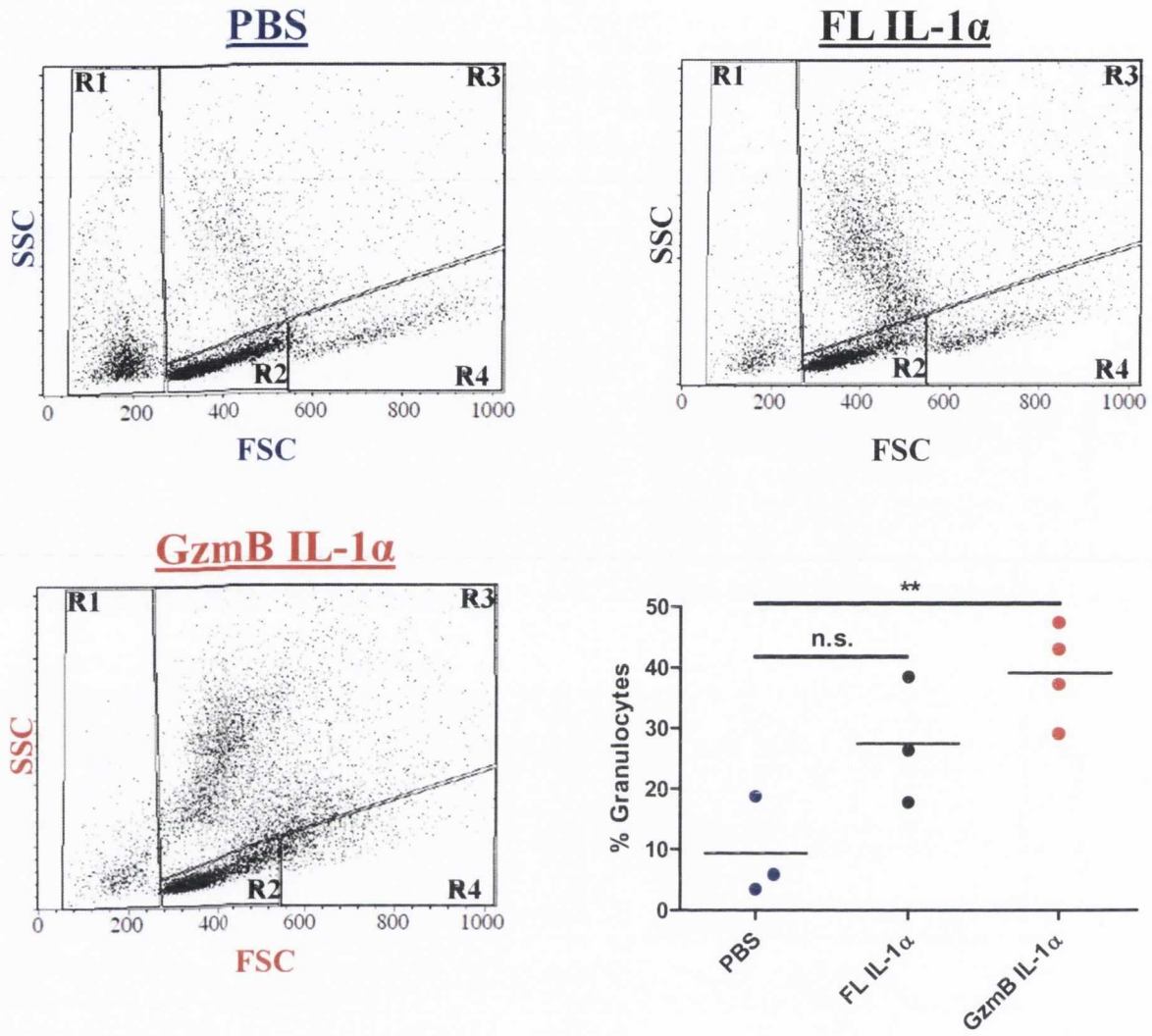

Figure 4.12 – GzmB IL-1α displays enhanced capacity for granulocyte recruitment into the peritoneum. Female BALB/c mice were injected as described in Figure 4.9. PECs were collected and analysed by flow cytometry. Granulocytes were identified on the basis of their high SSC/FSC profile (R3 in representative dot plots). Percentage of cells in R3 for each group is shown in the scatter plot. Versus PBS, n.s., not significant, ** $p<0.01$. FACS analysis was performed by Dr. Inna Afonina of the Molecular Cell Biology Laboratory in the Department of Genetics, TCD.

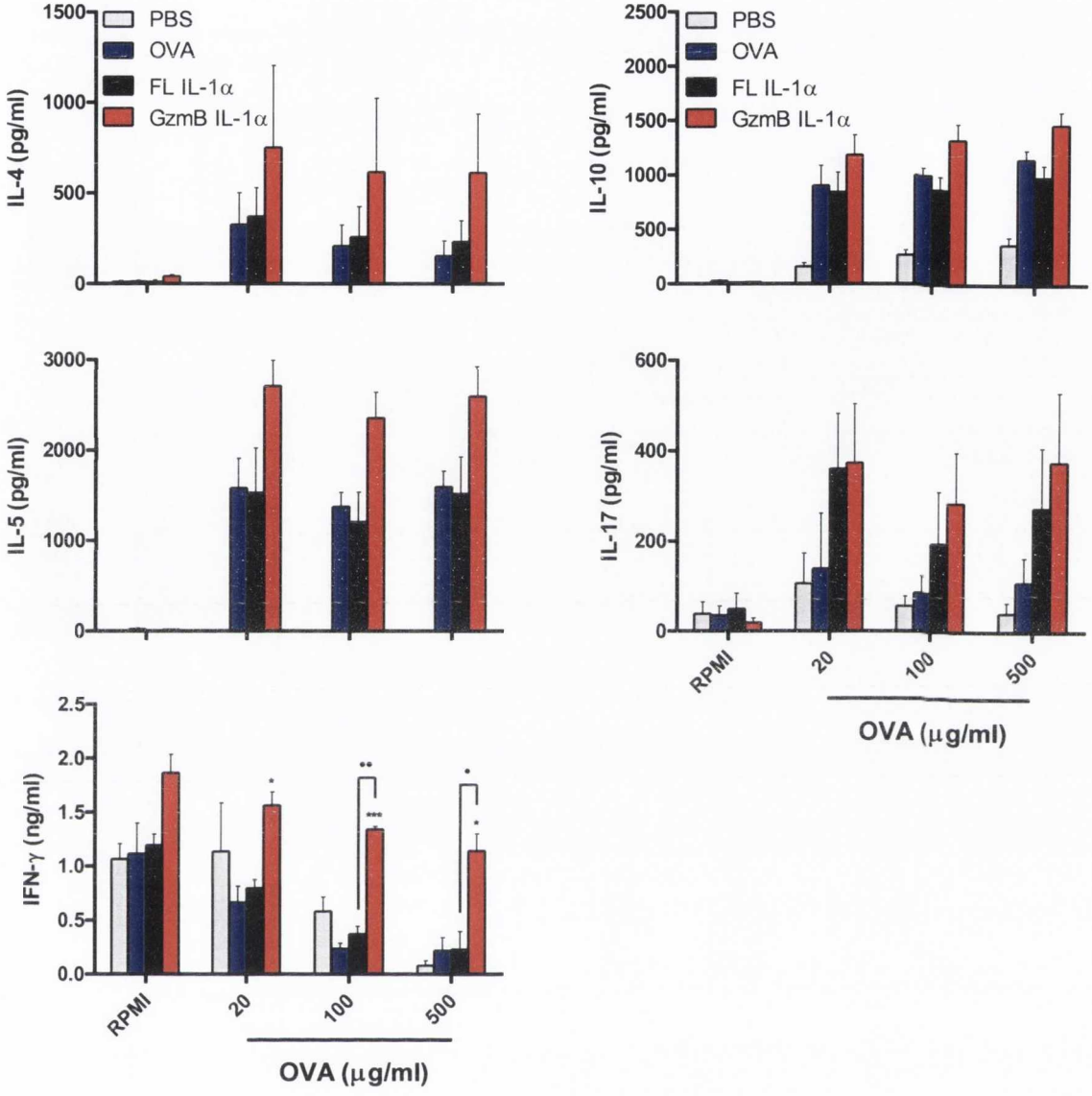

Figure 4.13 – Injection of antigen with GzmB IL-1α enhances antigen-specific IL-4, IL-5 and IL-10 production by PECs. Female BALB/c mice were immunised i.p. with PBS or OVA (200μg/mouse) either alone or in combination with FL IL-1α or GzmB IL-1α (5μg/mouse). The mice were boosted with these same treatments on day 14 and were sacrificed on day 21. PECs were recovered and restimulated *ex vivo* with RPMI or a range of concentrations of OVA (20, 100, 500μg/ml). After 72 hours, supernatants were collected and analysed for the cytokines IL-4, IL-5, IFN-γ, IL-10 and IL-17 by ELISA. Results are mean cytokine concentrations (+ SEM) for 5 mice per experimental group tested individually in triplicate. Versus OVA at corresponding concentrations of stimulus, * $p<0.05$, *** $p<0.001$, GzmB IL-1α versus FL IL-1α at corresponding concentration of stimulus, • $p<0.05$, •• $p<0.01$.

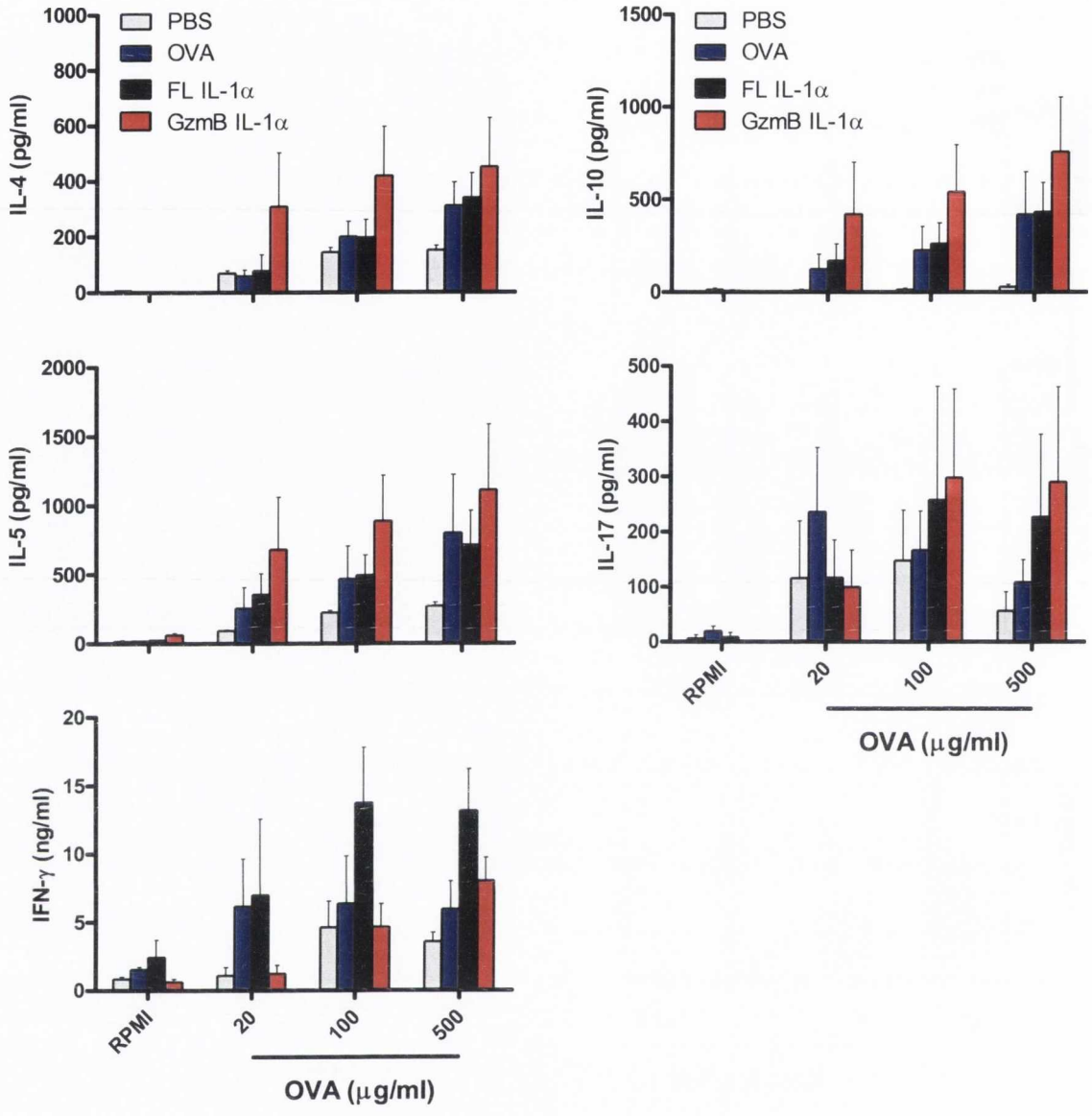

Figure 4.14 – Injection of antigen with GzmB IL-1α enhances the secretion of antigen-specific IL-4, IL-5 and IL-10 by splenocytes. Female BALB/c mice were immunised as described in Figure 4.13. Spleens were recovered and restimulated *ex vivo* with RPMI or a range of concentrations of OVA (20, 100, 500μg/ml). After 72 hours, supernatants were collected and analysed for the cytokines IL-4, IL-5, IFN-γ, IL-10 and IL-17 by ELISA. Results are mean cytokine concentrations (+ SEM) for 5 mice per experimental group tested individually in triplicate.

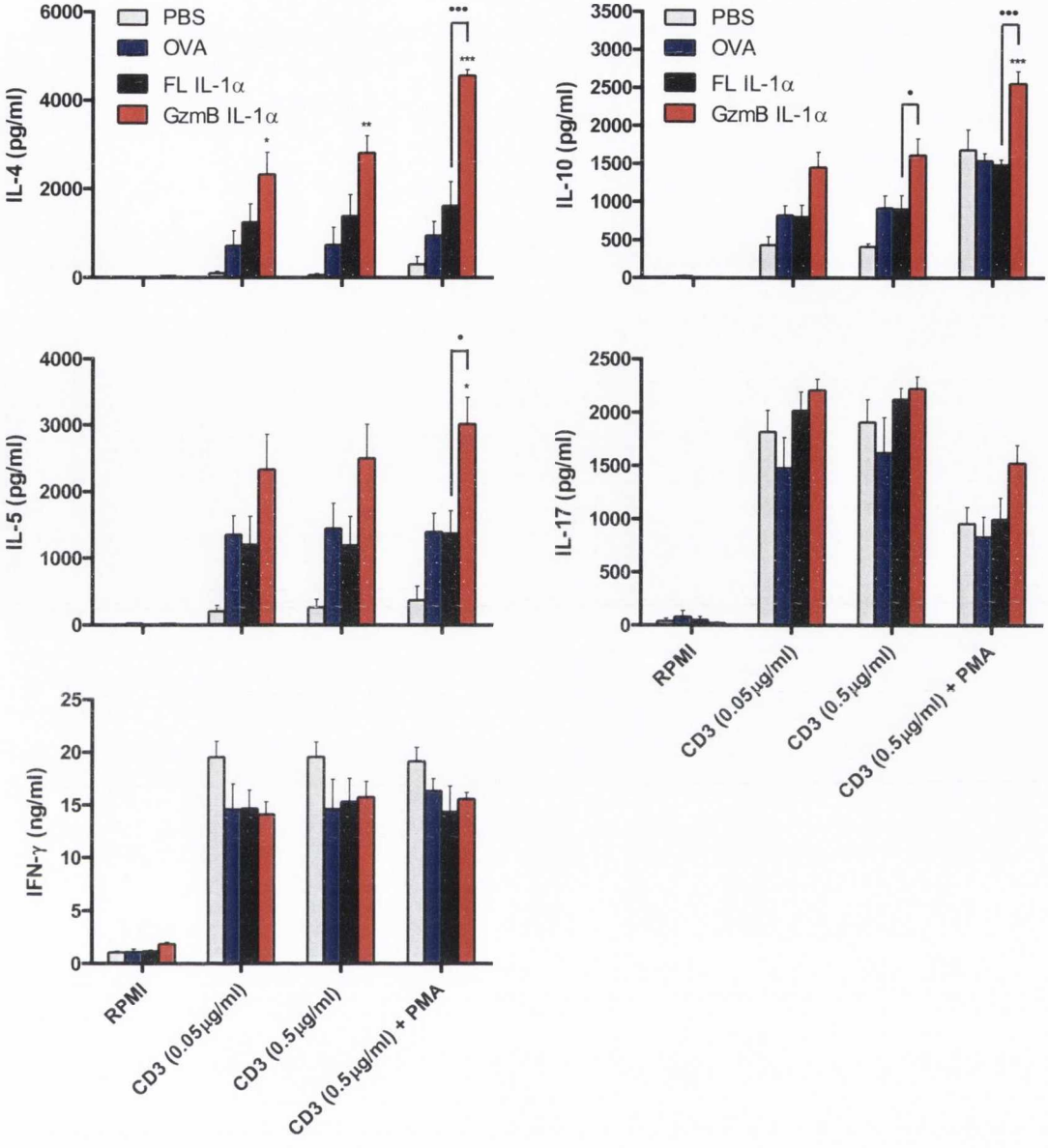

Figure 4.15 – Injection of antigen with GzmB IL-1α significantly enhances the secretion of IL-4, IL-5 and IL-10 by PECs following restimulation with anti-CD3. Female BALB/c mice were immunised as described in Figure 4.13. PECs were recovered and restimulated *ex vivo* with RPMI, anti-CD3 (0.05μg/ml and 0.5μg/ml) or anti-CD3 (0.5μg/ml) in combination with PMA (25ng/ml). After 72 hours, supernatants were collected and analysed for the cytokines IL-4, IL-5, IFN-γ, IL-10 and IL-17 by ELISA. Results are mean cytokine concentrations (+ SEM) for 5 mice per experimental group tested individually in triplicate. Versus OVA at corresponding concentration of stimulus, * $p<0.05$, ** $p<0.01$, *** $p<0.001$. GzmB IL-1α versus FL IL-1α at corresponding concentration of stimulus, • $p<0.05$, ••• $p<0.001$.

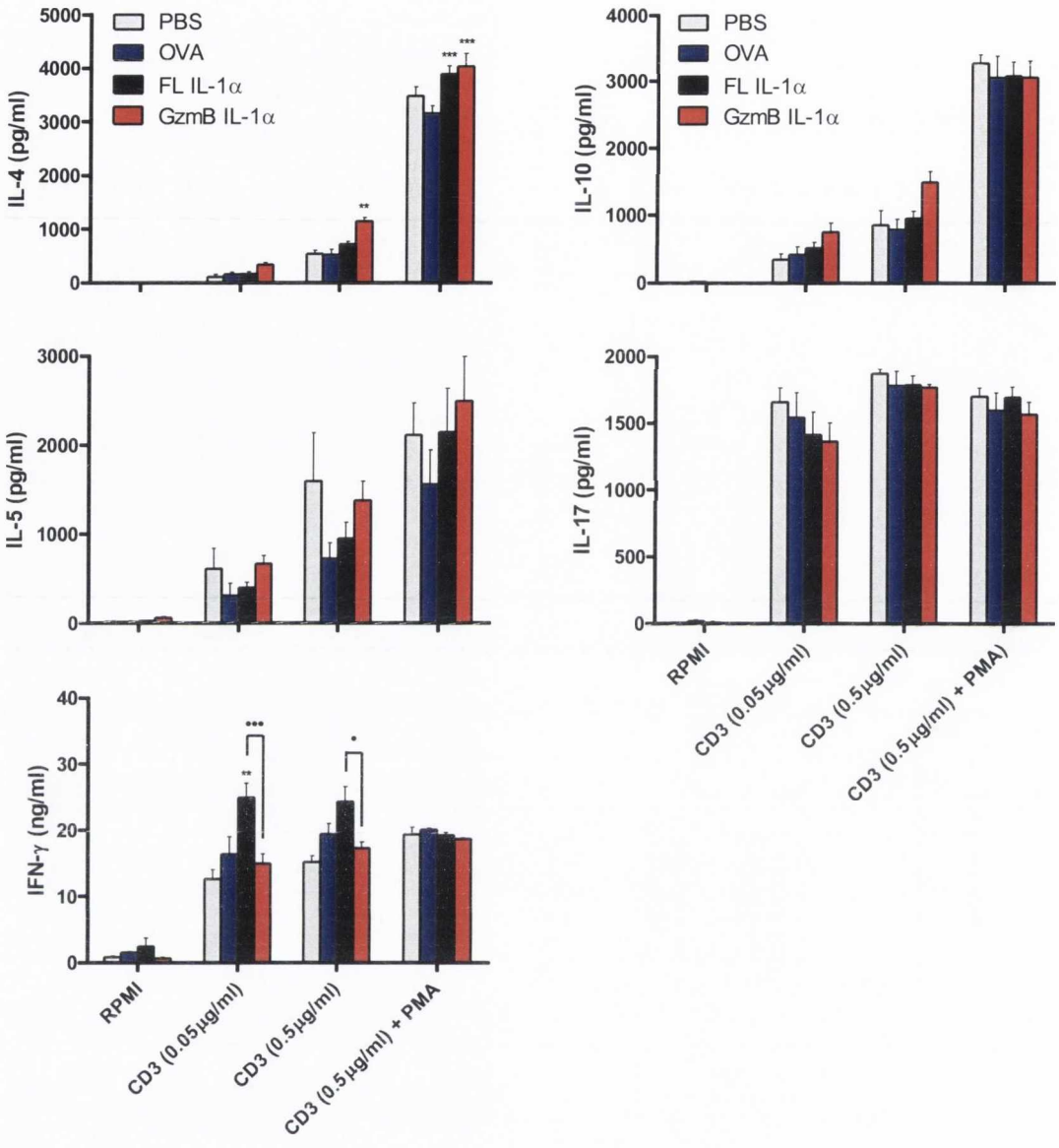

Figure 4.16 – Injection of antigen with GzmB IL-1α fails to enhance the secretion of T cell cytokines by splenocytes in response to anti-CD3. Female BALB/c mice were immunised as described in Figure 4.13. Spleens were recovered and restimulated *ex vivo* with RPMI, anti-CD3 (0.05µg/ml and 0.5µg/ml) or anti-CD3 (0.5µg/ml) in combination with PMA (25ng/ml). After 72 hours, supernatants were collected and analysed for the cytokines IL-4, IL-5, IFN-γ, IL-10 and IL-17 by ELISA. Results are mean cytokine concentrations (+ SEM) for 5 mice per experimental group tested individually in triplicate. Versus OVA at corresponding concentration of stimulus, ** $p<0.01$, *** $p<0.001$. GzmB IL-1α versus FL IL-1α at corresponding concentration of stimulus, • $p<0.05$, ••• $p<0.001$.

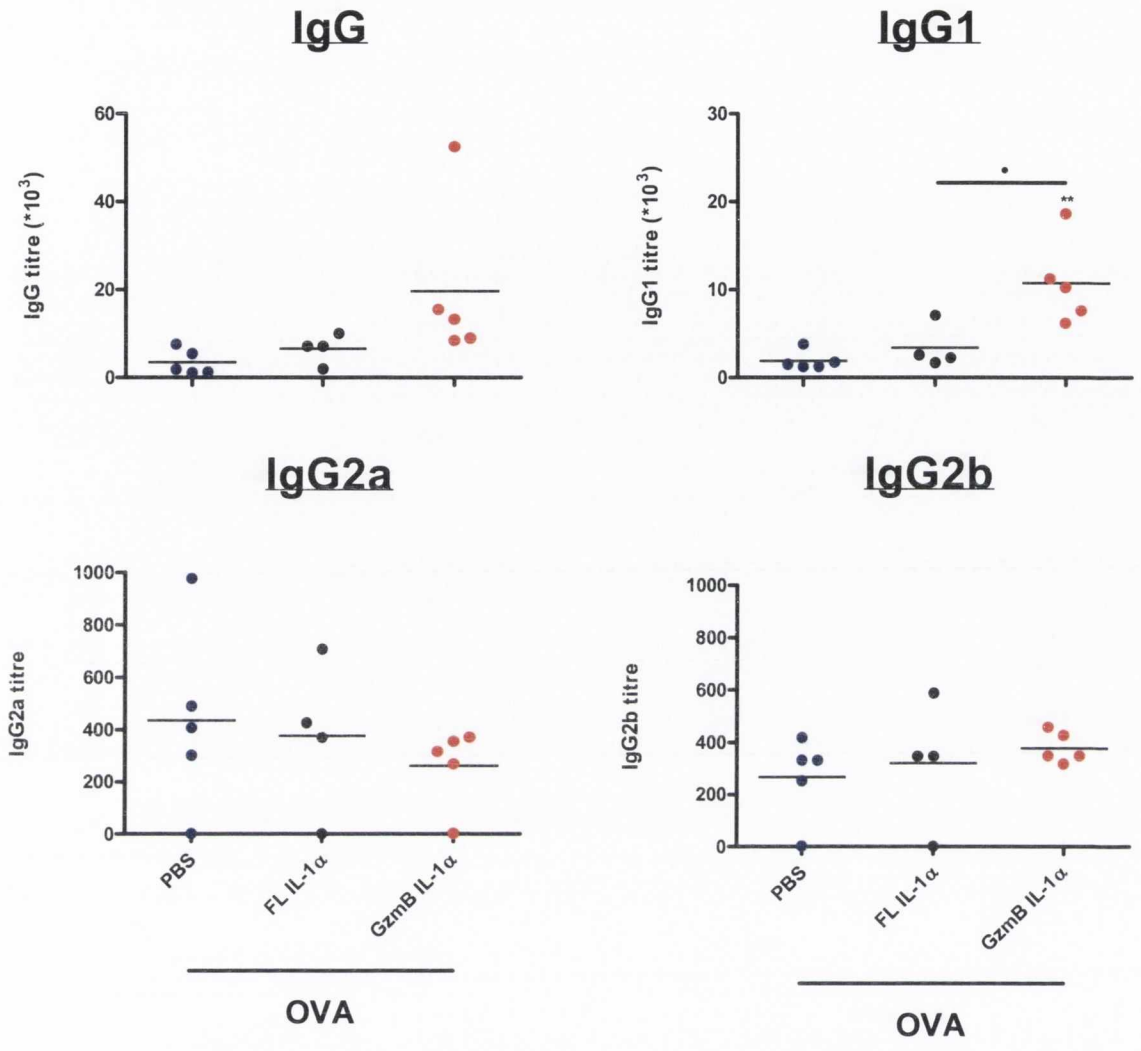

Figure 4.17 – GzmB-dependent proteolysis of IL-1α enhances OVA-specific antibody titres in the serum (Pre-Boost). Female BALB/c mice were immunised i.p. with PBS or OVA (200μg/mouse) either alone or in combination with FL IL-1α or GzmB IL-1α (5μg/mouse). Blood samples were recovered on day 13 and OVA-specific antibody titres (IgG, IgG1, IgG2a, IgG2b) in the serum were determined by ELISA. Scatter plot represents mean titre. Versus PBS (OVA), ** $p<0.01$. GzmB IL-1α (OVA) versus FL IL-1α (OVA), • $p<0.05$.

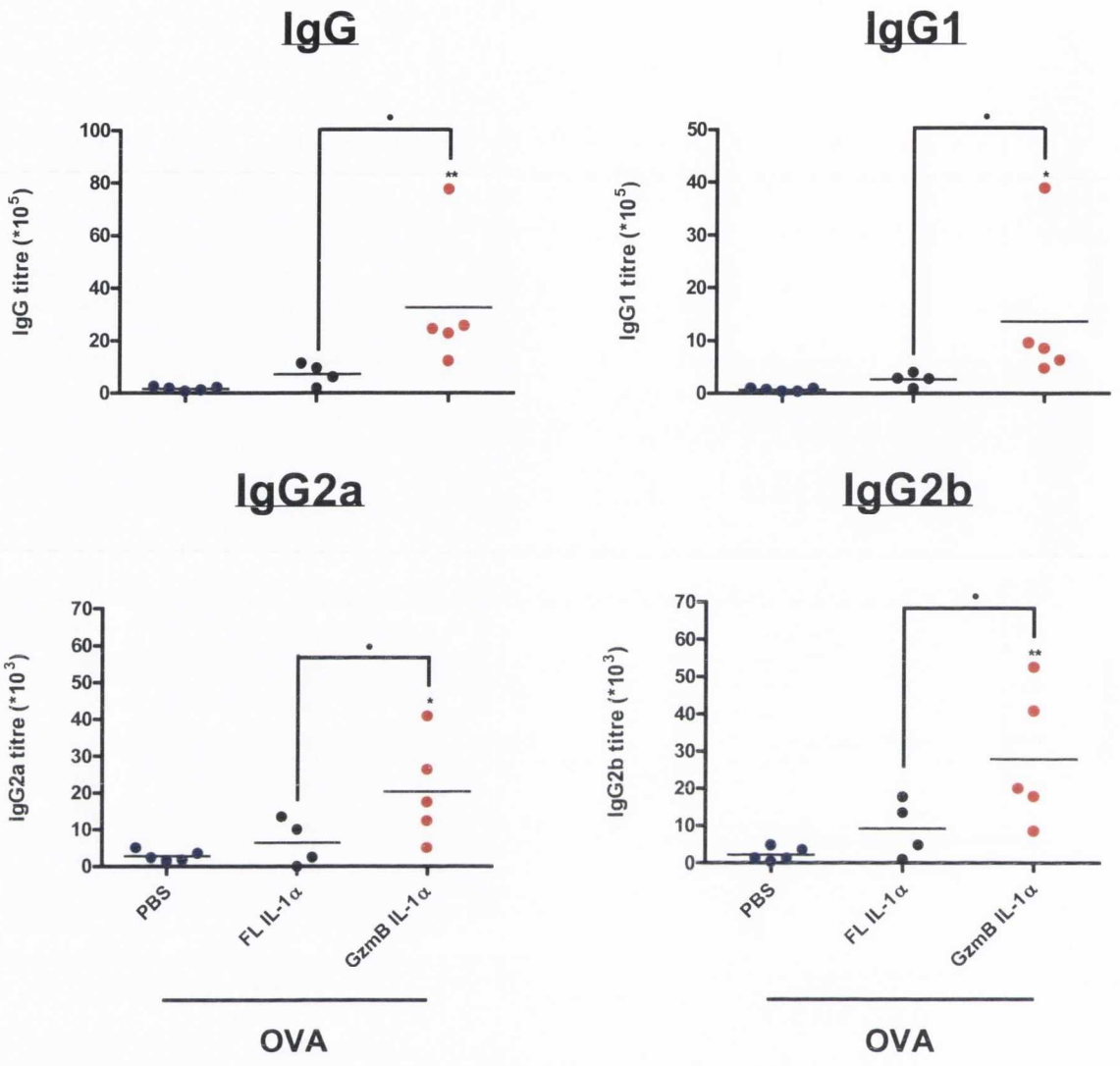

Figure 4.18 – GzmB processing of IL-1α significantly potentiates OVA-specific antibody titres in the serum (Post-Boost). Female BALB/c mice were immunised as described in Figure 4.13. Blood samples were recovered on day 21 and OVA-specific antibody titres (IgG, IgG1, IgG2a, IgG2b) in the serum were determined by ELISA. Scatter plot represents mean titre. Versus PBS (OVA), * $p<0.05$, ** $p<0.01$. GzmB IL-1α (OVA) versus FL IL-1α (OVA), • $p<0.05$.

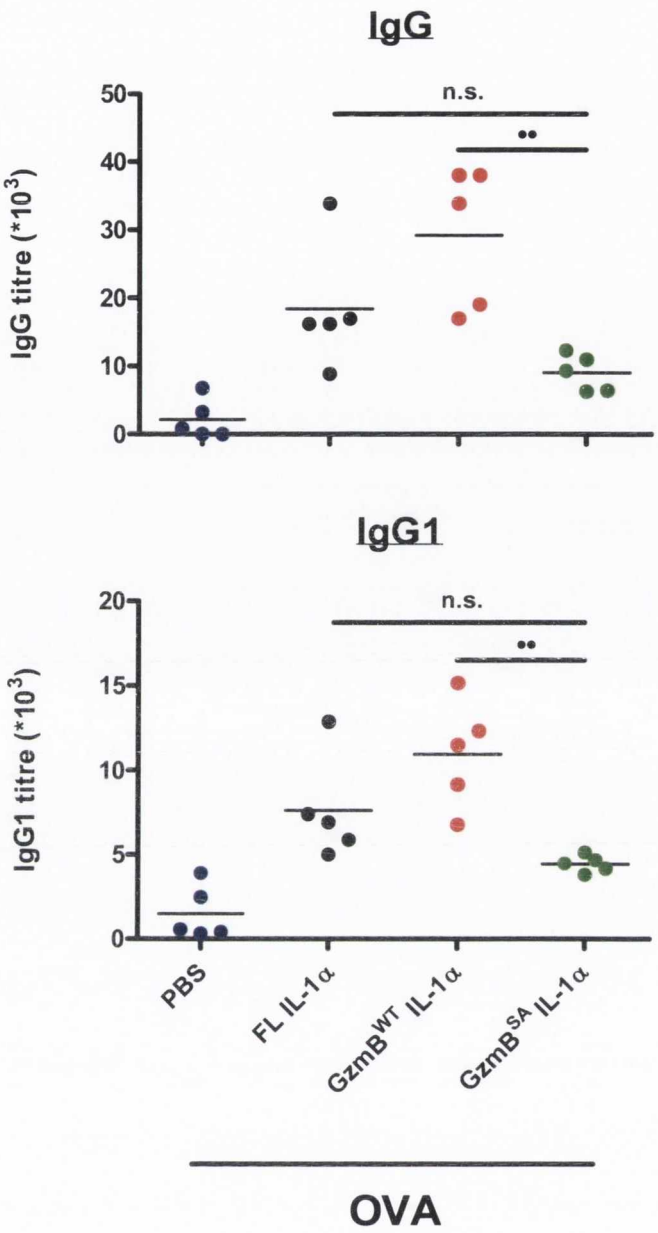

Figure 4.19 – GzmB contaminants are not responsible for enhanced IL-1α bioactivity *in vivo* (Pre-Boost). Female BALB/c mice were immunised i.p. with PBS or OVA (200μg/mouse) either alone or in combination with FL IL-1α, $GzmB^{WT}$ IL-1α or $GzmB^{SA}$ IL-1α (5μg/mouse). Blood samples were recovered on day 13 and OVA-specific antibody titres (IgG, IgG1) in the serum were determined by ELISA. Scatter plot represents mean titre for 5 mice per experimental group. Versus $GzmB^{SA}$ IL-1α (OVA), n.s., not significant, •• $p<0.01$.

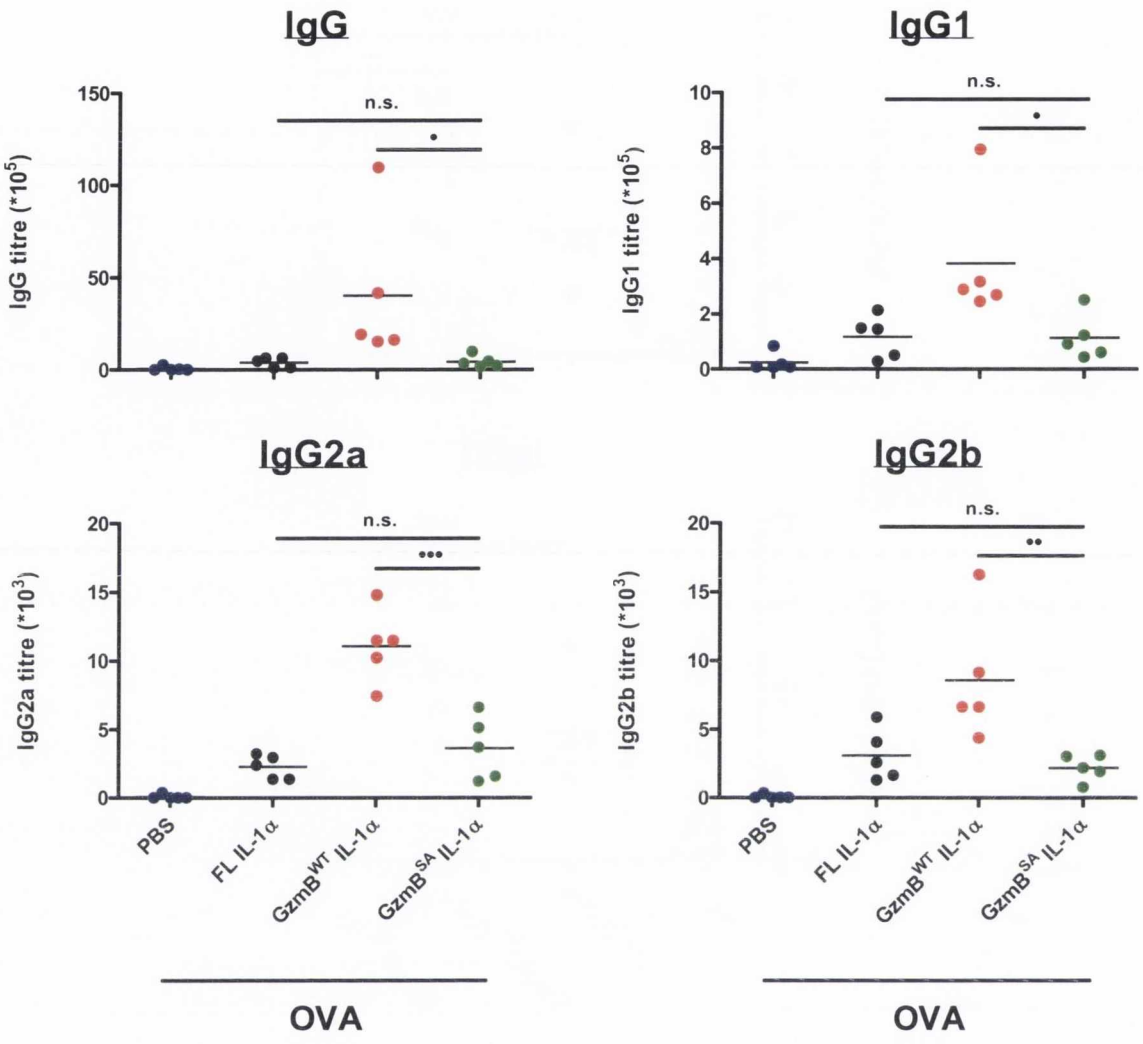

Figure 4.20 – GzmB contaminants are not responsible for enhanced IL-1α bioactivity *in vivo* (Post-Boost). Female BALB/c mice were immunised i.p. with PBS or OVA (200μg/mouse) either alone or in combination with FL IL-1α, $GzmB^{WT}$ IL-1α or $GzmB^{SA}$ IL-1α (5μg/mouse). The mice were boosted with these same treatments on day 14 and were sacrificed on day 21. Blood samples were recovered and OVA-specific antibody titres (IgG, IgG1, IgG2a, IgG2b) in the serum were determined by ELISA. Scatter plot represents mean titre for 5 mice per experimental group. Versus $GzmB^{SA}$ IL-1α (OVA), n.s., not significant, • $p<0.05$, •• $p<0.01$, ••• $p<0.001$.

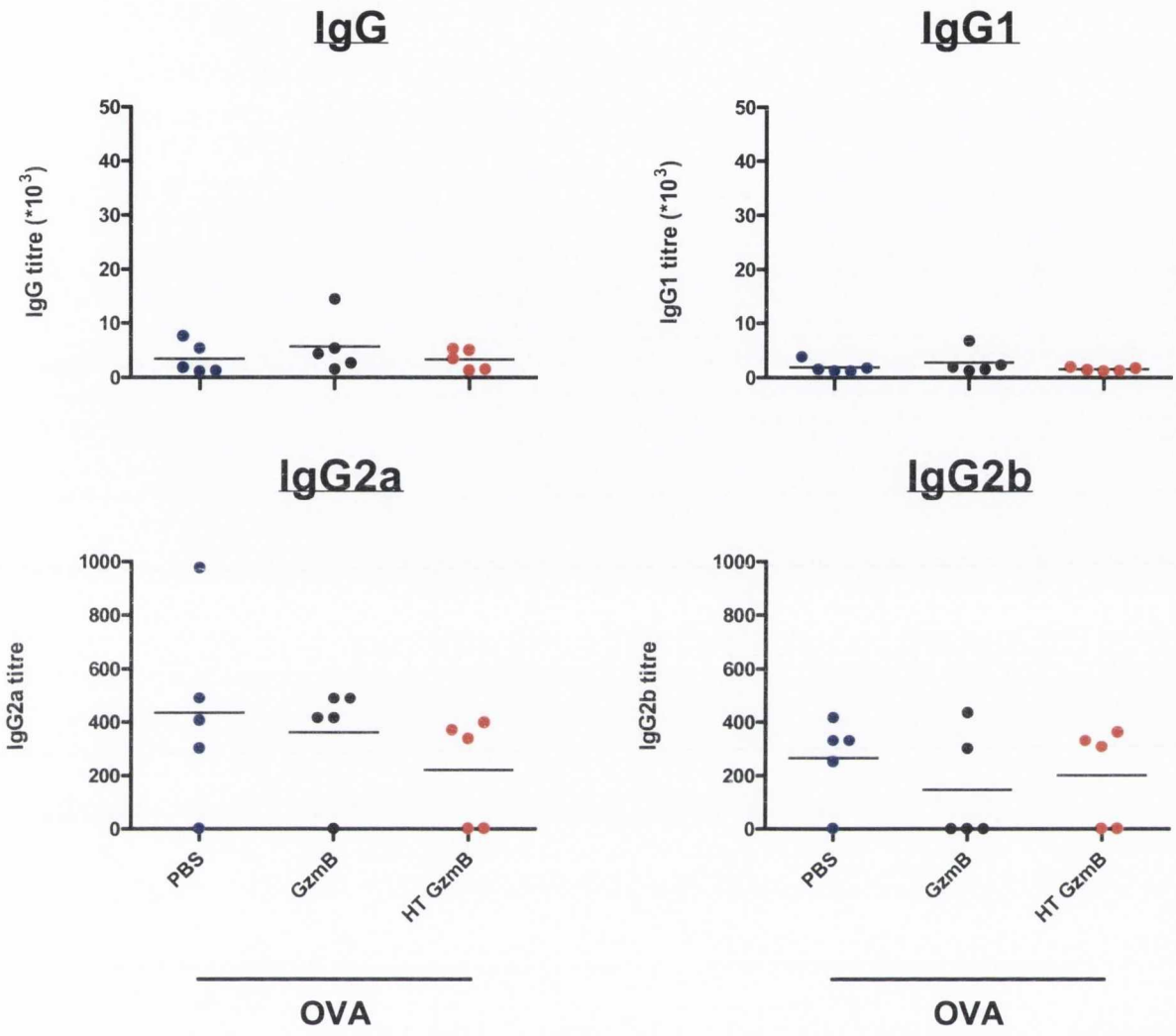

Figure 4.21 – GzmB does not possess adjuvanticity *in vivo* (Pre-Boost). Female BALB/c mice were immunised i.p. with PBS or OVA (200µg/mouse) either alone or in combination with active GzmB or HI GzmB (2µg/mouse). Blood samples were recovered on day 13 and OVA-specific antibody titres (IgG, IgG1, IgG2a, IgG2b) in the serum were determined by ELISA. Scatter plot represents mean titre for 5 mice per experimental group.

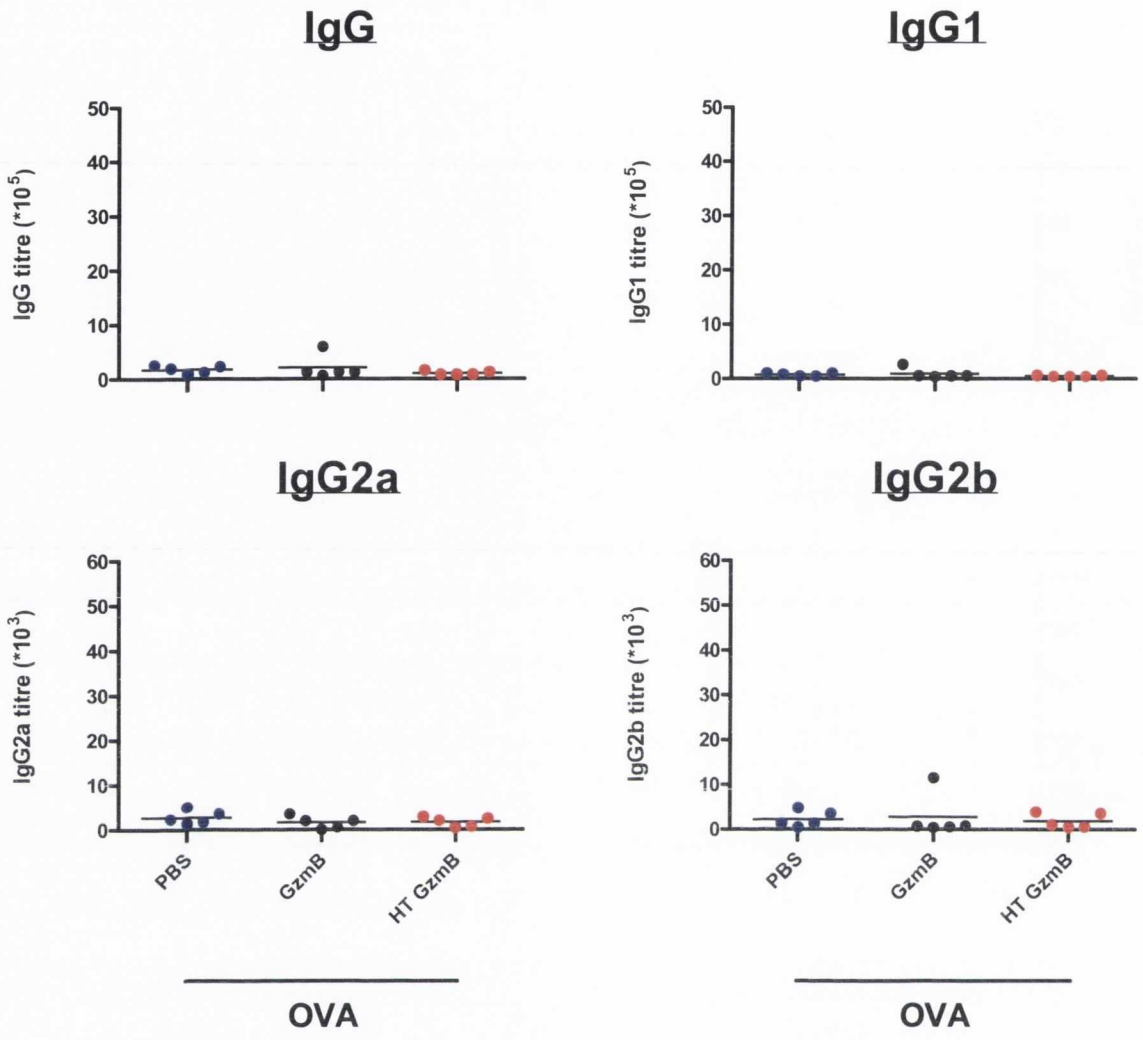

Figure 4.22 – GzmB does not possess adjuvanticity *in vivo* (Post-Boost). Female BALB/c mice were immunised i.p. with PBS or OVA (200µg/mouse) either alone or in combination with active GzmB or HI GzmB (2µg/mouse). The mice were boosted with these same treatments on day 14 and were sacrificed on day 21. Blood samples were recovered and OVA-specific antibody titres (IgG, IgG1, IgG2a, IgG2b) in the serum were determined by ELISA. Scatter plot represents mean titre for 5 mice per experimental group.

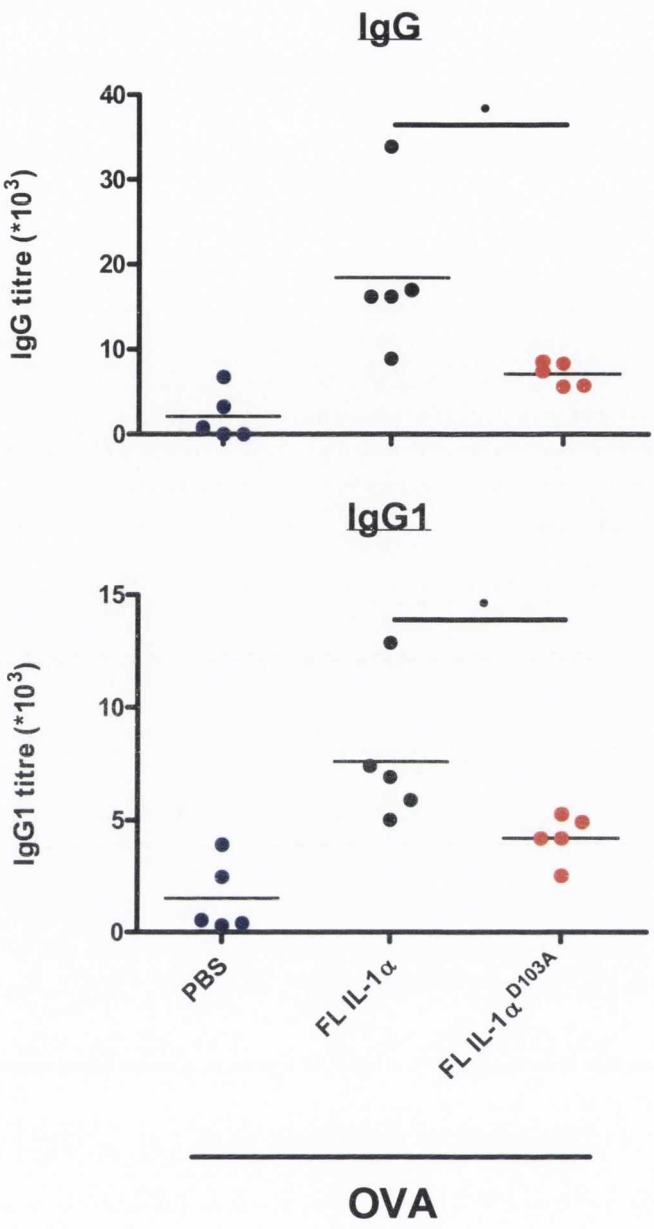

Figure 4.23 – IL-1α processing is mediated by GzmB *in vivo* (Pre-Boost). Female BALB/c mice were immunised i.p. with PBS or OVA (200μg/mouse) either alone or in combination with FL IL-1α or GzmB non-cleavable IL-1α (FL IL-1α^{D103A}) (5μg/mouse). Blood samples were recovered on day 13 and OVA-specific antibody titres (IgG, IgG1) in the serum were determined by ELISA. Scatter plot represents mean titre for 5 mice per experimental group. Versus FL IL-1α (OVA), • $p<0.05$.

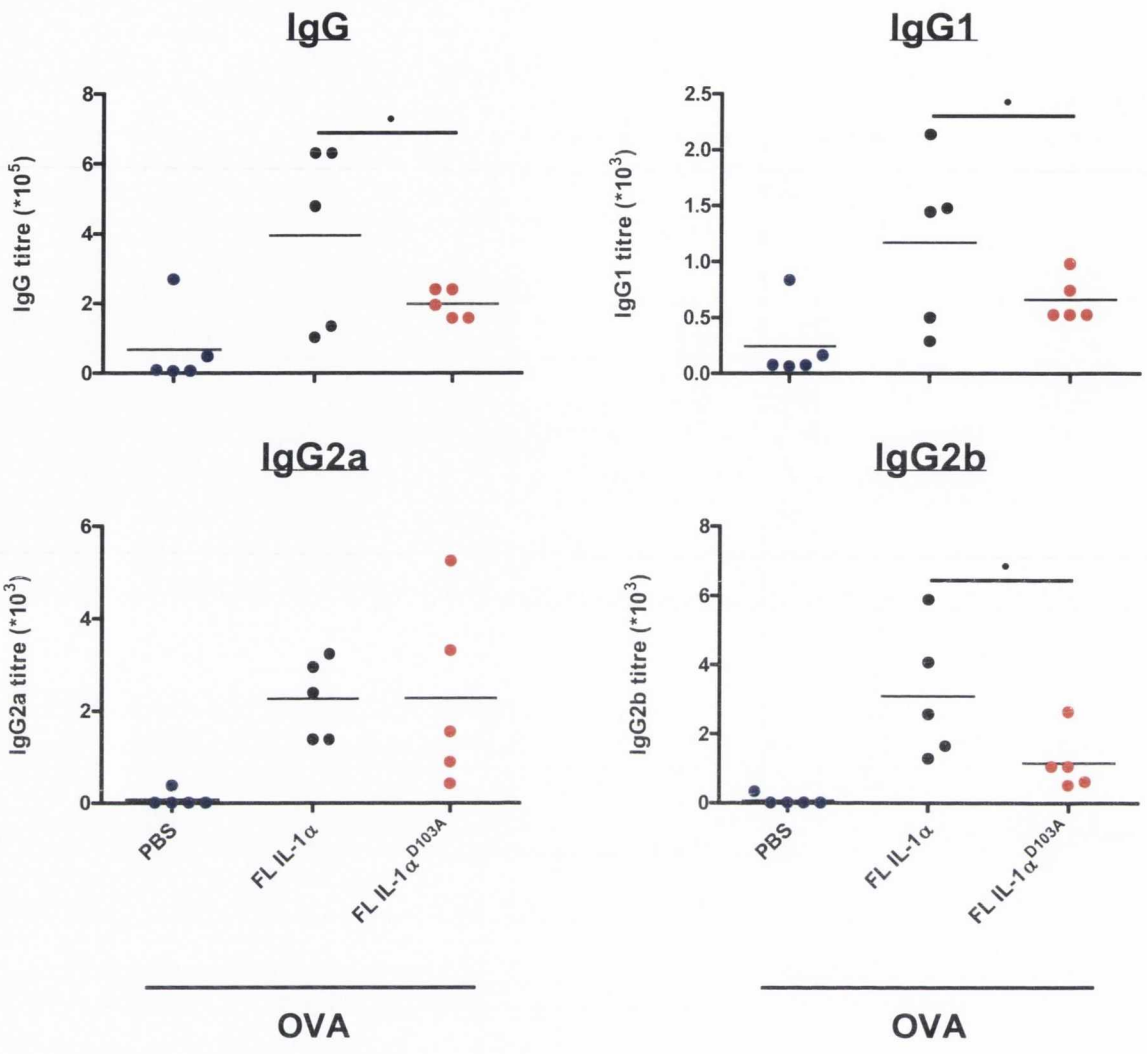

Figure 4.24 – IL-1α processing is mediated by GzmB *in vivo* (Post-Boost). Female BALB/c mice were immunised i.p. with PBS or OVA (200μg/mouse) either alone or in combination with FL IL-1α or GzmB non-cleavable IL-1α (FL IL-1α^{D103A}) (5μg/mouse). The mice were boosted with these same treatments on day 14 and were sacrificed on day 21. Blood samples were recovered and OVA-specific antibody titres (IgG, IgG1, IgG2a, IgG2b) in the serum were determined by ELISA. Scatter plot represents mean titre for 5 mice per experimental group. Versus FL IL-1α (OVA), • $p<0.05$.

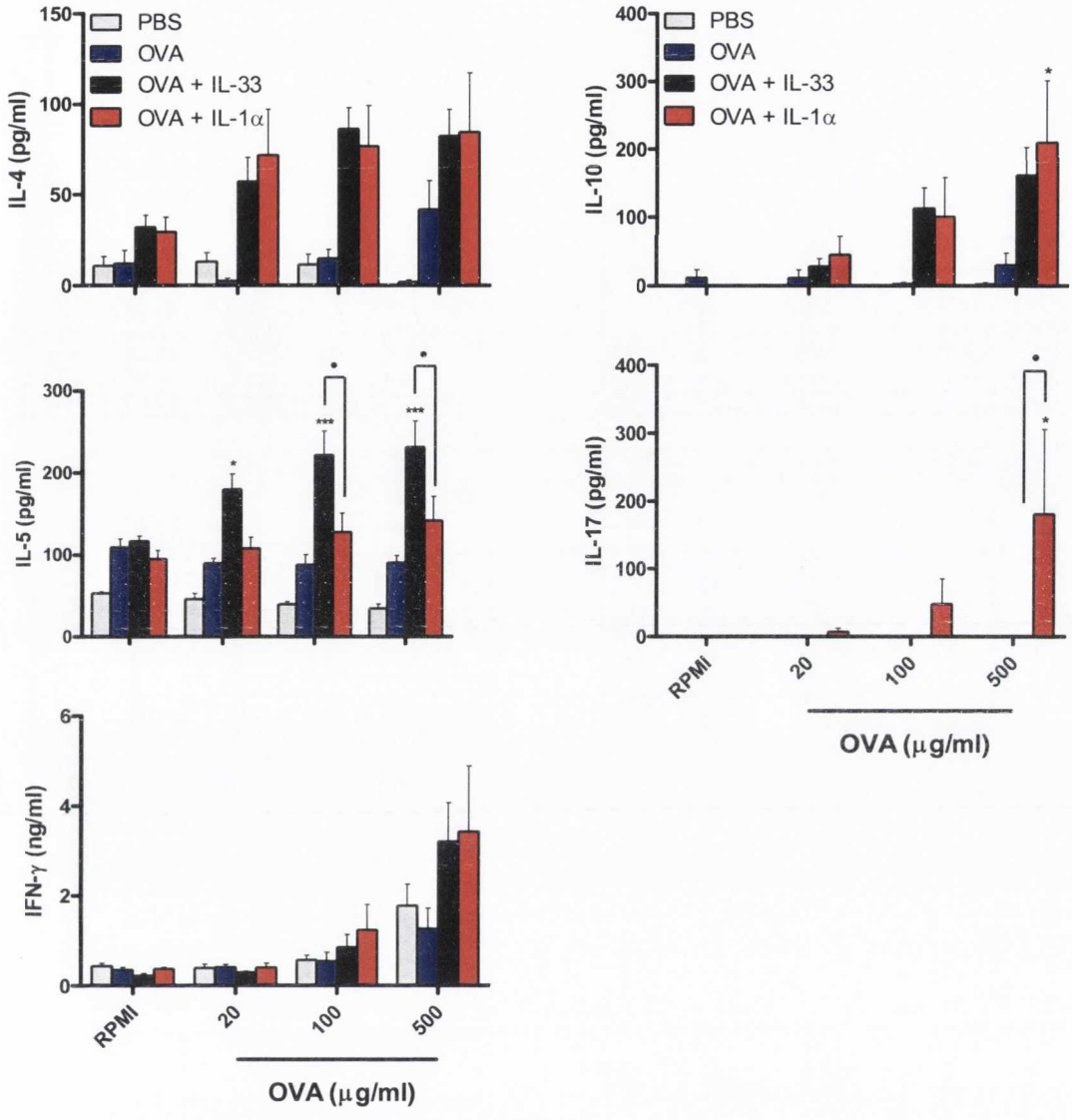

Figure 4.25 – Injection of antigen with IL-33$^{112-270}$ or IL-1α$^{104-271}$ as adjuvants enhances antigen-specific IL-4, IL-5 and IL-10 production by splenocytes. Female BALB/c mice were immunised i.p. with PBS or OVA (200μg/mouse) either alone or in combination with IL-33$^{112-270}$ (5μg/mouse) or IL-1α$^{104-271}$ (5μg/mouse). The mice were boosted with these same treatments on day 14 and were sacrificed on day 21. Spleens were recovered and restimulated *ex vivo* with RPMI or OVA (20, 100, 500μg/ml). After 72 hours, supernatants were collected and analysed for the cytokines IL-4, IL-5, IFN-γ, IL-10 and IL-17 by ELISA. Results are mean cytokine concentrations (+ SEM) for 5 mice per experimental group tested individually in triplicate. Versus OVA at corresponding concentration of stimulus, * $p<0.05$, *** $p<0.001$. IL-33 versus IL-1α at corresponding concentration of stimulus, • $p<0.05$.

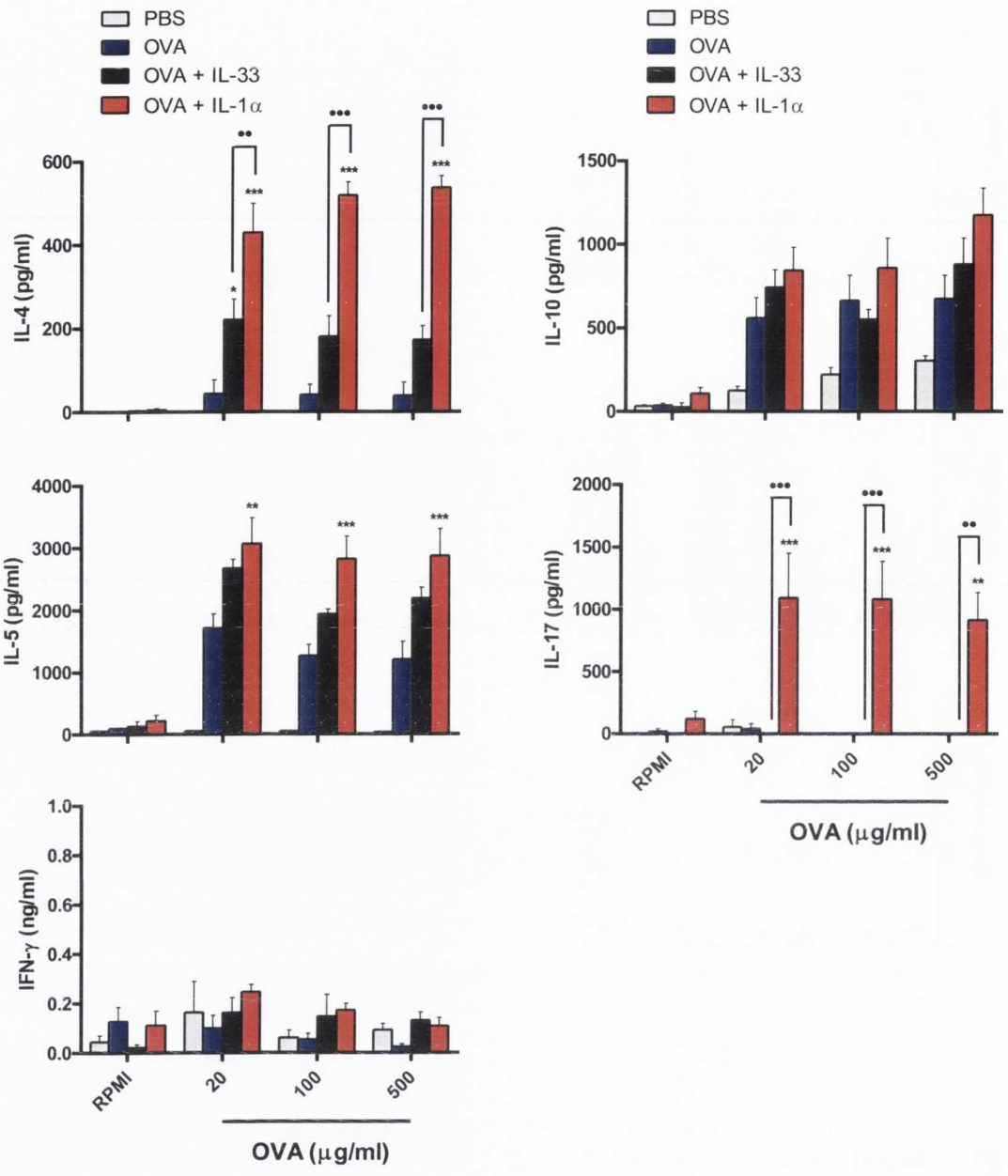

Figure 4.26 – Injection of antigen with IL-33$^{112-270}$ or IL-1α$^{104-271}$ as adjuvants induces qualitatively different T cell responses at the site of injection. Female BALB/c mice were immunised as described in Figure 4.25. PECs were recovered and restimulated *ex vivo* with RPMI or OVA (20, 100, 500μg/ml). After 72 hours, supernatants were collected and analysed for the cytokines IL-4, IL-5, IFN-γ, IL-10 and IL-17 by ELISA. Results are mean cytokine concentrations (+ SEM) for 5 mice per experimental group tested individually in triplicate. Versus OVA at corresponding concentration of stimulus, * $p<0.05$, ** $p<0.01$, *** $p<0.001$. IL-33 versus IL-1α at corresponding concentration of stimulus, •• $p<0.01$, ••• $p<0.001$.

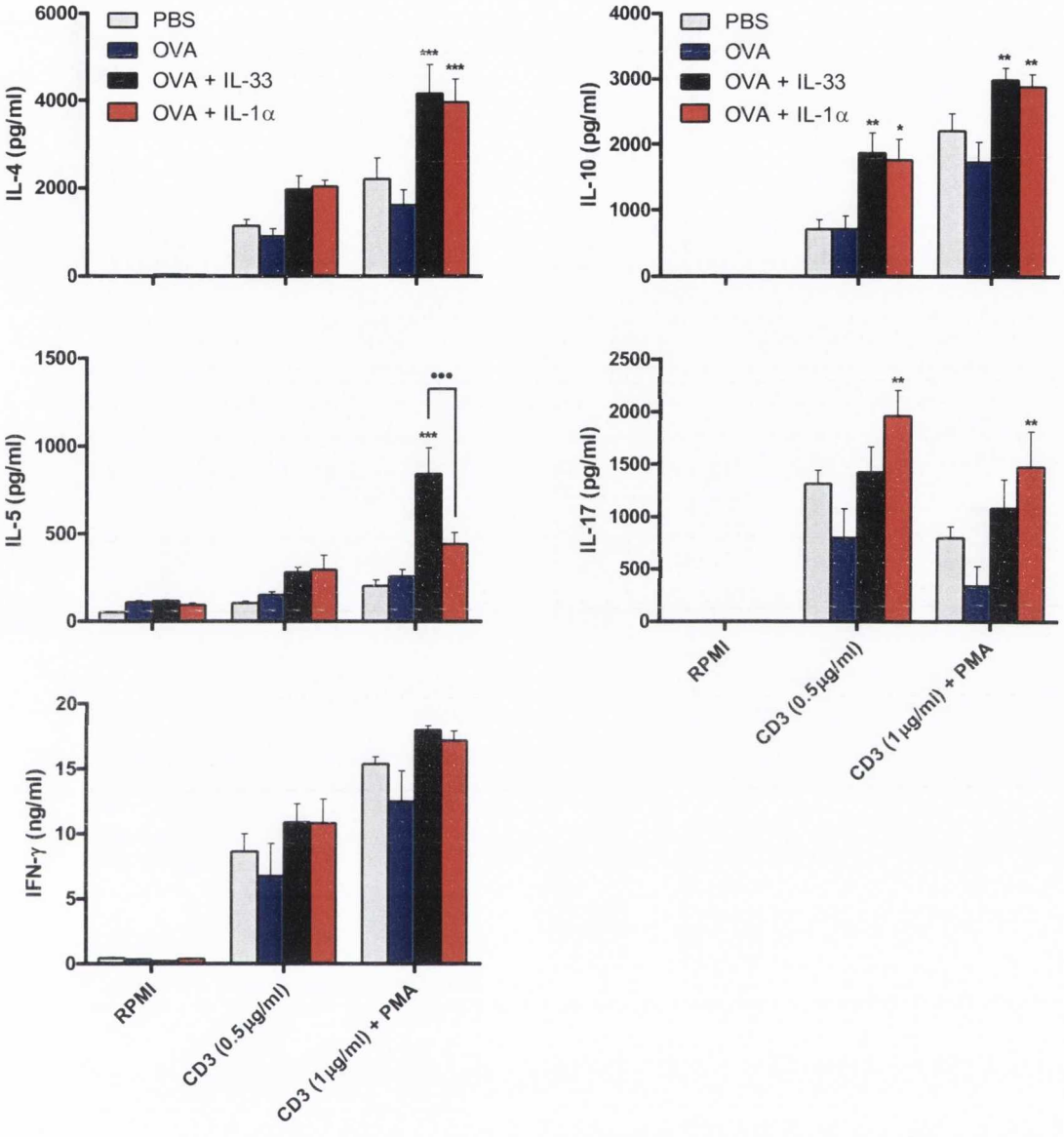

Figure 4.27 – Injection of antigen with IL-33$^{112-270}$ or IL-1α$^{104-271}$ as adjuvants enhances the secretion of IL-4 and IL-10 by splenocytes following restimulation with anti-CD3. Female BALB/c mice were immunised as described in Figure 4.25. Spleens were recovered and restimulated *ex vivo* with RPMI, anti-CD3 (0.5µg/ml) or anti-CD3 (1µg/ml) in combination with PMA (25ng/ml). After 72 hours, supernatants were collected and analysed for the cytokines IL-4, IL-5, IFN-γ, IL-10 and IL-17 by ELISA. Results are mean cytokine concentrations (+ SEM) for 5 mice per experimental group tested individually in triplicate. Versus OVA at corresponding concentration of stimulus, * $p<0.05$, ** $p<0.01$, *** $p<0.001$. IL-33 versus IL-1α at corresponding concentration of stimulus, ••• $p<0.001$.

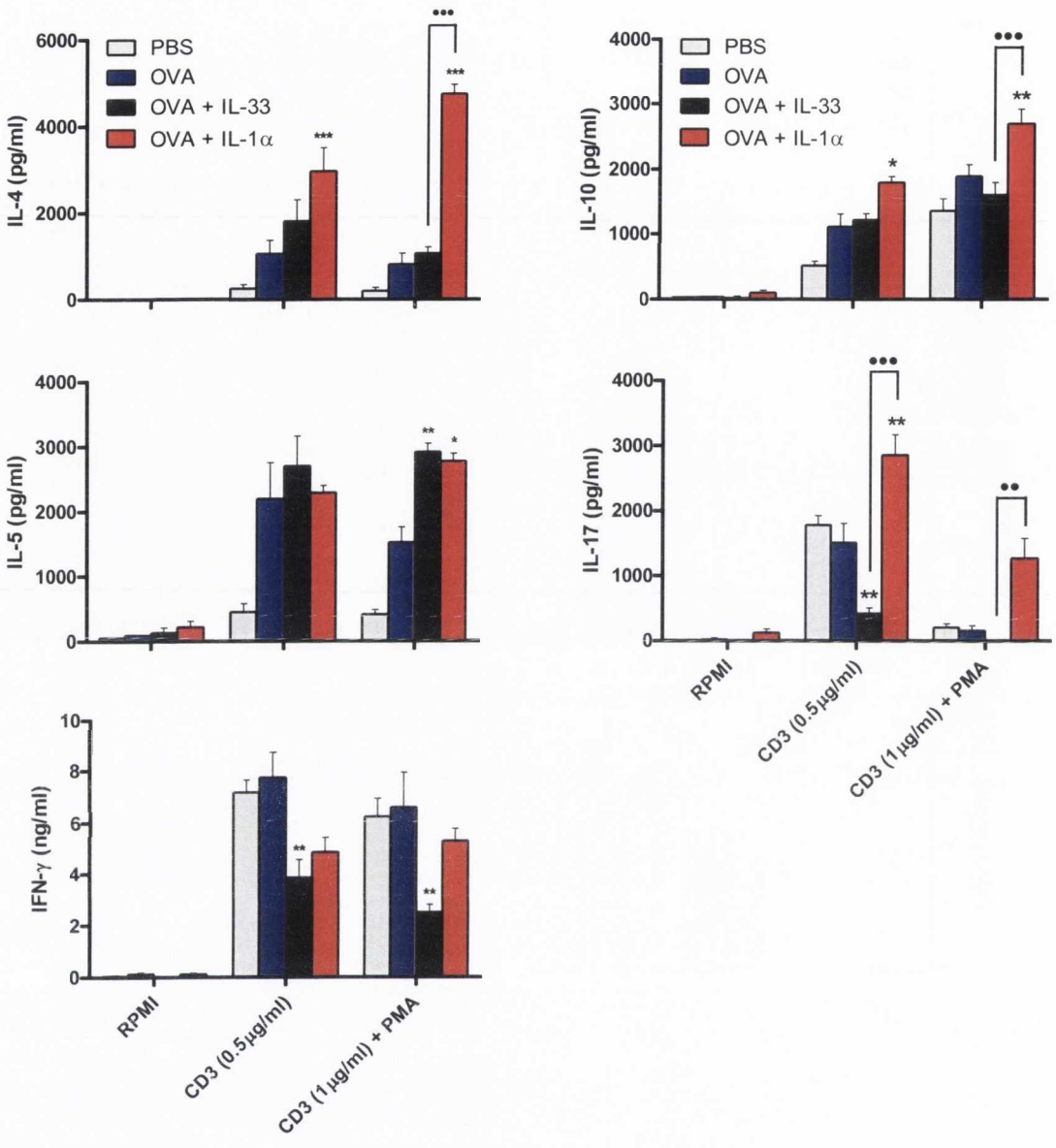

Figure 4.28 – Injection of antigen with IL-33$^{112-270}$ or IL-1α$^{104-271}$ as adjuvants induces qualitatively different T cell responses at the site of injection following restimulation with anti-CD3. Female BALB/c mice were immunised as described in Figure 4.25. PECs were recovered and restimulated *ex vivo* with RPMI, anti-CD3 (0.5µg/ml) or anti-CD3 (1µg/ml) in combination with PMA (25ng/ml). After 72 hours, supernatants were collected and analysed for the cytokines IL-4, IL-5, IFN-γ, IL-10 and IL-17 by ELISA. Results are mean cytokine concentrations (+ SEM) for 5 mice per experimental group tested individually in triplicate. Versus OVA at corresponding concentration of stimulus, * $p<0.05$, ** $p<0.01$, *** $p<0.001$. IL-33 versus IL-1α at corresponding concentration of stimulus, •• $p<0.01$, ••• $p<0.001$.

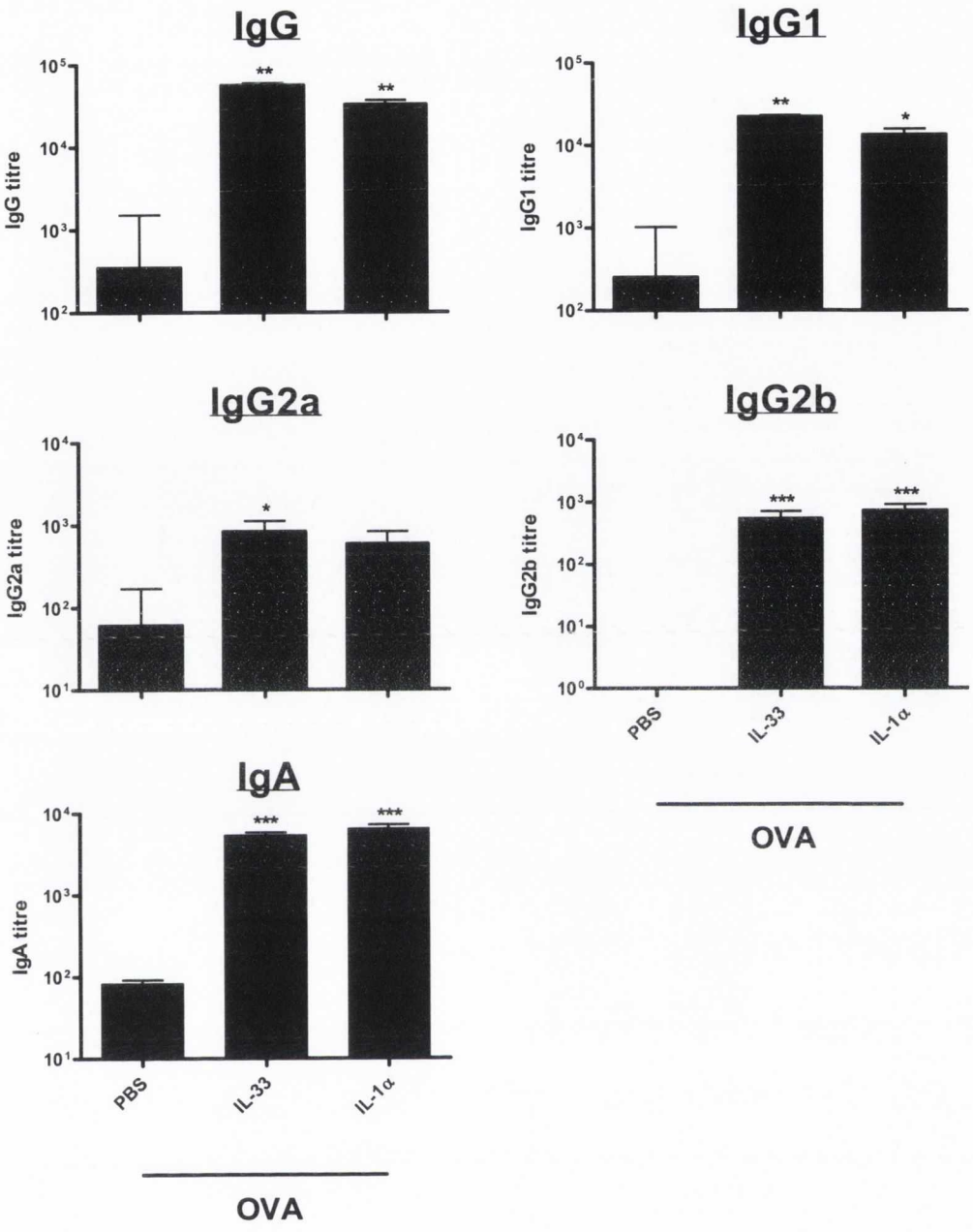

Figure 4.29 – IL-33$^{112-270}$ and IL-1α$^{104-271}$ both promote strong OVA-specific antibody responses in the serum but there are no differences in the magnitude of the response or the antibody isotypes elicited (Pre-Boost). Female BALB/c mice were immunised i.p. with PBS or OVA (200μg/mouse) either alone or in combination with IL-33$^{112-270}$ (5μg/mouse) or IL-1α$^{104-271}$ (5μg/mouse). Blood samples were recovered on day 13 and OVA-specific antibody titres (IgG, IgG1, IgG2a, IgG2b, IgA) in the serum were determined by ELISA. Results are mean titre (+ SEM) for 5 mice per experimental group. Versus PBS (OVA), * $p<0.05$, ** $p<0.01$, *** $p<0.001$.

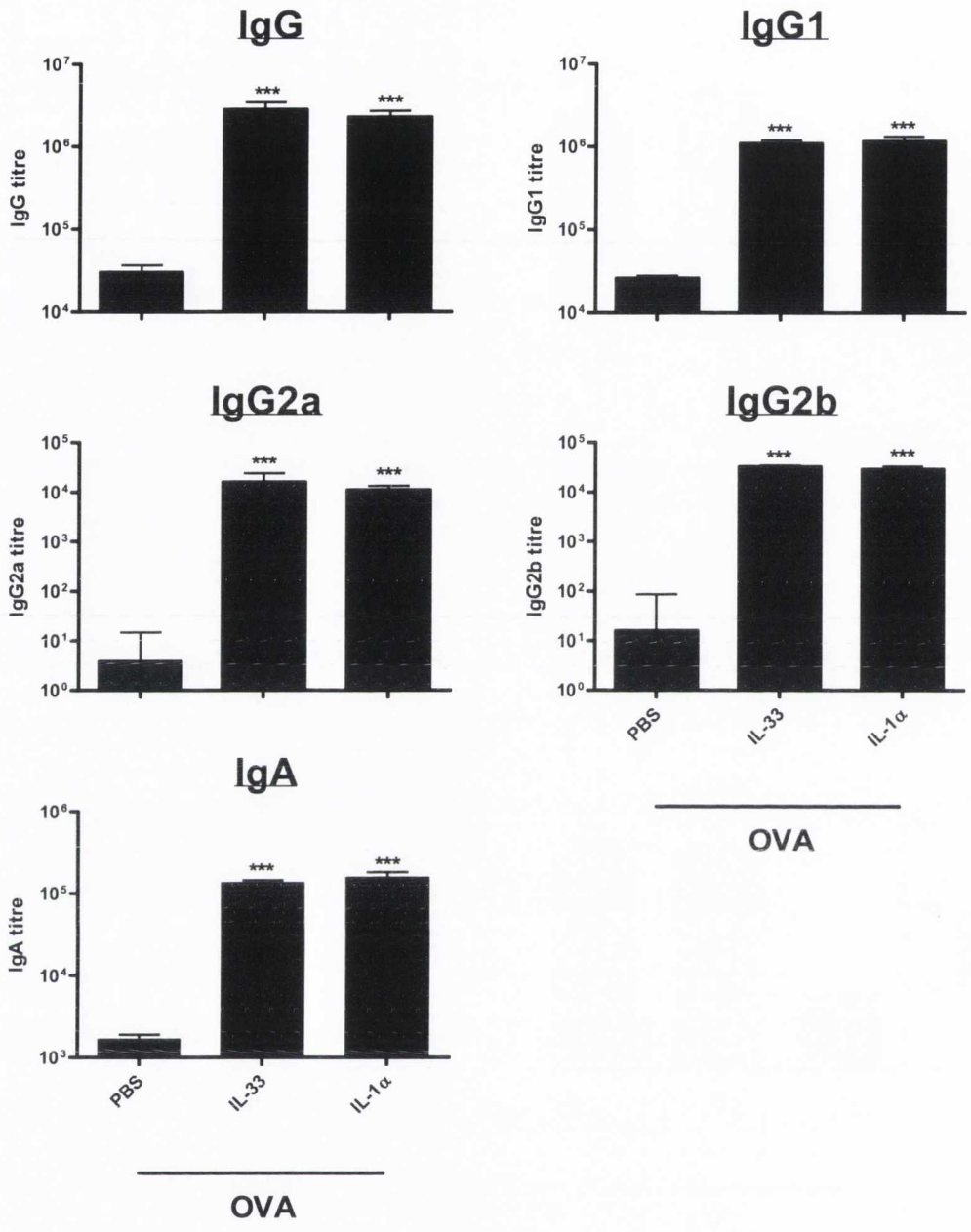

Figure 4.30 – IL-33$^{112-270}$ and IL-1α$^{104-271}$ both promote strong OVA-specific antibody responses in the serum but there are no differences in the magnitude of the response or the antibody isotypes elicited (Post-Boost). Female BALB/c mice were immunised as described in Figure 4.25. Blood samples were recovered on day 21 and OVA-specific antibody titres (IgG, IgG1, IgG2a, IgG2b, IgA) in the serum were determined by ELISA. Results are mean titre (+ SEM) for 5 mice per experimental group. Versus PBS (OVA), *** $p<0.001$.

Chapter 5

An Investigation of the Immunomodulatory Potential of Endogenous Oils Derived from the Human Omentum

5.1 – Introduction

The adipose organ is the largest endocrine organ in the body and is composed of brown adipose tissue (BAT) and white adipose tissue (WAT). While BAT is highly specialised for heat production by non-shivering thermogenesis, WAT serves as a long-term energy depot for the animal by storing fatty acids in the form of triglycerides. Indeed, WAT is the predominant energy reservoir in the body. Triglycerides comprise three fatty acids attached to a single glycerol molecule and are efficiently stored inside adipocytes which are the major constituent of WAT. Adipocytes contain a single cytoplasmic lipid droplet which facilitates storage of triglycerides. Lipid droplets are characterised by a phospholipid monolayer surrounding a core of neutral lipids predominantly consisting of triglycerides.

Some of the most powerful adjuvants in clinical and experimental use include oil-based emulsions such as MF59 and Freund's adjuvant, and indeed one of the earliest adjuvants discovered was starch oil. Therefore, adipocytes may harbour endogenous oils with immunostimulatory activity comparable to that of some of the most potent adjuvants currently known. Ultimately, necrotic adipocytes may signal danger to the host by rapidly releasing these endogenous immunomodulators from the droplet core, thus facilitating interactions with local APCs and stimulating potent immune responses.

Obesity is characterised by chronic, low-grade inflammation associated with recruitment of neutrophils and proinflammatory macrophages into WAT, resulting in insulin resistance and the onset of type 2 diabetes. Despite this, the cellular and molecular mechanisms responsible for macrophage infiltration into adipose tissue and the inflammatory response associated with obesity remain largely unknown. However, an important study by Cinti *et al.* has shown that adipocytes in WAT of obese mice exhibit features of necrosis, including loss of plasma membrane integrity, dilated ER, cell debris in the extracellular space and most importantly, degeneration of the lipid droplet. Cinti *et al.* demonstrate that macrophages are recruited exclusively to sites of necrotic adipocyte death where they aggregate to form crown-like structures (CLS). Interestingly, it remains unknown how scavenging of the residual lipid droplet by WAT macrophages promotes or prolongs the inflammatory response associated with obesity. Furthermore, both adipocyte necrosis and subsequent CLS formation are rare events in lean mice and humans but increase dramatically in obese mice (thirty-fold) and humans [513].

Based on the observations outlined above, it is hypothesised that endogenous oils released from necrotic adipocytes may function as a danger signal and initiate a potent immune response, thus providing an important link between obesity and inflammation. If passively released from hypertrophic adipocytes associated with obesity, these endogenous oils may have serious consequences for the host in terms of chronic immune stimulation.

Interestingly, inflammation is predominantly associated with visceral adiposity rather than subcutaneous adiposity. The omentum is a visceral fat depot and a major storage site for dietary oils. In humans, it hangs over the intestines inside the abdomen and is pathogenic in the context of obesity-induced inflammation. Therefore, the omentum was considered to be a good candidate for potentially harbouring endogenous oils capable of eliciting immuostimulatory effects.

5.2 – Aim

- To evaluate the immunomodulatory properties of endogenous oils derived from the human omentum.

5.3 – Results

5.3.1 – Endogenous oils fail to induce proinflammatory cytokine secretion from BMDCs

The first question addressed was whether endogenous oils derived from the human omentum of metabolically healthy obese (MHO) individuals (oils were derived from MHO individuals for each experiment, unless stated otherwise) could directly augment secretion of proinflammatory cytokines by BMDCs. Furthermore, if indeed these oils proved sufficient to promote cytokine secretion, this study sought to address whether this property was specific for oils derived from the omentum or was a general characteristic of most oils. This was achieved simply by using olive oil as a control. Therefore, C57BL/6 BMDCs were stimulated with a range of concentrations of endogenous oils or olive oil and secretion of IL-6 and TNF-α was measured. However, both preparations failed to potentiate secretion of these cytokines from BMDCs (Figure 5.1).

5.3.2 – Endogenous oils are toxic to BMDCs

This study next investigated whether the endogenous oils were toxic to BMDCs. These cells were stimulated with endogenous oils or olive oil before propidium iodide (PI) uptake by treated cells was measured by flow cytometry. Both the endogenous oils and olive oil significantly augmented levels of cell death compared with untreated control cells (Figure 5.2). Moreover, this toxicity was most marked at the highest concentrations of the respective oils.

5.3.3 – Endogenous oils fail to potentiate IL-1β or IL-1α release from BMDCs

Most stimuli capable of inducing NLRP3 inflammasome activation and promoting secretion of IL-1β, as well as release of IL-1α, are somewhat toxic to BMDCs. Since the endogenous oils were also toxic to BMDCs (Figure 5.2), this study next investigated whether these oils might activate the NLRP3 inflammasome and therefore synergise with TLR agonists to induce secretion of IL-1β. The possibility that endogenous oils may synergise with a TLR agonist to enhance IL-1α release by BMDCs was also explored. Again, olive oil was used as a control. C57BL/6 BMDCs were stimulated with a range of concentrations of endogenous oils, olive oil or alum, either alone or in the presence of the TLR9 agonist CpG. Subsequently, IL-1α and IL-1β release was measured in response to these stimuli.

Importantly, it is unclear whether the ELISA kits used in these experiments detect pro-IL-1β, mature IL-1β or indeed both forms of this proinflammatory cytokine. Therefore, in order to distinguish the 31kDa full-length form of IL-1β from the caspase-1 processed 17kDa mature form of this cytokine, a western blot assay was also performed. BMDCs from C57BL/6 mice were stimulated with alum or endogenous oils in combination with CpG. Protein was extracted from the supernatants 24 hours later and immunoblotted for IL-1β.

Both oil preparations failed to synergise with CpG in potentiating the release of IL-1β or IL-1α from BMDCs, unlike alum which in combination with CpG stimulated significant production of these cytokines. However, the endogenous oils and olive oil significantly reduced secretion of IL-1α by BMDCs compared to control cells stimulated with CpG alone (Figure 5.3A). This was possibly owing to the toxic effects of the oils on BMDCs. Western blot analysis confirmed that CpG in combination with endogenous oils was not sufficient to promote release of mature IL-1β into the supernatant, although these oils did promote release of pro-IL-1β (Figure 5.3B).

5.3.4 – Endogenous oils fail to enhance cytokine secretion from splenocytes

An important limitation associated with using BMDCs in testing for immunomodulatory properties of candidate molecules is that BMDC cultures comprise a single population of cells, thus eliminating the possibility of any communication between different cell types. Indeed, complex interactions between various different cell types are essential for generating immune responses *in vivo*. In order to address this issue, and possibly discover immunomodulatory activity for the endogenous oils *in vitro*, splenocytes were isolated from C57BL/6 mice and were stimulated with a range of concentrations of endogenous oils, olive oil, FIA or HK *E. coli* in the presence of plate-bound anti-CD3. Subsequently, secretion of the characteristic T cell cytokines IL-4, IL-5, IFN-γ, IL-10, IL-17 and IL-6 was measured. None of the oils induced secretion of any of the cytokines tested, unlike HK *E. coli*. In fact, stimulation of splenocytes with each of the oils at all concentrations tested significantly reduced secretion of IFN-γ, IL-17 and IL-10 compared to untreated control cells (Figure 5.4).

5.3.5 – Endogenous oils elicit adjuvanticity *in vivo*

Oil-based emulsions such as MF59 and Freund's adjuvant are some of the most potent adjuvants in clinical and experimental use. Therefore, in order to assess the immunomodulatory potential of the endogenous oils *in vivo*, an adjuvant study was employed using OVA as an antigen. Female C57BL/6 mice were immunised i.p. on day 0 with PBS as a control or OVA either alone or mixed with a crude preparation of endogenous oils. OVA was also mixed with FIA and this solution was emulsified by rigorous sonication. The mice were boosted with these same treatments on day 14 and were sacrificed on day 21 when blood samples were recovered. Crucially, the endogenous oils induced powerful OVA-specific antibody titres in the serum, thus confirming the potent biological activity of these oils *in vivo*. In particular, a significant enhancement in serum titres for total IgG as well as IgG1, IgG2b and IgG2c was evident (Figure 5.5).

5.3.6 – The organic phase of the preparation of endogenous oils is responsible for mediating adjuvanticity *in vivo*

In order to rule out the possibility that non-lipid components were responsible for the immunostimulatory activity attributed to the preparation of endogenous oils *in vivo*, a lipid extraction procedure was performed using chloroform and methanol. This extraction procedure was performed by Dr. Ken Mok of the Protein Folding and Biomolecular NMR Spectroscopy Group in the School of Biochemistry and Immunology, TCD. The aim of this procedure was to separate lipids from non-lipid components such as proteins, polysaccharides and amino acids. Lipids lacking polar groups, for example triglycerides, are very soluble in organic solvents such as chloroform, but are rather insoluble in polar solvents such as methanol.

In order to assess which fraction was responsible for potentiating antigen-specific antibody titres in the serum (Figure 5.5), C57BL/6 mice were immunised i.p. on day 0 with PBS as a control or OVA either alone or mixed with an equal volume of a crude preparation of endogenous oils. However, OVA was also mixed with an equal volume of either the aqueous or organic fraction derived from this crude preparation. As a positive control, OVA was combined with an equal volume of FIA and this solution was emulsified by rigorous sonication. The mice were boosted with these same treatments on day 14 and were sacrificed on day 21 when blood was recovered.

The aqueous phase containing non-lipid components failed to enhance any of the OVA-specific IgG subtypes tested. However, the organic fraction containing non-polar lipids potently enhanced OVA-specific antibody titres in the serum, including IgG, IgG1, IgG2b and IgG2c (Figure 5.6). Indeed, these titres were comparable to those mediated by the crude preparation of endogenous oils and also FIA. Thus, it is likely that lipids, and not non-lipid contaminants, are responsible for the enhanced biological activity of the preparation of endogenous oils *in vivo*.

Importantly, these findings were also confirmed in a separate adjuvant study using human serum albumin (HSA) as an antigen (Figure 5.7).

5.3.7 – Endogenous oils promote cell recruitment into the injection site

In addition to mediating potent antibody responses, the adjuvant MF59 is also a powerful chemoattractant for macrophages and granulocytes [152]. Furthermore, the activation of the innate immune system is paramount to the onset of obesity-induced inflammation as neutrophils and macrophages quickly infiltrate WAT. Therefore, it was important to determine the impact of the endogenous oils on the innate immune system and more specifically cell recruitment. In order to achieve this objective, it was crucial to assess the effects of these oils at a much earlier time point than that employed in the adjuvant model discussed above. The peritoneum is a particularly useful site to study modulation of the innate immune system as cell recruitment into this site in response to treatments can be assessed. Therefore, the immunostimulatory effects of the endogenous oils were investigated using a peritonitis model.

Female C57BL/6 mice were immunised i.p. with PBS or endogenous oils and the mice were sacrificed at a range of early time points, specifically 15 minutes, 1 hour, 3 hours and 24 hours. PECs were isolated and counted. The endogenous oils induced almost a three-fold increase in PEC numbers (Figure 5.8), thus confirming their ability to promote cell recruitment into the injection site and initiate an early immune response.

5.3.8 – Neutrophils, small peritoneal macrophages and eosinophils infiltrate the injection site in response to endogenous oils

Neutrophil and macrophage infiltration into WAT is the hallmark of obesity-induced inflammation. Considering the significant increase in the total number of PECs following injection with endogenous oils (Figure 5.8), this study next sought to investigate whether neutrophils and macrophages were amongst the recruited populations of cells in the peritoneum. Female C57BL/6 mice were immunised i.p. with PBS or endogenous oils and the mice were sacrificed after 15 minutes, 1 hour, 3 hours or 24 hours. PECs were isolated at the appropriate time points and analysed by flow cytometry.

There was almost a complete absence of neutrophils ($CD11b^{inter}$ $F4/80^{-}$ $Gr\text{-}1^{high}$) in the peritoneum of the control mice. However, the endogenous oils induced neutrophil recruitment into the peritoneum after only 15 minutes. Moreover, the magnitude of this response increased proportionally with time, being highest after 24 hours (Figure 5.9). The endogenous oils also promoted significant infiltration of small peritoneal macrophages (SPMs) ($CD11b^{inter}$ $F4/80^{inter}$ $Gr\text{-}1^{low/inter}$ $SiglecF^{-}$) into the injection site. However, recruitment of these cells was only detectable after 3 hours but was again most prominent after 24 hours (Figure 5.10). Furthermore, the endogenous oils increased the number of eosinophils ($SiglecF^{+}$ $ckit^{-}$) in the peritoneum after 24 hours (Figure 5.11), while concomitantly mediating the depletion of both mast cells ($SiglecF^{-}$ $ckit^{+}$) (Figure 5.11) and large peritoneal macrophages (LPMs) ($CD11b^{high}$ $F4/80^{high}$) (Figure 5.12).

5.3.9 – Endogenous oils are only moderately toxic to PECs *in vivo* in comparison to alum

The immunostimulatory activity of a number of adjuvants has been reported to be at least partially dependent on their ability to induce necrotic cell death at the injection site. In order to establish whether the immune activation capacity of endogenous oils was owing to their ability to elicit toxicity in the peritoneum, female C57BL/6 mice were immunised i.p. with PBS or endogenous oils and the mice were sacrificed after 15 minutes, 1 hour, 3 hours or 24 hours. As a positive control for toxicity, an additional experiment was also performed where C57BL/6 mice were immunised i.p. with PBS or alum for 15 minutes. PECs were isolated at the appropriate time points and the number of $AQUA^{+}$ cells was measured by flow cytometry.

The endogenous oils induced approximately a two-fold increase in cell death in the peritoneum after only 15 minutes and this effect was still evident after 1 hour. Cell death was reduced after 3 hours and 24 hours but was still only marginally higher than control levels (Figure 5.13A, 5.13B). However, the extent of necrosis in response to endogenous oils was only very moderate compared to alum. After 15 minutes, alum induced almost a twenty-fold increase in toxicity in the peritoneum as approximately 80% of isolated PECs were necrotic (Figure 5.13C). Ultimately, endogenous oils were only mildly toxic in comparison to the dramatic toxicity elicited by alum.

5.3.10 – Endogenous oils modulate the cytokine profile of PECs following *ex vivo* restimulation with PRR agonists

Under normal conditions, resident macrophages serve to dampen immune responses in WAT through secretion of anti-inflammatory cytokines such as IL-10. In obese conditions, however, WAT recruits macrophages that secrete proinflammatory cytokines such as TNF-α. In order to determine whether endogenous oils could modulate the cytokine profile of PECs in a similar fashion, female C57BL/6 mice were immunised i.p. with PBS or endogenous oils and the mice were sacrificed 24 hours later. PECs were isolated and restimulated *ex vivo* with a range of PRR agonists. Subsequently, secretion of the cytokines TNF-α, IL-10, IL-12p40 and IL-12p70 was measured.

PECs isolated from mice injected with endogenous oils exhibited a very significant increase in secretion of TNF-α and IL-12p40 following restimulation with all PRR agonists tested, whereas IL-12p70 release was only augmented following restimulation with HK *E. coli*. PECs isolated from mice injected with endogenous oils also synthesised significantly less IL-10 in comparison to those isolated from mice injected with PBS, and this robust trend was evident in response to all PRR agonists tested (Figure 5.14). Thus, endogenous oils generate a cytokine profile in the peritoneum which reflects that found in the inflamed WAT of obese individuals.

5.3.11 – TLR4 is dispensable for cell recruitment into the peritoneum in response to endogenous oils

Saturated fatty acids (SFAs) have previously been shown to promote NF-κB activation in macrophages *in vitro* in a TLR4-dependent manner [488]. The SFA palmitate has also been reported

to engage TLR4 and induce IL-6 and TNF-α mRNA expression in macrophages and adipocytes. Furthermore, TLR4-deficient mice are protected from high-fat diet-induced insulin resistance [489]. Since endogenous oils derived from the human omentum will contain free fatty acids, this study next investigated whether TLR4 is required for inflammatory cell recruitment into the peritoneum in response to these oils. Female wild-type C3H/HeN and TLR4-defective C3H/HeJ mice were immunised i.p. with PBS or endogenous oils and the mice were sacrificed 24 hours later. PECs were isolated, counted and analysed by flow cytometry.

Injection of endogenous oils increased total PEC numbers in both C3H/HeN and C3H/HeJ mice, but there was no significant difference in total PEC number between the two mouse strains (Figure 5.15). The endogenous oils also induced potent recruitment of neutrophils into the peritoneum of both C3H/HeN and C3H/HeJ mice, with no significant difference between the two (Figure 5.16). Similar results were also evident for SPMs (Figure 5.16) and eosinophils (Figure 5.17). Furthermore, the endogenous oils depleted the entire resident mast cell population in the peritoneum of both C3H/HeN and C3H/HeJ mice (Figure 5.17), with similar results also apparent for LPMs (Figure 5.18). Ultimately, TLR4 was entirely dispensable for the immunostimulatory effects of the endogenous oils in this peritonitis model. Therefore, signalling through TLR4 by free fatty acids does not appear to be responsible for mediating these effects.

5.3.12 – Endogenous oils promote release of IL-1α, IL-1β and KC in the peritoneum

Given the apparent dispensability of TLR4 in mediating cell recruitment into the peritoneum following injection with endogenous oils, this study aimed to further investigate a mechanism for these events. In order to help establish a mechanism for this process, it was first necessary to assess proinflammatory cytokine and chemokine levels in the peritoneum in response to the endogenous oils. IL-1α, IL-1β and KC are all powerful chemoattractants which may be involved in promoting cell recruitment into the peritoneum. IL-33, in addition to IL-1α, is a potent danger signal which may also contribute to these events if released from necrotic cells at the injection site. Although cell recruitment into the peritoneum was most evident after 24 hours (Figure 5.8), it is conceivable that the cytokines mediating this process might be elevated at a much earlier time point and may in fact be in decline after 24 hours. Therefore, it was also crucial to assess a relatively early time point when determining cytokine levels in the peritoneum.

Female C57BL/6 mice were immunised i.p. with PBS or endogenous oils and the mice were sacrificed either 3 hours or 24 hours later. PECs were isolated and PEC supernatants were collected. Subsequently, levels of IL-1α, IL-1β, KC and IL-33 were measured in PEC supernatants. IL-1α, IL-1β and KC were all elevated significantly in the peritoneum after 3 hours in response to injection with endogenous oils, whereas there was no statistical difference in levels of IL-33. After 24 hours, IL-1α, KC and IL-33 levels were all at baseline. Levels of IL-β were still elevated after 24 hours but were less than those detected after 3 hours (Figure 5.19).

5.3.13 – Cell recruitment into the peritoneum following injection with endogenous oils is dependent on the IL-1R

Considering that both IL-1α and IL-1β were augmented significantly in the peritoneum of mice injected with endogenous oils and are also powerful chemoattractants, this study next sought to determine whether these cytokines might play a role in the subsequent recruitment of different populations of cells into the injection site. Again using a peritonitis model, female C57BL/6, NLRP3 KO and IL-1R KO mice were immunised i.p. with PBS or endogenous oils and the mice were sacrificed 24 hours later. PECs were isolated, counted and analysed by flow cytometry.

The endogenous oils increased total PEC numbers in both C57BL/6 and NLRP3 KO mice, but there was no significant difference in total PEC number between the two mouse strains. However, cell recruitment into the peritoneum in response to endogenous oils was completely abrogated in IL-1R KO mice (Figure 5.20). Neutrophil recruitment was partially dependent on NLRP3, but was entirely dependent on the IL-1R (Figure 5.21). Moreover, SPM recruitment was also IL-1R-dependent but was totally independent of NLRP3 (Figure 5.21). The endogenous oils also promoted recruitment of eosinophils into the peritoneum of wild-type and NLRP3 KO mice, whereas this response was absent in IL-1R KO mice. However, IL-1R KO mice also possessed much lower eosinophil numbers compared to wild-type and NLRP3 KO mice following injection with PBS, thus suggesting that IL-1R KO mice simply contain far fewer resident eosinophils and that recruitment of these inflammatory cells in response to endogenous oils is independent of the IL-1R (Figure 5.22). This is supported by the observation that in comparison to PBS, endogenous oils still promoted an increase in eosinophils in the peritoneum of IL-1R KO mice (Figure 5.22). LPMs were depleted by endogenous oils in wild-type and NLRP3 KO mice, but were not entirely diminished in the peritoneum of IL-1R KO mice (Figure 5.23). Importantly, IL-1R KO mice also possessed fewer

LPMs than wild-type or NLRP3 KO mice in response to PBS. Moreover, there was a much smaller fold reduction in percentage of LPMs in IL-1R KO mice than in wild-type or NLRP3 KO mice following injection with endogenous oils (Figure 5.23). This suggests that the IL-1R may play a relatively minor role in depleting LPMs in response to endogenous oils.

The results outlined above raised the possibility that IL-1R KO mice were simply incapable of promoting neutrophil and SPM recruitment into the injection site. However, when injected with a different stimulus, namely 10μm polystyrene (PS) particles, these mice competently recruited both of these inflammatory cell types into the peritoneum (Figure 5.24). Thus, the requirement for the IL-1R in recruitment of neutrophils and SPMs was specific for injection with endogenous oils.

5.3.14 – Modulation of the cytokine profile of PECs by endogenous oils following *ex vivo* restimulation is dependent on the IL-1R

Since the endogenous oils were capable of modulating the cytokine profile of PECs from wild-type mice following *ex vivo* restimulation with PRR agonists (Figure 5.14), this study next addressed the question of whether this modulation was dependent on NLRP3 or the IL-1R. Female C57BL/6, NLRP3 KO and IL-1R KO mice were immunised i.p. with PBS or endogenous oils and the mice were sacrificed 24 hours later. PECs were isolated and restimulated *ex vivo* with a range of PRR agonists. Subsequently, secretion of the cytokines TNF-α, IL-10, IL-12p40 and IL-12p70 was measured.

PECs isolated from wild-type mice injected with endogenous oils exhibited an increase in secretion of TNF-α and IL-12p40 following restimulation with all PRR agonists tested, whereas IL-12p70 release was only augmented following restimulation with HK *E. coli*. PECs isolated from wild-type mice injected with endogenous oils also secreted less IL-10 in comparison to those injected with PBS, and this trend was apparent for all PRR agonists tested (Figure 5.25). PECs isolated from NLRP3 KO mice injected with endogenous oils elicited an almost identical trend to those isolated from wild-type mice with regard to each of the cytokines tested, with the exception of IL-12p70 which was secreted at higher concentrations by PECs isolated from NLRP3 KO mice following restimulation with CpG and HK *E. coli* (Figure 5.25). PECs isolated from IL-1R KO mice injected with endogenous oils failed to secrete detectable levels of IL-12p40 and IL-12p70 following restimulation with PRR agonists. Furthermore, secretion of TNF-α by these cells was completely

abrogated following restimulation with all PRR agonists, with the exception of HK *E. coli* where TNF-α was secreted but only at much lower levels than those secreted by PECs isolated from wild-type and NLRP3 KO mice. However, similarly to wild-type and NLRP3 KO mice, a reduction in IL-10 synthesis was still evident in PECs isolated from IL-1R KO mice injected with endogenous oils, and this was apparent for all PRR agonists tested (Figure 5.25). Ultimately, the ability of endogenous oils to modulate secretion of TNF-α, IL-12p40 and IL-12p70 by PECs following *ex vivo* restimulation with PRR agonists was NLRP3-independent but IL-1R-dependent.

5.3.15 – ASC possesses a NLRP3-independent role in depleting the large peritoneal macrophage population following injection with endogenous oils

ASC functions as an adaptor protein for NLRP3 [239] but it is also performs a similar role for other inflammasomes including NLRP1 [241], NLRC4 [249, 251, 255] and AIM2 [446]. Although NLRP3 was dispensable for infiltration of inflammatory cells into the peritoneum following injection with endogenous oils, it was plausible that other inflammasomes might be involved in this process. In addition, ASC has also been reported to exhibit numerous inflammasome-independent functions [170, 538-541]. In order to investigate the role of ASC in recruitment of neutrophils and SPMs in response to endogenous oils, female wild-type C57BL/6 and ASC KO mice were immunised i.p. with PBS or endogenous oils and the mice were sacrificed 24 hours later. PECs were isolated, counted and analysed by flow cytometry.

Total PEC numbers were similar in wild-type and ASC KO mice following injection with endogenous oils, thus suggesting that ASC is not required for infiltration of inflammatory cells into the peritoneum (Figure 5.26). Neutrophil and SPM recruitment was only partially dependent on ASC, although these results were indicative of a robust trend and were not statistically significant (Figure 5.27). Furthermore, eosinophil recruitment into the peritoneum was not compromised in the absence of ASC (Figure 5.28). Depletion of mast cells in the peritoneum of ASC KO mice following injection with endogenous oils was less apparent than in wild-type mice. However, this difference was not statistically significant. Furthermore, ASC KO mice also possessed a significantly higher percentage of mast cells compared to wild-type mice following injection with PBS, thus suggesting that there are simply a higher percentage of resident mast cells in the peritoneum of ASC KO mice and that depletion of these cells in response to endogenous oils is in fact independent of ASC (Figure 5.28). ASC however, possessed a NLRP3-independent function as it was intimately involved in

depletion of the LPM population at the injection site. Following injection of endogenous oils into the peritoneum of wild-type mice, the LPM population was diminished. However, this diminishing effect was significantly reduced in ASC KO mice (Figure 5.29).

PECs were also restimulated *ex vivo* with a range of TLR agonists. Subsequently, secretion of the cytokines TNF-α, IL-10, IL-12p40 and IL-12p70 was measured. PECs isolated from wild-type mice injected with endogenous oils exhibited an increase in secretion of TNF-α, IL-12p40 and IL-12p70. PECs isolated from ASC KO mice injected with endogenous oils secreted only marginally lower levels of these cytokines (Figure 5.30). PECs isolated from wild-type mice injected with endogenous oils also secreted less IL-10 in comparison to those injected with PBS, and this trend was apparent for all PRR agonists tested. However, unlike PECs isolated from NLRP3 KO mice (Figure 5.25), this effect was mostly absent in PECs isolated from ASC KO mice injected with endogenous oils as these cells secreted similar levels of IL-10 to those isolated from ASC KO mice injected with PBS (Figure 5.30).

5.3.16 – Endogenous oils derived from subcutaneous adipocytes promote innate immune responses comparable to those derived from omental adipocytes

Visceral fat is more pathogenic than subcutaneous fat in the context of obesity-induced inflammation. Therefore, this study next sought to address the question of whether cell recruitment into the injection site was an immunostimulatory property specific for endogenous oils derived from omental adipocytes or was also characteristic of endogenous oils derived from less pathogenic subcutaneous fat. In order to answer this question, female C57BL/6 mice were immunised i.p. with PBS or endogenous oils derived from omental adipocytes or subcutaneous adipocytes collected from the same obese individual. The mice were sacrificed 24 hours later. PECs were isolated, counted and analysed by flow cytometry.

Endogenous oils derived from subcutaneous and omental adipocytes both induced a comparable increase in PEC number, with no significant difference between the two treatments (Figure 5.31). Both forms of endogenous oils also promoted similar recruitment of neutrophils (Figure 5.32), SPMs (Figure 5.33) and eosinophils (Figure 5.34) into the injection site, while simultaneously depleting the mast cell (Figure 5.34) and LPM (Figure 5.35) populations. Ultimately, there was no significant

difference between endogenous oils derived from subcutaneous or omental adipocytes in their respective ability to promote immunostimulatory effects in the peritonitis model.

5.3.17 – Olive oil is comparable to endogenous oils in its ability to induce potent innate and adaptive immune responses

Since endogenous oils derived from subcutaneous adipocytes were as potent as those derived from omental adipocytes in promoting innate immune responses, it was hypothesised that the immunostimulatory properties observed may in fact be a general characteristic of most oil-based preparations. In order to test this hypothesis, the immunostimulatory effects of olive oil were assessed in a peritonitis study and also an adjuvant study.

Adapting the peritonitis model, female C57BL/6 mice were immunised i.p. with PBS or olive oil and were sacrificed after 24 hours. PECs were isolated, counted and analysed by flow cytometry. Total PEC numbers were significantly increased following injection with olive oil (Figure 5.36). Similar to endogenous oils, olive oil potently induced infiltration of neutrophils (Figure 5.37), SPMs (Figure 5.38) and eosinophils (Figure 5.39) while simultaneously depleting LPMs (Figure 5.40).

In order to assess the effect of olive oil on the adaptive immune response *in vivo*, an adjuvant study was employed using OVA as an antigen. Female C57BL/6 mice were immunised i.p. on day 0 with PBS as a control or OVA either alone or mixed with an equal volume of olive oil or endogenous oils. OVA was also mixed with an equal volume of FIA and this solution was emulsified by rigorous sonication. The mice were boosted with these same treatments on day 14 and were sacrificed on day 21 when blood samples were recovered. As before, endogenous oils derived from omental adipocytes induced a significant enhancement of OVA-specific serum antibody titres. However, olive oil also proved a very capable inducer of antigen-specific humoral immunity, although to a lesser extent than the endogenous oils. In particular, olive oil increased serum antibody titres for total IgG as well as IgG1, IgG2b and IgG2c (Figure 5.41).

5.3.18 – Metabolically unhealthy obese individuals have significantly larger adipocytes than metabolically healthy obese individuals

Since all of the oils tested thus far elicited immunostimulatory effects *in vivo*, it was hypothesised that the ability of endogenous oils to promote obesity-induced inflammation was entirely dependent on their passive release from adipocytes in WAT rather than their specific composition. Endogenous oils are known to be released from hypertrophic adipocytes undergoing necrosis. Therefore, it was hypothesised that metabolically unhealthy obese (MUO) individuals may possess adipocytes with a larger diameter (i.e. more hypertrophic) than those present in metabolically healthy obese (MHO) individuals and are therefore more likely to undergo necrosis and release endogenous oils. These oils will then subsequently drive potent inflammatory responses in the tissue. This would explain why MUO individuals and MHO individuals both possess adipocytes which contain endogenous adjuvants in the form of oils but only MUO individuals experience persistant inflammation and metabolic disorders.

In order to test this hypothesis, it was necessary to measure the hypertrophic state of omental adipocytes from both MUO individuals and MHO individuals. Therefore, the mean diameter of a range of adipocytes from 5 MUO individuals and 5 MHO individuals was calculated on H&E-stained WAT sections. MHO individuals possessed an average adipocyte diameter of approximately 75μm, but MUO individuals had significantly larger adipocytes which were approximately 85μm in diameter, thus representing almost a 15% increase in adipocyte size (Figure 5.42).

5.4 – Discussion

MF59 and Freund's adjuvant are oil-based emulsions with potent immunostimulatory activity. MF59 is an oil-in-water emulsion successfully licensed as part of an influenza vaccine formulation (Fluad). The predominant oil constituent of MF59 is squalene, a naturally occurring precursor of cholesterol derived from shark liver oil but also present in human sebum. Freund's adjuvant is a water-in-oil emulsion which is not used in clinical settings but is the most commonly used adjuvant for experimental work. Paraffin oil is the major oil component of Freund's adjuvant. Paraffin oil is a mineral oil, and is a liquid by-product of the distillation of petroleum. Despite years of extensive research, the precise immunostimulatory mechanism of action of MF59 and Freund's adjuvant remains unclear (Section 1.5). However, what has become apparent from using these adjuvants is that oils are undoubtedly powerful mediators of immunity with the ability to confer host protection when used as part of a vaccine formulation.

WAT adipocytes store dietary lipids, particularly triglycerides, as a means of fuel storage and energy conservation for the animal. However, obesity occurs when energy intake and triglyceride storage exceed the rate of lipolysis in adipocytes. Moreover, there is a strong positive correlation between obesity and inflammation. The cellular and molecular mechanisms responsible for the inflammatory response associated with obesity remain unclear. However, based on the renowned ability of oil-based adjuvants to induce potent immune responses, this study investigated the immunostimulatory potential of endogenous dietary oils recovered from adipocytes in the human omentum.

DCs are professional APCs capable of linking innate and adaptive immunity. Therefore, DC activation is commonly used as a means of assessing the immunomodulatory potential of endogenous danger signals. Based on the crucial role of DCs within the immune system, the effect of endogenous oils derived from adipocytes in the human omentum on these sentinel cells was investigated. Importantly, olive oil was used as a control in order to establish whether any immunomodulatory effects identified were exclusively mediated by endogenous oils. However, endogenous oils failed to induce cytokine secretion from DCs. Nevertheless, this finding was not altogether unexpected as many powerful immunomodulators, including the adjuvants MF59 and alum, also fail to directly activate DCs *in vitro* [152]. One plausible explanation for this observation is that endogenous oils may be toxic to DCs. In order to investigate this hypothesis, DCs were stimulated with a range of concentrations of endogenous oils before necrotic cell death was measured. Interestingly, both the endogenous oils and olive oil were toxic to DCs in a dose-

dependent manner. However, at lower concentrations, the resulting toxicity would not be expected to completely abrogate the ability of the entire DC culture to respond to an activating stimulus, therefore suggesting that endogenous oils derived from the omentum do not directly activate DCs. In order to confirm this finding, lower concentrations of endogenous oils which are not toxic to BMDCs must be used. However, the issue of toxicity is not as straightforward as it may appear. The endogenous oils are insoluble in RPMI and tend to reside on top of the aqueous solution. Therefore, it is unclear whether the endogenous oils are directly toxic to DCs through cell surface interactions or are indirectly toxic through CO_2 starvation. Further studies will be required to address this issue.

The toxic effects of endogenous oils on DCs inadvertently opened up a new avenue of investigation. Interestingly, most compounds capable of promoting activation of the NLRP3 inflammasome and subsequent secretion of IL-1β, as well as release of IL-1α, are somewhat toxic to DCs. Furthermore, a number of well-characterised particulate adjuvants including alum and chitosan which fail to directly promote proinflammatory cytokine secretion by DCs, are also capable of activating the NLRP3 inflammasome [245, 542]. It has recently been shown that cholesterol crystals, derived from the dietary lipid cholesterol, are also sufficient to promote assembly of this caspase-1 activation platform [543]. Since endogenous oils are toxic to DCs, fail to directly activate these sentinel cells, and constitute dietary lipids, this study next investigated whether these oils might also activate the NLRP3 inflammasome and therefore synergise with TLR agonists to induce secretion of IL-1β. The possibility that endogenous oils may synergise with a TLR agonist to enhance IL-1α release by DCs was also explored. However, stimulation of DCs with a range of concentrations of endogenous oils in the presence of a TLR agonist failed to promote the release of IL-1β or IL-1α. This data suggests that oils derived from the omentum are incapable of promoting NLRP3 inflammasome activation.

The above finding was surprising given that palmitate has been reported to directly activate NLRP3 and thus supply the second signal required for caspase-1 activation and IL-1β secretion [481]. Palmitate is an abundant saturated fatty acid and would be expected to be found in the preparation of endogenous oils derived from the omentum. However, palmitate is only capable of activating NLRP3 when conjugated to BSA at a 3:1 molar ratio in order to improve the solubility of this fatty acid. The endogenous oils were not conjugated to a carrier protein and this step could not be accomplished due to the fact that it was impossible to determine a single molecular weight for this mixed preparation of oils. Ultimately, fat solubility was a major issue for all of the experiments performed *in vitro*, although the physiological relevance of conjugating oils to proteins is questionable. Although free fatty acids and triglycerides are transported in the bloodstream by

albumin and lipoproteins respectively, hypertrophic adipocytes passively release fatty acids and triglycerides into the extracellular milieu in their non-solubilised form following necrotic cell death [513].

One major concern allied with using DC cultures as a means of assessing the immunomodulatory capacity of candidate molecules is undoubtedly the presence of only a single cell type. This scenario does not enable or account for communication between different cell types, thereby failing to address the fact that these complex interactions are crucial for mounting effective immune responses *in vivo*. In an attempt to address this issue, a mixed population of splenocytes was stimulated with a range of concentrations of endogenous oils, olive oil or FIA. However, each of the three different oil preparations tested not only failed to augment secretion of characteristic T cell cytokines by splenocytes, but also significantly reduced synthesis of IFN-γ, IL-17 and IL-10. This effect, however, is likely to be a result of toxicity rather than a direct suppressive effect attributed to the various oil preparations.

Notably, FIA, which as discussed in Section 1.5 is a powerful adjuvant that has been discontinued in humans because of unacceptable levels of reactogenicity, also failed to enhance cytokine secretion by splenocytes. Furthermore, FIA also failed to directly augment cytokine secretion by DCs or promote NLRP3 inflammasome activation (data not shown). However, numerous studies have shown that when injected in combination with an antigen, FIA generates powerful immune responses, in particular elevating serum antigen-specific antibody titres [544]. Based on these observations, the biological activity of endogenous oils was evaluated *in vivo* by employing an adjuvant model using OVA as an antigen. Interestingly, the endogenous oils promoted powerful OVA-specific antibody titres in the serum. Indeed, one particularly important point to highlight here is that, unlike FIA, the preparation of endogenous oils was not emulsified before being injected into mice. This course of action was taken in order to preserve the physiological relevance of the experiment and to replicate what may actually occur *in vivo,* rather than to generate an emulsified artefact with no credible existence in the animal. Thus, this consideration makes the antibody-inducing activity of endogenous oils even more impressive. Ultimately, adipocytes in the omentum contain endogenous adjuvants in the form of dietary oils.

In order to eliminate the possibility that non-lipid components were responsible for the observed immunostimulatory effects of the omental lipid preparation *in vivo,* a lipid extraction procedure was performed using chloroform and methanol. The aim of this procedure was to separate lipid

constituents from non-lipid components such as proteins, polysaccharides and amino acids. Once again, the biological activity of both the organic and aqueous fractions was assessed *in vivo* by employing an adjuvant model using OVA as an antigen. Interestingly, the aqueous phase containing non-lipid components failed to enhance any of the OVA-specific IgG subtypes tested. However, the organic fraction containing non-polar lipids potently induced OVA-specific antibody responses, including total IgG, IgG1, IgG2b and IgG2c. Indeed, these titres were comparable to those mediated by the crude preparation of endogenous oils and also FIA. These findings were also confirmed in an adjuvant study using HSA as an antigen. This data suggests that non-lipid components are not responsible for the observed adjuvanticity accredited to the preparation of endogenous oils.

The adjuvant studies described above were primarily employed to compare the immunostimulatory effects of endogenous oils with FIA in the most appropriate model, rather than to accurately portray actual physiological events in WAT. However, there is still some very significant physiological relevance to these findings in so far as that the adaptive immune system is now recognised as being very active in WAT in the context of obesity-induced inflammation. Interestingly, Winer *et al.* have reported that T cells isolated from visceral fat of DIO mice elicit biased TCR repertoires, thus suggesting that these cells undergo antigen-specific clonal expansion. Despite this however, it remains unconfirmed whether T cells recognise antigens in WAT and if so what the identities of these antigens are. IFN-γ secreting Th1 cells are also increased in visceral fat of DIO mice and these cells promote classical macrophage activation, thus contributing further to inflammation and insulin resistance. Importantly, depletion of Th1 cells impoves insulin sensitivity [545]. A study by Nishimura *et al.* found that $CD8^+$ T cell numbers are also increased in visceral adipose tissue of DIO mice. Depletion of $CD8^+$ T cells reduces macrophage infiltration into WAT and protects mice against obesity-induced inflammation and metabolic disorders, whereas adoptive transfer of $CD8^+$ T cells exacerbates WAT inflammation. Importantly, since infiltration of $CD8^+$ T cells into WAT precedes that of macrophages, it has been postulated that $CD8^+$ T cells may in fact mediate recruitment and activation of macrophages in WAT [546]. These findings suggest that upon release from necrotic adipocytes, the ability of endogenous oils to function as a potent adjuvant and mediate activation of the adaptive immune system may in fact be very important in driving obesity-induced inflammation.

In mice, it has been shown that MF59 promotes macrophage recruitment into the injection site [166]. Seubert *et al.* have also noted that human monocytes and granulocytes migrate towards MF59-conditioned culture supernatants and that this adjuvant enhances monocyte differentiation towards DCs [152]. Moreover, the antibody-inducing activity of alum is apparently mediated by a population

of Gr-1$^+$ cells, which may be granulocytes [547]. Based on these observations, as well as the fact that rapid infiltration of neutrophils and macrophages into WAT is characteristic of obesity-induced inflammation, the ability of endogenous oils to recruit innate immune cells into the injection site was assessed. For these studies, a peritonitis model was employed where mice were injected i.p. and PECs were isolated and analysed by flow cytometry.

In the peritonitis model, the endogenous oils increased total PEC number after 24 hours, specifically recruiting SPMs into the injection site while simultaneously depleting the LPM population. A simple M1/M2 macrophage paradigm has not been fully established in the peritoneum, although SPMs and LPMs are likely to represent the peritoneal equivalent of these respective subsets. A comprehensive study by Ghosn *et al.* has characterised the function of SPMs and LPMs and clearly distinguishes these coexisting populations. SPMs are derived from blood monocytes and are only present at very low levels in the peritoneum of naive mice. However, following injection with an inflammatory stimulus such as LPS or thioglycolate, SPMs become the dominant macrophage population in the peritoneum. LPMs are resident cells and are undoubtedly the dominant macrophage population in the peritoneum of naive mice. Unlike SPMs however, the LPM population is almost undetectable in the peritoneum following injection with an inflammatory stimulus. Since LPMs do not differentiate into SPMs, it is unclear how they become depleted, with different theories postulating that inflammatory stimuli may be toxic to LPMs or that LPMs may migrate out of the peritoneum or even adhere to the endothelial lining of the peritoneum in response to these stimuli [548].

NO synthesis is characteristic of a classically activated M1 macrophage phenotype and thus facilitates characterisation of macrophage subsets into the M1/M2 paradigm. Interestingly, only LPMs produce NO *in vitro* in response to stimulation with LPS, although at very low levels that are barely above those of the control. However, this scenario is completely different *in vivo* where SPMs produce much higher levels of NO than LPMs following injection with LPS [548]. Indeed, a recent study by Spence *et al.* has further characterised SPMs and LPMs with regard to the M1/M2 framework. Importantly, it was shown that SPMs express higher levels of Nos2, CD80, Ly6C and MHC II compared to LPMs, which are all markers characteristic of M1 macrophages. Moreover, LPMs express higher levels of IL-10, arginase and Ym1, which are markers characteristic of M2 macrophages. Therefore, SPMs and LPMs have now been referred to as 'M1-like' and 'M2-like' macrophages respectively [549]. Despite the difficulties associated with translating SPMs and LPMs into the M1/M2 framework, these results suggest that SPMs are the dominant inflammatory

macrophage subset in the peritoneum and are likely to be the peritoneal equivalent of M1 macrophages.

Endogenous oils mediate recruitment of inflammatory SPMs into the injection site and also deplete the resident LPM population, a scenario that resembles events in WAT of obese individuals where a phenotypic shift from M2 macrophages to M1 macrophages is prevalent. However, despite the fact that monocytes give rise to SPMs, future work should identify these blood leukocytes in the peritoneum and clearly distinguish them from SPMs. Indeed, it is conceivable that monocytes may also be present within the Gr-1$^{low/inter}$ population of cells. Nevertheless, these monocytes are essentially pre-SPMs and differentiate into inflammatory SPMs over a short period of time [548].

Endogenous oils also potently induced neutrophil recruitment into the peritoneum. In addition to inflammatory macrophages, these granulocytes infiltrate visceral fat during the early stages of high-fat feeding [474] and mediate tissue inflammation and insulin resistance in DIO mice through secretion of neutrophil elastase [475]. Indeed, the fact that endogenous oils are capable of mediating recruitment of the two most important cell populations in obesity-induced inflammation suggests that these oils may play a prominent role in this process.

Eosinophil infiltration into the peritoneum and also depletion of mast cells was evident 24 hours after injection with endogenous oils. However, these findings were very surprising given the apparent role of these respective innate cells in WAT. Eosinophils are the primary source of IL-4 in WAT and are therefore crucial for alternative activation of M2 macrophages. Eosinophil-deficient DIO mice elicit worse metabolic profiles than wild-type DIO mice, whereas IL-5 transgenic mice have tissue eosinophilia and have lower levels of adiposity with improved glucose tolerance. Furthermore, eosinophil numbers correlate inversely with adiposity [550]. In contrast, mast cells appear to promote obesity-induced inflammation as mast cell-deficient DIO mice have improved insulin resistance. Furthermore, mast cell numbers are increased in WAT of obese humans and mice compared to WAT from their lean counterparts. [551]. The discrepancy between the findings of this study and those in the literature will need to be investigated further, perhaps placing an emphasis on a later time point in the peritoneum. It is conceivable that mast cells may be recruited into the peritoneum at a later stage. Indeed, preliminary studies seem to indicate that this in fact the case and that mast cells may infiltrate the peritoneum after approximately 5 days (data not shown).

This study also concluded that of all of the time points tested, 24 hours was the optimal time point for assessing cell recruitment into the peritoneum following injection with endogenous oils.

Although changes in cell populations in the peritoneum were evident at much earlier time points, these changes were most prominent after 24 hours. Therefore, this particular time point was chosen for all subsequent experiments assessing cell recruitment into the peritoneum. Furthermore, 10µl of endogenous oils was the volume injected for each experiment. This was the smallest possible volume that could be drawn by the syringe and was deliberately chosen in order to maintain as much physiological relevance as possible compared to volumes which may be released by necrotic adipocytes in obese conditions.

The immune activation capacity of adjuvants has often been accredited to their tendency to elicit toxicity at the injection site. For example, it has been reported that DNA released by dying host cells mediates adjuvanticity *in vivo*, and the adjuvanticity of alum is partially attenuated when extracellular DNA is digested by treatment with DNase I [156]. Furthermore, recruitment of innate immune cells such as neutrophils and inflammatory monocytes, as well as T cell priming and humoral immunity, is abrogated in response to alum when uric acid is degraded by the enzyme uricase. Thus, uric acid released from dying host cells at the injection site has also been proposed to mediate the immunostimulatory effects of alum [78]. This study has confirmed that alum is extremely toxic to cells at the injection site, killing approximately 80% of PECs after only 15 minutes. Indeed, this finding highlights the importance of employing very early time points when assessing cell death in the peritoneum in response to adjuvants. Although cell recruitment is most prominent after 24 hours, many of the events which drive this process are likely to occur much earlier. The endogenous oils induced a two-fold increase in toxicity of PECs after 15 minutes, but this was only a very moderate increase compared to the toxicity elicited by alum. Furthermore, these effects were reduced over time, possibly owing to phagocytosis of necrotic debris by SPMs or LPMs, both of which have been reported to have significant phagocytic potential [548]. Interestingly, the endogenous oils are not toxic to PECs *in vitro* (data not shown). Taken together, this suggests that toxicity is unlikely to mediate the immunostimulatory effects of endogenous oils.

Another important observation made in this study was the ability of the endogenous oils to induce a complete shift in the cytokine profile of PECs. 24 hours after injection with endogenous oils, PECs isolated from these mice were restimulated *ex vivo* with a range of PRR agonists. Interestingly, PECs isolated from these mice secreted significantly more TNF-α, IL-12p40 and IL-12p70 than those isolated from control mice injected with PBS, while simultaneously producing less IL-10. Under normal conditions, M2 macrophages in WAT secrete anti-inflammatory cytokines such as IL-10 in order to dampen the immune environment and maintain homeostasis [470]. In obese conditions,

however, WAT recruits M1 macrophages that secrete proinflammatory cytokines such as TNF-α [469] and IL-12 [552-554]. Therefore, the endogenous oils very clearly induce a shift in the cytokine profile in the peritoneum which serves to establish an inflammatory environment resembling that of WAT in obese individuals. Furthermore, secretion of IL-12 may also serve to polarise Th1 cells which are increased in visceral fat of DIO mice. As discussed earlier, Th1 cells promote classical macrophage activation, thus contributing further to inflammation and insulin resistance [545]. It is hypothesised that SPMs are producing these inflammatory cytokines, whereas the LPMs are making IL-10. This further strengthens the case for SPMs and LPMs representing the peritoneal equivalent of M1 and M2 macrophages respectively. In support of this hypothesis, reduced levels of IL-10 secretion by PECs isolated from mice injected with endogenous oils coincides with the gradual disappearance of LPMs, whereas increased production of TNF-α and IL-12 corresponds with the recruitment of SPMs. However, it is possible that other infiltrating cells such as neutrophils may also produce these proinflammatory cytokines, whereas residual levels of IL-10 production by PECs isolated from mice injected with endogenous oils suggests that cell types other than LPMs also make this anti-inflammatory cytokine. Indeed, the fact that endogenous oils also mediate the depletion of mast cells suggests that these innate immune cells might provide a source of IL-10. This should be the focus of future work. However, it is imperative to be conscious of the fact that when PECs isolated from mice injected with endogenous oils are restimulated *ex vivo* with PRR agonists, the change in cytokine secretion profiles observed compared to those isolated from control mice is likely a result of altered cell populations in the peritoneum rather than secretion of different cytokines by similar cell types.

Since endogenous oils are capable of inducing comprehensive changes in cell populations in the peritoneum, it was important to establish a mechanism for this process. TLR4 was a primary candidate for mediating inflammatory cell recruitment into the peritoneum simply because the preparation of endogenous oils is expected to contain free fatty acids and these lipids have been shown previously to promote TLR4-dependent immunostimulatory responses both *in vitro* and *in vivo* [488-489]. However, TLR4-defective C3H/HeJ mice were as competent as wild-type C3H/HeN mice in their ability to recruit neutrophils, SPMs and eosinophils into the peritoneum while also depleting the LPM and mast cell populations. This suggests that TLR4 is not required for inflammatory cell recruitment into the peritoneum in response to these oils and eliminates the possibility that signalling through TLR4 by free fatty acids is mediating these effects. However, this result also extinguishes the possibility that contamination with a TLR4 agonist is responsible for the

observed effects. In the world of danger signals, this is a very encouraging finding. Nevertheless, it was still necessary to establish a mechanism for the inflammatory effects of the endogenous oils in the peritonitis model.

As mentioned previously, many events leading to cell recruitment into the injection site are likely to happen relatively early. Indeed, this study found that levels of IL-1α and IL-1β were elevated in the peritoneum 3 hours after injection with endogenous oils. IL-1α and IL-1β are powerful chemoattractants and were therefore considered prime candidates for promoting cell recruitment into the peritoneum following injection with endogenous oils. Interestingly, IL-1R KO mice failed to recruit neutrophils or SPMs and this was reflected in a significant reduction in overall PEC numbers, thus suggesting that IL-1α and/or IL-1β is mediating the effects of the endogenous oils *in vivo*. Interestingly, neutrophil recruitment was only partially dependent on NLRP3 and SPM recruitment was completely independent of this inflammasome. This suggests that a NLRP3-dependent source of IL-1β may be partially responsible for mediating neutrophil recruitment into the peritoneum, but is not involved in SPM infiltration. However, there are various other NLRP3-independent sources of IL-1β in the peritoneum which may be involved in these events, while IL-1α is also likely to contribute significantly.

Using a model of sterile inflammation, Rider *et al.* have shown that IL-1α initiates the inflammatory process by promoting neutrophil recruitment whereas IL-1β sustains inflammation by inducing infiltration and retention of macrophages [555]. Indeed, IL-1α has previously been shown to be important for the acute neutrophilic inflammatory response to cell injury, although mainly as a secondary mediator produced by inflammatory macrophages following initial recognition of necrotic cells by receptors not including the IL-1R [272]. Therefore, it is likely that effector cells in the peritoneum also secrete IL-1α following IL-1R-independent recognition of the endogenous oils. However, in order to establish the precise roles of IL-1α and IL-1β in the inflammatory response to endogenous oils in the peritoneum, it will be necessary to perform neutralisation experiments for each of these inflammatory cytokines. Alternatively, injecting IL-1α KO and IL-1β KO mice i.p. with endogenous oils and monitoring subsequent cell recruitment into the peritoneum would potentially be even more informative. Since levels of the chemoattractant KC were also raised 3 hours after injection with endogenous oils, it is conceivable that IL-1 may subsequently drive production of KC which in turn mediates some of the effects observed. Therefore, it will be interesting to assess KC levels in the peritoneum of IL-1R KO mice 3 hours after injection with endogenous oils. The IL-1R did not appear to play a role in recruiting eosinophils in response to

endogenous oils, although this is an effect likely to be mediated by eotaxin. However, the IL-1R may play a minor role in depleting LPMs given that the fold reduction in the percentage of LPMs following injection with endogenous oils is noticeably smaller in IL-1R KO mice compared to wild-type and NLRP3 KO mice, although this observation will need to be confirmed in future studies.

As mentioned, IL-1R KO mice failed to recruit neutrophils and SPMs following injection with endogenous oils. One concern here was that the IL-1R KO mice were severely compromised and simply did not have the capacity to mediate cell recruitment into the peritoneum, regardless of the stimulus. However, IL-1R KO mice were able to recruit both neutrophils and SPMs in response to 10μm PS particles, thus confirming that the requirement for the IL-1R in recruitment of these innate immune cells was specific for injection with endogenous oils and was not simply a defect associated with these mice.

Interestingly, the ability of the endogenous oils to induce a shift in the cytokine profile of PECs when restimulated *ex vivo* was also partially dependent on the IL-1R. Secretion of TNF-α, IL-12p40 and IL-12p70 by PECs isolated from IL-1R KO mice injected with endogenous oils was abrogated compared to PECs isolated from wild-type control mice. This result is likely due to the failure of IL-1R KO mice to recruit SPMs. However, a requirement for IL-1R expression on PECs for secreting proinflammatory cytokines following *ex vivo* restimulation with PRR agonists cannot be discounted. PECs isolated from IL-1R KO mice injected with endogenous oils still produced less IL-10 than PECs isolated from IL-1R KO mice injected with PBS. Furthermore, secretion of IL-10 by PECs isolated from IL-1R KO mice injected with endogenous oils was similar to that of PECs isolated from wild-type mice injected with the same treatment. Thus, the effects of endogenous oils on the synthesis of IL-10 remained intact in IL-1R KO mice. This is possibly owing to the fact that LPMs are still partially depleted in IL-1R KO mice in response to endogenous oils, thus diminishing a major cell population in the peritoneum that may provide a rich source of IL-10. Ultimately, the IL-1R appears to be crucial in establishing an inflammatory environment in the peritoneum following injection with endogenous oils. PECs isolated from NLRP3 KO mice injected with endogenous oils elicited a similar cytokine profile to those isolated from wild-type mice, thus complimenting the cell recruitment data in confirming only a relatively minor role for NLRP3.

Similar to NLRP3, neutrophil recruitment was partially dependent on the adaptor protein ASC, although SPM recruitment may also share this ASC dependency to a very limited extent. However, these findings represented a trend and were not found to be statistically significant. Eosinophil

recruitment and significant mast cell depletion were also evident in ASC KO mice. Nevertheless, ASC undoubtedly possesses a NLRP3-independent role in the peritoneum. LPMs were still present in the peritoneum of ASC KO mice following injection with endogenous oils, whereas this resident population completely disappeared in wild-type mice. In the previous experiment, LPMs also disappeared from the peritoneum of NLRP3 KO mice in response to endogenous oils, thus confirming a NLRP3-independent role for ASC in depleting the LPM population. As discussed above, the IL-1R may also play a relatively minor role in this depletion process, although this observation will need to be confirmed.

PECs isolated from ASC KO mice injected with endogenous oils secreted only marginally lower levels of TNF-α, IL-12p40 and IL-12p70 than those isolated from wild-type mice. This was not surprising given that ASC KO mice were still competent in their recruitment of neutrophils and particularly SPMs. PECs isolated from wild-type mice injected with endogenous oils secreted less IL-10 in comparison to those injected with PBS, and this trend was apparent for all PRR agonists tested. However, unlike PECs isolated from NLRP3 KO mice, this effect was mostly absent in PECs isolated from ASC KO mice injected with endogenous oils as these cells secreted similar levels of IL-10 to those isolated from ASC KO mice injected with PBS. This effect coincides with the retention of LPMs in ASC KO mice following injection with endogenous oils. It is conceivable that ASC KO mice fail to deplete LPMs and that these resident cells subsequently secrete IL-10 following restimulation with PRR agonists. However, it is surprising that IL-1R KO mice have a reduced number of LPMs compared to wild-type and NLRP3 KO mice following injection with PBS, yet IL-10 synthesis by PECs isolated from IL-1R KO mice remains intact following *ex vivo* restimulation. This suggests that LPMs may not be the primary source of IL-10. Indeed, endogenous oils also deplete the mast cell population in the peritoneum of wild-type mice but fail to entirely diminish this population in ASC KO mice. Although this effect appears to be independent of ASC, it raises the possibility that mast cells may provide a source of IL-10. Ultimately, intracellular cytokine staining and IL-10 reporter mice will be required to address this issue.

Although NLRP3 is not involved in the depletion of LPMs in response to endogenous oils, ASC also functions as an adaptor protein for NLRP1, NLRC4 and AIM2. Therefore, it will be interesting to establish whether these inflammasomes have an ASC-dependent role in depleting the LPM population in the peritoneum in response to endogenous oils. Alternatively, it is possible that ASC may possess an inflammasome-independent role in diminishing these resident macrophages. In order to address this issue it will be important to assess the LPM population in caspase-1 KO mice

following injection with endogenous oils and also to further characterise the role of the IL-1R in this process.

Importantly, it seems likely that the immunostimulatory activity of endogenous oils is in fact mediated by their physiochemical properties rather than by a specific danger signal present in the preparation. This hypothesis is supported by the fact that olive oil is also capable of modulating similar innate and adaptive immune responses. Thus, searching for a specific danger signal responsible for the observed effects is likely to prove fruitless. Alternatively, there may be a specific danger signal which is common to both olive oil and endogenous oils released from necrotic adipocytes in the omentum. Indeed, primary candidates might include triglycerides such as trioleylglycerol and tripalmitoylglycerol which are the first and second most abundant triglycerides in the adipocyte lipid droplet [556]. Nevertheless, this study hypothesises that most triglycerides are in fact immunostimulatory but only those that are released from necrotic adipocytes and are therefore exposed to the immune system will signal danger to the host and mediate inflammation. This is confirmed by the finding that endogenous oils derived from subcutaneous adipocytes are as potent as those derived from omental adipocytes of the same individual, despite the fact that visceral fat is significantly more pathogenic than subcutaneous fat in the context of obesity-induced inflammation.

The above findings suggest that the capacity of endogenous oils to drive immune activation is entirely dependent on their ability to be passively released from hypertrophic adipocytes undergoing necrosis. Ultimately, these oils will only act as endogenous adjuvants if they are discharged into the extracellular milieu. It is imperative to note that visceral fat depots are more pathogenic in MUO individuals than in MHO or lean individuals. Visceral fat is also more pathogenic than its subcutaneous counterpart in all of the above groups. Therefore, this study proposes that endogenous oils will have the highest propensity to be released from adipocytes in visceral fat of MUO individuals than in any of the other scenarios. In support of this hypothesis, Cinti *et al.* have shown that necrotic adipocytes are approximately thirty-fold more frequent in visceral fat of genetically obese mice than in visceral fat of lean mice. Furthermore, this finding was also confirmed in humans [513]. Murano *et al.* have reported that necrotic adipocytes are far more prevalent in visceral fat than in subcutaneous fat of genetically obese mice [557], and this occurrence has also been observed in humans [558]. Importantly, there is a positive correlation between adipocyte size and adipocyte necrosis in visceral fat of obese mice and humans [513]. In agreement with O'Connell *et al* [559], this study demonstrates that MUO individuals have significantly larger omental adipocytes than MHO individuals, increasing in diameter by approximately 15%. Given that adipocyte size is

correlated with death, this data suggests that adipocytes in visceral fat of MUO individuals are more likely to undergo necrosis than adipocytes in visceral fat of MHO individuals and are therefore more likely to subsequently release endogenous oils into the extracellular milieu which drive potent immunostimulatory responses. Ultimately, this study hypothesises that endogenous oils derived from all fat depots in individuals with various different BMIs and metabolic states are in fact immunostimulatory. However, it is the higher propensity of these oils to be released from visceral fat of MUO individuals which makes this profile more pathogenic than any other. Once released from necrotic adipocytes in visceral fat, the endogenous oils proceed to recruit neutrophils and inflammatory macrophages into the tissue in an IL-1R-dependent manner. These innate immune cells then initiate the inflammatory cascade associated with obesity (Figure 5.43).

It will be vital to further understand and indeed characterise the immunomodulatory potential of endogenous oils and also their role in the chronic low-grade inflammation associated with obesity. One very interesting avenue of exploration will be their chemotactic effects. Importantly, Seubert *et al.* have recently shown that both MF59 and alum induce secretion of chemokines such as MCP-1, MIP-1α, MIP-1β and IL-8 by human macrophages and monocytes while concomitantly failing to induce secretion of proinflammatory cytokines. Furthermore, both myeloid and monocyte-derived DCs were completely unresponsive to MF59 and alum [152]. This data not only suggests that BMDCs are an inappropriate cell type to be using in testing for immunomodulatory activity of these endogenous oils, but also that secretion of proinflammatory cytokines is an insufficient indicator of immune activation in this case. Therefore, it will be crucial to assess whether these oils can potentiate secretion of chemokines by macrophages both *in vitro* and in the more physiologically relevant *in vivo* setting.

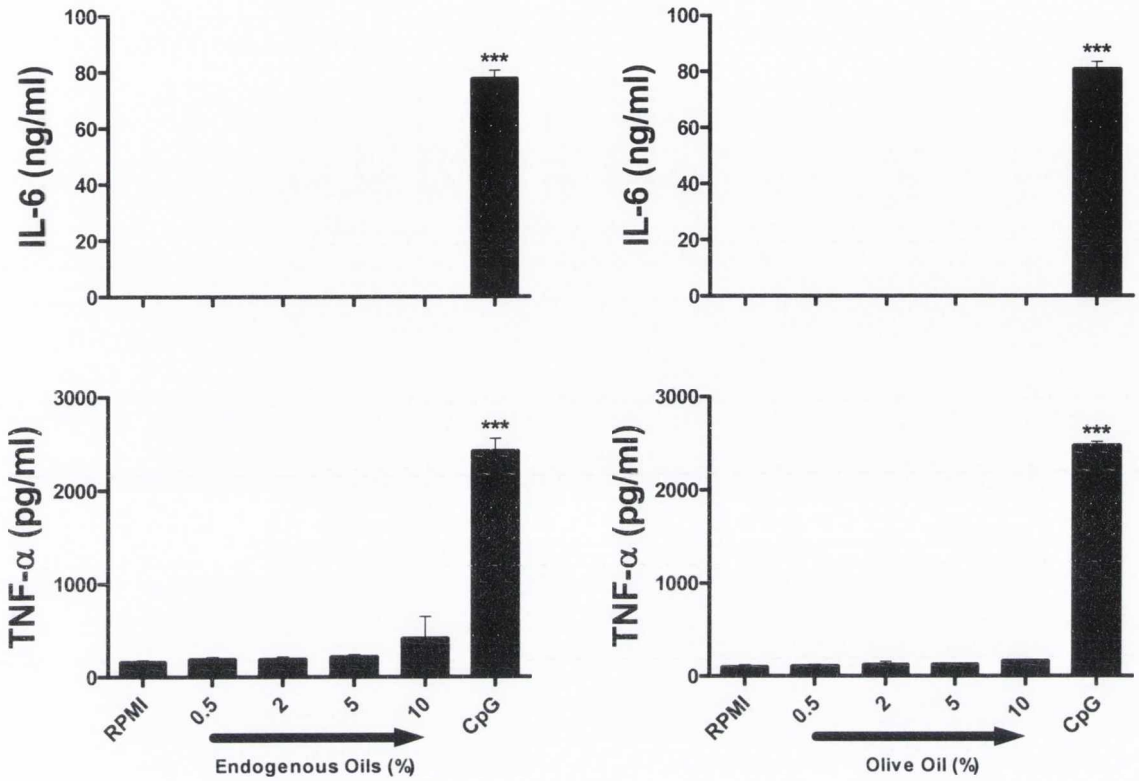

Figure 5.1 – BMDCs do not secrete proinflammatory cytokines following stimulation with endogenous oils. BMDCs (6.25 x 10^5 cells/ml) from C57BL/6 mice were stimulated with RPMI or the indicated concentrations of endogenous oils, olive oil or CpG (4μg/ml). Supernatants were collected 24 hours later and tested for the cytokines IL-6 and TNF-α by ELISA. Results are mean cytokine concentrations (+ SEM) for triplicate samples. Versus RPMI, *** $p<0.001$.

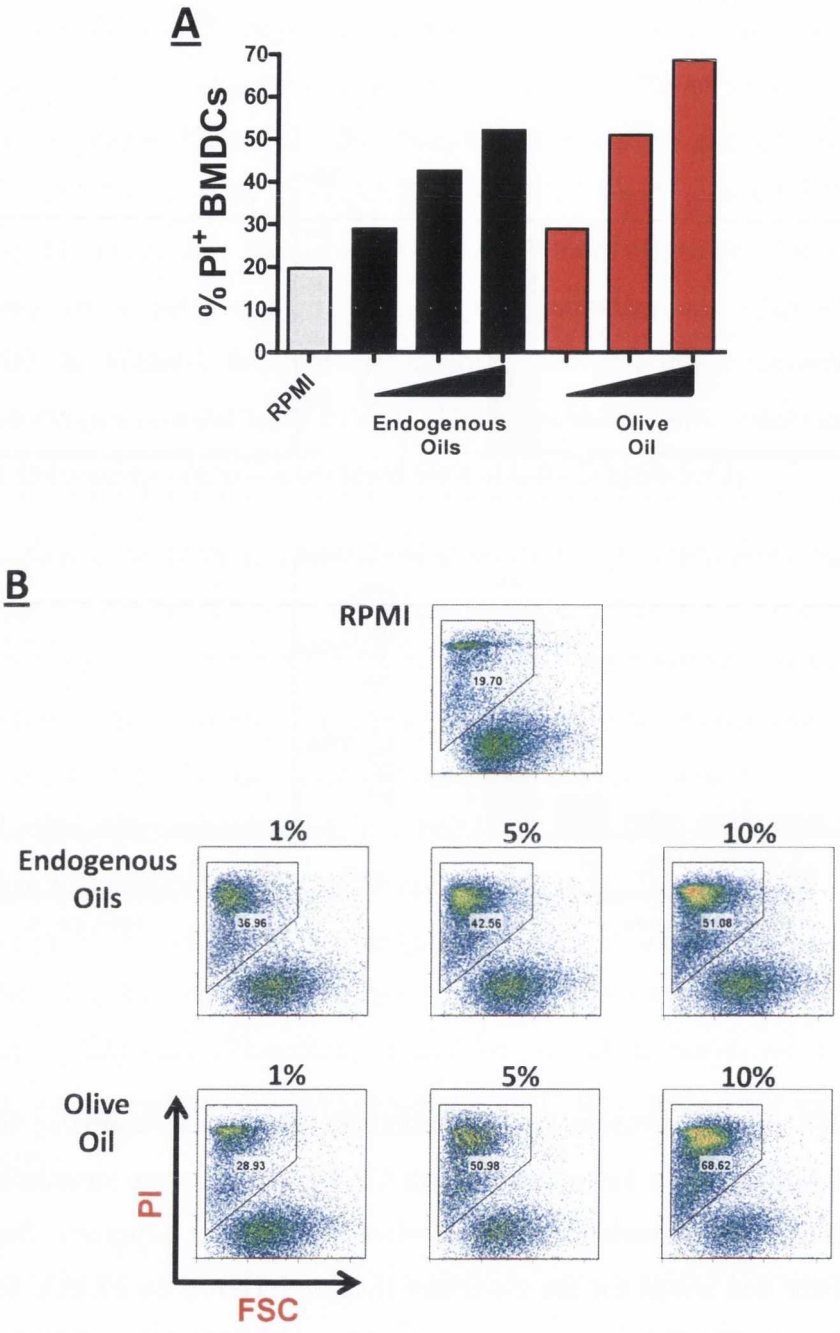

Figure 5.2 – Endogenous oils are toxic to BMDCs. BMDCs (6.25 x 10^5 cells/ml) from C57BL/6 mice were stimulated with RPMI, endogenous oils (1, 5, 10%) or olive oil (1, 5, 10%). Cells were harvested 24 hours later and stained with PI and an antibody specific for CD11c. The level of PI staining on $CD11c^+$ BMDCs was quantified for each treatment by flow cytometry. Cell death is expressed as the number of $CD11c^+$ cells that have incorporated PI as a percentage of the total number of $CD11c^+$ cells and is represented in (A) a bar graph and (B) dot plot format. Data are represented as MFI for triplicate samples.

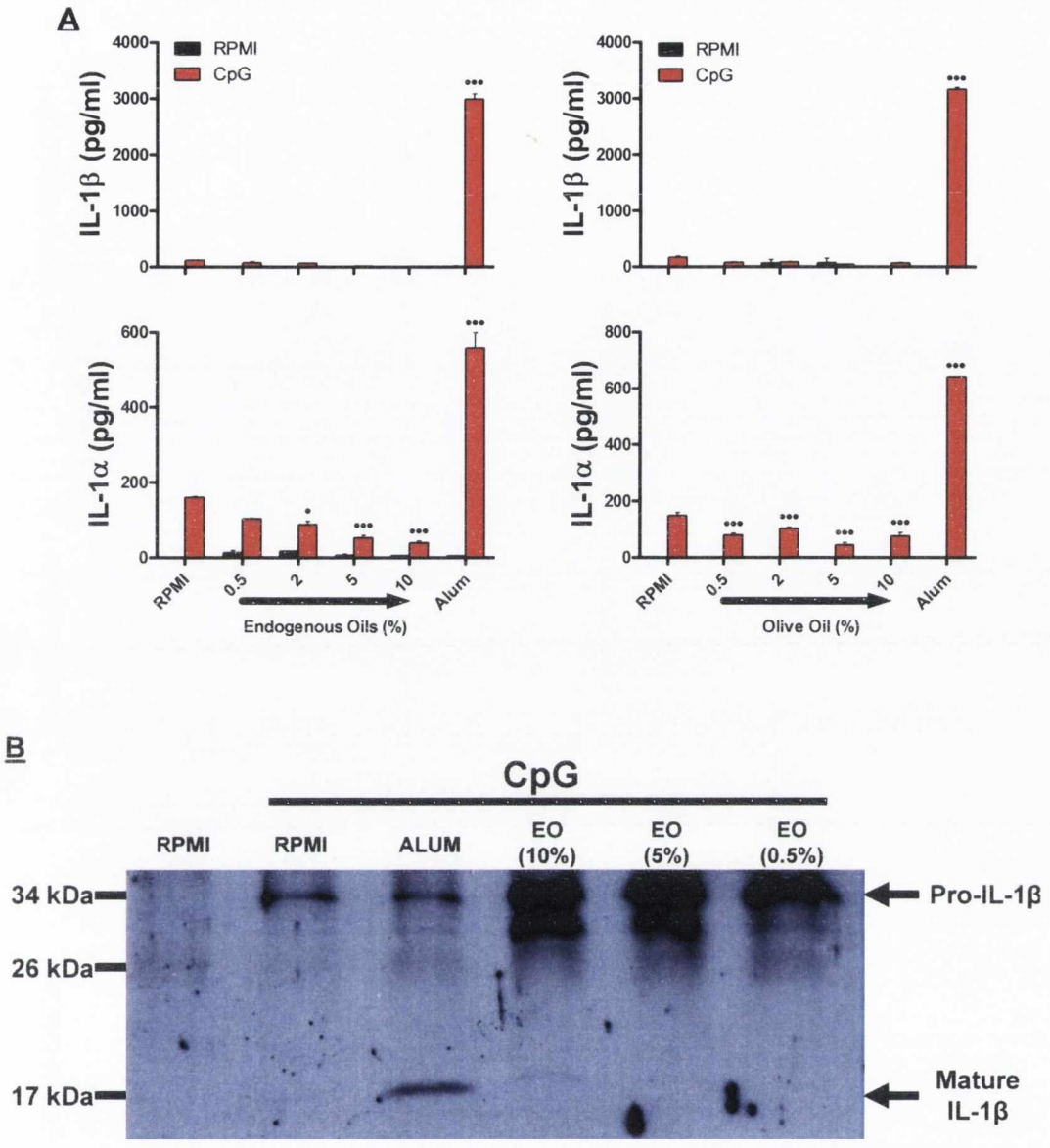

Figure 5.3 – Endogenous oils fail to synergise with CpG in releasing the proinflammatory cytokines IL-1β and IL-1α from BMDCs. (A) BMDCs (6.25 x 10^5 cells/ml) from C57BL/6 mice were stimulated with RPMI or CpG (4μg/ml) for 2 hours. These cells were then stimulated with the indicated concentrations of endogenous oils, olive oil or alum (5mM). Supernatants were collected 24 hours later and tested for the cytokines IL-1β and IL-1α by ELISA. Results are mean cytokine concentrations (+ SEM) for triplicate samples. CpG + treatment versus CpG alone, • $p<0.05$, ••• $p<0.001$. (B) BMDCs (1 x 10^6 cells/ml) from C57BL/6 mice were stimulated with CpG (4μg/ml) for 2 hours. These cells were then stimulated with RPMI, alum (5mM) or the indicated concentrations of endogenous oils. Supernatants were collected 24 hours later. Protein was extracted from the supernatants and immunoblotted for IL-1β.

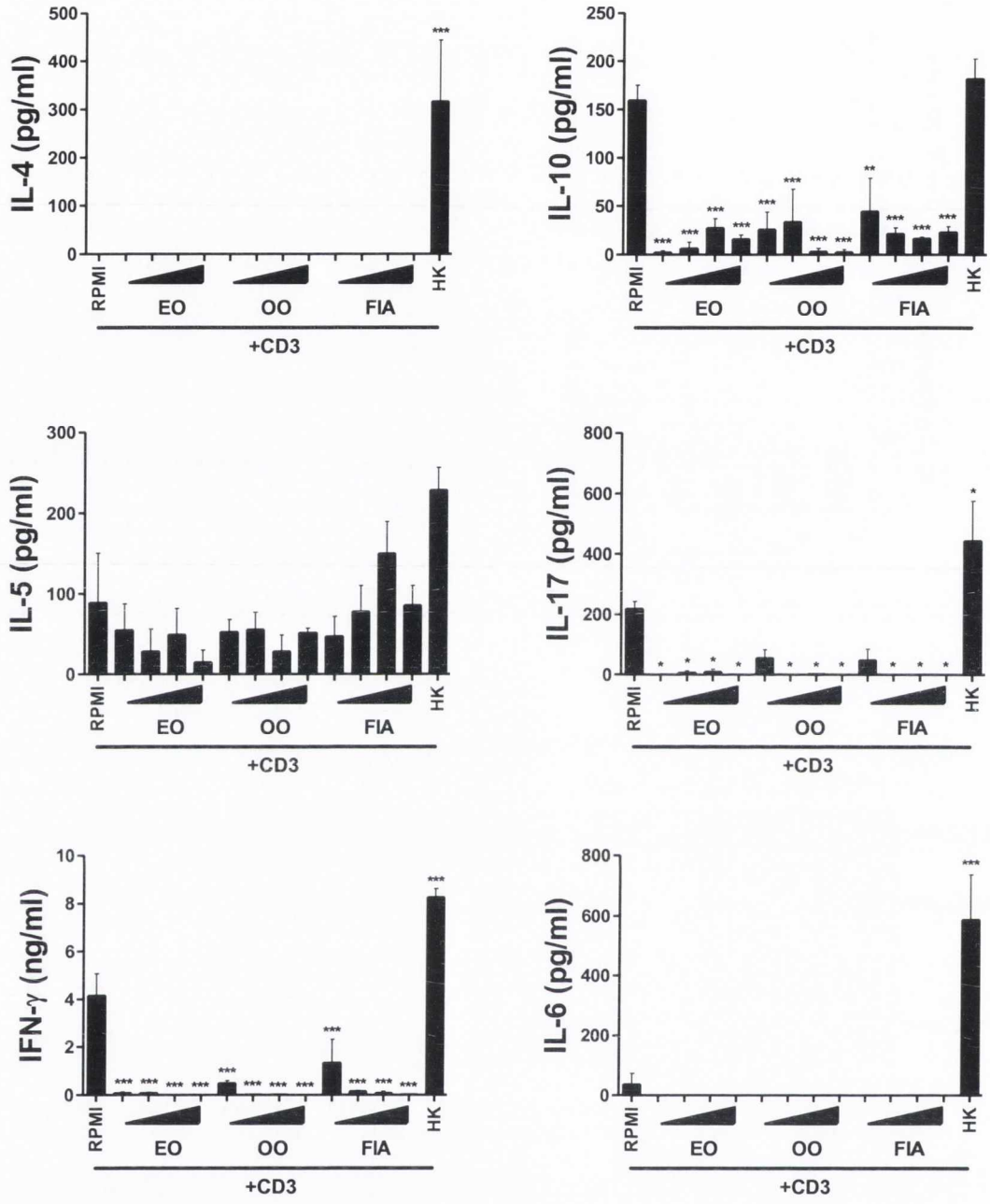

Figure 5.4 – Endogenous oils do not augment, but rather suppress secretion of characteristic T cell cytokines by splenocytes. Splenocytes (2 x 10^6 cells/ml) from C57BL/6 mice were stimulated with RPMI, endogenous oils (EO) (0.5, 2, 5, 10%), olive oil (OO) (0.5, 2, 5, 10%), FIA (0.5, 2, 5, 10%) or HK *E. coli* (HK) (10 *E. coli* : 1 BMDC) in the presence of plate-bound anti-CD3 (0.5μg/ml). Supernatants were collected 72 hours later and tested for the cytokines IL-4, IL-5, IFN-γ, IL-10, IL-17 and IL-6 by ELISA. Results are mean cytokine concentrations (+ SEM) for triplicate samples. Versus RPMI, * $p<0.05$, ** $p<0.01$, *** $p<0.001$.

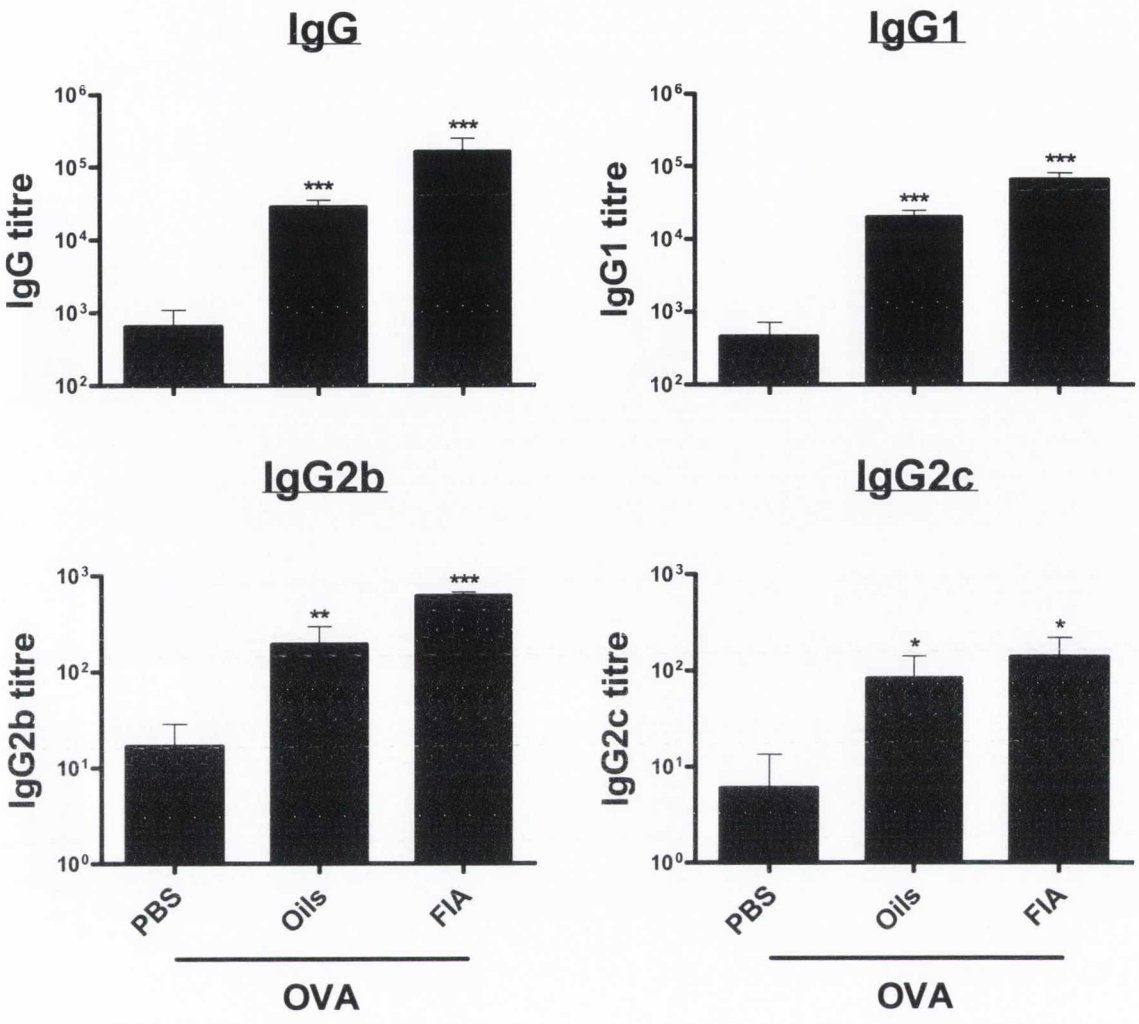

Figure 5.5 – Endogenous oils significantly boost OVA-specific serum antibody titres. Female C57BL/6 mice were immunised i.p. on day 0 with PBS as a control or OVA (200µg per mouse) either alone or mixed with an equal volume (100µl) of a crude preparation of endogenous oils derived from the human omentum. OVA was also mixed with an equal volume (100µl) of FIA and this solution was emulsified by rigorous sonication. The mice were boosted with these same treatments on day 14 and were sacrificed on day 21. Blood samples were recovered and the serum was removed following centrifugation. OVA-specific antibody titres (IgG, IgG1, IgG2b, IgG2c) in the serum were determined by ELISA. Results are mean titres (+ SEM) for 5 mice per experimental group. Versus PBS (OVA), * $p<0.05$, ** $p<0.01$, *** $p<0.001$.

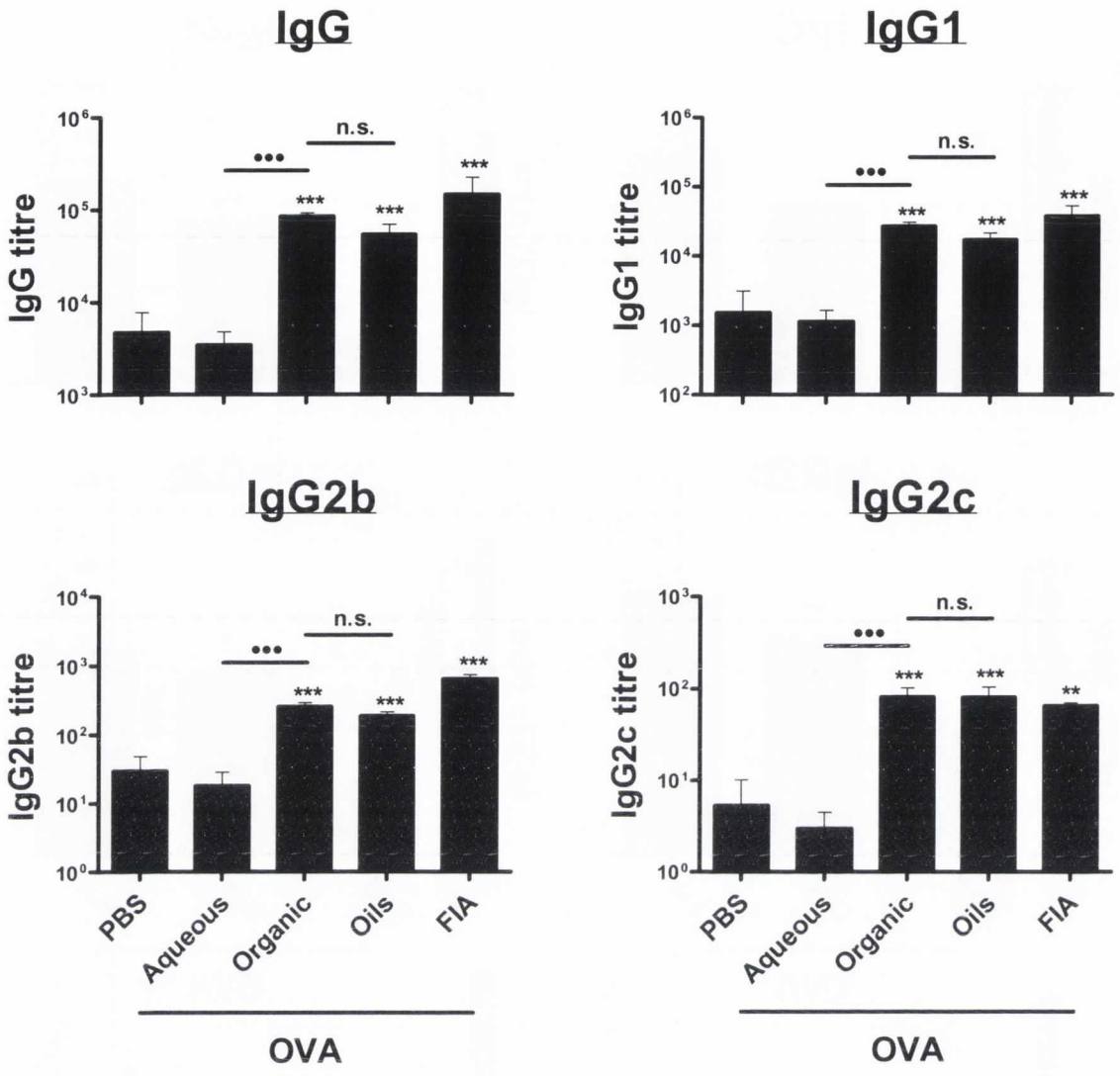

Figure 5.6 – The organic phase of the omental lipid preparation mediates enhancement of OVA-specific antibody titres in the serum. Female C57BL/6 mice were immunised i.p. with PBS or OVA (200μg/mouse) either alone or mixed with an equal volume (100μl) of a crude preparation of endogenous oils, or an aqueous or organic fraction derived from this crude preparation. OVA was also mixed with an equal volume (100μl) of FIA and this solution was emulsified by rigorous sonication. The mice were boosted with these same treatments on day 14 and were sacrificed on day 21. Blood samples were recovered and the serum was removed following centrifugation. OVA-specific antibody titres (IgG, IgG1, IgG2b, IgG2c) in the serum were determined by ELISA. Results are mean titres (+ SEM) for 4 mice per experimental group. Versus PBS (OVA), ** $p<0.01$, *** $p<0.001$. Organic fraction (OVA) versus aqueous fraction (OVA), ••• $p<0.001$.

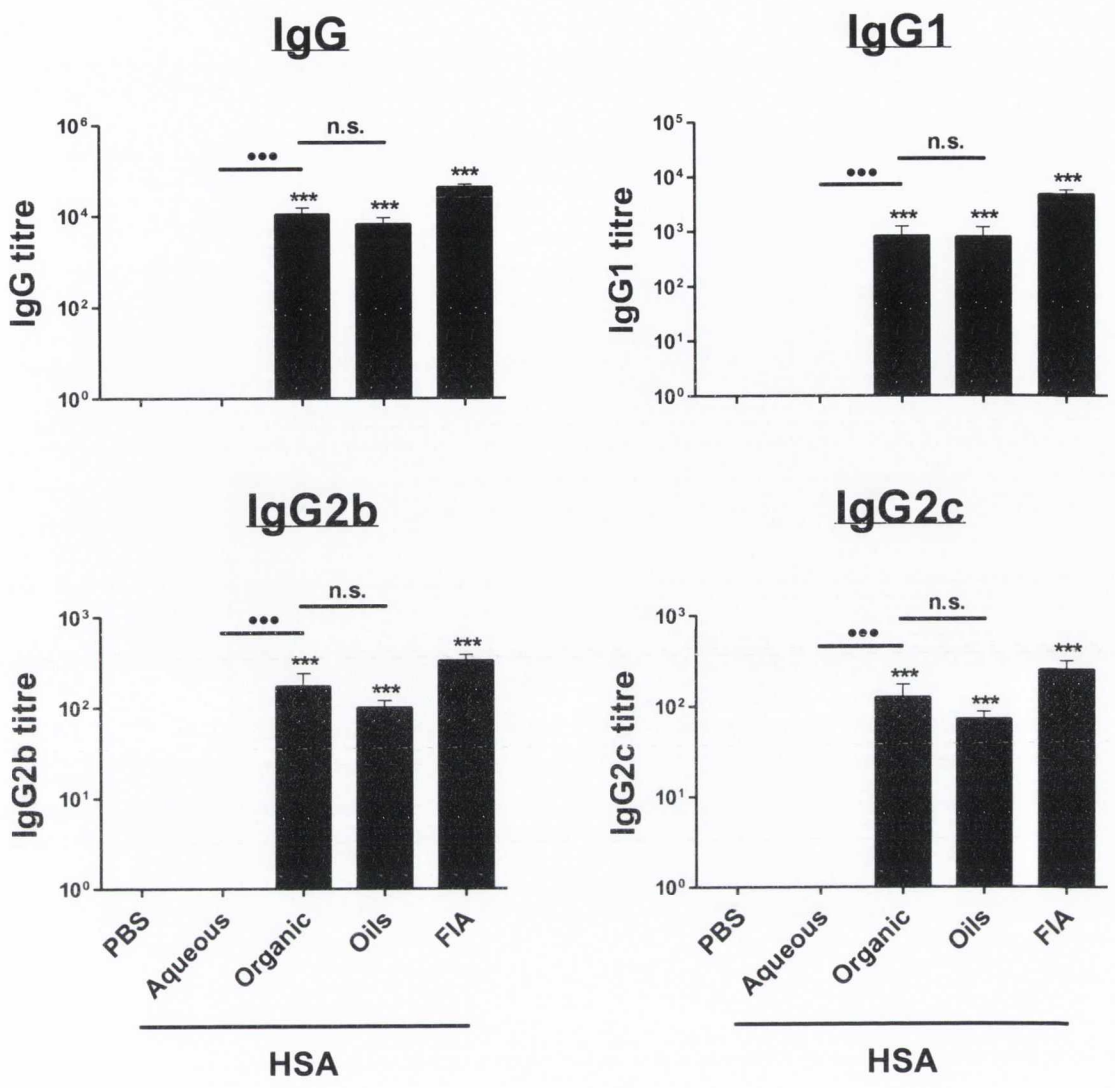

Figure 5.7 – The organic phase of the omental lipid preparation mediates enhancement of HSA-specific antibody titres in the serum. Female C57BL/6 mice were immunised i.p. with PBS or HSA (50μg/mouse) either alone or mixed with an equal volume (100μl) of a crude preparation of endogenous oils, or an aqueous or organic fraction derived from this crude preparation. HSA was also mixed with an equal volume (100μl) of FIA and this solution was emulsified by rigorous sonication. The mice were boosted with these same treatments on day 14 and were sacrificed on day 21. Blood samples were recovered and the serum was removed following centrifugation. HSA-specific antibody titres (IgG, IgG1, IgG2b, IgG2c) in the serum were determined by ELISA. Results are mean titres (+ SEM) for 4 mice per experimental group. Versus PBS (HSA), *** $p<0.001$. Organic fraction (HSA) versus aqueous fraction (HSA), ••• $p<0.001$.

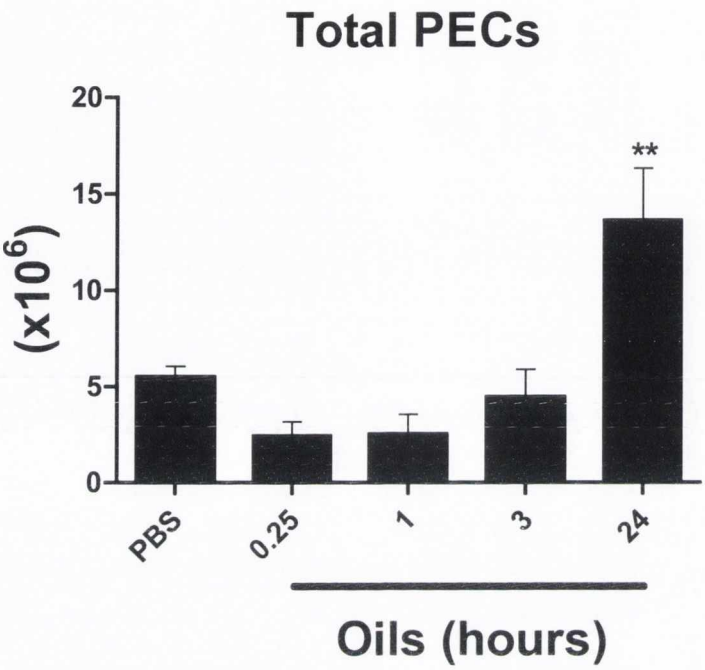

Figure 5.8 – Endogenous oils promote cell recruitment into the peritoneum. Female C57BL/6 mice were immunised i.p. with PBS (10µl/mouse) as a control or endogenous oils (10µl/mouse). The mice were sacrificed after the indicated number of hours (0.25, 1, 3, or 24) and PECs were isolated. PEC numbers were determined using a Glasstic cell counter slide with grids following trypan blue staining. Results are mean PEC number (+ SEM) for 3 mice per experimental group. Versus PBS, ** $p<0.01$.

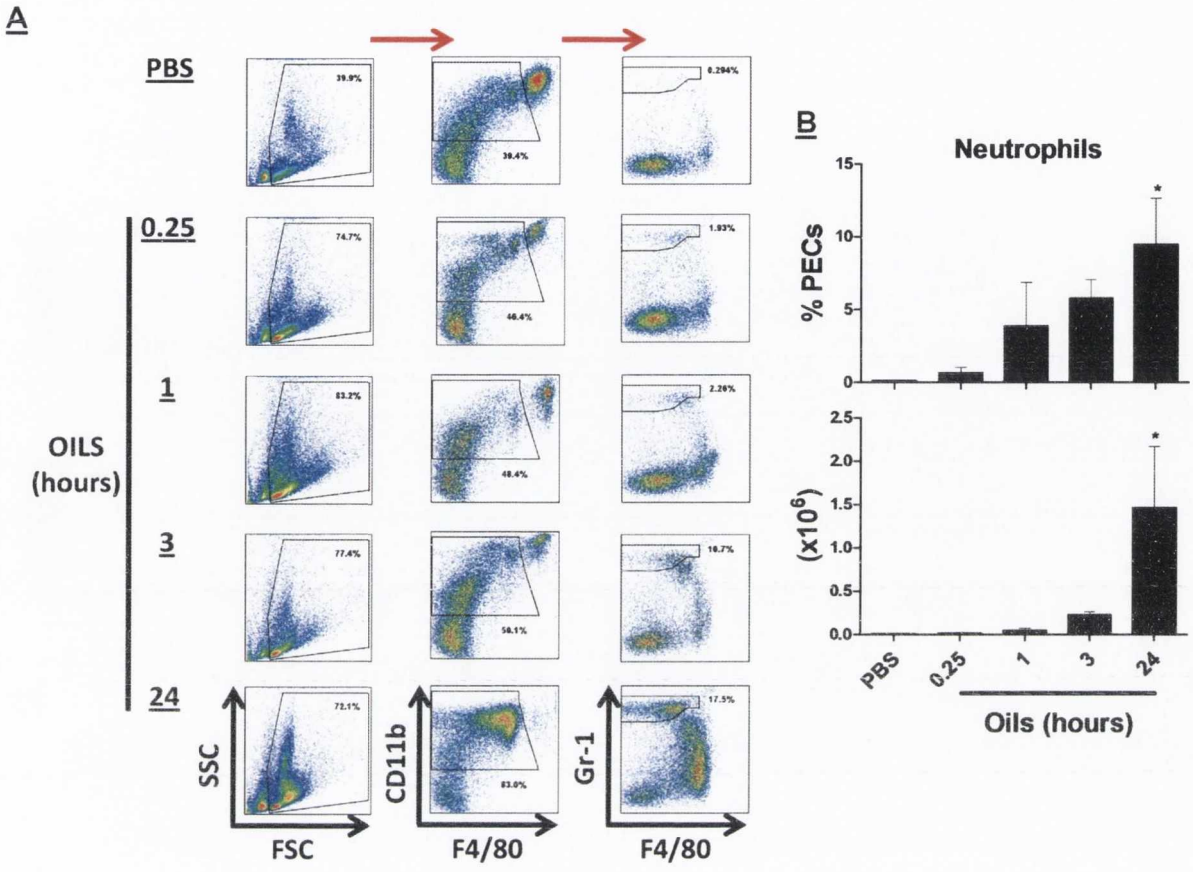

Figure 5.9 – Endogenous oils mediate neutrophil recruitment into the peritoneum. Female C57BL/6 mice were immunised as described in Figure 5.8. PECS were isolated and stained with antibodies specific for CD11b, F4/80 and Gr-1 (5 x 10^5 PECs/sample). The level of positive staining was quantified for each sample by flow cytometry. Neutrophils were identified ($CD11b^{inter}$ F4/80$^-$ Gr-1^{high}) and are represented in (A) dot plot and (B) bar graph format. Dot plots are shown as a single representative population from each treatment group and are indicative of the gating strategy employed. Bar graphs represent mean (+ SEM) for 3 mice per experimental group. Versus PBS, * $p<0.05$.

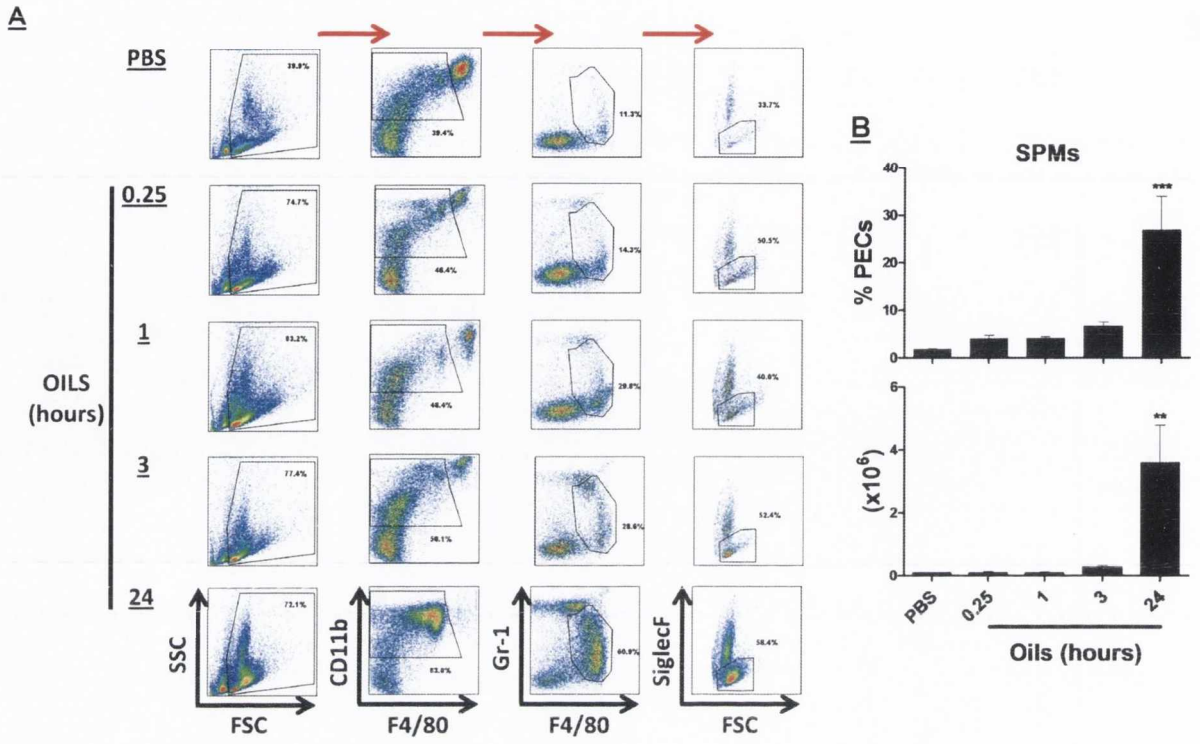

Figure 5.10 – Small peritoneal macrophages infiltrate the peritoneum following injection with endogenous oils. Female C57BL/6 mice were immunised as described in Figure 5.8. PECs were isolated and stained with antibodies specific for CD11b, F4/80, Gr-1 and SiglecF (5 x 10^5 PECs/sample). The level of positive staining was quantified for each sample by flow cytometry. SPMs were identified (CD11b^{inter} F4/80^{inter} Gr-1$^{low/inter}$ SiglecF$^-$) and are represented in (A) dot plot and (B) bar graph format. Dot plots are shown as a single representative population from each treatment group and are indicative of the gating strategy employed. Bar graphs represent mean (+ SEM) for 3 mice per experimental group. Versus PBS, ** $p<0.01$, *** $p<0.001$.

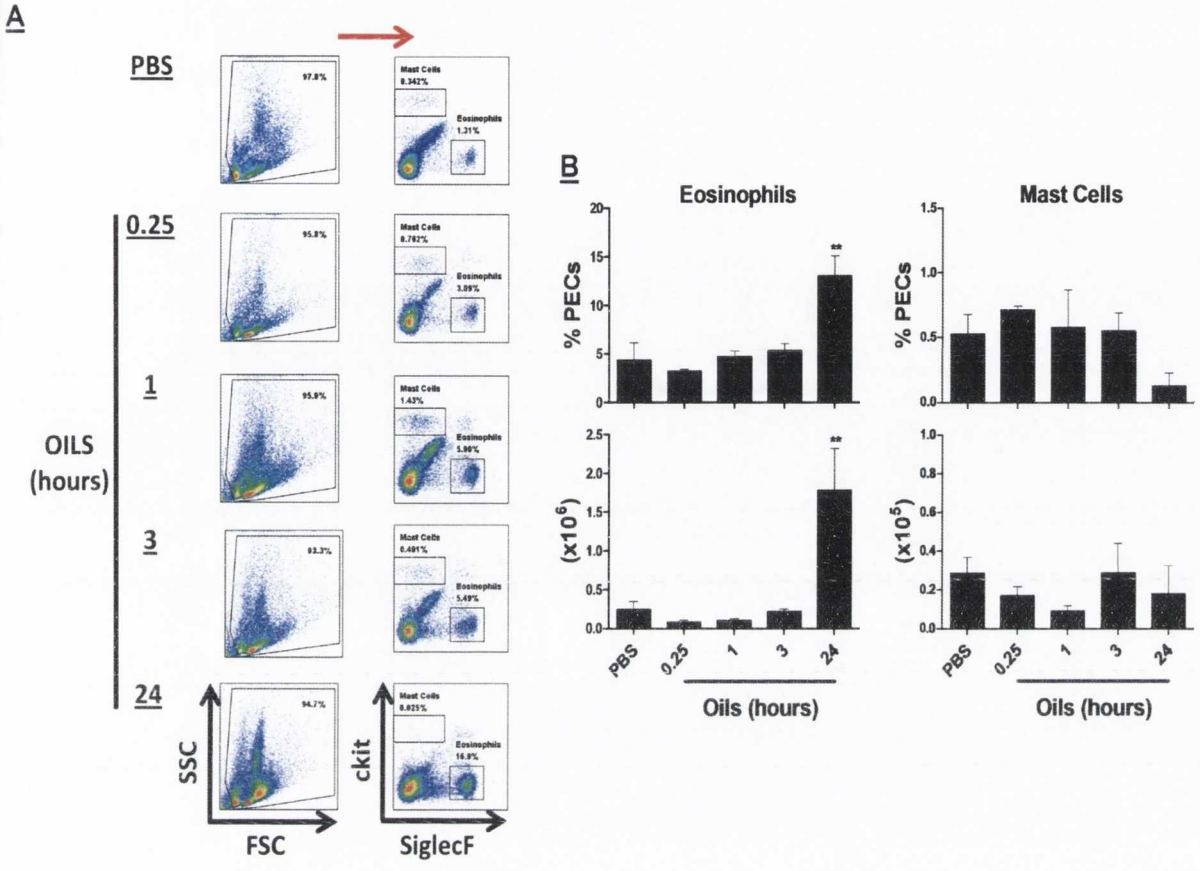

Figure 5.11 – Endogenous oils promote eosinophil recruitment into the peritoneum after 24 hours but deplete resident mast cells. Female C57BL/6 mice were immunised as described in Figure 5.8. PECs were isolated and stained with antibodies specific for SiglecF and ckit (5×10^5 PECs/sample). The level of positive staining was quantified for each sample by flow cytometry. Eosinophils ($SiglecF^+$ $ckit^-$) and mast cells ($SiglecF^-$ $ckit^+$) were identified and are represented in (A) dot plot and (B) bar graph format. Dot plots are shown as a single representative population from each treatment group and are indicative of the gating strategy employed. Bar graphs represent mean (+ SEM) for 3 mice per experimental group. Versus PBS, ** $p<0.01$.

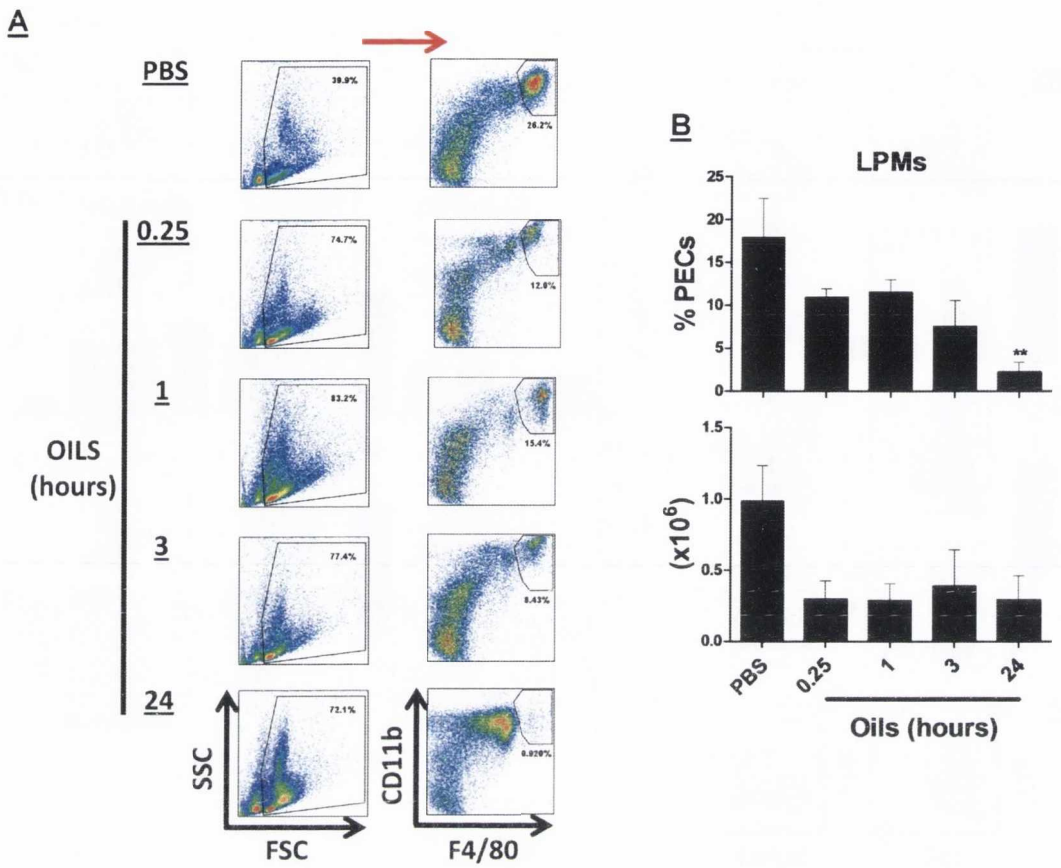

Figure 5.12 – Endogenous oils deplete resident large peritoneal macrophages at the injection site. Female C57BL/6 mice were immunised as described in Figure 5.8. PECs were isolated and stained with antibodies specific for CD11b and F4/80 (5 x 10^5 PECs/sample). The level of positive staining was quantified for each sample by flow cytometry. LPMs were identified ($CD11b^{high}$ $F4/80^{high}$) and are represented in (A) dot plot and (B) bar graph format. Dot plots are shown as a single representative population from each treatment group and are indicative of the gating strategy employed. Bar graphs represent mean (+ SEM) for 3 mice per experimental group. Versus PBS, ** $p<0.01$.

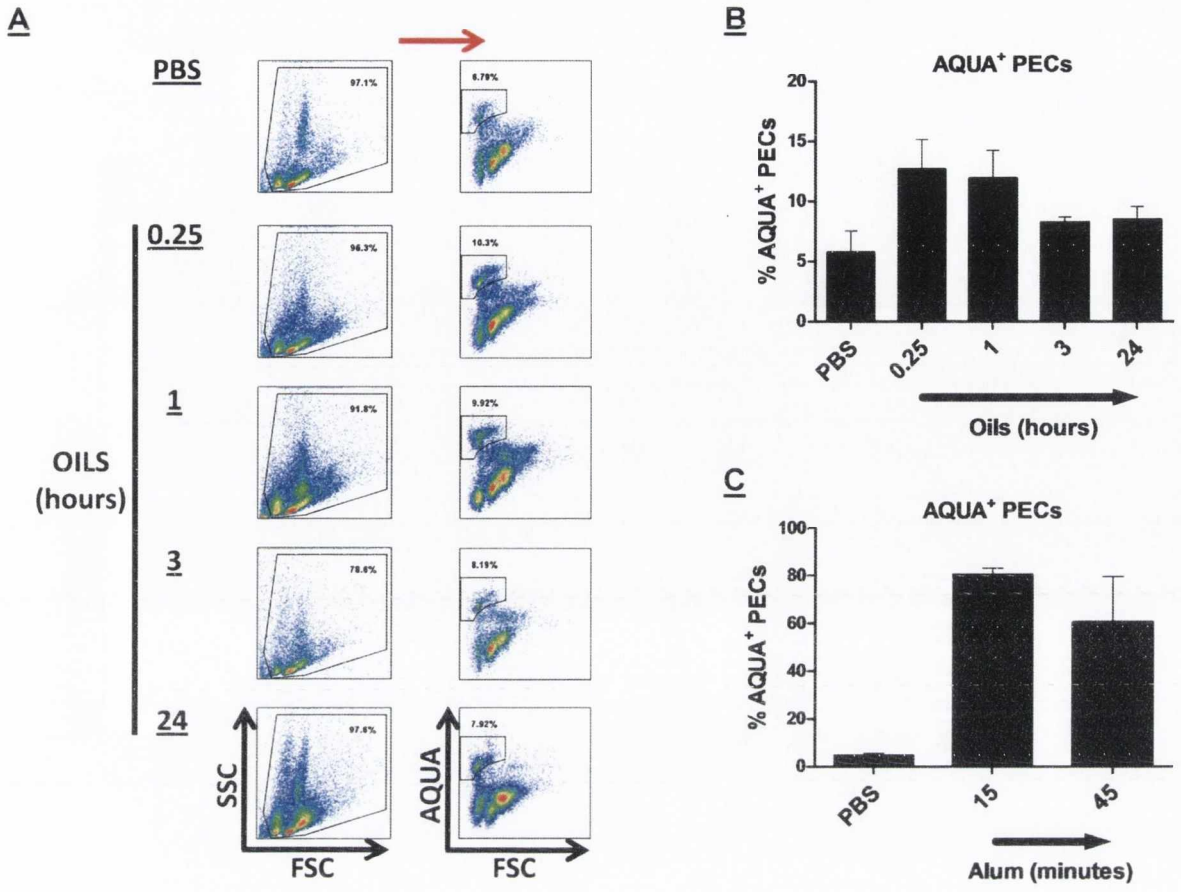

Figure 5.13 – Endogenous oils are only moderately toxic to PECs *in vivo*. Female C57BL/6 mice were immunised as described in Figure 5.8. PECS were isolated and stained with AQUA (5 x 10^5 PECs/sample). The level of AQUA staining was quantified for each sample by flow cytometry. Cell death is expressed as the number of PECs that have stained positive for AQUA as a percentage of the total number of PECs and is represented in (A) dot plot and (B) bar graph format. Dot plots are shown as a single representative population from each treatment group and are indicative of the gating strategy employed. Bar graph represents mean percentage of $AQUA^+$ PECs (+ SEM) for 3 mice per experimental group. (C) Female C57BL/6 mice were immunised i.p. with PBS (200µl/mouse) as a control or alum (1mg/mouse in 200µl volume). This experiment was performed by Ewa Oleszycka of the Adjuvant Research Group in the School of Biochemistry and Immunology, TCD. The mice were sacrificed after 15 minutes and PECs were isolated. Cell death was determined as described above and is expressed in bar graph format.

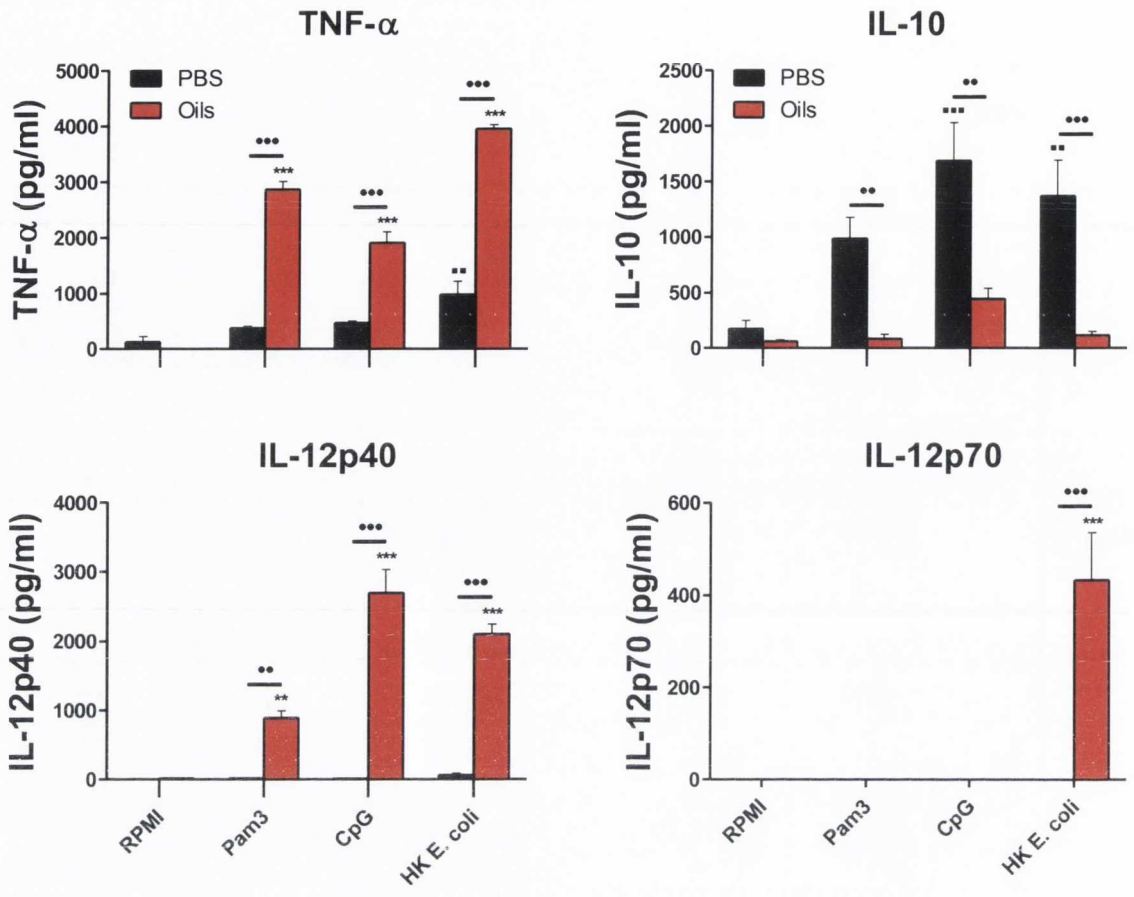

Figure 5.14 – Endogenous oils modulate the cytokine profile of PECs following *ex vivo* restimulation with PRR agonists. Female C57BL/6 mice were immunised i.p. with PBS (10µl/mouse) or endogenous oils (10µl/mouse). The mice were sacrificed 24 hours later and PECs were isolated. PECs were restimulated with RPMI, Pam3 (5µg/ml), CpG (5µg/ml) or HK *E. coli* (10 *E. coli* : 1 PEC). After 24 hours, supernatants were collected and analysed for the cytokines TNF-α, IL-10, IL-12p40 and IL-12p70 by ELISA. Results are mean cytokine concentrations (+ SEM) for 4 mice per experimental group tested individually in triplicate. Versus PECs from mice injected with endogenous oils and restimulated with RPMI, ** $p<0.01$, *** $p<0.001$. Versus PECs from mice injected with PBS and restimulated with RPMI, ▪▪ $p<0.01$, ▪▪▪ $p<0.001$. PECs from mice injected with endogenous oils versus PECs from mice injected with PBS for corresponding stimulus, •• $p<0.01$, ••• $p<0.001$.

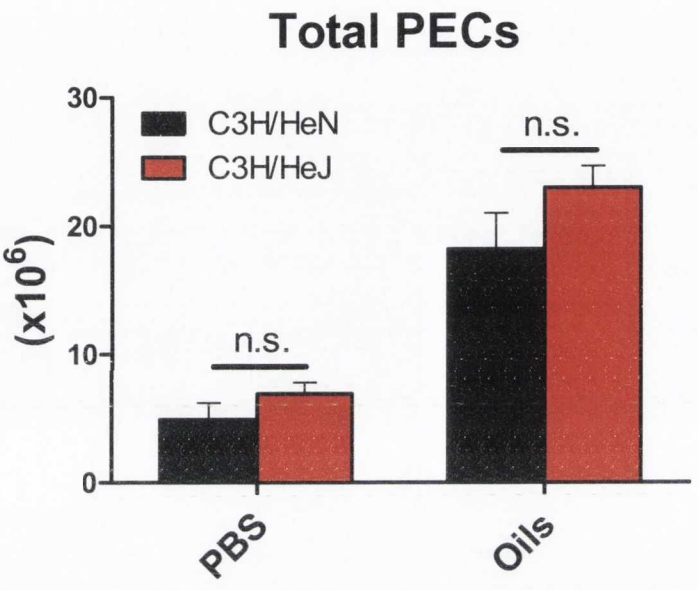

Figure 5.15 – TLR4 is not required for increased PEC numbers following injection with endogenous oils. Female C3H/HeN and C3H/HeJ mice were immunised i.p. with PBS (10µl/mouse) as a control or endogenous oils (10µl/mouse). The mice were sacrificed 24 hours later and PECs were isolated. PEC numbers were determined using a Glasstic cell counter slide with grids following trypan blue staining. Results are mean PEC number (+ SEM) for 4 mice per experimental group.

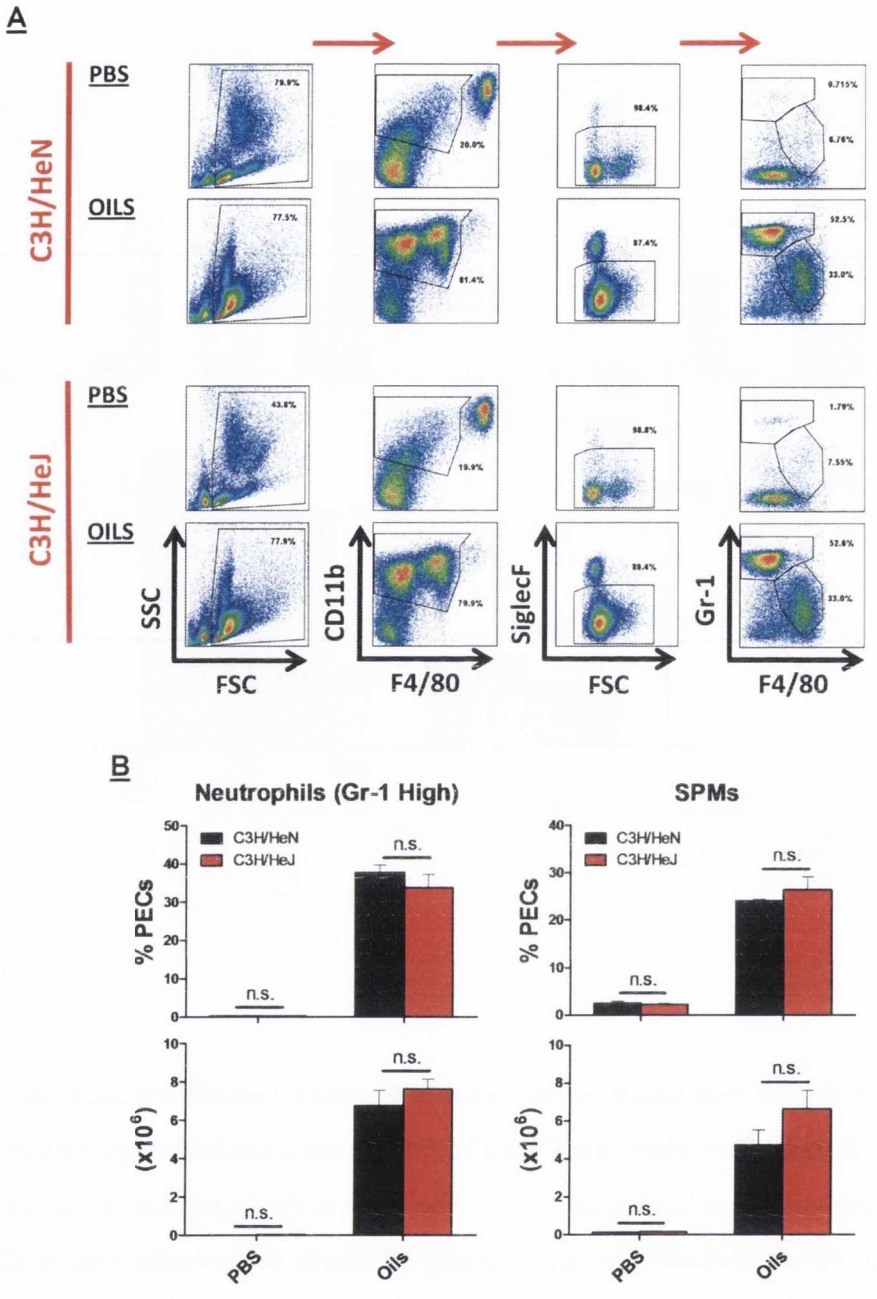

Figure 5.16 – Neutrophil and small peritoneal macrophage recruitment in response to endogenous oils is independent of TLR4. Female C3H/HeN and C3H/HeJ mice were immunised as described in Figure 5.15. PECS were isolated and stained with antibodies specific for CD11b, F4/80, SiglecF and Gr-1 (5 x 10^5 PECs/sample). The level of positive staining was quantified for each sample by flow cytometry. Neutrophils (CD11b^{inter} SiglecF$^-$ F4/80$^-$ Gr-1^{high}) and SPMs (CD11b^{inter} SiglecF$^-$ F4/80^{inter} Gr-1$^{low/inter}$) were identified and are represented in (A) dot plot and (B) bar graph format. Dot plots are shown as a single representative population from each treatment group and are indicative of the gating strategy employed. Bar graphs represent mean (+ SEM) for 4 mice per experimental group.

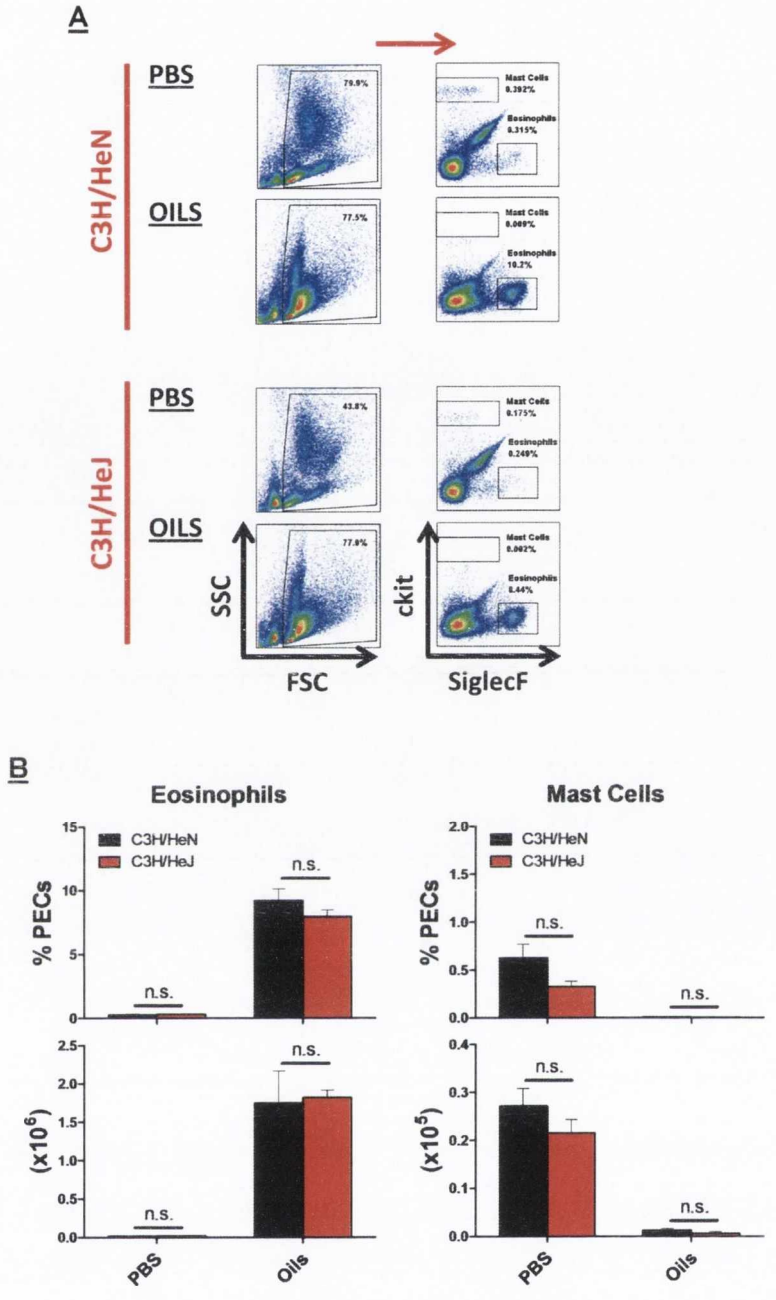

Figure 5.17 – Eosinophil recruitment and mast cell depletion in response to endogenous oils is TLR4-independent. Female C57BL/6 mice were immunised as described in Figure 5.15. PECs were isolated and stained with antibodies specific for SiglecF and ckit (5 x 10^5 PECs/sample). The level of positive staining was quantified for each sample by flow cytometry. Eosinophils (SiglecF$^+$ ckit$^-$) and mast cells (SiglecF$^-$ ckit$^+$) were identified and are represented in (A) dot plot and (B) bar graph format. Dot plots are shown as a single representative population from each treatment group and are indicative of the gating strategy employed. Bar graphs represent mean (+ SEM) for 4 mice per experimental group.

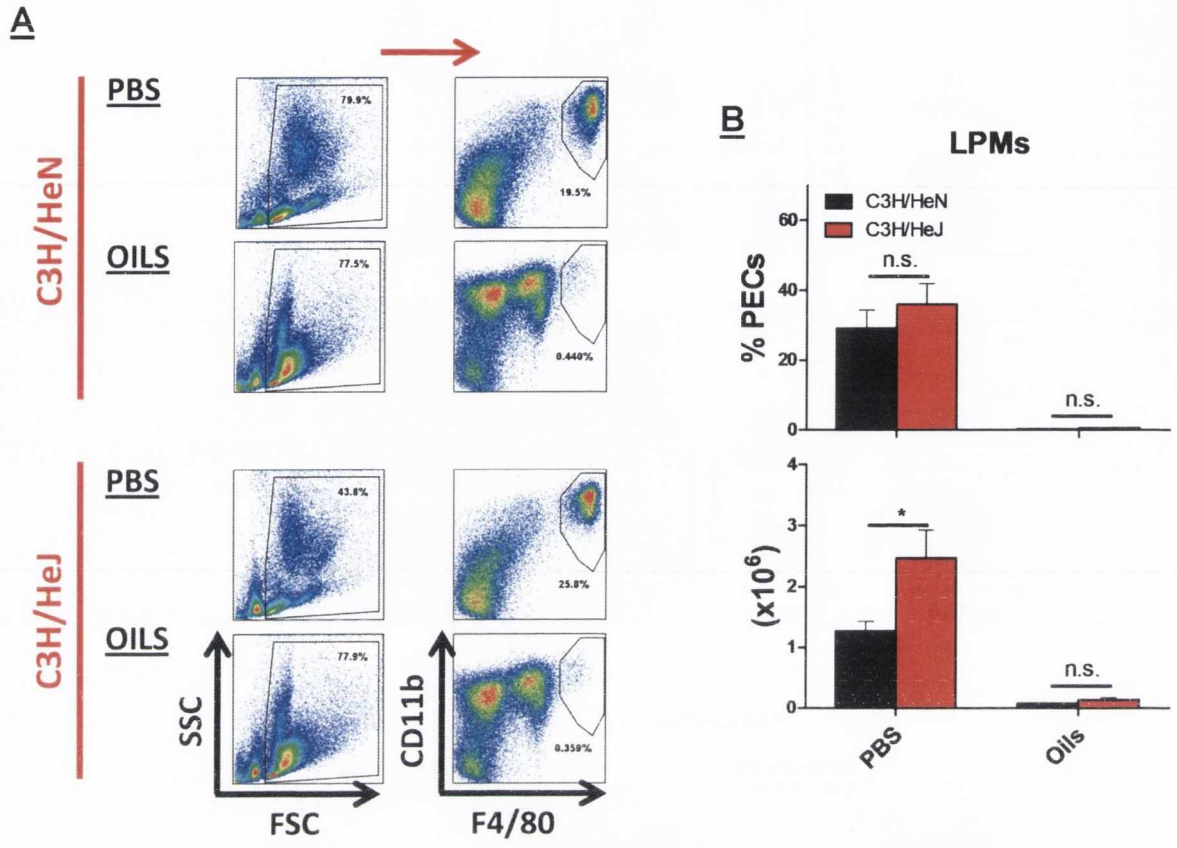

Figure 5.18 – Endogenous oils diminish resident large peritoneal macrophages in both C3H/HeN and C3H/HeJ mice. Female C57BL/6 mice were immunised as described in Figure 5.15. PECs were isolated and stained with antibodies specific for CD11b and F4/80 (5 x 10^5 PECs/sample). The level of positive staining was quantified for each sample by flow cytometry. LPMs were identified ($CD11b^{high}$ $F4/80^{high}$) and are represented in (A) dot plot and (B) bar graph format. Dot plots are shown as a single representative population from each treatment group and are indicative of the gating strategy employed. Bar graphs represent mean (+ SEM) for 4 mice per experimental group. C3H/HeJ versus C3H/HeN for corresponding treatment, n.s., not significant, * $p<0.05$.

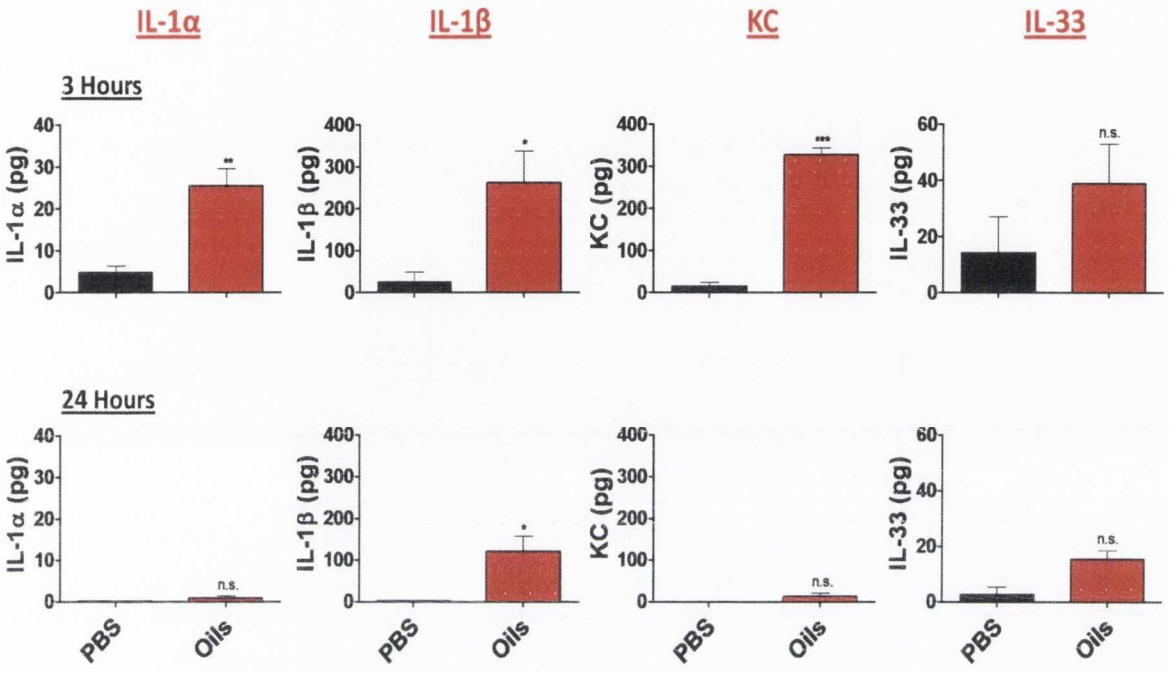

Figure 5.19 – Endogenous oils increase levels of IL-1α, IL-1β and KC in the peritoneum after 3 hours. Female C57BL/6 mice were immunised i.p. with PBS (10µl/mouse) as a control or endogenous oils (10µl/mouse). The mice were sacrificed either 3 hours or 24 hours later. PECs were isolated and PEC supernatants were collected. PEC supernatants were tested for the cytokines IL-1α, IL-1β, KC and IL-33 by ELISA. Results are mean cytokine concentrations (+ SEM) for 3 mice per experimental group. Versus PBS, n.s., not significant, * $p<0.05$, ** $p<0.01$, *** $p<0.001$.

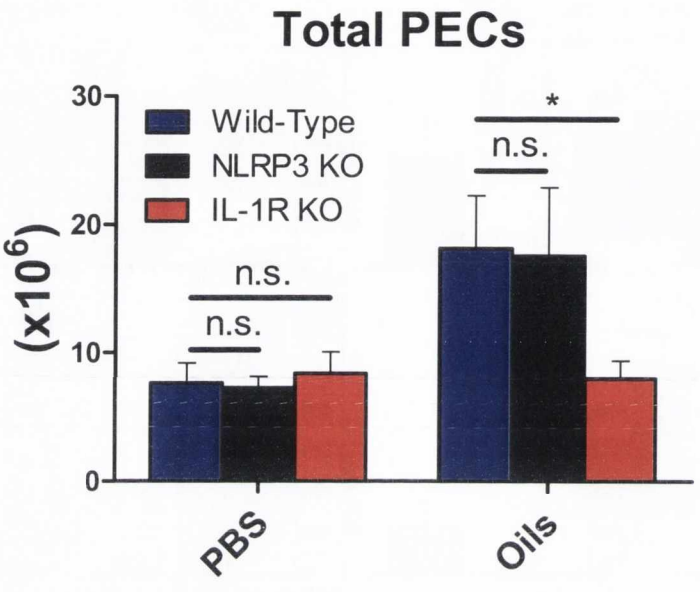

Figure 5.20 – Endogenous oils mediate cell recruitment into the peritoneum through a process dependent on the IL-1R. Female wild-type C57BL/6, NLRP3 KO and IL-1R KO mice were immunised i.p. with PBS (10µl/mouse) as a control or endogenous oils (10µl/mouse). The mice were sacrificed 24 hours later and PECs were isolated. PEC numbers were determined using a Glasstic cell counter slide with grids following trypan blue staining. Results are mean PEC number (+ SEM) for 4 mice per experimental group. Versus wild-type for corresponding treatment, n.s., not significant, * $p<0.05$.

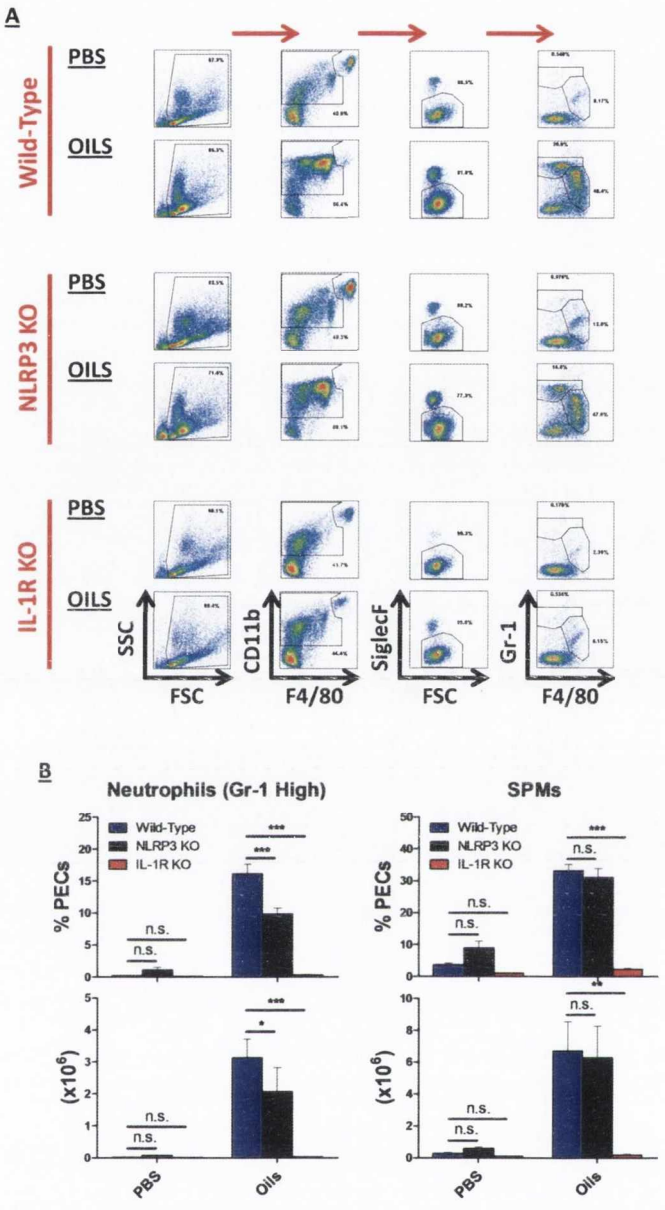

Figure 5.21 – Neutrophil and small peritoneal macrophage recruitment in response to endogenous oils is entirely dependent on the IL-1R. Female wild-type C57BL/6, NLRP3 KO and IL-1R KO mice were immunised as described in Figure 5.20. PECS were isolated and stained with antibodies specific for CD11b, F4/80, SiglecF and Gr-1 (5 x 10^5 PECs/sample). The level of positive staining was quantified for each sample by flow cytometry. Neutrophils ($CD11b^{inter}$ $SiglecF^-$ $F4/80^-$ $Gr\text{-}1^{high}$) and SPMs ($CD11b^{inter}$ $SiglecF^-$ $F4/80^{inter}$ $Gr\text{-}1^{low/inter}$) were identified and are represented in (A) dot plot and (B) bar graph format. Dot plots are shown as a single representative population from each treatment group and are indicative of the gating strategy employed. Bar graphs represent mean (+ SEM) for 4 mice per experimental group. Versus wild-type for corresponding treatment, n.s., not significant, * $p<0.05$, *** $p<0.001$.

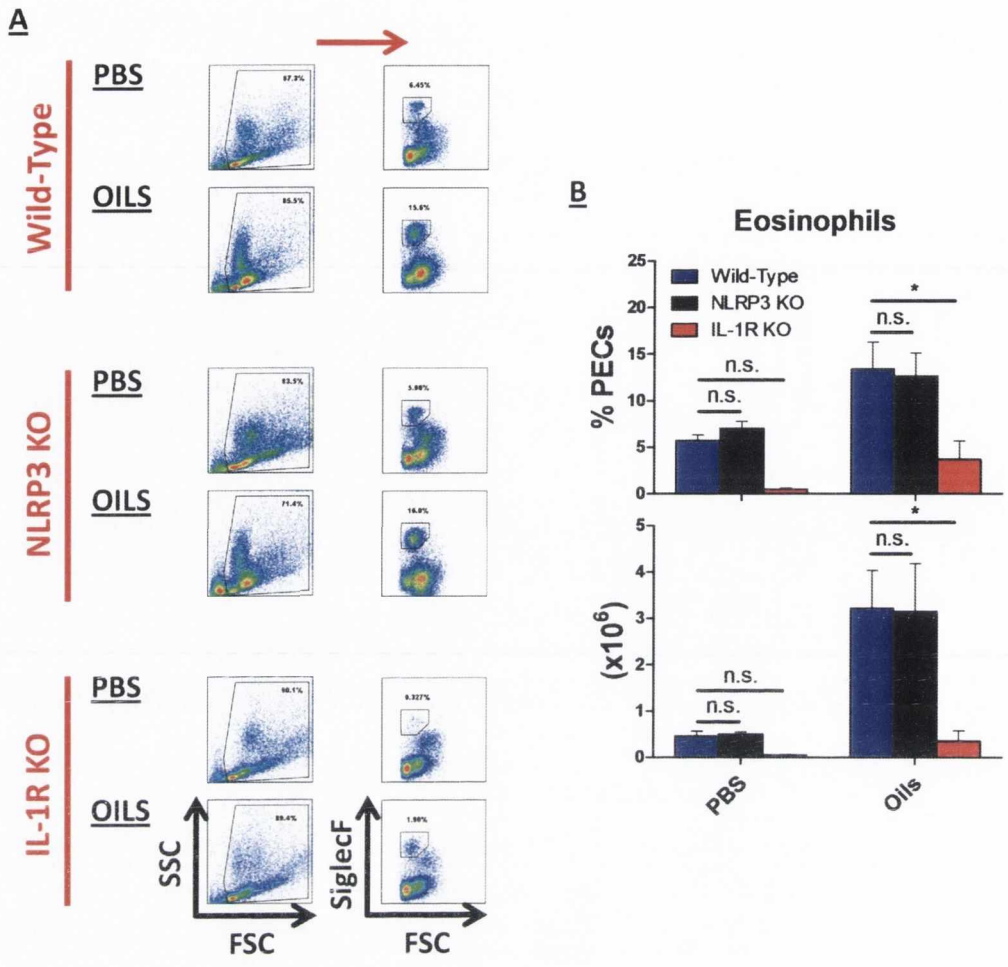

Figure 5.22 – Eosinophil recruitment following injection with endogenous oils is independent of NLRP3. Female wild-type C57BL/6, NLRP3 KO and IL-1R KO mice were immunised as described in Figure 5.20. PECs were isolated and stained with an antibody specific for SiglecF (5 x 10^5 PECs/sample). The level of positive staining was quantified for each sample by flow cytometry. Eosinophils ($SiglecF^+$) were identified and are represented in (A) dot plot and (B) bar graph format. Dot plots are shown as a single representative population from each treatment group and are indicative of the gating strategy employed. Bar graphs represent mean (+ SEM) for 4 mice per experimental group. Versus wild-type for corresponding treatment, n.s., not significant, * $p<0.05$.

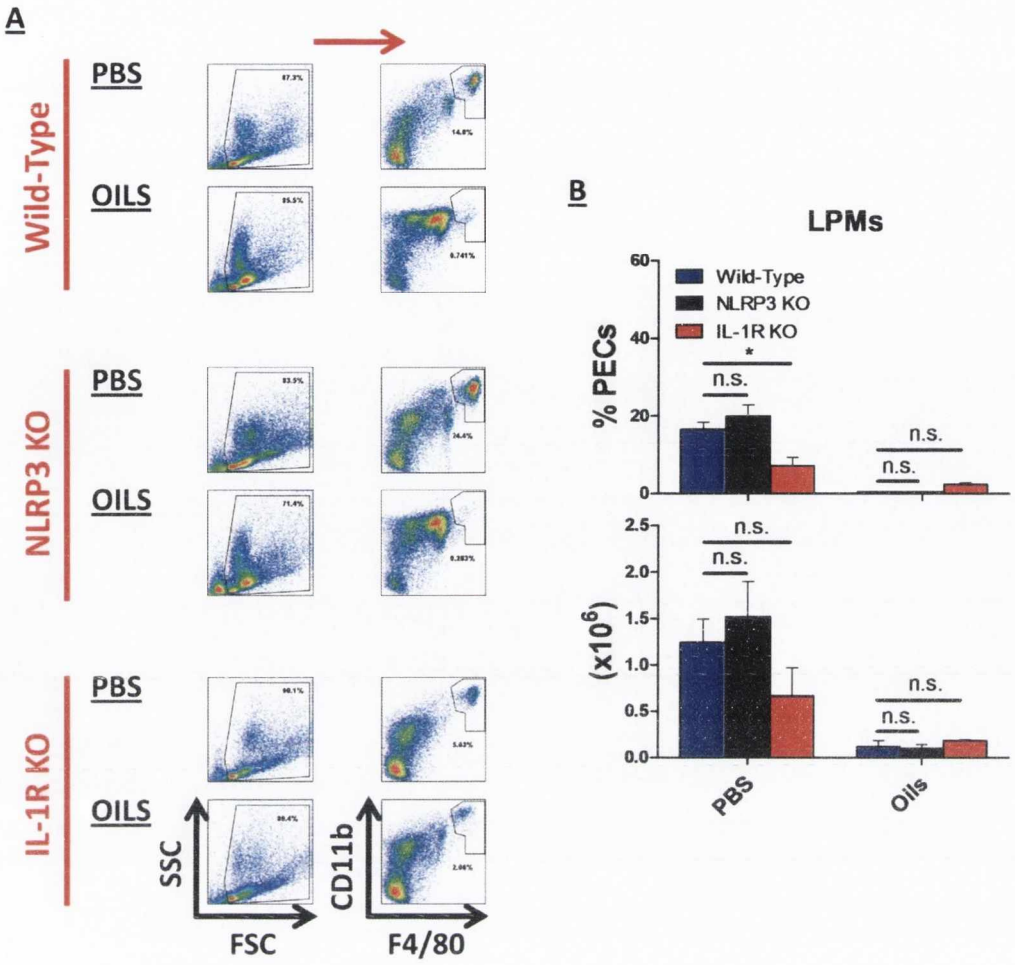

Figure 5.23 – Depletion of resident large peritoneal macrophages by endogenous oils is independent of NLRP3. Female wild-type C57BL/6, NLRP3 KO and IL-1R KO mice were immunised as described in Figure 5.20. PECs were isolated and stained with antibodies specific for CD11b and F4/80 (5 x 10^5 PECs/sample). The level of positive staining was quantified for each sample by flow cytometry. LPMs were identified ($CD11b^{high}$ $F4/80^{high}$) and are represented in (A) dot plot and (B) bar graph format. Dot plots are shown as a single representative population from each treatment group and are indicative of the gating strategy employed. Bar graphs represent mean (+ SEM) for 4 mice per experimental group. Versus wild-type for corresponding treatment, n.s., not significant, * $p<0.05$.

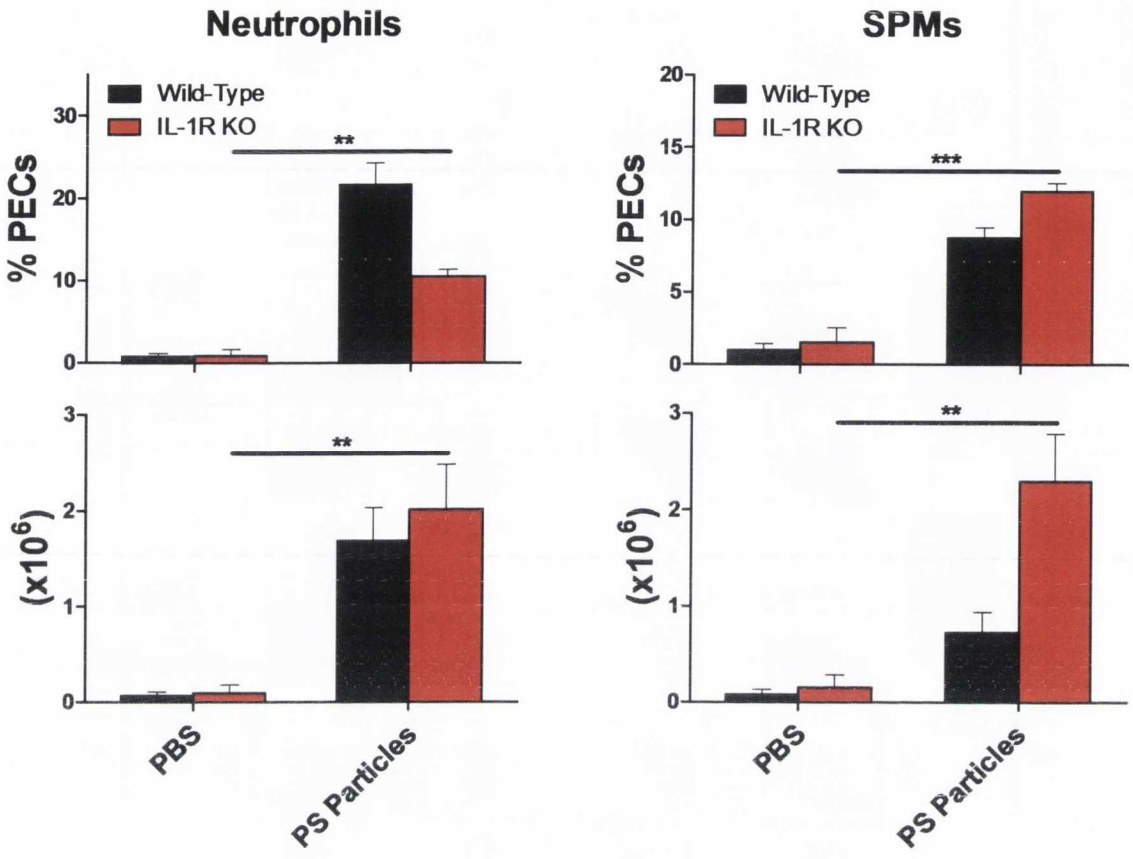

Figure 5.24 – IL-1R KO mice are capable of recruiting neutrophils and small peritoneal macrophages. Female wild-type C57BL/6 and IL-1R KO mice were immunised i.p. with PBS (200µl) or 10µm PS particles (4mg/mouse in 200µl volume). The mice were sacrificed 24 hours later. PECS were isolated and stained with antibodies specific for CD11b, F4/80, SiglecF and Gr-1 (5 x 10^5 PECs/sample). The level of positive staining was quantified for each sample by flow cytometry. Neutrophils ($CD11b^{inter}$ $SiglecF^-$ $F4/80^-$ $Gr\text{-}1^{high}$) and SPMs ($CD11b^{inter}$ $SiglecF^-$ $F4/80^{inter}$ $Gr\text{-}1^{low/inter}$) were identified and are shown in bar graph format. Bar graphs represent mean (+ SEM) for 3 mice per experimental group. IL-1R KO mice injected with PS particles versus IL-1R KO mice injected with PBS, ** $p<0.01$, *** $p<0.001$. This experiment was performed by Claire Hearnden of the Adjuvant Research Group in the School of Biochemistry and Immunology, TCD.

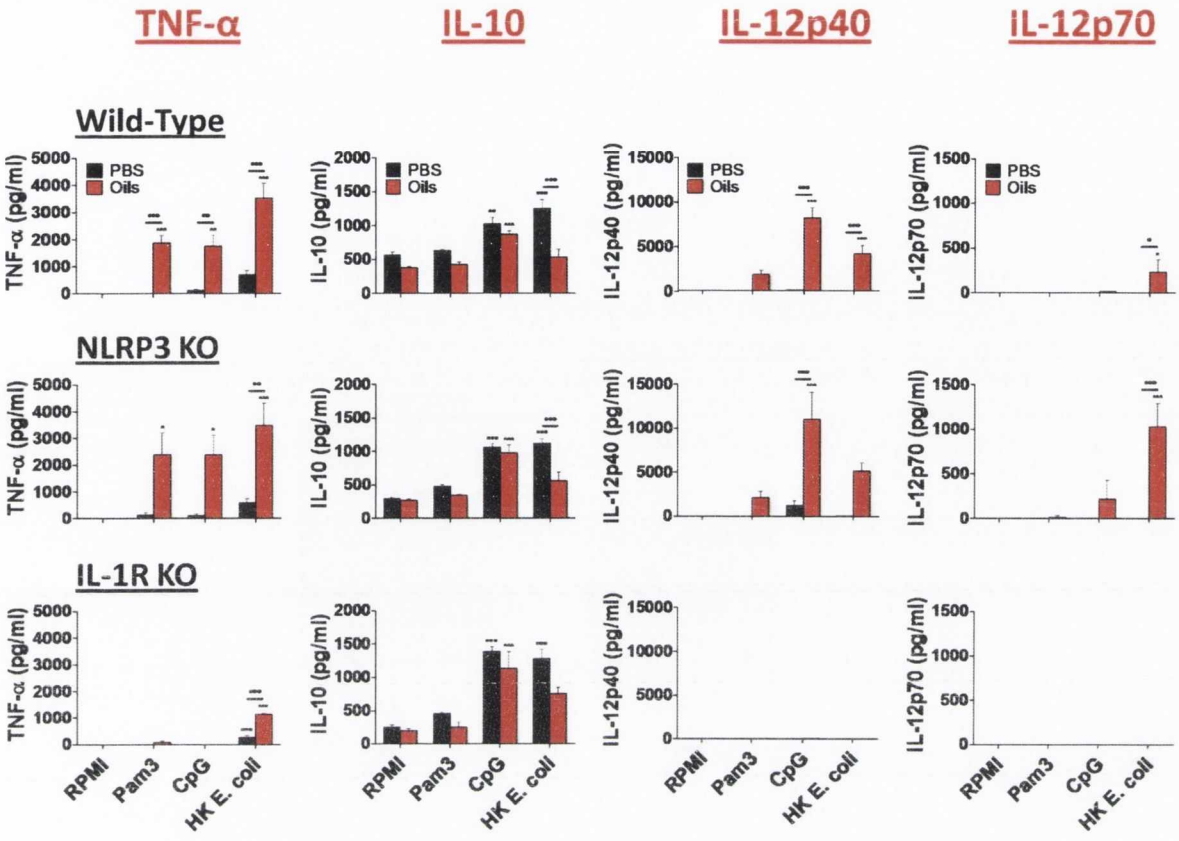

Figure 5.25 – The IL-1R is required for modulation of the cytokine profile of PECs following injection with endogenous oils. Female wild-type C57BL/6, NLRP3 KO and IL-1R KO mice were immunised as described in Figure 5.20. The mice were sacrificed 24 hours later and PECs were isolated. PECs were restimulated with RPMI, Pam3 (5μg/ml), CpG (5μg/ml) or HK *E. coli* (10 *E. coli* : 1 PEC). After 24 hours, supernatants were collected and analysed for the cytokines TNF-α, IL-10, IL-12p40 and IL-12p70 by ELISA. Results are mean cytokine concentrations (+ SEM) for 4 mice per experimental group tested individually in triplicate Versus PECs from mice injected with endogenous oils and restimulated with RPMI, * $p<0.05$, ** $p<0.01$, *** $p<0.001$. Versus PECs from mice injected with PBS and restimulated with RPMI, ▪▪ $p<0.01$, ▪▪▪ $p<0.001$. PECs from mice injected with endogenous oils versus PECs from mice injected with PBS at corresponding stimulus, •• $p<0.01$, ••• $p<0.001$.

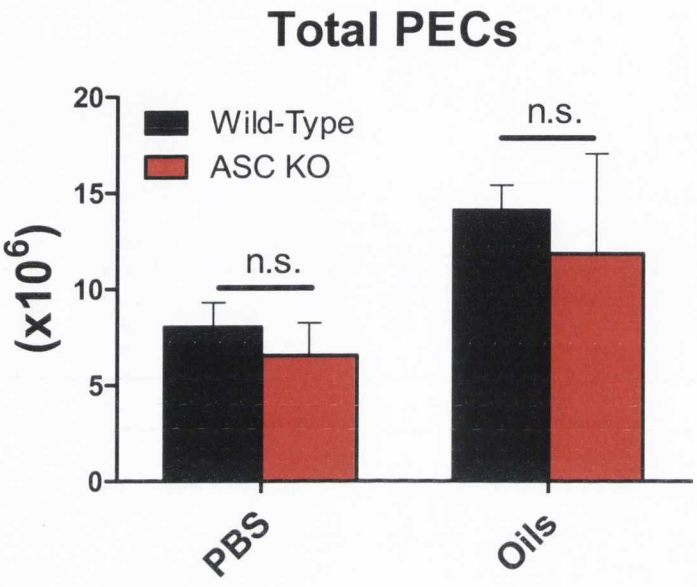

Figure 5.26 – ASC is not required for increased PEC numbers following injection with endogenous oils. Female wild-type C57BL/6 and ASC KO mice were immunised i.p. with PBS (10µl/mouse) as a control or endogenous oils (10µl/mouse). The mice were sacrificed 24 hours later and PECs were isolated. PEC numbers were determined using a Glasstic cell counter slide with grids following trypan blue staining. Results are mean PEC number (+ SEM) for 4 mice per experimental group.

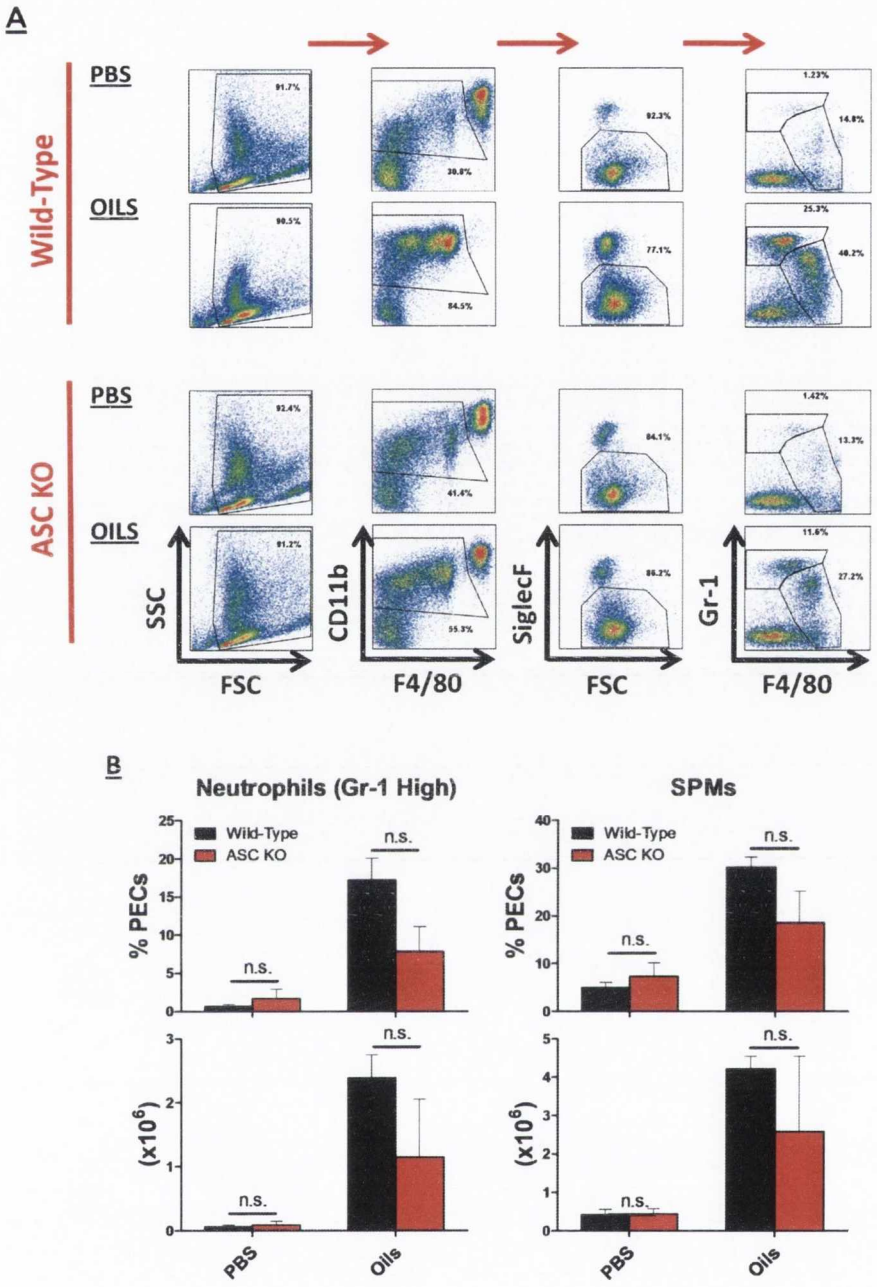

Figure 5.27 – Neutrophil and small peritoneal macrophage recruitment in response to endogenous oils is partially dependent on ASC. Female C57BL/6 and ASC KO mice were immunised as described in Figure 5.26. PECS were isolated and stained with antibodies specific for CD11b, F4/80, SiglecF and Gr-1 (5 x 10^5 PECs/sample). The level of positive staining was quantified for each sample by flow cytometry. Neutrophils ($CD11b^{inter}$ $SiglecF^-$ $F4/80^-$ $Gr\text{-}1^{high}$) and SPMs ($CD11b^{inter}$ $SiglecF^-$ $F4/80^{inter}$ $Gr\text{-}1^{low/inter}$) were identified and are represented in (A) dot plot and (B) bar graph format. Dot plots are shown as a single representative population from each treatment group and are indicative of the gating strategy employed. Bar graphs represent mean (+ SEM) for 4 mice per experimental group.

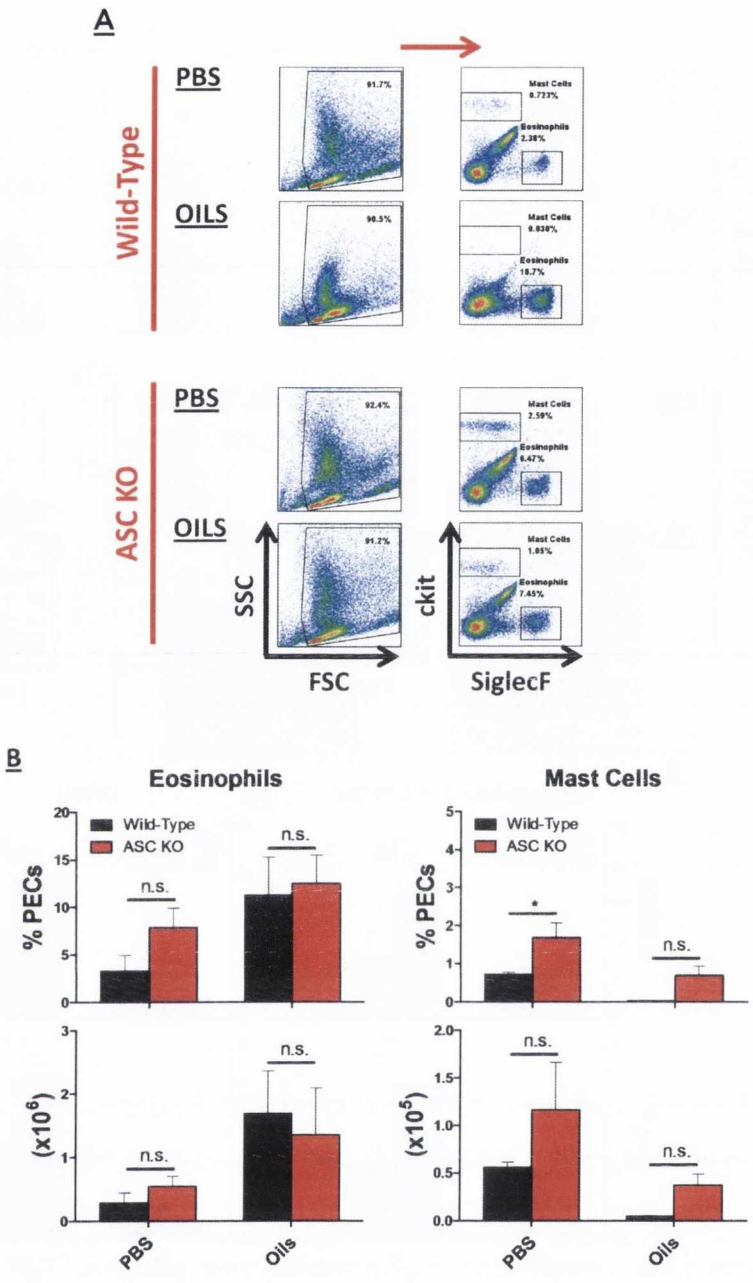

Figure 5.28 – Eosinophil recruitment and mast cell depletion in response to endogenous oils is independent of ASC. Female C57BL/6 mice were immunised as described in Figure 5.26. PECs were isolated and stained with antibodies specific for SiglecF and ckit (5 x 10^5 PECs/sample). The level of positive staining was quantified for each sample by flow cytometry. Eosinophils (SiglecF$^+$ ckit$^-$) and mast cells (SiglecF$^-$ ckit$^+$) were identified and are represented in (A) dot plot and (B) bar graph format. Dot plots are shown as a single representative population from each treatment group and are indicative of the gating strategy employed. Bar graphs represent mean (+ SEM) for 4 mice per experimental group.

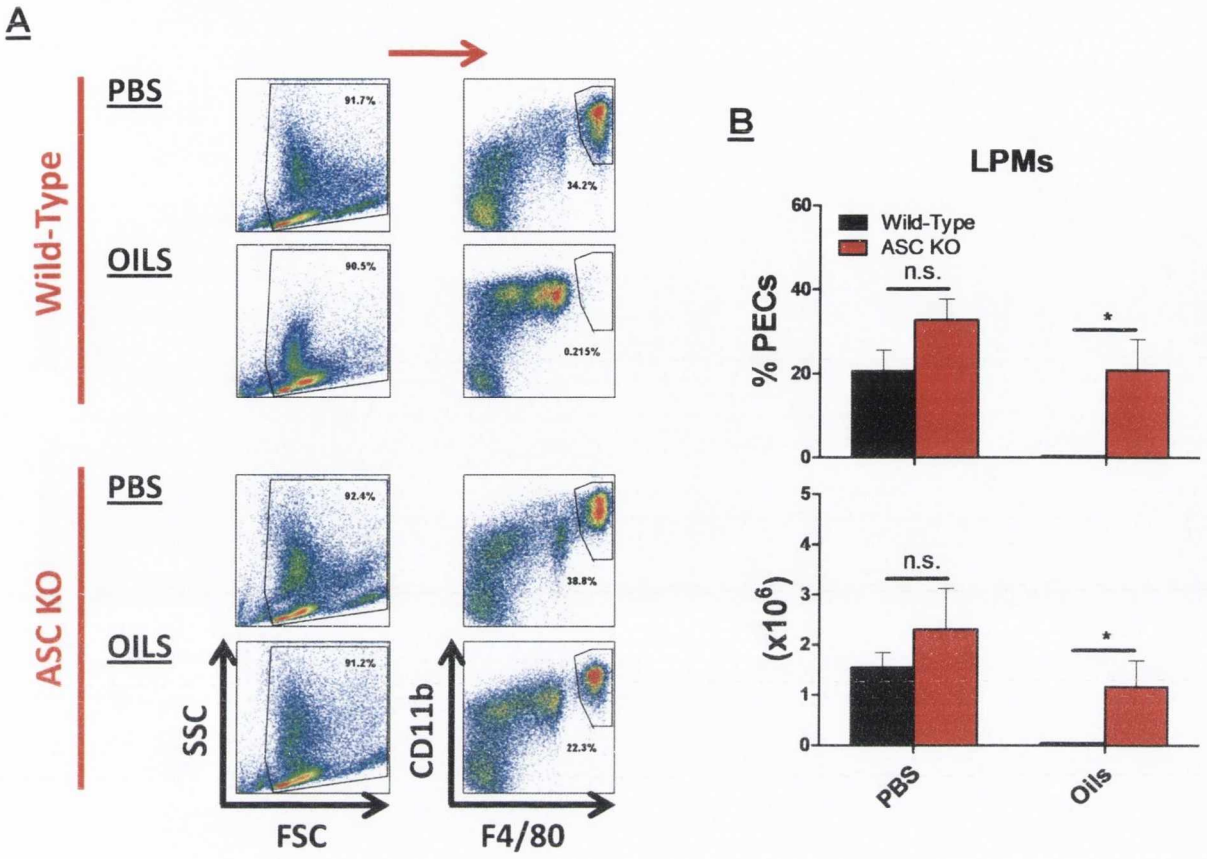

Figure 5.29 – Depletion of resident large peritoneal macrophages by endogenous oils is ASC-dependent. Female wild-type C57BL/6, NLRP3 KO and IL-1R KO mice were immunised as described in Figure 5.26. PECs were isolated and stained with antibodies specific for CD11b and F4/80 (5 x 10^5 PECs/sample). The level of positive staining was quantified for each sample by flow cytometry. LPMs were identified ($CD11b^{high}$ $F4/80^{high}$) and are represented in (A) dot plot and (B) bar graph format. Dot plots are shown as a single representative population from each treatment group and are indicative of the gating strategy employed. Bar graphs represent mean (+ SEM) for 4 mice per experimental group. C3H/HeJ versus C3H/HeN for corresponding treatment, n.s., not significant, * $p<0.05$.

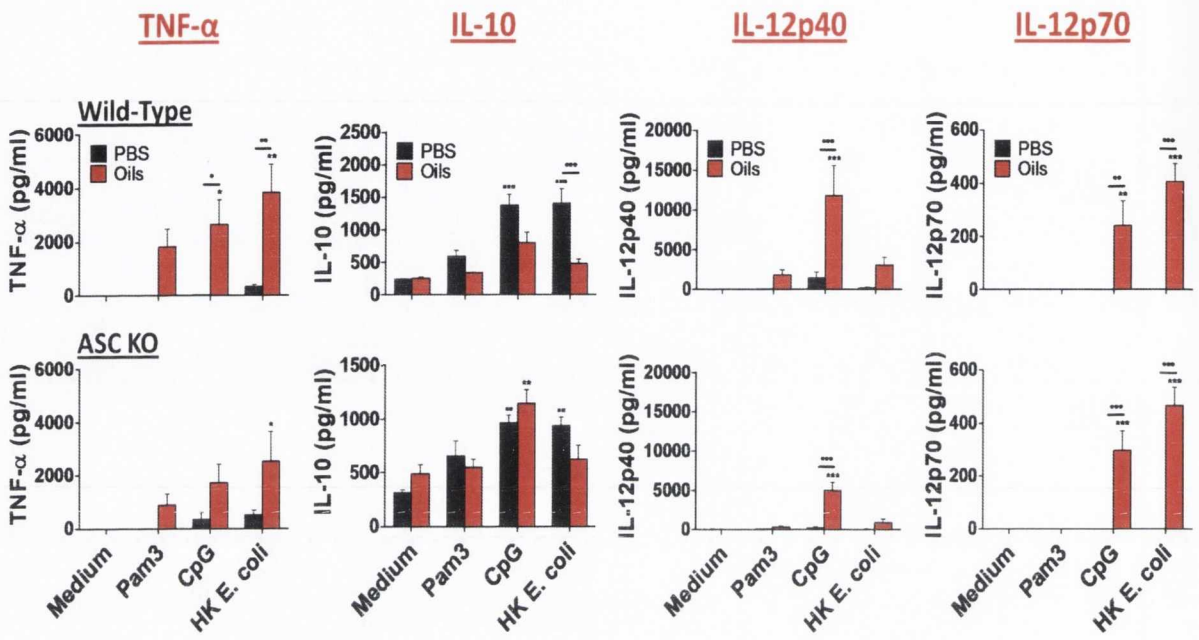

Figure 5.30 – Endogenous oils diminish IL-10 secretion by PECs derived from wild-type mice but not ASC KO mice following *ex vivo* restimulation with PRR agonists. Female wild-type C57BL/6, NLRP3 KO and IL-1R KO mice were immunised as described in Figure 5.26. The mice were sacrificed 24 hours later and PECs were isolated. PECs were restimulated with RPMI, Pam3 (5μg/ml), CpG (5μg/ml) or HK *E. coli* (10 *E. coli* : 1 PEC). After 24 hours, supernatants were collected and analysed for the cytokines TNF-α, IL-10, IL-12p40 and IL-12p70 by ELISA. Results are mean cytokine concentrations (+ SEM) for 4 mice per experimental group tested individually in triplicate Versus PECs from mice injected with endogenous oils and restimulated with RPMI, * $p<0.05$, ** $p<0.01$, *** $p<0.001$. Versus PECs from mice injected with PBS and restimulated with RPMI, ▪▪ $p<0.01$, ▪▪▪ $p<0.001$. PECs from mice injected with endogenous oils versus PECs from mice injected with PBS at corresponding stimulus, • $p<0.05$, •• $p<0.01$, ••• $p<0.001$.

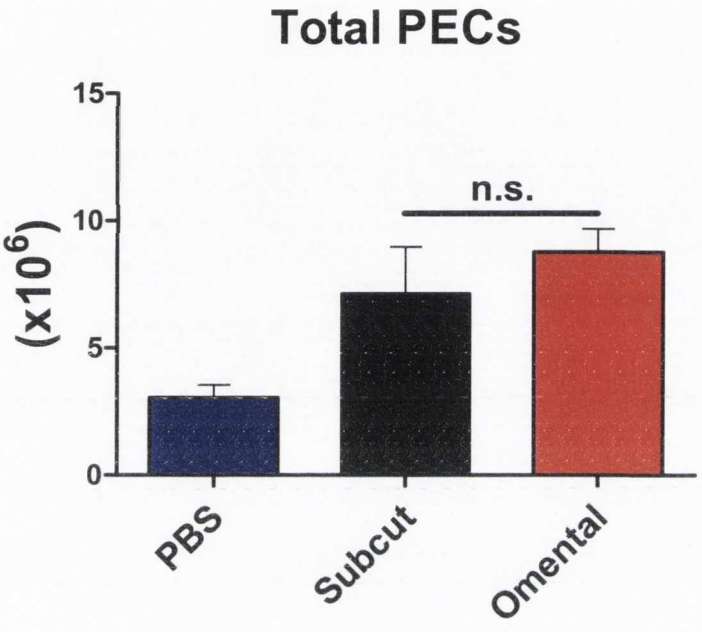

Figure 5.31 – Endogenous oils derived from subcutaneous adipocytes and omental adipocytes both increase total PEC numbers. Female C57BL/6 mice were immunised i.p. with PBS (10µl/mouse) as a control or endogenous oils derived from either subcutaneous adipocytes or omental adipocytes (10µl/mouse) from the same obese individual. The mice were sacrificed 24 hours later and PECs were isolated. PEC numbers were determined using a Glasstic cell counter slide with grids following trypan blue staining. Results are mean PEC number (+ SEM) for 3 mice per experimental group.

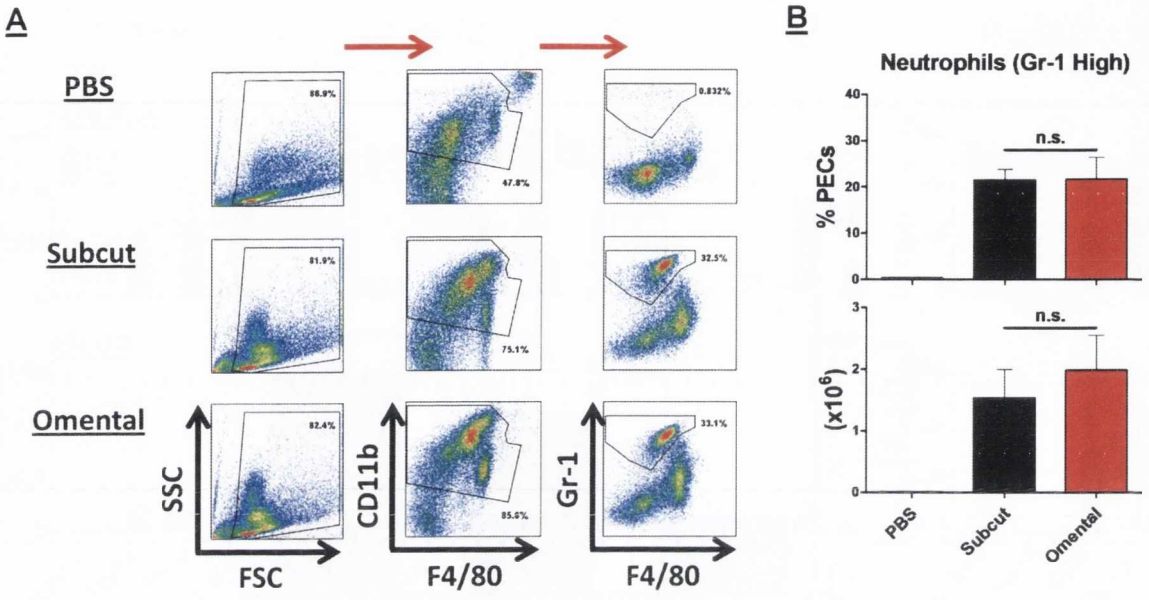

Figure 5.32 – Endogenous oils derived from subcutaneous adipocytes and omental adipocytes both mediate neutrophil recruitment into the peritoneum. Female C57BL/6 mice were immunised as described in Figure 5.31. PECS were isolated and stained with antibodies specific for CD11b, F4/80 and Gr-1 (5 x 10^5 PECs/sample). The level of positive staining was quantified for each sample by flow cytometry. Neutrophils were identified ($CD11b^{inter}$ $F4/80^-$ $Gr\text{-}1^{high}$) and are represented in (A) dot plot and (B) bar graph format. Dot plots are shown as a single representative population from each treatment group and are indicative of the gating strategy employed. Bar graphs represent mean (+ SEM) for 3 mice per experimental group.

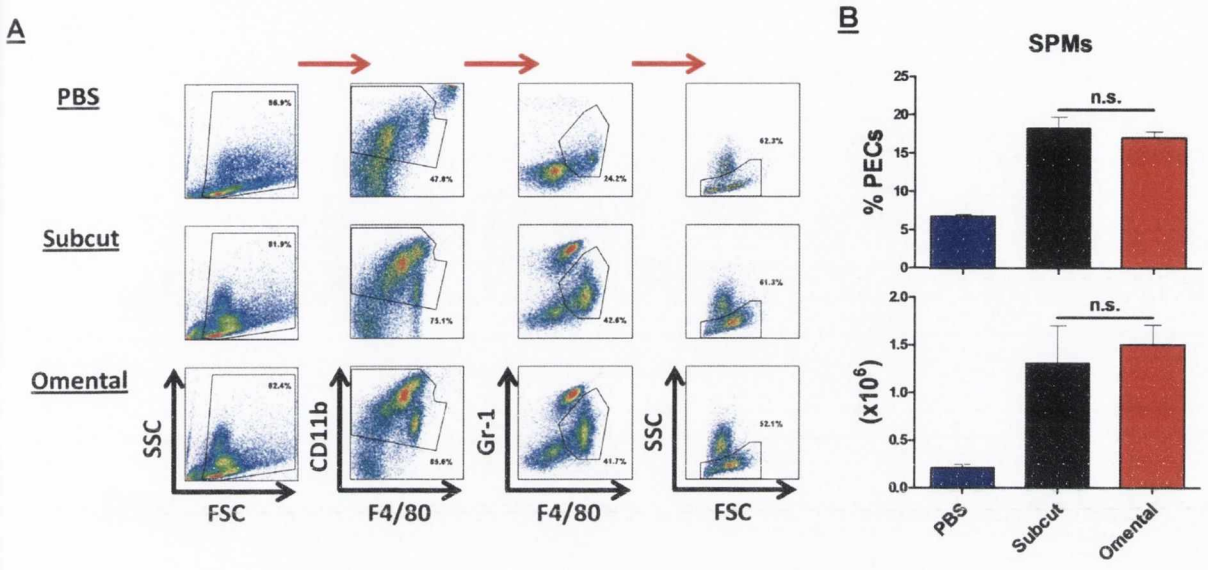

Figure 5.33 – There is no significant difference between endogenous oils derived from subcutaneous adipocytes and omental adipocytes in their ability to promote small peritoneal macrophage recruitment into the injection site. Female C57BL/6 mice were immunised as described in Figure 5.31. PECs were isolated and stained with antibodies specific for CD11b, F4/80 and Gr-1 (5 x 10^5 PECs/sample). The level of positive staining was quantified for each sample by flow cytometry. SPMs were identified (CD11b^{inter} F4/80^{inter} Gr-1$^{low/inter}$ SSc^{low}) and are represented in (A) dot plot and (B) bar graph format. Dot plots are shown as a single representative population from each treatment group and are indicative of the gating strategy employed. Bar graphs represent mean (+ SEM) for 3 mice per experimental group.

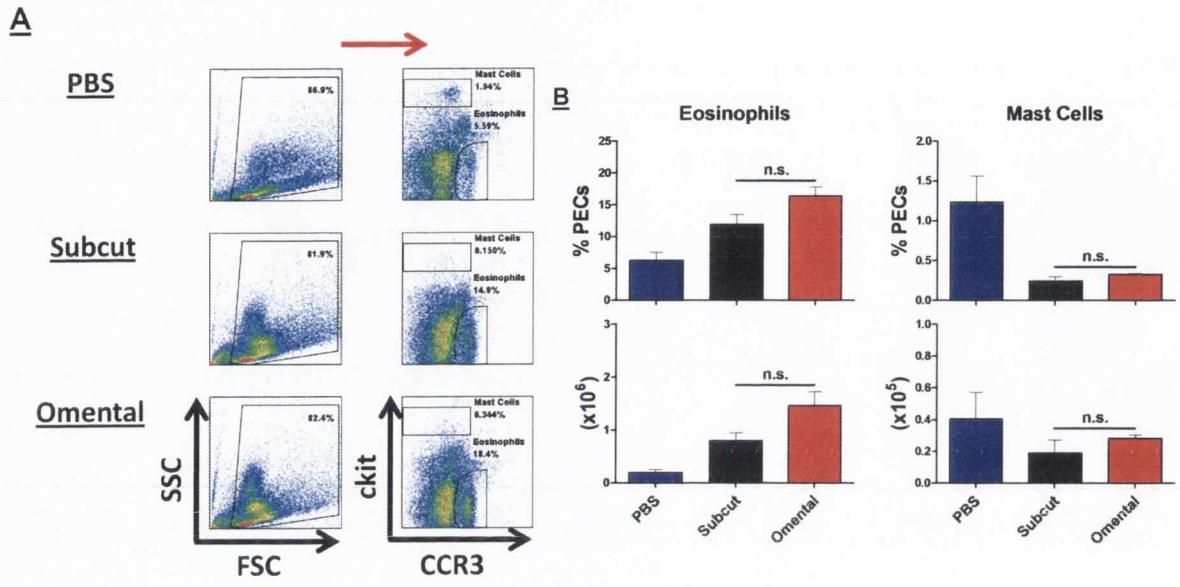

Figure 5.34 – Both endogenous oils derived from subcutaneous adipocytes and omental adipocytes promote eosinophil recruitment into the peritoneum but deplete resident mast cells. Female C57BL/6 mice were immunised as described in Figure 5.31. PECs were isolated and stained with antibodies specific for CCR3 and ckit (5 x 10^5 PECs/sample). The level of positive staining was quantified for each sample by flow cytometry. Eosinophils ($CCR3^+$ $ckit^-$) and mast cells ($CCR3^-$ $ckit^+$) were identified and are represented in (A) dot plot and (B) bar graph format. Dot plots are shown as a single representative population from each treatment group and are indicative of the gating strategy employed. Bar graphs represent mean (+ SEM) for 3 mice per experimental group.

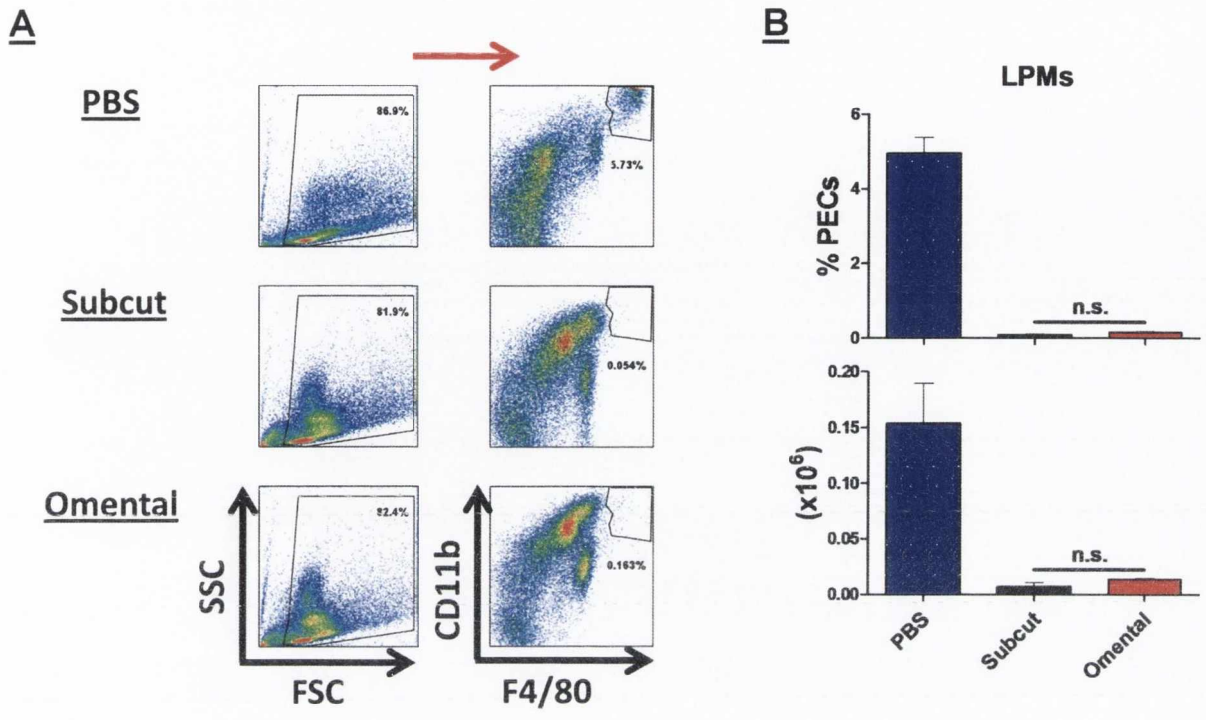

Figure 5.35 – Endogenous oils derived from subcutaneous adipocytes and omental adipocytes both deplete resident large peritoneal macrophages. Female C57BL/6 mice were immunised as described in Figure 5.31. PECs were isolated and stained with antibodies specific for CD11b and F4/80 (5 x 10^5 PECs/sample). The level of positive staining was quantified for each sample by flow cytometry. LPMs were identified ($CD11b^{high}$ $F4/80^{high}$) and are represented in (A) dot plot and (B) bar graph format. Dot plots are shown as a single representative population from each treatment group and are indicative of the gating strategy employed. Bar graphs represent mean (+ SEM) for 3 mice per experimental group.

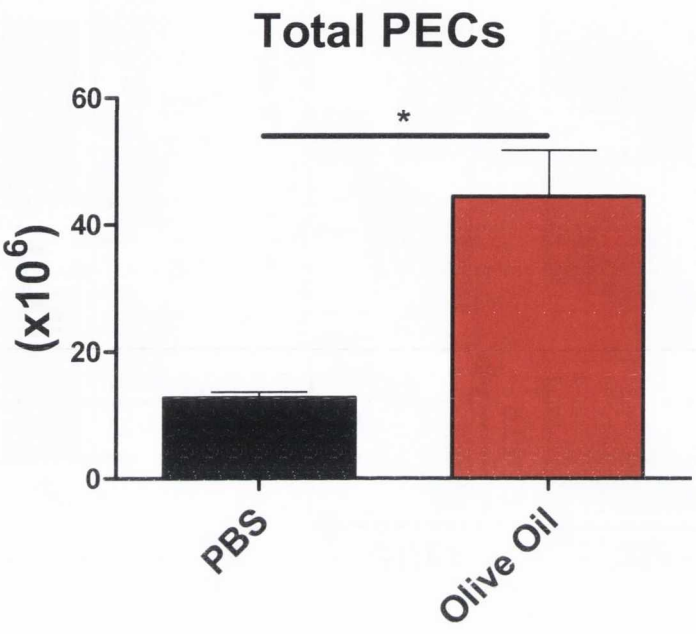

Figure 5.36 – Olive oil promotes cell recruitment into the peritoneum. Female C57BL/6 mice were immunised i.p. with PBS (10µl/mouse) as a control or olive oil (10µl/mouse). The mice were sacrificed 24 hours later and PECs were isolated. PEC numbers were determined using a Glasstic cell counter slide with grids following trypan blue staining. Results are mean PEC number (+ SEM) for 3 mice per experimental group. Versus PBS, * $p<0.05$.

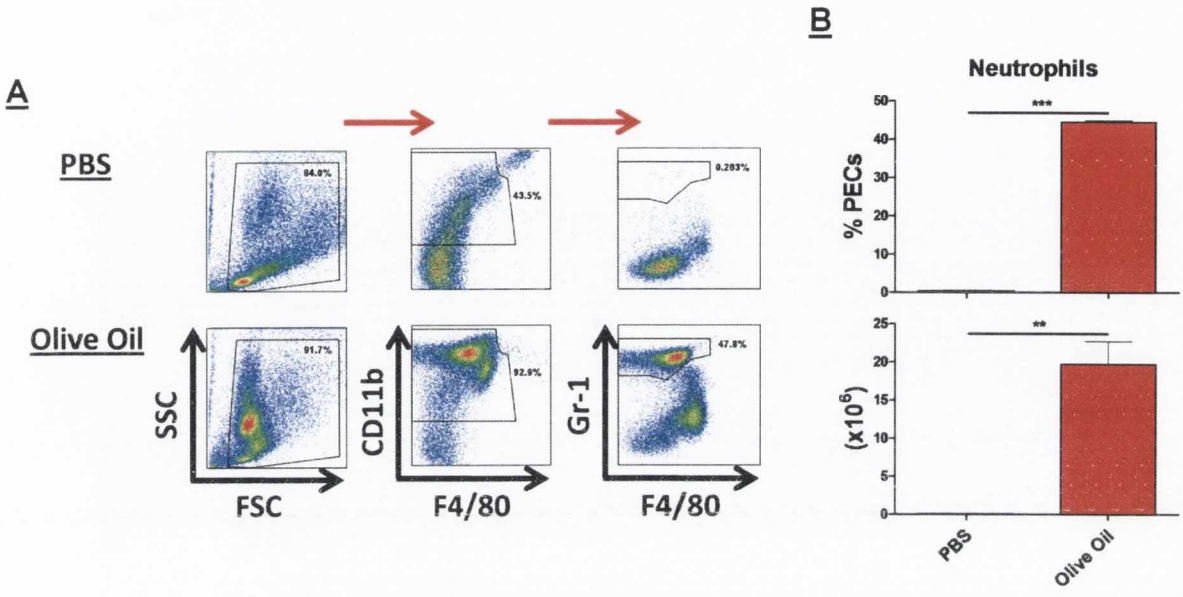

Figure 5.37 – Neutrophils infiltrate the peritoneum following injection with olive oil. Female C57BL/6 mice were immunised as described in Figure 5.36. PECS were isolated and stained with antibodies specific for CD11b, F4/80 and Gr-1 (5 x 10^5 PECs/sample). The level of positive staining was quantified for each sample by flow cytometry. Neutrophils were identified ($CD11b^{inter}$ $F4/80^{-}$ $Gr\text{-}1^{high}$) and are represented in (A) dot plot and (B) bar graph format. Dot plots are shown as a single representative population from each treatment group and are indicative of the gating strategy employed. Bar graphs represent mean (+ SEM) for 3 mice per experimental group. Versus PBS, ** $p<0.01$, *** $p<0.001$.

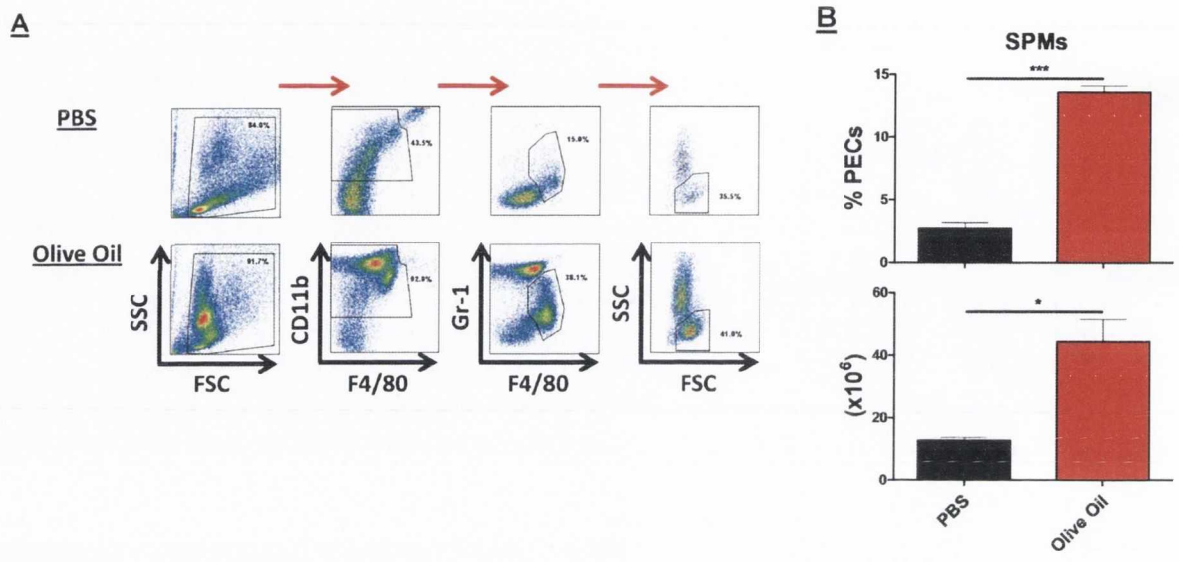

Figure 5.38 – Olive oil mediates recruitment of small peritoneal macrophages. Female C57BL/6 mice were immunised as described in Figure 5.36. PECs were isolated and stained with antibodies specific for CD11b, F4/80 and Gr-1 (5 x 10^5 PECs/sample). The level of positive staining was quantified for each sample by flow cytometry. SPMs were identified (CD11b^{inter} F4/80^{inter} Gr-1$^{low/inter}$ SSc^{low}) and are represented in (A) dot plot and (B) bar graph format. Dot plots are shown as a single representative population from each treatment group and are indicative of the gating strategy employed. Bar graphs represent mean (+ SEM) for 3 mice per experimental group. Versus PBS, * $p<0.05$, *** $p<0.001$.

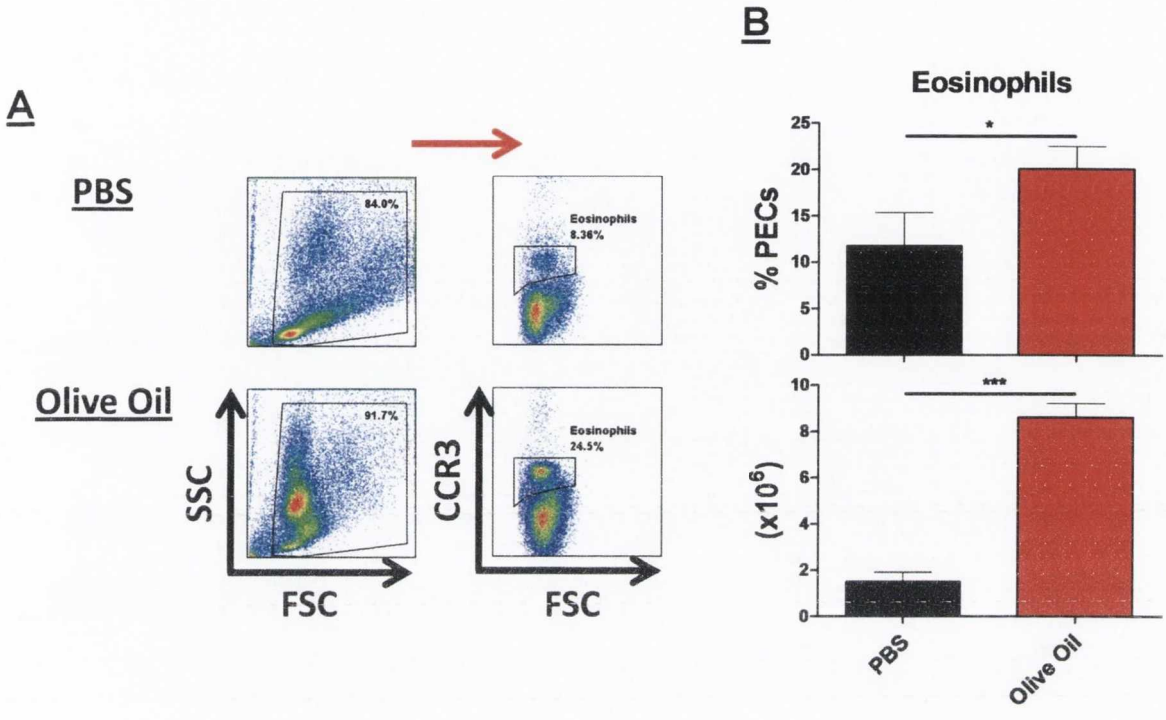

Figure 5.39 – Olive oil promotes eosinophil recruitment into the peritoneum. Female C57BL/6 mice were immunised as described in Figure 5.36. PECs were isolated and stained with an antibody specific for CCR3 (5 x 10^5 PECs/sample). The level of positive staining was quantified for each sample by flow cytometry. Eosinophils ($CCR3^+$) were identified and are represented in (A) dot plot and (B) bar graph format. Dot plots are shown as a single representative population from each treatment group and are indicative of the gating strategy employed. Bar graphs represent mean (+ SEM) for 3 mice per experimental group. Versus PBS, * $p<0.05$, *** $p<0.001$.

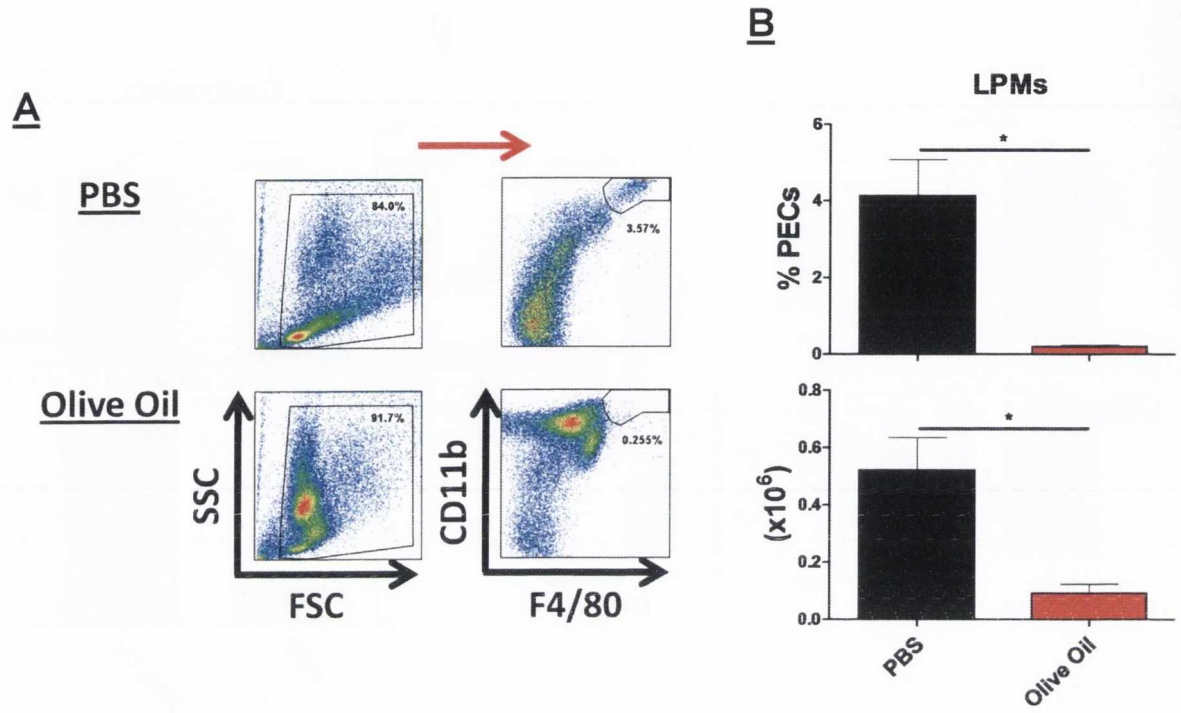

Figure 5.40 – Olive oil depletes resident large peritoneal macrophages at the injection site. Female C57BL/6 mice were immunised as described in Figure 5.36. PECs were isolated and stained with antibodies specific for CD11b and F4/80 (5 x 10^5 PECs/sample). The level of positive staining was quantified for each sample by flow cytometry. LPMs were identified ($CD11b^{high}$ $F4/80^{high}$) and are represented in (A) dot plot and (B) bar graph format. Dot plots are shown as a single representative population from each treatment group and are indicative of the gating strategy employed. Bar graphs represent mean (+ SEM) for 3 mice per experimental group. Versus PBS, * $p<0.05$.

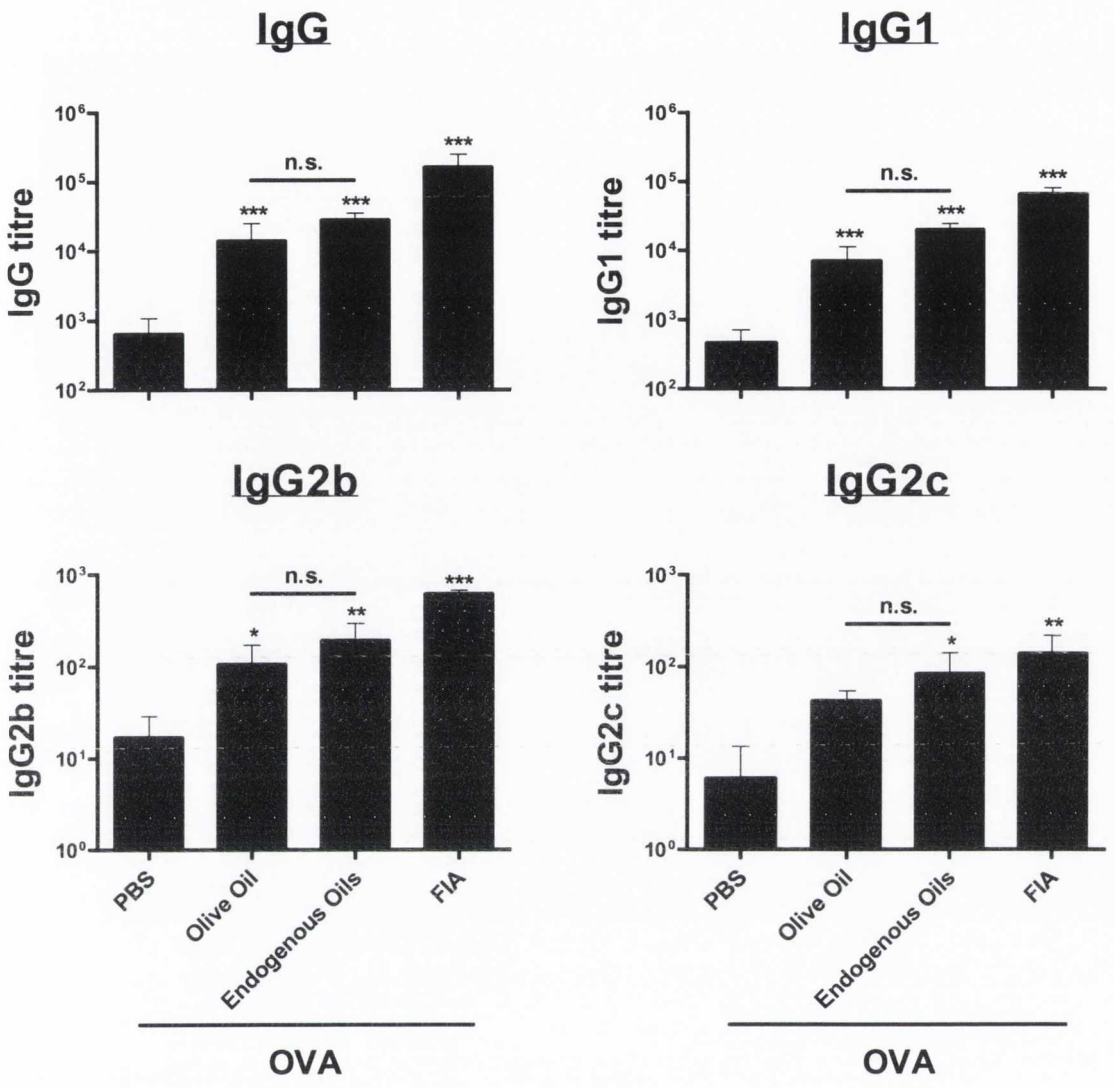

Figure 5.41 – Olive oil significantly boosts OVA-specific serum antibody titres. Female C57BL/6 mice were immunised i.p. on day 0 with PBS as a control or OVA (200μg per mouse) either alone or mixed with an equal volume (100μl) of olive oil or endogenous oils derived from the human omentum. OVA was also mixed with an equal volume (100μl) of FIA and this solution was emulsified by rigorous sonication. The mice were boosted with these same treatments on day 14 and were sacrificed on day 21. Blood samples were recovered and the serum was removed following centrifugation. OVA-specific antibody titres (IgG, IgG1, IgG2b, IgG2c) in the serum were determined by ELISA. Results are mean titres (+ SEM) for 5 mice per experimental group. Versus PBS (OVA), * $p<0.05$, ** $p<0.01$, *** $p<0.001$. Olive oil (OVA) versus endogenous oils (OVA), n.s., not significant.

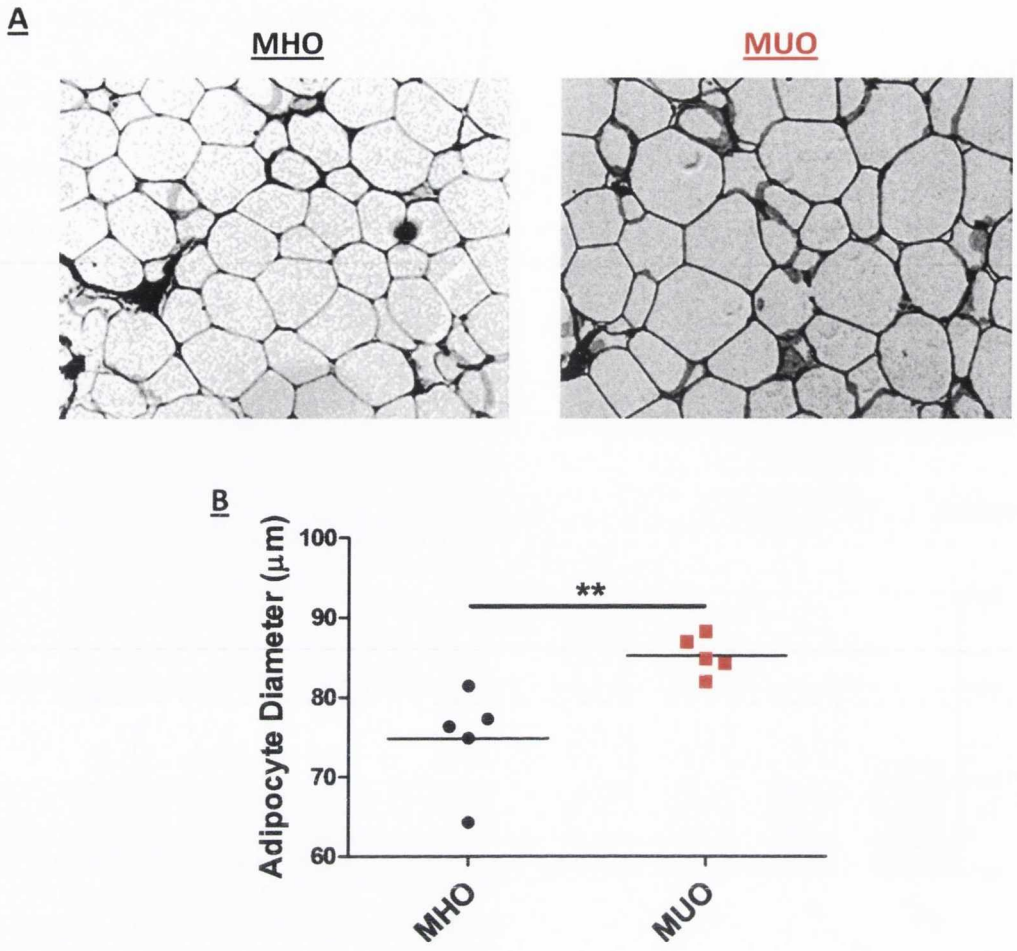

Figure 5.42 – Adipocyte diameter is significantly larger in MUO individuals than in MHO individuals. Approximately 10-30 grams of omental adipose tissue was obtained during bariatric surgery. A piece of this tissue was immediately fixed in formalin, prior to paraffin mounting and preparation of H&E sections. Adipocyte size was determined using Image Pro Plus 7 Software. The mean diameter of a range of adipocytes from 5 MHO individuals and 5 MUO individuals was calculated from 10 separate photographs of randomised areas of the same section. (A) Single representative image of a section containing WAT from MHO individual and also a section containing WAT from MUO individual. (B) Scatter plot represents mean for 5 individuals per experimental group. Versus MHO, ** $p<0.01$. The embedding and sectioning of the samples was carried out by Dr. Jean O'Connell of the Obesity Group, St. Vincent's University Hospital, Elm Park, Dublin 4, Ireland and the H&E staining was performed by Prof. Sean Callanan of the School of Agriculture, Food Science and Veterinary Medicine, University College Dublin, Belfield, Dublin 4, Ireland.

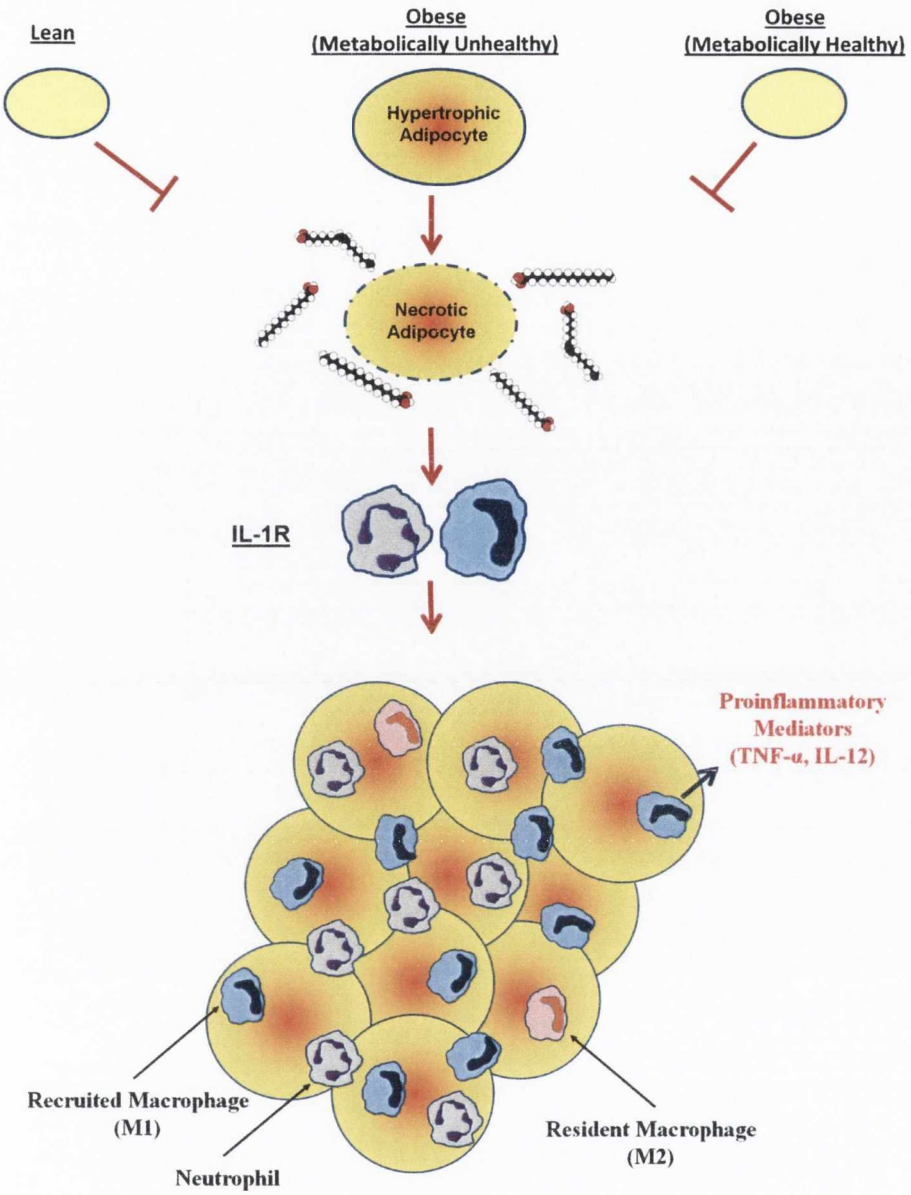

Figure 5.43 – Proposed model for obesity-induced inflammation through release of endogenous oils from adipocytes in visceral fat depots of MUO individuals. Adipocytes in visceral fat depots of MUO individuals are more hypertrophic than those in MHO or lean individuals. Hypertrophy induces adipocyte necrosis and release of endogenous oils from the core of the lipid droplet. These endogenous oils subsequently mediate IL-1R-dependent recruitment of neutrophils and M1 macrophages into WAT. M1 macrophages become more numerous than M2 macrophages and secrete cytokines such as TNF-α and IL-12 which function to initiate the inflammatory cascade associated with MUO individuals.

Chapter 6

General Discussion

6 – General Discussion

'Most of us are far more influential alive than dead. But a chosen few achieve power and influence of prodigal proportions only in their death'. Bali Pulendran once used these words to describe the role of necrotic cells in the immune response [560]. Indeed, the immunostimulatory activity of necrotic cells is a major component of the danger model. This model was first proposed by Polly Matzinger in 1994 [267] in an attempt to address perceived deficiencies in the late Charles Janeway's stranger model [176]. Janeway's model, which was revolutionary at the time, postulated the idea that the immune system responds only to infectious nonself rather than simply to anything that is foreign. However, Matzinger asked clever questions of this model, for example why is transplant rejection characterised by a potent immune response against a foreign body in the apparent absence of microbes? Questions such as this resulted in the proposal of Matzinger's danger model which outlines the concept that the immune system responds specifically to molecules associated with dangerous situations rather than those simply recognised as infectious or foreign. More specifically, necrotic cells associated with infection or trauma release endogenous danger signals into the extracellular milieu following loss of membrane integrity. These endogenous danger signals can activate APCs and induce robust innate and adaptive immune responses [267]. Interestingly, transplants cannot be performed without surgical or ischemic damage, thus initiating the release of endogenous danger signals which results in immune activation and can compromise survival of the transplanted organ. Since 1994, the danger model has been gaining increased scientific acceptance. Although the aims of this thesis were diverse, the danger model was the central theme and was a fundamental component to each of these respective aims.

The first major achievement of this work was in proving that residual LPS contamination of sample preparations is unquestionably the biggest thorn in the side of the danger model. The most important criterion for danger signals is that their biological activity is not owing to contamination with PAMPs. However, the literature contains many studies accrediting immunostimulatory activity to endogenous danger signals when in fact contaminating LPS is responsible for the observed effects (Section 3.1). Although LPS contamination certainly cannot account for the immunostimulatory activity of many of these danger signals *in vivo*, this is in stark contrast to *in vitro* studies where contamination is a very serious concern. There are many studies that neglect the tremendous potency of LPS, often assuming that residual levels of this PAMP cannot account for the immunostimulatory activity ascribed to the candidate molecule of interest. Therefore, this work aimed to confirm the

minimum LPS concentration required to induce murine DC activation, and to assess the ability of PmB to inhibit this process.

The finding that 10pg/ml LPS is sufficient to induce DC activation is certainly a major concern, particularly given the fact that many proteins such as HMGB1 and Hsps bind specifically to this PAMP. The discovery that PmB is exceedingly limited in its capacity to inhibit DC activation in response to LPS further emphasises the significance of the problem concerning residual contamination. Low concentrations of LPS also fail to promote secretion of proinflammatory cytokines by DCs following heat treatment, thus eradicating the old notion that LPS is heat resistant and seriously jeopardising the credibility of a second control commonly used to eliminate the possibility of residual LPS contamination. Interestingly, this study found that LPS is capable of promoting DC activation at concentrations of at least two hundred times less than the minimal concentrations being used to test for heat sensitivity in the literature. Therefore, even if 99.5% of LPS is inactivated by heat treatment, the active residual LPS is still adequate to promote DC activation, thus leading to the erroneous conclusion that LPS is heat resistant. These problems are only compounded by the observation that as little as 5pg/ml LPS is sufficient to promote secretion of the proinflammatory cytokine IL-6 in the presence of *E. coli* LT. Indeed, LPS concentrations which are incapable of promoting DC secretion of proinflammatory cytokines independently may synergise with candidate immunomodulators to enhance this effect, thus reducing even further the minimal LPS concentration required for DC activation. This generates the incorrect conclusion that the candidate molecule can induce cytokine secretion independently of LPS.

Ultimately, chapter 3 of this thesis meticulously quantifies exactly how little LPS is required to induce DC activation and confirms what researchers have perhaps suspected for many years but have never directly tested. These findings also serve as an important reminder that LPS contamination is a concern which must not be casually overlooked. In addition, the limitations and deficiencies associated with the controls commonly used to address this issue only serve to further heighten these concerns. Given the extreme potency of LPS in DC activation and the inability of common controls to successfully reverse the effects of this PAMP, it is advisable to fully deplete LPS from candidate danger signals prior to testing for potential immunostimulatory activity using murine DCs. However, the complete removal of LPS from sample preparations is not always achievable. In these cases, it is proposed that the only definitive way to eliminate the possibility of residual LPS contamination is to use TLR4-deficient DCs or immortalised cell lines which do not express TLR4. However, the clear

disadvantage of this approach is that danger signals that genuinely signal through TLR4 may not be identified.

Moving on from the issue of residual LPS contamination but keeping in tune with the principles of the danger model, the next aim of this thesis was to investigate the immunomodulatory activity of novel GzmB substrates. Indeed, this work has successfully shown that GzmB processing of the endogenous danger signal IL-1α at Asp103 significantly potentiates its immunostimulatory potential *in vivo*. This observation contradicts the dogma that processing of IL-1α has no effect on its biological activity. Although it is unclear exactly how GzmB processing of IL-1α augments the immune activation capacity of this endogenous cytokine, it is possible that conformational changes in GzmB IL-1α may enhance its affinity for the IL-1R. It is also feasible that the N-terminus of IL-1α may partially obstruct the receptor binding domain. Therefore, removing the N-terminus of the cytokine may facilitate more efficient binding to the IL-1R.

IL-1α is passively released from necrotic cells but is retained in the nucleus of cells undergoing apoptosis [432]. The nuclear localisation of IL-1α is facilitated by an N-terminal nuclear retention sequence. However, GzmB processing of IL-1α removes this region. Therefore, it is entirely plausible that GzmB processing of IL-1α may also override nuclear retention mechanisms employed during apoptosis, thus facilitating its rapid release into the extracellular milieu. However, proving this will require further study.

Another key question concerning GzmB processing of IL-1α is how this protease might come into contact with IL-1α in a physiological setting. Indeed, there are several scenarios where this contact may occur. Firstly, cytotoxic cells such as CTLs and NK cells secrete GzmB in response to virally infected and transformed cells [126]. If these target cells express endogenous IL-1α, it is likely to be processed by GzmB and released from secondary necrotic cells into the extracellular milieu. Secondly, necrotic cells may release endogenous IL-1α following loss of membrane integrity and this danger signal may encounter GzmB that has been secreted into the extracellular environment by immune cells. This particular hypothesis is supported by the fact that patients with RA and melioidosis express elevated levels of circulating GzmB [286-287]. Furthermore, GzmB has also been shown to be secreted by a range of immune cells not associated with cytotoxicity (Section 1.8.1).

The possibility that co-purifying microbial contaminants were responsible for mediating the enhanced adjuvanticity of GzmB IL-1α *in vivo* was rigorously tested. Firstly, a catalytically inactive

GzmB mutant ($GzmB^{SA}$) was expressed and purified in the same yeast system as that used to produce wild-type GzmB ($GzmB^{WT}$). Importantly, $GzmB^{SA}$ IL-1α failed to elicit the same adjuvanticity displayed by $GzmB^{WT}$ IL-1α. This confirmed that the catalytic activity of GzmB is necessary for potentiating IL-1α bioactivity *in vivo* and that co-purifying microbial contaminants present within the respective GzmB preparations are not responsible for this effect. Furthermore, HeLa cells were an ideal cell line to use when testing IL-1α for immunostimulatory activity *in vitro* as these cells are very sensitive to this cytokine but fail to respond to a wide range of PAMPs including LPS. More specifically, HeLa cells express TLR4 but not MD-2, which is necessary for the response to LPS. In order to eliminate the possibility that residual GzmB activity within the IL-1α preparations was responsible for mediating the immunostimulatory effects of IL-1α *in vivo*, the adjuvanticity of both active GzmB and HI GzmB was assessed. However, both active and HI GzmB failed to increase antigen-specific antibody titres in the serum.

Indeed, it is reasonable to conclude that GzmB may process intracellular substrates with downstream consequences distinct from apoptosis. IL-1α is one example of such an endogenous danger signal. Ultimately, GzmB processing of intracellular targets may generate novel immunostimulatory danger signals or enhance the immune activation capacity of pre-existing danger signals. Importantly, HRF was also identified as a GzmB substrate and is cleaved at Asn51. Initially, both FL HRF and GzmB HRF were shown to induce proinflammatory cytokine secretion from DCs and were comparable to LPS in their ability to promote this effect. However, these effects were found to be mediated exclusively by LPS contamination. This finding, although disappointing, was a perfect example of how residual LPS contamination can be extremely potent and how it can generate misleading conclusions. Ultimately, this finding served to validate earlier work in this thesis. Despite this setback, it is clear that GzmB possesses immune functions and can potentiate the bioactivity of IL-1α. It will be interesting to establish whether this protease is also capable of modulating the immune activation capacity of additional substrates.

Matzinger's danger model encapsulates the idea that the host tissue is in control of the immune system. Microbes that reside in mammalian host tissues but do not cause tissue destruction will be tolerated by the host, whereas microbes that induce tissue damage and release of danger signals will trigger effector immune responses. However, it is intriguing to ask the question of whether different danger signals may drive distinct immune responses. Therefore, the next objective of this work was to assess the adjuvant properties of the endogenous danger signals IL-33 and IL-1α as measured by their ability to drive antigen-specific cellular and humoral immunity and also to compare the nature

of the responses induced. Interestingly, this study found that IL-1α promotes a strong antigen-specific Th17 response in PECs whereas a Th17 response is not detectable when IL-33 is used as an adjuvant. Therefore, the type of T cell response induced by IL-1α and IL-33 is qualitatively different. This raises the possibility that different tissues may possess distinct danger signals which promote specific immune responses following necrosis. Ultimately, the consequences of necrotic cell death on the adaptive immune system may be dependent on the repertoire of intracellular danger signals present. Indeed, this is an exciting concept which certainly merits further study. In addition, it would be most interesting to compare the effects of IL-1α and IL-33 on the innate immune system using a mouse peritonitis model.

In addition to GzmB substrates, WAT may also represent a potentially rich source of novel danger signals. Oils have been recognised as immunostimulatory since the discovery of starch oil as a 'dirty little secret of the immunologist'. Indeed, oil-based emulsions have proved to be some of the most potent adjuvants in clinical and experimental use. For example, MF59 is an oil-in-water emulsion containing squalene and Freund's adjuvant is a water-in-oil emulsion containing paraffin oil. Significantly, adipocytes in WAT contain a lipid droplet that is filled with dietary oils and is large enough to push other organelles out to the periphery of the cell. Given the principles of the danger model, it was hypothesised that WAT adipocytes may in fact harbour an endogenous adjuvant in the form of dietary oils. Therefore, the final objective of this thesis was to investigate the immunomodulatory potential of endogenous oils released from necrotic adipocytes. Importantly, it was first demonstrated that endogenous oils enhance antigen-specific antibody titres in the serum and are comparable to FIA in their ability to promote this effect. The significance of this is only highlighted further by the fact that, unlike FIA, the endogenous oils were not emulsified before being injected into mice. Ultimately, this work demonstrates that adipocytes contain their own endogenous adjuvant.

Endogenous oils also induce rapid recruitment of neutrophils and inflammatory SPMs into the injection site in an IL-1R-dependent manner. Importantly, neutrophils [474-475] and inflammatory macrophages [469-471, 502] are the two most important cell types in mediating obesity-induced inflammation in WAT, thus suggesting that release of endogenous oils from hypertrophic adipocytes undergoing necrosis may play a prominent role in the pathology of this condition. Furthermore, endogenous oils also modulate the cytokine profile of PECs following *ex vivo* restimulation with PRR agonists. This was reflected in an increase in secretion of the proinflammatory cytokines TNF-α

and IL-12 and a simultaneous reduction in synthesis of the anti-inflammatory cytokine IL-10. This modulatory effect is dependent on the IL-1R but is largely independent of NLRP3.

Interestingly, resident macrophages serve to dampen immune responses in WAT in normal conditions through secretion of IL-10 [470]. In obese conditions, however, WAT recruits macrophages that secrete proinflammatory cytokines such as TNF-α [469] and IL-12 [552-553]. Work performed as part of this thesis suggests that LPMs could be the cell type predominantly responsible for secretion of IL-10 in the peritoneum whereas SPMs and possibly neutrophils may be responsible for production of TNF-α and IL-12. This is due to the fact that the disappearance of LPMs from the peritoneum after injection with endogenous oils coincides with a reduction in IL-10 secretion by the mixed PEC population following restimulation with PRR agonists, whereas an increase in SPMs and neutrophils in the peritoneum coincides with an increase in production of TNF-α and IL-12 by the PEC population. This finding strongly supports the hypothesis that release of an endogenous adjuvant from necrotic adipocytes may initiate obesity-induced inflammation, a process that is well-characterised but poorly understood. However, future work should further characterise the source of TNF-α, IL-12 and IL-10 using intracellular cytokine staining techniques.

The precise role of the IL-1R in cell recruitment into the peritoneum in response to endogenous oils remains ambiguous. It is clear that infiltration of neutrophils and SPMs into the injection site is completely abrogated in the absence of the IL-1R. However, the current consensus in the literature is that IL-1 is crucial for the acute inflammatory response following immune recognition of necrotic cells, although mainly as a secondary mediator following initial recognition of necrotic cells by receptors not including the IL-1R [272, 274]. This may also be the case for endogenous oils, meaning that events preceding synthesis of IL-1 need to be unravelled. However, the identification of a specific receptor responsible for initial recognition of endogenous oils in the peritoneum will be a very difficult task. Firstly, the receptor on $CD11b^+$ macrophages responsible for initial recognition of necrotic cells has so far proved elusive. Although CLEC9A has been identified as a sensor of necrotic cells [460-461], the expression of this receptor is restricted to $CD8\alpha^+$ DCs in mice and $BDCA3^+$ DCs in humans [561]. Furthermore, given the heterogenous nature and physiochemical properties of the endogenous oils, as well as the fact that olive oil can replicate the immunostimulatory effects of these oils, it is unlikely that a single receptor-ligand interaction is responsible for the initial recognition step. Perhaps a more likely scenario is that endogenous oils function in a similar manner to alum and MSU. A specific receptor for these immunomodulators has

not yet been identified. However, both alum and MSU engage cholesterol in the plasma membrane of DCs and induce lipid sorting [158, 354]. Undoubtedly, this will require further study.

An additional point of interest that needs to be addressed further is the relative contributions of IL-1α and IL-1β in the recruitment of distinct cell populations into the peritoneum. Although the IL-1R is crucial for this effect, IL-1R KO mice are not sufficient to characterise the relative importance of IL-1α and IL-1β in this process as both of these respective cytokines signal through the IL-1R. Neutrophil and SPM recruitment in NLRP3 KO and ASC KO mice is still predominantly intact following injection with endogenous oils. However, this does not rule out a major role for IL-1β in recruitment of either of these cell populations as there are additional sources of this proinflammatory cytokine that are independent of NLRP3 and ASC. According to the literature, IL-1α initiates the inflammatory response to necrotic cells by promoting neutrophil recruitment whereas IL-1β sustains inflammation by inducing recruitment and retention of macrophages [555]. However, this will need to be confirmed in the response to endogenous oils. Furthermore, chemokines such as KC and MCP-1 may be important players in this process downstream of IL-1, particularly given that levels of KC are elevated after 3 hours in the peritoneum of mice injected with endogenous oils. It will be interesting to assess chemokine levels in the peritoneum of oil injected IL-1R KO mice.

Importantly, cell recruitment in response to endogenous oils remains completely intact in TLR4-defective C3H/HeJ mice and is therefore not mediated by residual LPS contamination. However, this was not surprising given that the samples were not derived from a bacterial expression system. Furthermore, residual LPS contamination is typically more of a concern *in vitro* than in the more physiological *in vivo* setting. The effects of the endogenous oils do not appear to be a result of toxicity either. Therefore, it is unlikely that the release of endogenous danger signals such as MSU and IL-33 is responsible for promoting infiltration of inflammatory cells into the peritoneum. Indeed, there is no significant difference in levels of IL-33 after 3 hours in the peritoneum of mice injected with PBS or endogenous oils, thus suggesting that this endogenous cytokine is not involved in this process. However, the use of IL-33 KO mice, or indeed ST2 KO mice, would represent a superior means of establishing the role of IL-33. Perhaps assessing responses at an even earlier time point might also be beneficial. Regarding a role for MSU in this process, preliminary studies have been performed using uricase but have proved inconclusive thus far.

One important point to draw attention to was the lack of success in testing the endogenous oils for immunostimulatory activity *in vitro*. However, there is a strong precedent here in so far as that DCs

are completely unresponsive to MF59 and alum [152]. Importantly, future work should instead characterise the chemotactic effects of endogenous oils as MF59 and alum both induce MCP-1, MIP-1α, MIP-1β and IL-8 synthesis in human macrophages and monocytes while failing to induce secretion of proinflammatory cytokines [152].

Solubility issues were also a significant obstacle in assessing the immunostimulatory activity of endogenous oils *in vitro*. The preparation of oils was immiscible with RPMI and therefore consistently resided on top of this aqueous solution. This raises the possibility that the oils were incapable of promoting DC activation simply because they did not come into contact with these innate sentinel cells. Solubility was also an issue when assessing cell death. Endogenous oils were toxic to DCs in a dose-dependent manner, although it is unclear whether they are directly toxic to DCs through cell surface interactions or are indirectly toxic through CO_2 starvation. Further studies will be required to tackle this issue. In the literature, solubility issues have been successfully addressed simply by conjugating lipids to proteins. [481]. However, this step could not be accomplished here due to the fact that it is impossible to determine a single molecular weight for the mixed preparation of endogenous oils.

Finally, this work established that endogenous oils derived from subcutaneous adipocytes are as potent as those derived from omental adipocytes of the same obese individual, despite the fact that visceral fat is significantly more pathogenic than subcutaneous fat in the context of obesity-induced inflammation. In addition, olive oil is also capable of mediating potent activation of the immune system. This ultimately reflects Matzinger's belief that the tissue is indeed the master regulator of the immune system. First and foremost, endogenous adjuvants will only drive immunity if released from the confines of the cell and membrane integrity will only be compromised following necrotic cell death. Importantly, hypertrophy induces adipocyte necrosis and release of endogenous oils. This work has shown that adipocytes in visceral fat of MUO individuals are more hypertrophic than those in visceral fat of MHO individuals. It is also well-established that obese individuals have significantly larger adipocytes than lean individuals [513]. Furthermore, adipocytes in visceral fat are more susceptible to necrosis than their counterparts in subcutaneous fat [557-558]. Ultimately, endogenous oils are far more likely to be released from necrotic adipocytes in visceral fat of MUO individuals than in any of the other conditions or depots outlined above. These endogenous oils subsequently drive obesity-induced inflammation and therefore might explain why MUO individuals have a significantly more pathogenic metabolic profile than any other cohort.

In summary, this thesis has successfully explored the concept of the danger model on various fronts, from the perennial issue of residual LPS contamination right through to identifying novel sources of danger signals in the form of GzmB substrates as well as an endogenous adjuvant found inside adipocytes. This work strongly supports the danger model and may help to further enhance its acceptance within the scientific community. Moreover, this work may also facilitate new avenues of investigation into Matzinger's model, with particular emphasis on potential new sources of endogenous danger signals as well as the different types of responses that distinct tissues and ultimately specific danger signals might promote.

Chapter 7

References

7 - References

1. Turvey, S.E. and D.H. Broide, *Innate immunity.* J Allergy Clin Immunol, 2010. **125**(2 Suppl 2): p. S24-32.
2. Walker, W.A., *Development of the intestinal mucosal barrier.* J Pediatr Gastroenterol Nutr, 2002. **34 Suppl 1**: p. S33-9.
3. Gallo, R.L., et al., *Biology and clinical relevance of naturally occurring antimicrobial peptides.* J Allergy Clin Immunol, 2002. **110**(6): p. 823-31.
4. Parkin, J. and B. Cohen, *An overview of the immune system.* Lancet, 2001. **357**(9270): p. 1777-89.
5. Janeway, C.A., Jr. and R. Medzhitov, *Innate immune recognition.* Annu Rev Immunol, 2002. **20**: p. 197-216.
6. Vestweber, D., *Adhesion and signaling molecules controlling the transmigration of leukocytes through endothelium.* Immunol Rev, 2007. **218**: p. 178-96.
7. Rankin, J.A., *Biological mediators of acute inflammation.* AACN Clin Issues, 2004. **15**(1): p. 3-17.
8. van der Poll, T., *Coagulation and inflammation.* J Endotoxin Res, 2001. **7**(4): p. 301-4.
9. Steinman, R.M. and Z.A. Cohn, *Identification of a novel cell type in peripheral lymphoid organs of mice. I. Morphology, quantitation, tissue distribution.* J Exp Med, 1973. **137**(5): p. 1142-62.
10. Steinman, R.M. and M.D. Witmer, *Lymphoid dendritic cells are potent stimulators of the primary mixed leukocyte reaction in mice.* Proc Natl Acad Sci U S A, 1978. **75**(10): p. 5132-6.
11. Nussenzweig, M.C., et al., *Dendritic cells are accessory cells for the development of anti-trinitrophenyl cytotoxic T lymphocytes.* J Exp Med, 1980. **152**(4): p. 1070-84.
12. Colonna, M., G. Trinchieri, and Y.J. Liu, *Plasmacytoid dendritic cells in immunity.* Nat Immunol, 2004. **5**(12): p. 1219-26.
13. Mellman, I. and R.M. Steinman, *Dendritic cells: specialized and regulated antigen processing machines.* Cell, 2001. **106**(3): p. 255-8.
14. Fogg, D.K., et al., *A clonogenic bone marrow progenitor specific for macrophages and dendritic cells.* Science, 2006. **311**(5757): p. 83-7.
15. Liu, K., et al., *In vivo analysis of dendritic cell development and homeostasis.* Science, 2009. **324**(5925): p. 392-7.
16. Varol, C., et al., *Intestinal lamina propria dendritic cell subsets have different origin and functions.* Immunity, 2009. **31**(3): p. 502-12.
17. Varol, C., et al., *Monocytes give rise to mucosal, but not splenic, conventional dendritic cells.* J Exp Med, 2007. **204**(1): p. 171-80.
18. Narni-Mancinelli, E., et al., *Memory CD8+ T cells mediate antibacterial immunity via CCL3 activation of TNF/ROI+ phagocytes.* J Exp Med, 2007. **204**(9): p. 2075-87.
19. Chorro, L., et al., *Langerhans cell (LC) proliferation mediates neonatal development, homeostasis, and inflammation-associated expansion of the epidermal LC network.* J Exp Med, 2009. **206**(13): p. 3089-100.
20. Ajami, B., et al., *Local self-renewal can sustain CNS microglia maintenance and function throughout adult life.* Nat Neurosci, 2007. **10**(12): p. 1538-43.
21. Meredith, M.M., et al., *Zinc finger transcription factor zDC is a negative regulator required to prevent activation of classical dendritic cells in the steady state.* J Exp Med, 2012. **209**(9): p. 1583-93.
22. Meredith, M.M., et al., *Expression of the zinc finger transcription factor zDC (Zbtb46, Btbd4) defines the classical dendritic cell lineage.* J Exp Med, 2012. **209**(6): p. 1153-65.
23. Lutz, M.B., et al., *An advanced culture method for generating large quantities of highly pure dendritic cells from mouse bone marrow.* J Immunol Methods, 1999. **223**(1): p. 77-92.
24. Scheicher, C., et al., *Dendritic cells from mouse bone marrow: in vitro differentiation using low doses of recombinant granulocyte-macrophage colony-stimulating factor.* J Immunol Methods, 1992. **154**(2): p. 253-64.

25. Naik, S.H., et al., *Cutting edge: generation of splenic CD8+ and CD8- dendritic cell equivalents in Fms-like tyrosine kinase 3 ligand bone marrow cultures.* J Immunol, 2005. **174**(11): p. 6592-7.
26. McKenna, H.J., et al., *Mice lacking flt3 ligand have deficient hematopoiesis affecting hematopoietic progenitor cells, dendritic cells, and natural killer cells.* Blood, 2000. **95**(11): p. 3489-97.
27. Maraskovsky, E., et al., *Dramatic increase in the numbers of functionally mature dendritic cells in Flt3 ligand-treated mice: multiple dendritic cell subpopulations identified.* J Exp Med, 1996. **184**(5): p. 1953-62.
28. Takeuchi, O. and S. Akira, *Pattern recognition receptors and inflammation.* Cell, 2010. **140**(6): p. 805-20.
29. Lennon-Dumenil, A.M., et al., *A closer look at proteolysis and MHC-class-II-restricted antigen presentation.* Curr Opin Immunol, 2002. **14**(1): p. 15-21.
30. Koopmann, J.O., G.J. Hammerling, and F. Momburg, *Generation, intracellular transport and loading of peptides associated with MHC class I molecules.* Curr Opin Immunol, 1997. **9**(1): p. 80-8.
31. Bevan, M.J., *Minor H antigens introduced on H-2 different stimulating cells cross-react at the cytotoxic T cell level during in vivo priming.* J Immunol, 1976. **117**(6): p. 2233-8.
32. Bevan, M.J., *Cross-priming for a secondary cytotoxic response to minor H antigens with H-2 congenic cells which do not cross-react in the cytotoxic assay.* J Exp Med, 1976. **143**(5): p. 1283-8.
33. den Haan, J.M., S.M. Lehar, and M.J. Bevan, *CD8(+) but not CD8(-) dendritic cells cross-prime cytotoxic T cells in vivo.* J Exp Med, 2000. **192**(12): p. 1685-96.
34. Burgdorf, S., et al., *Distinct pathways of antigen uptake and intracellular routing in CD4 and CD8 T cell activation.* Science, 2007. **316**(5824): p. 612-6.
35. Luster, A.D., *The role of chemokines in linking innate and adaptive immunity.* Curr Opin Immunol, 2002. **14**(1): p. 129-35.
36. Germain, R.N., *MHC-dependent antigen processing and peptide presentation: providing ligands for T lymphocyte activation.* Cell, 1994. **76**(2): p. 287-99.
37. Bour-Jordan, H. and J.A. Blueston, *CD28 function: a balance of costimulatory and regulatory signals.* J Clin Immunol, 2002. **22**(1): p. 1-7.
38. Reis e Sousa, C., *Dendritic cells in a mature age.* Nat Rev Immunol, 2006. **6**(6): p. 476-83.
39. Nossal, G.J. and J. Lederberg, *Antibody production by single cells.* Nature, 1958. **181**(4620): p. 1419-20.
40. Pancer, Z. and M.D. Cooper, *The evolution of adaptive immunity.* Annu Rev Immunol, 2006. **24**: p. 497-518.
41. Fagraeus, A., *The plasma cellular reaction and its relation to the formation of antibodies in vitro.* J Immunol, 1948. **58**(1): p. 1-13.
42. Cooper, M.D., R.D. Peterson, and R.A. Good, *Delineation of the Thymic and Bursal Lymphoid Systems in the Chicken.* Nature, 1965. **205**: p. 143-6.
43. Cooper, M.D., et al., *The functions of the thymus system and the bursa system in the chicken.* J Exp Med, 1966. **123**(1): p. 75-102.
44. Miller, J.F. and G.F. Mitchell, *Cell to cell interaction in the immune response. I. Hemolysin-forming cells in neonatally thymectomized mice reconstituted with thymus or thoracic duct lymphocytes.* J Exp Med, 1968. **128**(4): p. 801-20.
45. Mitchell, G.F. and J.F. Miller, *Cell to cell interaction in the immune response. II. The source of hemolysin-forming cells in irradiated mice given bone marrow and thymus or thoracic duct lymphocytes.* J Exp Med, 1968. **128**(4): p. 821-37.
46. Coombs, R.R., A. Feinstein, and A.B. Wilson, *Immunoglobulin determinants on the surface of human lymphocytes.* Lancet, 1969. **2**(7631): p. 1157-60.
47. Froland, S., J.B. Natvig, and P. Berdal, *Surface-bound immunoglobulin as a marker of B lymphocytes in man.* Nat New Biol, 1971. **234**(51): p. 251-2.
48. Edelman, G.M. and J.A. Gally, *A Model for the 7s Antibody Molecule.* Proc Natl Acad Sci U S A, 1964. **51**: p. 846-53.

49. Porter, R.R., *Chemical Structure of Gamma-Globulin and Antibodies.* Br Med Bull, 1963. **19**: p. 197-201.
50. Brack, C., et al., *A complete immunoglobulin gene is created by somatic recombination.* Cell, 1978. **15**(1): p. 1-14.
51. Hardy, R.R., et al., *Resolution and characterization of pro-B and pre-pro-B cell stages in normal mouse bone marrow.* J Exp Med, 1991. **173**(5): p. 1213-25.
52. Hardy, R.R., P.W. Kincade, and K. Dorshkind, *The protean nature of cells in the B lymphocyte lineage.* Immunity, 2007. **26**(6): p. 703-14.
53. LeBien, T.W., *Fates of human B-cell precursors.* Blood, 2000. **96**(1): p. 9-23.
54. Coleclough, C., D. Cooper, and R.P. Perry, *Rearrangement of immunoglobulin heavy chain genes during B-lymphocyte development as revealed by studies of mouse plasmacytoma cells.* Proc Natl Acad Sci U S A, 1980. **77**(3): p. 1422-6.
55. Ward, E.S. and V. Ghetie, *The effector functions of immunoglobulins: implications for therapy.* Ther Immunol, 1995. **2**(2): p. 77-94.
56. Chen, K. and A. Cerutti, *New insights into the enigma of immunoglobulin D.* Immunol Rev, 2010. **237**(1): p. 160-79.
57. Fearon, D.T. and M.C. Carroll, *Regulation of B lymphocyte responses to foreign and self-antigens by the CD19/CD21 complex.* Annu Rev Immunol, 2000. **18**: p. 393-422.
58. Parker, D.C., *T cell-dependent B cell activation.* Annu Rev Immunol, 1993. **11**: p. 331-60.
59. Pierce, S.K., *Lipid rafts and B-cell activation.* Nat Rev Immunol, 2002. **2**(2): p. 96-105.
60. Kuhn, R., K. Rajewsky, and W. Muller, *Generation and analysis of interleukin-4 deficient mice.* Science, 1991. **254**(5032): p. 707-10.
61. Defrance, T., et al., *Interleukin 10 and transforming growth factor beta cooperate to induce anti-CD40-activated naive human B cells to secrete immunoglobulin A.* J Exp Med, 1992. **175**(3): p. 671-82.
62. Snapper, C.M. and W.E. Paul, *Interferon-gamma and B cell stimulatory factor-1 reciprocally regulate Ig isotype production.* Science, 1987. **236**(4804): p. 944-7.
63. Harris, D.P., et al., *Reciprocal regulation of polarized cytokine production by effector B and T cells.* Nat Immunol, 2000. **1**(6): p. 475-82.
64. Yanaba, K., et al., *A regulatory B cell subset with a unique CD1dhiCD5+ phenotype controls T cell-dependent inflammatory responses.* Immunity, 2008. **28**(5): p. 639-50.
65. Lund, F.E. and T.D. Randall, *Effector and regulatory B cells: modulators of CD4(+) T cell immunity.* Nat Rev Immunol, 2010. **10**(4): p. 236-47.
66. LeBien, T.W. and T.F. Tedder, *B lymphocytes: how they develop and function.* Blood, 2008. **112**(5): p. 1570-80.
67. Mosmann, T.R., et al., *Two types of murine helper T cell clone. I. Definition according to profiles of lymphokine activities and secreted proteins.* J Immunol, 1986. **136**(7): p. 2348-57.
68. Wan, Y.Y., *Multi-tasking of helper T cells.* Immunology, 2010. **130**(2): p. 166-71.
69. Paul, W.E. and R.A. Seder, *Lymphocyte responses and cytokines.* Cell, 1994. **76**(2): p. 241-51.
70. Seder, R.A., et al., *Interleukin 12 acts directly on CD4+ T cells to enhance priming for interferon gamma production and diminishes interleukin 4 inhibition of such priming.* Proc Natl Acad Sci U S A, 1993. **90**(21): p. 10188-92.
71. Sims, J.E. and D.E. Smith, *The IL-1 family: regulators of immunity.* Nat Rev Immunol, 2010. **10**(2): p. 89-102.
72. Szabo, S.J., et al., *Molecular mechanisms regulating Th1 immune responses.* Annu Rev Immunol, 2003. **21**: p. 713-58.
73. Kurata, H., et al., *Ectopic expression of activated Stat6 induces the expression of Th2-specific cytokines and transcription factors in developing Th1 cells.* Immunity, 1999. **11**(6): p. 677-88.
74. Zheng, W. and R.A. Flavell, *The transcription factor GATA-3 is necessary and sufficient for Th2 cytokine gene expression in CD4 T cells.* Cell, 1997. **89**(4): p. 587-96.

75. Min, B., et al., *Basophils produce IL-4 and accumulate in tissues after infection with a Th2-inducing parasite.* J Exp Med, 2004. **200**(4): p. 507-17.
76. MacGlashan, D., Jr., et al., *Secretion of IL-4 from human basophils. The relationship between IL-4 mRNA and protein in resting and stimulated basophils.* J Immunol, 1994. **152**(6): p. 3006-16.
77. Sokol, C.L., et al., *Basophils function as antigen-presenting cells for an allergen-induced T helper type 2 response.* Nat Immunol, 2009. **10**(7): p. 713-20.
78. Kool, M., et al., *Alum adjuvant boosts adaptive immunity by inducing uric acid and activating inflammatory dendritic cells.* J Exp Med, 2008. **205**(4): p. 869-82.
79. Perrigoue, J.G., et al., *MHC class II-dependent basophil-CD4+ T cell interactions promote T(H)2 cytokine-dependent immunity.* Nat Immunol, 2009. **10**(7): p. 697-705.
80. Zhu, J., et al., *Stat5 activation plays a critical role in Th2 differentiation.* Immunity, 2003. **19**(5): p. 739-48.
81. Paul, W.E. and J. Zhu, *How are T(H)2-type immune responses initiated and amplified?* Nat Rev Immunol, 2010. **10**(4): p. 225-35.
82. Weaver, C.T., et al., *IL-17 family cytokines and the expanding diversity of effector T cell lineages.* Annu Rev Immunol, 2007. **25**: p. 821-52.
83. McKenzie, B.S., R.A. Kastelein, and D.J. Cua, *Understanding the IL-23-IL-17 immune pathway.* Trends Immunol, 2006. **27**(1): p. 17-23.
84. Korn, T., et al., *IL-17 and Th17 Cells.* Annu Rev Immunol, 2009. **27**: p. 485-517.
85. Torchinsky, M.B., et al., *Innate immune recognition of infected apoptotic cells directs T(H)17 cell differentiation.* Nature, 2009. **458**(7234): p. 78-82.
86. Ivanov, II, et al., *The orphan nuclear receptor RORgammat directs the differentiation program of proinflammatory IL-17+ T helper cells.* Cell, 2006. **126**(6): p. 1121-33.
87. Sakaguchi, S., et al., *Regulatory T cells and immune tolerance.* Cell, 2008. **133**(5): p. 775-87.
88. Baecher-Allan, C. and D.A. Hafler, *Human regulatory T cells and their role in autoimmune disease.* Immunol Rev, 2006. **212**: p. 203-16.
89. Kretschmer, K., et al., *Making regulatory T cells with defined antigen specificity: role in autoimmunity and cancer.* Immunol Rev, 2006. **212**: p. 163-9.
90. Fontenot, J.D., M.A. Gavin, and A.Y. Rudensky, *Foxp3 programs the development and function of CD4+CD25+ regulatory T cells.* Nat Immunol, 2003. **4**(4): p. 330-6.
91. Lio, C.W. and C.S. Hsieh, *A two-step process for thymic regulatory T cell development.* Immunity, 2008. **28**(1): p. 100-11.
92. Malek, T.R., et al., *IL-2 family of cytokines in T regulatory cell development and homeostasis.* J Clin Immunol, 2008. **28**(6): p. 635-9.
93. Schmitt, E., et al., *IL-9 production of naive CD4+ T cells depends on IL-2, is synergistically enhanced by a combination of TGF-beta and IL-4, and is inhibited by IFN-gamma.* J Immunol, 1994. **153**(9): p. 3989-96.
94. Nowak, E.C., et al., *IL-9 as a mediator of Th17-driven inflammatory disease.* J Exp Med, 2009. **206**(8): p. 1653-60.
95. Elyaman, W., et al., *IL-9 induces differentiation of TH17 cells and enhances function of FoxP3+ natural regulatory T cells.* Proc Natl Acad Sci U S A, 2009. **106**(31): p. 12885-90.
96. Groux, H., et al., *A CD4+ T-cell subset inhibits antigen-specific T-cell responses and prevents colitis.* Nature, 1997. **389**(6652): p. 737-42.
97. Anderson, C.F., et al., *CD4(+)CD25(-)Foxp3(-) Th1 cells are the source of IL-10-mediated immune suppression in chronic cutaneous leishmaniasis.* J Exp Med, 2007. **204**(2): p. 285-97.
98. McGeachy, M.J., et al., *TGF-beta and IL-6 drive the production of IL-17 and IL-10 by T cells and restrain T(H)-17 cell-mediated pathology.* Nat Immunol, 2007. **8**(12): p. 1390-7.
99. Rubtsov, Y.P., et al., *Regulatory T cell-derived interleukin-10 limits inflammation at environmental interfaces.* Immunity, 2008. **28**(4): p. 546-58.

100. Schaerli, P., et al., *CXC chemokine receptor 5 expression defines follicular homing T cells with B cell helper function.* J Exp Med, 2000. **192**(11): p. 1553-62.
101. Nurieva, R.I., et al., *Generation of T follicular helper cells is mediated by interleukin-21 but independent of T helper 1, 2, or 17 cell lineages.* Immunity, 2008. **29**(1): p. 138-49.
102. Yu, D., et al., *The transcriptional repressor Bcl-6 directs T follicular helper cell lineage commitment.* Immunity, 2009. **31**(3): p. 457-68.
103. Fazilleau, N., et al., *Follicular helper T cells: lineage and location.* Immunity, 2009. **30**(3): p. 324-35.
104. Palmer, M.T. and C.T. Weaver, *Autoimmunity: increasing suspects in the CD4+ T cell lineup.* Nat Immunol, 2010. **11**(1): p. 36-40.
105. Mullen, A.C., et al., *Role of T-bet in commitment of TH1 cells before IL-12-dependent selection.* Science, 2001. **292**(5523): p. 1907-10.
106. Chtanova, T., et al., *Gene microarrays reveal extensive differential gene expression in both CD4(+) and CD8(+) type 1 and type 2 T cells.* J Immunol, 2001. **167**(6): p. 3057-63.
107. Djuretic, I.M., et al., *Transcription factors T-bet and Runx3 cooperate to activate Ifng and silence Il4 in T helper type 1 cells.* Nat Immunol, 2007. **8**(2): p. 145-53.
108. Wei, G., et al., *Global mapping of H3K4me3 and H3K27me3 reveals specificity and plasticity in lineage fate determination of differentiating CD4+ T cells.* Immunity, 2009. **30**(1): p. 155-67.
109. Mathur, A.N., et al., *T-bet is a critical determinant in the instability of the IL-17-secreting T-helper phenotype.* Blood, 2006. **108**(5): p. 1595-601.
110. Zhu, J., et al., *Down-regulation of Gfi-1 expression by TGF-beta is important for differentiation of Th17 and CD103+ inducible regulatory T cells.* J Exp Med, 2009. **206**(2): p. 329-41.
111. Zhu, J. and W.E. Paul, *Heterogeneity and plasticity of T helper cells.* Cell Res, 2010. **20**(1): p. 4-12.
112. Zhou, L., et al., *TGF-beta-induced Foxp3 inhibits T(H)17 cell differentiation by antagonizing RORgammat function.* Nature, 2008. **453**(7192): p. 236-40.
113. Ichiyama, K., et al., *Foxp3 inhibits RORgammat-mediated IL-17A mRNA transcription through direct interaction with RORgammat.* J Biol Chem, 2008. **283**(25): p. 17003-8.
114. Bettelli, E., et al., *Reciprocal developmental pathways for the generation of pathogenic effector TH17 and regulatory T cells.* Nature, 2006. **441**(7090): p. 235-8.
115. Chen, W., et al., *Conversion of peripheral CD4+CD25- naive T cells to CD4+CD25+ regulatory T cells by TGF-beta induction of transcription factor Foxp3.* J Exp Med, 2003. **198**(12): p. 1875-86.
116. Davidson, T.S., et al., *Cutting Edge: IL-2 is essential for TGF-beta-mediated induction of Foxp3+ T regulatory cells.* J Immunol, 2007. **178**(7): p. 4022-6.
117. Peng, Y., et al., *TGF-beta regulates in vivo expansion of Foxp3-expressing CD4+CD25+ regulatory T cells responsible for protection against diabetes.* Proc Natl Acad Sci U S A, 2004. **101**(13): p. 4572-7.
118. Benson, M.J., et al., *All-trans retinoic acid mediates enhanced T reg cell growth, differentiation, and gut homing in the face of high levels of co-stimulation.* J Exp Med, 2007. **204**(8): p. 1765-74.
119. Xu, L., et al., *Cutting edge: regulatory T cells induce CD4+CD25-Foxp3- T cells or are self-induced to become Th17 cells in the absence of exogenous TGF-beta.* J Immunol, 2007. **178**(11): p. 6725-9.
120. Zheng, S.G., J. Wang, and D.A. Horwitz, *Cutting edge: Foxp3+CD4+CD25+ regulatory T cells induced by IL-2 and TGF-beta are resistant to Th17 conversion by IL-6.* J Immunol, 2008. **180**(11): p. 7112-6.
121. Wan, Y.Y. and R.A. Flavell, *Regulatory T-cell functions are subverted and converted owing to attenuated Foxp3 expression.* Nature, 2007. **445**(7129): p. 766-70.
122. Zhou, L., M.M. Chong, and D.R. Littman, *Plasticity of CD4+ T cell lineage differentiation.* Immunity, 2009. **30**(5): p. 646-55.
123. Annunziato, F., et al., *Phenotypic and functional features of human Th17 cells.* J Exp Med, 2007. **204**(8): p. 1849-61.
124. Lexberg, M.H., et al., *Th memory for interleukin-17 expression is stable in vivo.* Eur J Immunol, 2008. **38**(10): p. 2654-64.
125. Podack, E.R., J.D. Young, and Z.A. Cohn, *Isolation and biochemical and functional characterization of perforin 1 from cytolytic T-cell granules.* Proc Natl Acad Sci U S A, 1985. **82**(24): p. 8629-33.

126. Lowin, B., M.C. Peitsch, and J. Tschopp, *Perforin and granzymes: crucial effector molecules in cytolytic T lymphocyte and natural killer cell-mediated cytotoxicity.* Curr Top Microbiol Immunol, 1995. **198**: p. 1-24.
127. Kupfer, A. and G. Dennert, *Reorientation of the microtubule-organizing center and the Golgi apparatus in cloned cytotoxic lymphocytes triggered by binding to lysable target cells.* J Immunol, 1984. **133**(5): p. 2762-6.
128. Allan, V.J., H.M. Thompson, and M.A. McNiven, *Motoring around the Golgi.* Nat Cell Biol, 2002. **4**(10): p. E236-42.
129. Stinchcombe, J.C., et al., *The immunological synapse of CTL contains a secretory domain and membrane bridges.* Immunity, 2001. **15**(5): p. 751-61.
130. Nakajima, H., H.L. Park, and P.A. Henkart, *Synergistic roles of granzymes A and B in mediating target cell death by rat basophilic leukemia mast cell tumors also expressing cytolysin/perforin.* J Exp Med, 1995. **181**(3): p. 1037-46.
131. Shiver, J.W. and P.A. Henkart, *A noncytotoxic mast cell tumor line exhibits potent IgE-dependent cytotoxicity after transfection with the cytolysin/perforin gene.* Cell, 1991. **64**(6): p. 1175-81.
132. Shiver, J.W., L. Su, and P.A. Henkart, *Cytotoxicity with target DNA breakdown by rat basophilic leukemia cells expressing both cytolysin and granzyme A.* Cell, 1992. **71**(2): p. 315-22.
133. Heusel, J.W., et al., *Cytotoxic lymphocytes require granzyme B for the rapid induction of DNA fragmentation and apoptosis in allogeneic target cells.* Cell, 1994. **76**(6): p. 977-87.
134. Fong, T.A. and T.R. Mosmann, *Alloreactive murine CD8+ T cell clones secrete the Th1 pattern of cytokines.* J Immunol, 1990. **144**(5): p. 1744-52.
135. Seder, R.A., et al., *CD8+ T cells can be primed in vitro to produce IL-4.* J Immunol, 1992. **148**(6): p. 1652-6.
136. Salgame, P., et al., *Differing lymphokine profiles of functional subsets of human CD4 and CD8 T cell clones.* Science, 1991. **254**(5029): p. 279-82.
137. Croft, M., et al., *Generation of polarized antigen-specific CD8 effector populations: reciprocal action of interleukin (IL)-4 and IL-12 in promoting type 2 versus type 1 cytokine profiles.* J Exp Med, 1994. **180**(5): p. 1715-28.
138. Vukmanovic-Stejic, M., et al., *Human Tc1 and Tc2/Tc0 CD8 T-cell clones display distinct cell surface and functional phenotypes.* Blood, 2000. **95**(1): p. 231-40.
139. Kaech, S.M., E.J. Wherry, and R. Ahmed, *Effector and memory T-cell differentiation: implications for vaccine development.* Nat Rev Immunol, 2002. **2**(4): p. 251-62.
140. Bachmann, M.F., et al., *Distinct kinetics of cytokine production and cytolysis in effector and memory T cells after viral infection.* Eur J Immunol, 1999. **29**(1): p. 291-9.
141. Veiga-Fernandes, H., et al., *Response of naive and memory CD8+ T cells to antigen stimulation in vivo.* Nat Immunol, 2000. **1**(1): p. 47-53.
142. Teague, T.K., et al., *Activation changes the spectrum but not the diversity of genes expressed by T cells.* Proc Natl Acad Sci U S A, 1999. **96**(22): p. 12691-6.
143. Sallusto, F., et al., *Two subsets of memory T lymphocytes with distinct homing potentials and effector functions.* Nature, 1999. **401**(6754): p. 708-12.
144. Murali-Krishna, K., et al., *Counting antigen-specific CD8 T cells: a reevaluation of bystander activation during viral infection.* Immunity, 1998. **8**(2): p. 177-87.
145. Zhang, X., et al., *Potent and selective stimulation of memory-phenotype CD8+ T cells in vivo by IL-15.* Immunity, 1998. **8**(5): p. 591-9.
146. Ku, C.C., et al., *Control of homeostasis of CD8+ memory T cells by opposing cytokines.* Science, 2000. **288**(5466): p. 675-8.
147. Schluns, K.S., et al., *Interleukin-7 mediates the homeostasis of naive and memory CD8 T cells in vivo.* Nat Immunol, 2000. **1**(5): p. 426-32.

148. Verdier, F., et al., *Aluminium assay and evaluation of the local reaction at several time points after intramuscular administration of aluminium containing vaccines in the Cynomolgus monkey.* Vaccine, 2005. **23**(11): p. 1359-67.
149. Gupta, R.K., et al., *In vivo distribution of radioactivity in mice after injection of biodegradable polymer microspheres containing 14C-labeled tetanus toxoid.* Vaccine, 1996. **14**(15): p. 1412-6.
150. Lindblad, E.B., *Aluminium adjuvants--in retrospect and prospect.* Vaccine, 2004. **22**(27-28): p. 3658-68.
151. Morefield, G.L., et al., *Role of aluminum-containing adjuvants in antigen internalization by dendritic cells in vitro.* Vaccine, 2005. **23**(13): p. 1588-95.
152. Seubert, A., et al., *The adjuvants aluminum hydroxide and MF59 induce monocyte and granulocyte chemoattractants and enhance monocyte differentiation toward dendritic cells.* J Immunol, 2008. **180**(8): p. 5402-12.
153. Sun, H., K.G. Pollock, and J.M. Brewer, *Analysis of the role of vaccine adjuvants in modulating dendritic cell activation and antigen presentation in vitro.* Vaccine, 2003. **21**(9-10): p. 849-55.
154. Eisenbarth, S.C., et al., *Crucial role for the Nalp3 inflammasome in the immunostimulatory properties of aluminium adjuvants.* Nature, 2008. **453**(7198): p. 1122-6.
155. Franchi, L. and G. Nunez, *The Nlrp3 inflammasome is critical for aluminium hydroxide-mediated IL-1beta secretion but dispensable for adjuvant activity.* Eur J Immunol, 2008. **38**(8): p. 2085-9.
156. Marichal, T., et al., *DNA released from dying host cells mediates aluminum adjuvant activity.* Nat Med, 2011. **17**(8): p. 996-1002.
157. Kool, M., et al., *An unexpected role for uric acid as an inducer of T helper 2 cell immunity to inhaled antigens and inflammatory mediator of allergic asthma.* Immunity, 2011. **34**(4): p. 527-40.
158. Flach, T.L., et al., *Alum interaction with dendritic cell membrane lipids is essential for its adjuvanticity.* Nat Med, 2011. **17**(4): p. 479-87.
159. Higgins, D.A., J.R. Carlson, and G. Van Nest, *MF59 adjuvant enhances the immunogenicity of influenza vaccine in both young and old mice.* Vaccine, 1996. **14**(6): p. 478-84.
160. Singh, M., et al., *A comparison of biodegradable microparticles and MF59 as systemic adjuvants for recombinant gD from HSV-2.* Vaccine, 1998. **16**(19): p. 1822-7.
161. Singh, M., et al., *A preliminary evaluation of alternative adjuvants to alum using a range of established and new generation vaccine antigens.* Vaccine, 2006. **24**(10): p. 1680-6.
162. Valensi, J.P., J.R. Carlson, and G.A. Van Nest, *Systemic cytokine profiles in BALB/c mice immunized with trivalent influenza vaccine containing MF59 oil emulsion and other advanced adjuvants.* J Immunol, 1994. **153**(9): p. 4029-39.
163. Wack, A., et al., *Combination adjuvants for the induction of potent, long-lasting antibody and T-cell responses to influenza vaccine in mice.* Vaccine, 2008. **26**(4): p. 552-61.
164. Dupuis, M., et al., *Dendritic cells internalize vaccine adjuvant after intramuscular injection.* Cell Immunol, 1998. **186**(1): p. 18-27.
165. Dupuis, M., D.M. McDonald, and G. Ott, *Distribution of adjuvant MF59 and antigen gD2 after intramuscular injection in mice.* Vaccine, 1999. **18**(5-6): p. 434-9.
166. Dupuis, M., et al., *Immunization with the adjuvant MF59 induces macrophage trafficking and apoptosis.* Eur J Immunol, 2001. **31**(10): p. 2910-8.
167. Calabro, S., et al., *Vaccine adjuvants alum and MF59 induce rapid recruitment of neutrophils and monocytes that participate in antigen transport to draining lymph nodes.* Vaccine, 2011. **29**(9): p. 1812-23.
168. O'Hagan, D.T., et al., *The mechanism of action of MF59 - an innately attractive adjuvant formulation.* Vaccine, 2012. **30**(29): p. 4341-8.
169. Seubert, A., et al., *Adjuvanticity of the oil-in-water emulsion MF59 is independent of Nlrp3 inflammasome but requires the adaptor protein MyD88.* Proc Natl Acad Sci U S A, 2011. **108**(27): p. 11169-74.

170. Ellebedy, A.H., et al., *Inflammasome-independent role of the apoptosis-associated speck-like protein containing CARD (ASC) in the adjuvant effect of MF59.* Proc Natl Acad Sci U S A, 2011. **108**(7): p. 2927-32.
171. Hui, G.S. and C.N. Hashimoto, *Adjuvant formulations possess differing efficacy in the potentiation of antibody and cell mediated responses to a human malaria vaccine under selective immune genes knockout environment.* Int Immunopharmacol, 2008. **8**(7): p. 1012-22.
172. Lederberg, J., *Genes and antibodies.* Science, 1959. **129**(3364): p. 1649-53.
173. Billingham, R.E., L. Brent, and P.B. Medawar, *Actively acquired tolerance of foreign cells.* Nature, 1953. **172**(4379): p. 603-6.
174. Bretscher, P. and M. Cohn, *A theory of self-nonself discrimination.* Science, 1970. **169**(950): p. 1042-9.
175. Lafferty, K.J. and A.J. Cunningham, *A new analysis of allogeneic interactions.* Aust J Exp Biol Med Sci, 1975. **53**(1): p. 27-42.
176. Janeway, C.A., Jr., *Approaching the asymptote? Evolution and revolution in immunology.* Cold Spring Harb Symp Quant Biol, 1989. **54 Pt 1**: p. 1-13.
177. Kawai, T. and S. Akira, *The role of pattern-recognition receptors in innate immunity: update on Toll-like receptors.* Nat Immunol, 2010. **11**(5): p. 373-84.
178. Rock, F.L., et al., *A family of human receptors structurally related to Drosophila Toll.* Proc Natl Acad Sci U S A, 1998. **95**(2): p. 588-93.
179. Ulevitch, R.J. and P.S. Tobias, *Receptor-dependent mechanisms of cell stimulation by bacterial endotoxin.* Annu Rev Immunol, 1995. **13**: p. 437-57.
180. Lemaitre, B., et al., *The dorsoventral regulatory gene cassette spatzle/Toll/cactus controls the potent antifungal response in Drosophila adults.* Cell, 1996. **86**(6): p. 973-83.
181. Medzhitov, R., P. Preston-Hurlburt, and C.A. Janeway, Jr., *A human homologue of the Drosophila Toll protein signals activation of adaptive immunity.* Nature, 1997. **388**(6640): p. 394-7.
182. Poltorak, A., et al., *Defective LPS signaling in C3H/HeJ and C57BL/10ScCr mice: mutations in Tlr4 gene.* Science, 1998. **282**(5396): p. 2085-8.
183. Qureshi, S.T., et al., *Endotoxin-tolerant mice have mutations in Toll-like receptor 4 (Tlr4).* J Exp Med, 1999. **189**(4): p. 615-25.
184. Hoshino, K., et al., *Cutting edge: Toll-like receptor 4 (TLR4)-deficient mice are hyporesponsive to lipopolysaccharide: evidence for TLR4 as the Lps gene product.* J Immunol, 1999. **162**(7): p. 3749-52.
185. Takeuchi, O., et al., *TLR6: A novel member of an expanding toll-like receptor family.* Gene, 1999. **231**(1-2): p. 59-65.
186. Du, X., et al., *Three novel mammalian toll-like receptors: gene structure, expression, and evolution.* Eur Cytokine Netw, 2000. **11**(3): p. 362-71.
187. Hemmi, H., et al., *A Toll-like receptor recognizes bacterial DNA.* Nature, 2000. **408**(6813): p. 740-5.
188. Chuang, T. and R.J. Ulevitch, *Identification of hTLR10: a novel human Toll-like receptor preferentially expressed in immune cells.* Biochim Biophys Acta, 2001. **1518**(1-2): p. 157-61.
189. Aliprantis, A.O., et al., *Cell activation and apoptosis by bacterial lipoproteins through toll-like receptor-2.* Science, 1999. **285**(5428): p. 736-9.
190. Brightbill, H.D., et al., *Host defense mechanisms triggered by microbial lipoproteins through toll-like receptors.* Science, 1999. **285**(5428): p. 732-6.
191. Lien, E., et al., *Toll-like receptor 2 functions as a pattern recognition receptor for diverse bacterial products.* J Biol Chem, 1999. **274**(47): p. 33419-25.
192. Means, T.K., et al., *The CD14 ligands lipoarabinomannan and lipopolysaccharide differ in their requirement for Toll-like receptors.* J Immunol, 1999. **163**(12): p. 6748-55.
193. Underhill, D.M., et al., *The Toll-like receptor 2 is recruited to macrophage phagosomes and discriminates between pathogens.* Nature, 1999. **401**(6755): p. 811-5.

194. Ozinsky, A., et al., *The repertoire for pattern recognition of pathogens by the innate immune system is defined by cooperation between toll-like receptors.* Proc Natl Acad Sci U S A, 2000. **97**(25): p. 13766-71.
195. Hayashi, F., et al., *The innate immune response to bacterial flagellin is mediated by Toll-like receptor 5.* Nature, 2001. **410**(6832): p. 1099-103.
196. Alexopoulou, L., et al., *Recognition of double-stranded RNA and activation of NF-kappaB by Toll-like receptor 3.* Nature, 2001. **413**(6857): p. 732-8.
197. Hemmi, H., et al., *Small anti-viral compounds activate immune cells via the TLR7 MyD88-dependent signaling pathway.* Nat Immunol, 2002. **3**(2): p. 196-200.
198. Heil, F., et al., *Species-specific recognition of single-stranded RNA via toll-like receptor 7 and 8.* Science, 2004. **303**(5663): p. 1526-9.
199. Jurk, M., et al., *Human TLR7 or TLR8 independently confer responsiveness to the antiviral compound R-848.* Nat Immunol, 2002. **3**(6): p. 499.
200. O'Neill, L.A. and A.G. Bowie, *The family of five: TIR-domain-containing adaptors in Toll-like receptor signalling.* Nat Rev Immunol, 2007. **7**(5): p. 353-64.
201. Carty, M., et al., *The human adaptor SARM negatively regulates adaptor protein TRIF-dependent Toll-like receptor signaling.* Nat Immunol, 2006. **7**(10): p. 1074-81.
202. Medzhitov, R., et al., *MyD88 is an adaptor protein in the hToll/IL-1 receptor family signaling pathways.* Mol Cell, 1998. **2**(2): p. 253-8.
203. Fitzgerald, K.A., et al., *Mal (MyD88-adapter-like) is required for Toll-like receptor-4 signal transduction.* Nature, 2001. **413**(6851): p. 78-83.
204. Yamamoto, M., et al., *Essential role for TIRAP in activation of the signalling cascade shared by TLR2 and TLR4.* Nature, 2002. **420**(6913): p. 324-9.
205. Kawai, T., et al., *Unresponsiveness of MyD88-deficient mice to endotoxin.* Immunity, 1999. **11**(1): p. 115-22.
206. Kaisho, T., et al., *Endotoxin-induced maturation of MyD88-deficient dendritic cells.* J Immunol, 2001. **166**(9): p. 5688-94.
207. Yamamoto, M., et al., *Role of adaptor TRIF in the MyD88-independent toll-like receptor signaling pathway.* Science, 2003. **301**(5633): p. 640-3.
208. Yamamoto, M., et al., *TRAM is specifically involved in the Toll-like receptor 4-mediated MyD88-independent signaling pathway.* Nat Immunol, 2003. **4**(11): p. 1144-50.
209. Hacker, H. and M. Karin, *Regulation and function of IKK and IKK-related kinases.* Sci STKE, 2006. **2006**(357): p. re13.
210. Yoneyama, M., et al., *The RNA helicase RIG-I has an essential function in double-stranded RNA-induced innate antiviral responses.* Nat Immunol, 2004. **5**(7): p. 730-7.
211. Kato, H., et al., *Differential roles of MDA5 and RIG-I helicases in the recognition of RNA viruses.* Nature, 2006. **441**(7089): p. 101-5.
212. Takahasi, K., et al., *Nonself RNA-sensing mechanism of RIG-I helicase and activation of antiviral immune responses.* Mol Cell, 2008. **29**(4): p. 428-40.
213. Satoh, T., et al., *LGP2 is a positive regulator of RIG-I- and MDA5-mediated antiviral responses.* Proc Natl Acad Sci U S A, 2010. **107**(4): p. 1512-7.
214. Kawai, T., et al., *IPS-1, an adaptor triggering RIG-I- and Mda5-mediated type I interferon induction.* Nat Immunol, 2005. **6**(10): p. 981-8.
215. Michallet, M.C., et al., *TRADD protein is an essential component of the RIG-like helicase antiviral pathway.* Immunity, 2008. **28**(5): p. 651-61.
216. Zelensky, A.N. and J.E. Gready, *The C-type lectin-like domain superfamily.* FEBS J, 2005. **272**(24): p. 6179-217.
217. van Kooyk, Y. and G.A. Rabinovich, *Protein-glycan interactions in the control of innate and adaptive immune responses.* Nat Immunol, 2008. **9**(6): p. 593-601.

218. Geijtenbeek, T.B. and S.I. Gringhuis, *Signalling through C-type lectin receptors: shaping immune responses.* Nat Rev Immunol, 2009. **9**(7): p. 465-79.
219. Geijtenbeek, T.B., et al., *Mycobacteria target DC-SIGN to suppress dendritic cell function.* J Exp Med, 2003. **197**(1): p. 7-17.
220. Bergman, M.P., et al., *Helicobacter pylori modulates the T helper cell 1/T helper cell 2 balance through phase-variable interaction between lipopolysaccharide and DC-SIGN.* J Exp Med, 2004. **200**(8): p. 979-90.
221. Geijtenbeek, T.B., et al., *DC-SIGN, a dendritic cell-specific HIV-1-binding protein that enhances trans-infection of T cells.* Cell, 2000. **100**(5): p. 587-97.
222. Gringhuis, S.I., et al., *C-type lectin DC-SIGN modulates Toll-like receptor signaling via Raf-1 kinase-dependent acetylation of transcription factor NF-kappaB.* Immunity, 2007. **26**(5): p. 605-16.
223. Dzionek, A., et al., *BDCA-2, a novel plasmacytoid dendritic cell-specific type II C-type lectin, mediates antigen capture and is a potent inhibitor of interferon alpha/beta induction.* J Exp Med, 2001. **194**(12): p. 1823-34.
224. Marshall, A.S., et al., *Identification and characterization of a novel human myeloid inhibitory C-type lectin-like receptor (MICL) that is predominantly expressed on granulocytes and monocytes.* J Biol Chem, 2004. **279**(15): p. 14792-802.
225. Richards, A., et al., *Implications of the initial mutations in membrane cofactor protein (MCP; CD46) leading to atypical hemolytic uremic syndrome.* Mol Immunol, 2007. **44**(1-3): p. 111-22.
226. Meyer-Wentrup, F., et al., *DCIR is endocytosed into human dendritic cells and inhibits TLR8-mediated cytokine production.* J Leukoc Biol, 2009. **85**(3): p. 518-25.
227. Meyer-Wentrup, F., et al., *Targeting DCIR on human plasmacytoid dendritic cells results in antigen presentation and inhibits IFN-alpha production.* Blood, 2008. **111**(8): p. 4245-53.
228. Chen, C.H., et al., *Dendritic-cell-associated C-type lectin 2 (DCAL-2) alters dendritic-cell maturation and cytokine production.* Blood, 2006. **107**(4): p. 1459-67.
229. Taylor, P.R., et al., *Dectin-1 is required for beta-glucan recognition and control of fungal infection.* Nat Immunol, 2007. **8**(1): p. 31-8.
230. Gross, O., et al., *Card9 controls a non-TLR signalling pathway for innate anti-fungal immunity.* Nature, 2006. **442**(7103): p. 651-6.
231. Sato, K., et al., *Dectin-2 is a pattern recognition receptor for fungi that couples with the Fc receptor gamma chain to induce innate immune responses.* J Biol Chem, 2006. **281**(50): p. 38854-66.
232. Yamasaki, S., et al., *C-type lectin Mincle is an activating receptor for pathogenic fungus, Malassezia.* Proc Natl Acad Sci U S A, 2009. **106**(6): p. 1897-902.
233. Yamasaki, S., et al., *Mincle is an ITAM-coupled activating receptor that senses damaged cells.* Nat Immunol, 2008. **9**(10): p. 1179-88.
234. Ting, J.P., et al., *The NLR gene family: a standard nomenclature.* Immunity, 2008. **28**(3): p. 285-7.
235. Mayor, A., et al., *A crucial function of SGT1 and HSP90 in inflammasome activity links mammalian and plant innate immune responses.* Nat Immunol, 2007. **8**(5): p. 497-503.
236. Chamaillard, M., et al., *An essential role for NOD1 in host recognition of bacterial peptidoglycan containing diaminopimelic acid.* Nat Immunol, 2003. **4**(7): p. 702-7.
237. Girardin, S.E., et al., *Nod2 is a general sensor of peptidoglycan through muramyl dipeptide (MDP) detection.* J Biol Chem, 2003. **278**(11): p. 8869-72.
238. Schroder, K. and J. Tschopp, *The inflammasomes.* Cell, 2010. **140**(6): p. 821-32.
239. Martinon, F., K. Burns, and J. Tschopp, *The inflammasome: a molecular platform triggering activation of inflammatory caspases and processing of proIL-beta.* Mol Cell, 2002. **10**(2): p. 417-26.
240. Boyden, E.D. and W.F. Dietrich, *Nalp1b controls mouse macrophage susceptibility to anthrax lethal toxin.* Nat Genet, 2006. **38**(2): p. 240-4.
241. Faustin, B., et al., *Reconstituted NALP1 inflammasome reveals two-step mechanism of caspase-1 activation.* Mol Cell, 2007. **25**(5): p. 713-24.

242. Gross, O., et al., *Syk kinase signalling couples to the Nlrp3 inflammasome for anti-fungal host defence.* Nature, 2009. **459**(7245): p. 433-6.
243. Mariathasan, S., et al., *Cryopyrin activates the inflammasome in response to toxins and ATP.* Nature, 2006. **440**(7081): p. 228-32.
244. Dostert, C., et al., *Innate immune activation through Nalp3 inflammasome sensing of asbestos and silica.* Science, 2008. **320**(5876): p. 674-7.
245. Sharp, F.A., et al., *Uptake of particulate vaccine adjuvants by dendritic cells activates the NALP3 inflammasome.* Proc Natl Acad Sci U S A, 2009. **106**(3): p. 870-5.
246. Martinon, F., et al., *Gout-associated uric acid crystals activate the NALP3 inflammasome.* Nature, 2006. **440**(7081): p. 237-41.
247. Gurcel, L., et al., *Caspase-1 activation of lipid metabolic pathways in response to bacterial pore-forming toxins promotes cell survival.* Cell, 2006. **126**(6): p. 1135-45.
248. Franchi, L., et al., *Cytosolic flagellin requires Ipaf for activation of caspase-1 and interleukin 1beta in salmonella-infected macrophages.* Nat Immunol, 2006. **7**(6): p. 576-82.
249. Suzuki, T., et al., *Differential regulation of caspase-1 activation, pyroptosis, and autophagy via Ipaf and ASC in Shigella-infected macrophages.* PLoS Pathog, 2007. **3**(8): p. e111.
250. Amer, A., et al., *Regulation of Legionella phagosome maturation and infection through flagellin and host Ipaf.* J Biol Chem, 2006. **281**(46): p. 35217-23.
251. Franchi, L., et al., *Critical role for Ipaf in Pseudomonas aeruginosa-induced caspase-1 activation.* Eur J Immunol, 2007. **37**(11): p. 3030-9.
252. Fink, S.L. and B.T. Cookson, *Pyroptosis and host cell death responses during Salmonella infection.* Cell Microbiol, 2007. **9**(11): p. 2562-70.
253. Zamboni, D.S., et al., *The Birc1e cytosolic pattern-recognition receptor contributes to the detection and control of Legionella pneumophila infection.* Nat Immunol, 2006. **7**(3): p. 318-25.
254. Sutterwala, F.S., et al., *Immune recognition of Pseudomonas aeruginosa mediated by the IPAF/NLRC4 inflammasome.* J Exp Med, 2007. **204**(13): p. 3235-45.
255. Mariathasan, S., et al., *Differential activation of the inflammasome by caspase-1 adaptors ASC and Ipaf.* Nature, 2004. **430**(6996): p. 213-8.
256. Kanneganti, T.D., et al., *Pannexin-1-mediated recognition of bacterial molecules activates the cryopyrin inflammasome independent of Toll-like receptor signaling.* Immunity, 2007. **26**(4): p. 433-43.
257. Hornung, V., et al., *Silica crystals and aluminum salts activate the NALP3 inflammasome through phagosomal destabilization.* Nat Immunol, 2008. **9**(8): p. 847-56.
258. Meissner, F., et al., *Inflammasome activation in NADPH oxidase defective mononuclear phagocytes from patients with chronic granulomatous disease.* Blood, 2010. **116**(9): p. 1570-3.
259. Kahlenberg, J.M. and G.R. Dubyak, *Mechanisms of caspase-1 activation by P2X7 receptor-mediated K+ release.* Am J Physiol Cell Physiol, 2004. **286**(5): p. C1100-8.
260. Fernandes-Alnemri, T., et al., *The pyroptosome: a supramolecular assembly of ASC dimers mediating inflammatory cell death via caspase-1 activation.* Cell Death Differ, 2007. **14**(9): p. 1590-604.
261. Franchi, L., et al., *Differential requirement of P2X7 receptor and intracellular K+ for caspase-1 activation induced by intracellular and extracellular bacteria.* J Biol Chem, 2007. **282**(26): p. 18810-8.
262. Petrilli, V., et al., *Activation of the NALP3 inflammasome is triggered by low intracellular potassium concentration.* Cell Death Differ, 2007. **14**(9): p. 1583-9.
263. Shio, M.T., et al., *Malarial hemozoin activates the NLRP3 inflammasome through Lyn and Syk kinases.* PLoS Pathog, 2009. **5**(8): p. e1000559.
264. Cassel, S.L., et al., *The Nalp3 inflammasome is essential for the development of silicosis.* Proc Natl Acad Sci U S A, 2008. **105**(26): p. 9035-40.
265. Cruz, C.M., et al., *ATP activates a reactive oxygen species-dependent oxidative stress response and secretion of proinflammatory cytokines in macrophages.* J Biol Chem, 2007. **282**(5): p. 2871-9.

266. Zhou, R., et al., *Thioredoxin-interacting protein links oxidative stress to inflammasome activation.* Nat Immunol, 2010. **11**(2): p. 136-40.
267. Matzinger, P., *Tolerance, danger, and the extended family.* Annu Rev Immunol, 1994. **12**: p. 991-1045.
268. Matzinger, P., *The danger model: a renewed sense of self.* Science, 2002. **296**(5566): p. 301-5.
269. Gallucci, S., M. Lolkema, and P. Matzinger, *Natural adjuvants: endogenous activators of dendritic cells.* Nat Med, 1999. **5**(11): p. 1249-55.
270. Shi, Y. and K.L. Rock, *Cell death releases endogenous adjuvants that selectively enhance immune surveillance of particulate antigens.* Eur J Immunol, 2002. **32**(1): p. 155-62.
271. Kono, H. and K.L. Rock, *How dying cells alert the immune system to danger.* Nat Rev Immunol, 2008. **8**(4): p. 279-89.
272. Chen, C.J., et al., *Identification of a key pathway required for the sterile inflammatory response triggered by dying cells.* Nat Med, 2007. **13**(7): p. 851-6.
273. Levy, R.M., et al., *Systemic inflammation and remote organ damage following bilateral femur fracture requires Toll-like receptor 4.* Am J Physiol Regul Integr Comp Physiol, 2006. **291**(4): p. R970-6.
274. Kono, H., et al., *Identification of the cellular sensor that stimulates the inflammatory response to sterile cell death.* J Immunol, 2010. **184**(8): p. 4470-8.
275. Kerr, J.F., A.H. Wyllie, and A.R. Currie, *Apoptosis: a basic biological phenomenon with wide-ranging implications in tissue kinetics.* Br J Cancer, 1972. **26**(4): p. 239-57.
276. Wyllie, A.H., J.F. Kerr, and A.R. Currie, *Cell death: the significance of apoptosis.* Int Rev Cytol, 1980. **68**: p. 251-306.
277. Ewen, C.L., K.P. Kane, and R.C. Bleackley, *A quarter century of granzymes.* Cell Death Differ, 2012. **19**(1): p. 28-35.
278. Kagi, D., et al., *Cytotoxicity mediated by T cells and natural killer cells is greatly impaired in perforin-deficient mice.* Nature, 1994. **369**(6475): p. 31-7.
279. McGuire, M.J., P.E. Lipsky, and D.L. Thiele, *Generation of active myeloid and lymphoid granule serine proteases requires processing by the granule thiol protease dipeptidyl peptidase I.* J Biol Chem, 1993. **268**(4): p. 2458-67.
280. Ebnet, K., et al., *In vivo primed mouse T cells selectively express T cell-specific serine proteinase-1 and the proteinase-like molecules granzyme B and C.* Int Immunol, 1991. **3**(1): p. 9-19.
281. Poe, M., et al., *Human cytotoxic lymphocyte granzyme B. Its purification from granules and the characterization of substrate and inhibitor specificity.* J Biol Chem, 1991. **266**(1): p. 98-103.
282. Pardo, J., et al., *Apoptotic pathways are selectively activated by granzyme A and/or granzyme B in CTL-mediated target cell lysis.* J Cell Biol, 2004. **167**(3): p. 457-68.
283. Fehniger, T.A., et al., *Acquisition of murine NK cell cytotoxicity requires the translation of a pre-existing pool of granzyme B and perforin mRNAs.* Immunity, 2007. **26**(6): p. 798-811.
284. Mullbacher, A., et al., *Granzymes are the essential downstream effector molecules for the control of primary virus infections by cytolytic leukocytes.* Proc Natl Acad Sci U S A, 1999. **96**(24): p. 13950-5.
285. Revell, P.A., et al., *Granzyme B and the downstream granzymes C and/or F are important for cytotoxic lymphocyte functions.* J Immunol, 2005. **174**(4): p. 2124-31.
286. Tak, P.P., et al., *The levels of soluble granzyme A and B are elevated in plasma and synovial fluid of patients with rheumatoid arthritis (RA).* Clin Exp Immunol, 1999. **116**(2): p. 366-70.
287. Lauw, F.N., et al., *Soluble granzymes are released during human endotoxemia and in patients with severe infection due to gram-negative bacteria.* J Infect Dis, 2000. **182**(1): p. 206-13.
288. Rissoan, M.C., et al., *Subtractive hybridization reveals the expression of immunoglobulin-like transcript 7, Eph-B1, granzyme B, and 3 novel transcripts in human plasmacytoid dendritic cells.* Blood, 2002. **100**(9): p. 3295-303.
289. Kim, W.J., et al., *Macrophages express granzyme B in the lesion areas of atherosclerosis and rheumatoid arthritis.* Immunol Lett, 2007. **111**(1): p. 57-65.

290. Strik, M.C., et al., *Human mast cells produce and release the cytotoxic lymphocyte associated protease granzyme B upon activation.* Mol Immunol, 2007. **44**(14): p. 3462-72.
291. Tschopp, C.M., et al., *Granzyme B, a novel mediator of allergic inflammation: its induction and release in blood basophils and human asthma.* Blood, 2006. **108**(7): p. 2290-9.
292. Hagn, M., et al., *Human B cells secrete granzyme B when recognizing viral antigens in the context of the acute phase cytokine IL-21.* J Immunol, 2009. **183**(3): p. 1838-45.
293. Freishtat, R.J., et al., *Sepsis alters the megakaryocyte-platelet transcriptional axis resulting in granzyme B-mediated lymphotoxicity.* Am J Respir Crit Care Med, 2009. **179**(6): p. 467-73.
294. Hernandez-Pigeon, H., et al., *Human keratinocytes acquire cellular cytotoxicity under UV-B irradiation. Implication of granzyme B and perforin.* J Biol Chem, 2006. **281**(19): p. 13525-32.
295. Horiuchi, K., et al., *Expression of granzyme B in human articular chondrocytes.* J Rheumatol, 2003. **30**(8): p. 1799-810.
296. Hu, S.X., et al., *Expression of endogenous granzyme B in a subset of human primary breast carcinomas.* Br J Cancer, 2003. **89**(1): p. 135-9.
297. Metkar, S.S., et al., *Human and mouse granzyme A induce a proinflammatory cytokine response.* Immunity, 2008. **29**(5): p. 720-33.
298. Mosley, B., et al., *The interleukin-1 receptor binds the human interleukin-1 alpha precursor but not the interleukin-1 beta precursor.* J Biol Chem, 1987. **262**(7): p. 2941-4.
299. Goodwin, G.H., C. Sanders, and E.W. Johns, *A new group of chromatin-associated proteins with a high content of acidic and basic amino acids.* Eur J Biochem, 1973. **38**(1): p. 14-9.
300. Muller, S., L. Ronfani, and M.E. Bianchi, *Regulated expression and subcellular localization of HMGB1, a chromatin protein with a cytokine function.* J Intern Med, 2004. **255**(3): p. 332-43.
301. Weir, H.M., et al., *Structure of the HMG box motif in the B-domain of HMG1.* EMBO J, 1993. **12**(4): p. 1311-9.
302. Hardman, C.H., et al., *Structure of the A-domain of HMG1 and its interaction with DNA as studied by heteronuclear three- and four-dimensional NMR spectroscopy.* Biochemistry, 1995. **34**(51): p. 16596-607.
303. Read, C.M., et al., *Solution structure of a DNA-binding domain from HMG1.* Nucleic Acids Res, 1993. **21**(15): p. 3427-36.
304. Melvin, V.S. and D.P. Edwards, *Coregulatory proteins in steroid hormone receptor action: the role of chromatin high mobility group proteins HMG-1 and -2.* Steroids, 1999. **64**(9): p. 576-86.
305. Jayaraman, L., et al., *High mobility group protein-1 (HMG-1) is a unique activator of p53.* Genes Dev, 1998. **12**(4): p. 462-72.
306. Agrawal, A. and D.G. Schatz, *RAG1 and RAG2 form a stable postcleavage synaptic complex with DNA containing signal ends in V(D)J recombination.* Cell, 1997. **89**(1): p. 43-53.
307. Calogero, S., et al., *The lack of chromosomal protein Hmg1 does not disrupt cell growth but causes lethal hypoglycaemia in newborn mice.* Nat Genet, 1999. **22**(3): p. 276-80.
308. Paonessa, G., R. Frank, and R. Cortese, *Nucleotide sequence of rat liver HMG1 cDNA.* Nucleic Acids Res, 1987. **15**(21): p. 9077.
309. Wen, L., et al., *A human placental cDNA clone that encodes nonhistone chromosomal protein HMG-1.* Nucleic Acids Res, 1989. **17**(3): p. 1197-214.
310. Hock, R., et al., *HMG chromosomal proteins in development and disease.* Trends Cell Biol, 2007. **17**(2): p. 72-9.
311. Wang, H., et al., *HMG-1 as a late mediator of endotoxin lethality in mice.* Science, 1999. **285**(5425): p. 248-51.
312. Gardella, S., et al., *The nuclear protein HMGB1 is secreted by monocytes via a non-classical, vesicle-mediated secretory pathway.* EMBO Rep, 2002. **3**(10): p. 995-1001.
313. Wang, H., et al., *Proinflammatory cytokines (tumor necrosis factor and interleukin 1) stimulate release of high mobility group protein-1 by pituicytes.* Surgery, 1999. **126**(2): p. 389-92.

314. Liu, S., et al., *HMGB1 is secreted by immunostimulated enterocytes and contributes to cytomix-induced hyperpermeability of Caco-2 monolayers.* Am J Physiol Cell Physiol, 2006. **290**(4): p. C990-9.
315. Semino, C., et al., *NK/iDC interaction results in IL-18 secretion by DCs at the synaptic cleft followed by NK cell activation and release of the DC maturation factor HMGB1.* Blood, 2005. **106**(2): p. 609-16.
316. Tsung, A., et al., *HMGB1 release induced by liver ischemia involves Toll-like receptor 4 dependent reactive oxygen species production and calcium-mediated signaling.* J Exp Med, 2007. **204**(12): p. 2913-23.
317. Scaffidi, P., T. Misteli, and M.E. Bianchi, *Release of chromatin protein HMGB1 by necrotic cells triggers inflammation.* Nature, 2002. **418**(6894): p. 191-5.
318. Kazama, H., et al., *Induction of immunological tolerance by apoptotic cells requires caspase-dependent oxidation of high-mobility group box-1 protein.* Immunity, 2008. **29**(1): p. 21-32.
319. Park, J.S., et al., *Activation of gene expression in human neutrophils by high mobility group box 1 protein.* Am J Physiol Cell Physiol, 2003. **284**(4): p. C870-9.
320. Orlova, V.V., et al., *A novel pathway of HMGB1-mediated inflammatory cell recruitment that requires Mac-1-integrin.* EMBO J, 2007. **26**(4): p. 1129-39.
321. Abraham, E., et al., *HMG-1 as a mediator of acute lung inflammation.* J Immunol, 2000. **165**(6): p. 2950-4.
322. Levy, R.M., et al., *Systemic inflammation and remote organ injury following trauma require HMGB1.* Am J Physiol Regul Integr Comp Physiol, 2007. **293**(4): p. R1538-44.
323. Ombrellino, M., et al., *Increased serum concentrations of high-mobility-group protein 1 in haemorrhagic shock.* Lancet, 1999. **354**(9188): p. 1446-7.
324. Kokkola, R., et al., *High mobility group box chromosomal protein 1: a novel proinflammatory mediator in synovitis.* Arthritis Rheum, 2002. **46**(10): p. 2598-603.
325. Messmer, D., et al., *High mobility group box protein 1: an endogenous signal for dendritic cell maturation and Th1 polarization.* J Immunol, 2004. **173**(1): p. 307-13.
326. Yang, D., et al., *High mobility group box-1 protein induces the migration and activation of human dendritic cells and acts as an alarmin.* J Leukoc Biol, 2007. **81**(1): p. 59-66.
327. Rovere-Querini, P., et al., *HMGB1 is an endogenous immune adjuvant released by necrotic cells.* EMBO Rep, 2004. **5**(8): p. 825-30.
328. Mitola, S., et al., *Cutting edge: extracellular high mobility group box-1 protein is a proangiogenic cytokine.* J Immunol, 2006. **176**(1): p. 12-5.
329. Palumbo, R., et al., *Extracellular HMGB1, a signal of tissue damage, induces mesoangioblast migration and proliferation.* J Cell Biol, 2004. **164**(3): p. 441-9.
330. Limana, F., et al., *Exogenous high-mobility group box 1 protein induces myocardial regeneration after infarction via enhanced cardiac C-kit+ cell proliferation and differentiation.* Circ Res, 2005. **97**(8): p. e73-83.
331. Yang, H., et al., *HMGB1 as a cytokine and therapeutic target.* J Endotoxin Res, 2002. **8**(6): p. 469-72.
332. Dumitriu, I.E., et al., *HMGB1: guiding immunity from within.* Trends Immunol, 2005. **26**(7): p. 381-7.
333. Hori, O., et al., *The receptor for advanced glycation end products (RAGE) is a cellular binding site for amphoterin. Mediation of neurite outgrowth and co-expression of rage and amphoterin in the developing nervous system.* J Biol Chem, 1995. **270**(43): p. 25752-61.
334. Huttunen, H.J., C. Fages, and H. Rauvala, *Receptor for advanced glycation end products (RAGE)-mediated neurite outgrowth and activation of NF-kappaB require the cytoplasmic domain of the receptor but different downstream signaling pathways.* J Biol Chem, 1999. **274**(28): p. 19919-24.
335. Bierhaus, A., et al., *Understanding RAGE, the receptor for advanced glycation end products.* J Mol Med, 2005. **83**(11): p. 876-86.
336. Treutiger, C.J., et al., *High mobility group 1 B-box mediates activation of human endothelium.* J Intern Med, 2003. **254**(4): p. 375-85.
337. Liliensiek, B., et al., *Receptor for advanced glycation end products (RAGE) regulates sepsis but not the adaptive immune response.* J Clin Invest, 2004. **113**(11): p. 1641-50.

338. Park, J.S., et al., *Involvement of toll-like receptors 2 and 4 in cellular activation by high mobility group box 1 protein.* J Biol Chem, 2004. **279**(9): p. 7370-7.
339. Rouhiainen, A., et al., *Pivotal advance: analysis of proinflammatory activity of highly purified eukaryotic recombinant HMGB1 (amphoterin).* J Leukoc Biol, 2007. **81**(1): p. 49-58.
340. Yang, H., et al., *Redox modification of cysteine residues regulates the cytokine activity of high mobility group box-1 (HMGB1).* Mol Med, 2012. **18**(1): p. 250-9.
341. Venereau, E., et al., *Mutually exclusive redox forms of HMGB1 promote cell recruitment or proinflammatory cytokine release.* J Exp Med, 2012.
342. Bianchi, M.E., *HMGB1 loves company.* J Leukoc Biol, 2009. **86**(3): p. 573-6.
343. Youn, J.H., et al., *High mobility group box 1 protein binding to lipopolysaccharide facilitates transfer of lipopolysaccharide to CD14 and enhances lipopolysaccharide-mediated TNF-alpha production in human monocytes.* J Immunol, 2008. **180**(7): p. 5067-74.
344. Sha, Y., et al., *HMGB1 develops enhanced proinflammatory activity by binding to cytokines.* J Immunol, 2008. **180**(4): p. 2531-7.
345. Tian, J., et al., *Toll-like receptor 9-dependent activation by DNA-containing immune complexes is mediated by HMGB1 and RAGE.* Nat Immunol, 2007. **8**(5): p. 487-96.
346. Ivanov, S., et al., *A novel role for HMGB1 in TLR9-mediated inflammatory responses to CpG-DNA.* Blood, 2007. **110**(6): p. 1970-81.
347. Bell, C.W., et al., *The extracellular release of HMGB1 during apoptotic cell death.* Am J Physiol Cell Physiol, 2006. **291**(6): p. C1318-25.
348. Urbonaviciute, V., et al., *Induction of inflammatory and immune responses by HMGB1-nucleosome complexes: implications for the pathogenesis of SLE.* J Exp Med, 2008. **205**(13): p. 3007-18.
349. Tang, D., et al., *The anti-inflammatory effects of heat shock protein 72 involve inhibition of high-mobility-group box 1 release and proinflammatory function in macrophages.* J Immunol, 2007. **179**(2): p. 1236-44.
350. Chen, G.Y., et al., *CD24 and Siglec-10 selectively repress tissue damage-induced immune responses.* Science, 2009. **323**(5922): p. 1722-5.
351. Shi, Y., J.E. Evans, and K.L. Rock, *Molecular identification of a danger signal that alerts the immune system to dying cells.* Nature, 2003. **425**(6957): p. 516-21.
352. Chen, C.J., et al., *MyD88-dependent IL-1 receptor signaling is essential for gouty inflammation stimulated by monosodium urate crystals.* J Clin Invest, 2006. **116**(8): p. 2262-71.
353. Liu-Bryan, R., et al., *Innate immunity conferred by Toll-like receptors 2 and 4 and myeloid differentiation factor 88 expression is pivotal to monosodium urate monohydrate crystal-induced inflammation.* Arthritis Rheum, 2005. **52**(9): p. 2936-46.
354. Ng, G., et al., *Receptor-independent, direct membrane binding leads to cell-surface lipid sorting and Syk kinase activation in dendritic cells.* Immunity, 2008. **29**(5): p. 807-18.
355. Terkeltaub, R., et al., *Plasma protein binding by monosodium urate crystals. Analysis by two-dimensional gel electrophoresis.* Arthritis Rheum, 1983. **26**(6): p. 775-83.
356. Fields, T.R., et al., *Activation of the alternative pathway of complement by monosodium urate crystals.* Clin Immunol Immunopathol, 1983. **26**(2): p. 249-57.
357. Tramontini, N., et al., *Central role of complement membrane attack complex in monosodium urate crystal-induced neutrophilic rabbit knee synovitis.* Arthritis Rheum, 2004. **50**(8): p. 2633-9.
358. Kono, H., et al., *Uric acid promotes an acute inflammatory response to sterile cell death in mice.* J Clin Invest, 2010. **120**(6): p. 1939-49.
359. Srivastava, P.K., A.B. DeLeo, and L.J. Old, *Tumor rejection antigens of chemically induced sarcomas of inbred mice.* Proc Natl Acad Sci U S A, 1986. **83**(10): p. 3407-11.
360. Ishii, T., et al., *Isolation of MHC class I-restricted tumor antigen peptide and its precursors associated with heat shock proteins hsp70, hsp90, and gp96.* J Immunol, 1999. **162**(3): p. 1303-9.
361. Blachere, N.E., et al., *Heat shock protein-peptide complexes, reconstituted in vitro, elicit peptide-specific cytotoxic T lymphocyte response and tumor immunity.* J Exp Med, 1997. **186**(8): p. 1315-22.

362. Basu, S., et al., *CD91 is a common receptor for heat shock proteins gp96, hsp90, hsp70, and calreticulin.* Immunity, 2001. **14**(3): p. 303-13.
363. Arnold-Schild, D., et al., *Cutting edge: receptor-mediated endocytosis of heat shock proteins by professional antigen-presenting cells.* J Immunol, 1999. **162**(7): p. 3757-60.
364. Flohe, S.B., et al., *Human heat shock protein 60 induces maturation of dendritic cells versus a Th1-promoting phenotype.* J Immunol, 2003. **170**(5): p. 2340-8.
365. Basu, S., et al., *Necrotic but not apoptotic cell death releases heat shock proteins, which deliver a partial maturation signal to dendritic cells and activate the NF-kappa B pathway.* Int Immunol, 2000. **12**(11): p. 1539-46.
366. Bethke, K., et al., *Different efficiency of heat shock proteins (HSP) to activate human monocytes and dendritic cells: superiority of HSP60.* J Immunol, 2002. **169**(11): p. 6141-8.
367. Vabulas, R.M., et al., *The endoplasmic reticulum-resident heat shock protein Gp96 activates dendritic cells via the Toll-like receptor 2/4 pathway.* J Biol Chem, 2002. **277**(23): p. 20847-53.
368. Panjwani, N.N., L. Popova, and P.K. Srivastava, *Heat shock proteins gp96 and hsp70 activate the release of nitric oxide by APCs.* J Immunol, 2002. **168**(6): p. 2997-3003.
369. Chen, W., et al., *Human 60-kDa heat-shock protein: a danger signal to the innate immune system.* J Immunol, 1999. **162**(6): p. 3212-9.
370. Radsak, M.P., et al., *The heat shock protein Gp96 binds to human neutrophils and monocytes and stimulates effector functions.* Blood, 2003. **101**(7): p. 2810-5.
371. Cohen-Sfady, M., et al., *Heat shock protein 60 activates B cells via the TLR4-MyD88 pathway.* J Immunol, 2005. **175**(6): p. 3594-602.
372. Multhoff, G., et al., *Heat shock protein 70 (Hsp70) stimulates proliferation and cytolytic activity of natural killer cells.* Exp Hematol, 1999. **27**(11): p. 1627-36.
373. Vabulas, R.M., et al., *Endocytosed HSP60s use toll-like receptor 2 (TLR2) and TLR4 to activate the toll/interleukin-1 receptor signaling pathway in innate immune cells.* J Biol Chem, 2001. **276**(33): p. 31332-9.
374. Asea, A., et al., *Novel signal transduction pathway utilized by extracellular HSP70: role of toll-like receptor (TLR) 2 and TLR4.* J Biol Chem, 2002. **277**(17): p. 15028-34.
375. Ohashi, K., et al., *Cutting edge: heat shock protein 60 is a putative endogenous ligand of the toll-like receptor-4 complex.* J Immunol, 2000. **164**(2): p. 558-61.
376. Vabulas, R.M., et al., *HSP70 as endogenous stimulus of the Toll/interleukin-1 receptor signal pathway.* J Biol Chem, 2002. **277**(17): p. 15107-12.
377. Breloer, M., B. Fleischer, and A. von Bonin, *In vivo and in vitro activation of T cells after administration of Ag-negative heat shock proteins.* J Immunol, 1999. **162**(6): p. 3141-7.
378. Osterloh, A., et al., *Synergistic and differential modulation of immune responses by Hsp60 and lipopolysaccharide.* J Biol Chem, 2007. **282**(7): p. 4669-80.
379. Osterloh, A., et al., *Lipopolysaccharide-free heat shock protein 60 activates T cells.* J Biol Chem, 2004. **279**(46): p. 47906-11.
380. Dentener, M.A., et al., *Antagonistic effects of lipopolysaccharide binding protein and bactericidal/permeability-increasing protein on lipopolysaccharide-induced cytokine release by mononuclear phagocytes. Competition for binding to lipopolysaccharide.* J Immunol, 1993. **151**(8): p. 4258-65.
381. Gao, B. and M.F. Tsan, *Recombinant human heat shock protein 60 does not induce the release of tumor necrosis factor alpha from murine macrophages.* J Biol Chem, 2003. **278**(25): p. 22523-9.
382. Erridge, C., *Endogenous ligands of TLR2 and TLR4: agonists or assistants?* J Leukoc Biol, 2010. **87**(6): p. 989-99.
383. Gao, B. and M.F. Tsan, *Endotoxin contamination in recombinant human heat shock protein 70 (Hsp70) preparation is responsible for the induction of tumor necrosis factor alpha release by murine macrophages.* J Biol Chem, 2003. **278**(1): p. 174-9.

384. Wallin, R.P., et al., *Heat-shock proteins as activators of the innate immune system.* Trends Immunol, 2002. **23**(3): p. 130-5.
385. Bausinger, H., et al., *Endotoxin-free heat-shock protein 70 fails to induce APC activation.* Eur J Immunol, 2002. **32**(12): p. 3708-13.
386. Reed, R.C., et al., *GRP94/gp96 elicits ERK activation in murine macrophages. A role for endotoxin contamination in NF-kappa B activation and nitric oxide production.* J Biol Chem, 2003. **278**(34): p. 31853-60.
387. Byrd, C.A., et al., *Heat shock protein 90 mediates macrophage activation by Taxol and bacterial lipopolysaccharide.* Proc Natl Acad Sci U S A, 1999. **96**(10): p. 5645-50.
388. Habich, C., et al., *Heat shock protein 60: specific binding of lipopolysaccharide.* J Immunol, 2005. **174**(3): p. 1298-305.
389. Warger, T., et al., *Interaction of TLR2 and TLR4 ligands with the N-terminal domain of Gp96 amplifies innate and adaptive immune responses.* J Biol Chem, 2006. **281**(32): p. 22545-53.
390. Zheng, L., et al., *Pathogen-induced apoptotic neutrophils express heat shock proteins and elicit activation of human macrophages.* J Immunol, 2004. **173**(10): p. 6319-26.
391. Tsukamoto, Y., W.E. Helsel, and S.M. Wahl, *Macrophage production of fibronectin, a chemoattractant for fibroblasts.* J Immunol, 1981. **127**(2): p. 673-8.
392. Bowersox, J.C. and N. Sorgente, *Chemotaxis of aortic endothelial cells in response to fibronectin.* Cancer Res, 1982. **42**(7): p. 2547-51.
393. Norris, D.A., et al., *Fibronectin fragment(s) are chemotactic for human peripheral blood monocytes.* J Immunol, 1982. **129**(4): p. 1612-8.
394. Gondokaryono, S.P., et al., *The extra domain A of fibronectin stimulates murine mast cells via toll-like receptor 4.* J Leukoc Biol, 2007. **82**(3): p. 657-65.
395. Tobiasova-Czetoova, Z., et al., *Effects of human plasma proteins on maturation of monocyte-derived dendritic cells.* Immunol Lett, 2005. **100**(2): p. 113-9.
396. Fan, S.T. and T.S. Edgington, *Integrin regulation of leukocyte inflammatory functions. CD11b/CD18 enhancement of the tumor necrosis factor-alpha responses of monocytes.* J Immunol, 1993. **150**(7): p. 2972-80.
397. Smiley, S.T., J.A. King, and W.W. Hancock, *Fibrinogen stimulates macrophage chemokine secretion through toll-like receptor 4.* J Immunol, 2001. **167**(5): p. 2887-94.
398. Postlethwaite, A.E. and A.H. Kang, *Collagen-and collagen peptide-induced chemotaxis of human blood monocytes.* J Exp Med, 1976. **143**(6): p. 1299-307.
399. Chang, C. and J.C. Houck, *Demonstration of the chemotactic properties of collagen.* Proc Soc Exp Biol Med, 1970. **134**(1): p. 22-6.
400. Senior, R.M., G.L. Griffin, and R.P. Mecham, *Chemotactic activity of elastin-derived peptides.* J Clin Invest, 1980. **66**(4): p. 859-62.
401. Mahnke, K., et al., *Interaction of murine dendritic cells with collagen up-regulates allostimulatory capacity, surface expression of heat stable antigen, and release of cytokines.* J Leukoc Biol, 1996. **60**(4): p. 465-72.
402. Johnson, G.B., G.J. Brunn, and J.L. Platt, *Cutting edge: an endogenous pathway to systemic inflammatory response syndrome (SIRS)-like reactions through Toll-like receptor 4.* J Immunol, 2004. **172**(1): p. 20-4.
403. Kodaira, Y., et al., *Phenotypic and functional maturation of dendritic cells mediated by heparan sulfate.* J Immunol, 2000. **165**(3): p. 1599-604.
404. Johnson, G.B., et al., *Receptor-mediated monitoring of tissue well-being via detection of soluble heparan sulfate by Toll-like receptor 4.* J Immunol, 2002. **168**(10): p. 5233-9.
405. Taylor, K.R., et al., *Hyaluronan fragments stimulate endothelial recognition of injury through TLR4.* J Biol Chem, 2004. **279**(17): p. 17079-84.
406. Scheibner, K.A., et al., *Hyaluronan fragments act as an endogenous danger signal by engaging TLR2.* J Immunol, 2006. **177**(2): p. 1272-81.

407. Campo, G.M., et al., *Molecular size hyaluronan differently modulates toll-like receptor-4 in LPS-induced inflammation in mouse chondrocytes.* Biochimie, 2010. **92**(2): p. 204-15.
408. Termeer, C.C., et al., *Oligosaccharides of hyaluronan are potent activators of dendritic cells.* J Immunol, 2000. **165**(4): p. 1863-70.
409. Termeer, C., et al., *Oligosaccharides of Hyaluronan activate dendritic cells via toll-like receptor 4.* J Exp Med, 2002. **195**(1): p. 99-111.
410. Krejcova, D., et al., *The effect of different molecular weight hyaluronan on macrophage physiology.* Neuro Endocrinol Lett, 2009. **30 Suppl 1**: p. 106-11.
411. Orend, G., *Potential oncogenic action of tenascin-C in tumorigenesis.* Int J Biochem Cell Biol, 2005. **37**(5): p. 1066-83.
412. Chiquet-Ehrismann, R. and M. Chiquet, *Tenascins: regulation and putative functions during pathological stress.* J Pathol, 2003. **200**(4): p. 488-99.
413. Midwood, K., et al., *Tenascin-C is an endogenous activator of Toll-like receptor 4 that is essential for maintaining inflammation in arthritic joint disease.* Nat Med, 2009. **15**(7): p. 774-80.
414. Kanayama, M., et al., *alpha9beta1 integrin-mediated signaling serves as an intrinsic regulator of pathogenic Th17 cell generation.* J Immunol, 2011. **187**(11): p. 5851-64.
415. Piccinini, A.M. and K.S. Midwood, *Endogenous Control of Immunity against Infection: Tenascin-C Regulates TLR4-Mediated Inflammation via MicroRNA-155.* Cell Rep, 2012.
416. Ruhmann, M., et al., *Endogenous activation of adaptive immunity: tenascin-C drives interleukin-17 synthesis in murine arthritic joint disease.* Arthritis Rheum, 2012. **64**(7): p. 2179-90.
417. van den Berg, W.B. and P. Miossec, *IL-17 as a future therapeutic target for rheumatoid arthritis.* Nat Rev Rheumatol, 2009. **5**(10): p. 549-53.
418. Dinarello, C., et al., *IL-1 family nomenclature.* Nat Immunol, 2010. **11**(11): p. 973.
419. Taylor, S.L., et al., *Genomic organization of the interleukin-1 locus.* Genomics, 2002. **79**(5): p. 726-33.
420. Dinarello, C.A., *Interleukin-1 in the pathogenesis and treatment of inflammatory diseases.* Blood, 2011. **117**(14): p. 3720-32.
421. Lin, H., et al., *Cloning and characterization of IL-1HY2, a novel interleukin-1 family member.* J Biol Chem, 2001. **276**(23): p. 20597-602.
422. Dinarello, C.A., *Biologic basis for interleukin-1 in disease.* Blood, 1996. **87**(6): p. 2095-147.
423. Dinarello, C.A., *Immunological and inflammatory functions of the interleukin-1 family.* Annu Rev Immunol, 2009. **27**: p. 519-50.
424. Mosley, B., et al., *Determination of the minimum polypeptide lengths of the functionally active sites of human interleukins 1 alpha and 1 beta.* Proc Natl Acad Sci U S A, 1987. **84**(13): p. 4572-6.
425. Horai, R., et al., *Production of mice deficient in genes for interleukin (IL)-1alpha, IL-1beta, IL-1alpha/beta, and IL-1 receptor antagonist shows that IL-1beta is crucial in turpentine-induced fever development and glucocorticoid secretion.* J Exp Med, 1998. **187**(9): p. 1463-75.
426. Howard, A.D., et al., *IL-1-converting enzyme requires aspartic acid residues for processing of the IL-1 beta precursor at two distinct sites and does not cleave 31-kDa IL-1 alpha.* J Immunol, 1991. **147**(9): p. 2964-9.
427. Kurt-Jones, E.A., et al., *Identification of a membrane-associated interleukin 1 in macrophages.* Proc Natl Acad Sci U S A, 1985. **82**(4): p. 1204-8.
428. Werman, A., et al., *The precursor form of IL-1alpha is an intracrine proinflammatory activator of transcription.* Proc Natl Acad Sci U S A, 2004. **101**(8): p. 2434-9.
429. Kobayashi, Y., et al., *Identification of calcium-activated neutral protease as a processing enzyme of human interleukin 1 alpha.* Proc Natl Acad Sci U S A, 1990. **87**(14): p. 5548-52.
430. Carruth, L.M., S. Demczuk, and S.B. Mizel, *Involvement of a calpain-like protease in the processing of the murine interleukin 1 alpha precursor.* J Biol Chem, 1991. **266**(19): p. 12162-7.
431. Gross, O., et al., *Inflammasome activators induce interleukin-1alpha secretion via distinct pathways with differential requirement for the protease function of caspase-1.* Immunity, 2012. **36**(3): p. 388-400.

432. Cohen, I., et al., *Differential release of chromatin-bound IL-1alpha discriminates between necrotic and apoptotic cell death by the ability to induce sterile inflammation.* Proc Natl Acad Sci U S A, 2010. **107**(6): p. 2574-9.
433. Schmitz, J., et al., *IL-33, an interleukin-1-like cytokine that signals via the IL-1 receptor-related protein ST2 and induces T helper type 2-associated cytokines.* Immunity, 2005. **23**(5): p. 479-90.
434. Palmer, G., et al., *The IL-1 receptor accessory protein (AcP) is required for IL-33 signaling and soluble AcP enhances the ability of soluble ST2 to inhibit IL-33.* Cytokine, 2008. **42**(3): p. 358-64.
435. Carriere, V., et al., *IL-33, the IL-1-like cytokine ligand for ST2 receptor, is a chromatin-associated nuclear factor in vivo.* Proc Natl Acad Sci U S A, 2007. **104**(1): p. 282-7.
436. Allakhverdi, Z., et al., *Cutting edge: The ST2 ligand IL-33 potently activates and drives maturation of human mast cells.* J Immunol, 2007. **179**(4): p. 2051-4.
437. Pecaric-Petkovic, T., et al., *Human basophils and eosinophils are the direct target leukocytes of the novel IL-1 family member IL-33.* Blood, 2009. **113**(7): p. 1526-34.
438. Cayrol, C. and J.P. Girard, *The IL-1-like cytokine IL-33 is inactivated after maturation by caspase-1.* Proc Natl Acad Sci U S A, 2009. **106**(22): p. 9021-6.
439. Luthi, A.U., et al., *Suppression of interleukin-33 bioactivity through proteolysis by apoptotic caspases.* Immunity, 2009. **31**(1): p. 84-98.
440. Lamkanfi, M. and V.M. Dixit, *IL-33 raises alarm.* Immunity, 2009. **31**(1): p. 5-7.
441. Gallucci, S. and P. Matzinger, *Danger signals: SOS to the immune system.* Curr Opin Immunol, 2001. **13**(1): p. 114-9.
442. Lefrancais, E., et al., *IL-33 is processed into mature bioactive forms by neutrophil elastase and cathepsin G.* Proc Natl Acad Sci U S A, 2012. **109**(5): p. 1673-8.
443. Ni, H., et al., *Extracellular mRNA induces dendritic cell activation by stimulating tumor necrosis factor-alpha secretion and signaling through a nucleotide receptor.* J Biol Chem, 2002. **277**(15): p. 12689-96.
444. Kariko, K., et al., *mRNA is an endogenous ligand for Toll-like receptor 3.* J Biol Chem, 2004. **279**(13): p. 12542-50.
445. Takaoka, A., et al., *DAI (DLM-1/ZBP1) is a cytosolic DNA sensor and an activator of innate immune response.* Nature, 2007. **448**(7152): p. 501-5.
446. Hornung, V., et al., *AIM2 recognizes cytosolic dsDNA and forms a caspase-1-activating inflammasome with ASC.* Nature, 2009. **458**(7237): p. 514-8.
447. Unterholzner, L., et al., *IFI16 is an innate immune sensor for intracellular DNA.* Nat Immunol, 2010. **11**(11): p. 997-1004.
448. Bird, A.P., et al., *Non-methylated CpG-rich islands at the human alpha-globin locus: implications for evolution of the alpha-globin pseudogene.* EMBO J, 1987. **6**(4): p. 999-1004.
449. Ishii, K.J., et al., *Genomic DNA released by dying cells induces the maturation of APCs.* J Immunol, 2001. **167**(5): p. 2602-7.
450. Zhang, Q., et al., *Circulating mitochondrial DAMPs cause inflammatory responses to injury.* Nature, 2010. **464**(7285): p. 104-7.
451. Schnurr, M., et al., *Extracellular ATP and TNF-alpha synergize in the activation and maturation of human dendritic cells.* J Immunol, 2000. **165**(8): p. 4704-9.
452. Wilkin, F., et al., *The P2Y11 receptor mediates the ATP-induced maturation of human monocyte-derived dendritic cells.* J Immunol, 2001. **166**(12): p. 7172-7.
453. Idzko, M., et al., *Nucleotides induce chemotaxis and actin polymerization in immature but not mature human dendritic cells via activation of pertussis toxin-sensitive P2y receptors.* Blood, 2002. **100**(3): p. 925-32.
454. Cronstein, B.N., et al., *The adenosine/neutrophil paradox resolved: human neutrophils possess both A1 and A2 receptors that promote chemotaxis and inhibit O2 generation, respectively.* J Clin Invest, 1990. **85**(4): p. 1150-7.

455. Zhang, M., et al., *Identification of the target self-antigens in reperfusion injury.* J Exp Med, 2006. **203**(1): p. 141-52.
456. Williams, J.P., et al., *Intestinal reperfusion injury is mediated by IgM and complement.* J Appl Physiol, 1999. **86**(3): p. 938-42.
457. Zhang, M., et al., *The role of natural IgM in myocardial ischemia-reperfusion injury.* J Mol Cell Cardiol, 2006. **41**(1): p. 62-7.
458. Weiser, M.R., et al., *Reperfusion injury of ischemic skeletal muscle is mediated by natural antibody and complement.* J Exp Med, 1996. **183**(5): p. 2343-8.
459. Zhang, M., et al., *Identification of a specific self-reactive IgM antibody that initiates intestinal ischemia/reperfusion injury.* Proc Natl Acad Sci U S A, 2004. **101**(11): p. 3886-91.
460. Sancho, D., et al., *Identification of a dendritic cell receptor that couples sensing of necrosis to immunity.* Nature, 2009. **458**(7240): p. 899-903.
461. Ahrens, S., et al., *F-actin is an evolutionarily conserved damage-associated molecular pattern recognized by DNGR-1, a receptor for dead cells.* Immunity, 2012. **36**(4): p. 635-45.
462. Cinti, S., *The adipose organ.* Prostaglandins Leukot Essent Fatty Acids, 2005. **73**(1): p. 9-15.
463. Reid, J., *A new outlook on the action of salicylate.* Scott Med J, 1957. **2**(3): p. 91-6.
464. Hotamisligil, G.S., N.S. Shargill, and B.M. Spiegelman, *Adipose expression of tumor necrosis factor-alpha: direct role in obesity-linked insulin resistance.* Science, 1993. **259**(5091): p. 87-91.
465. Uysal, K.T., et al., *Protection from obesity-induced insulin resistance in mice lacking TNF-alpha function.* Nature, 1997. **389**(6651): p. 610-4.
466. Bastard, J.P., et al., *Adipose tissue IL-6 content correlates with resistance to insulin activation of glucose uptake both in vivo and in vitro.* J Clin Endocrinol Metab, 2002. **87**(5): p. 2084-9.
467. Mohamed-Ali, V., et al., *Subcutaneous adipose tissue releases interleukin-6, but not tumor necrosis factor-alpha, in vivo.* J Clin Endocrinol Metab, 1997. **82**(12): p. 4196-200.
468. Soukas, A., et al., *Leptin-specific patterns of gene expression in white adipose tissue.* Genes Dev, 2000. **14**(8): p. 963-80.
469. Weisberg, S.P., et al., *Obesity is associated with macrophage accumulation in adipose tissue.* J Clin Invest, 2003. **112**(12): p. 1796-808.
470. Lumeng, C.N., J.L. Bodzin, and A.R. Saltiel, *Obesity induces a phenotypic switch in adipose tissue macrophage polarization.* J Clin Invest, 2007. **117**(1): p. 175-84.
471. Weisberg, S.P., et al., *CCR2 modulates inflammatory and metabolic effects of high-fat feeding.* J Clin Invest, 2006. **116**(1): p. 115-24.
472. Charriere, G., et al., *Preadipocyte conversion to macrophage. Evidence of plasticity.* J Biol Chem, 2003. **278**(11): p. 9850-5.
473. Zeyda, M., et al., *Human adipose tissue macrophages are of an anti-inflammatory phenotype but capable of excessive pro-inflammatory mediator production.* Int J Obes (Lond), 2007. **31**(9): p. 1420-8.
474. Elgazar-Carmon, V., et al., *Neutrophils transiently infiltrate intra-abdominal fat early in the course of high-fat feeding.* J Lipid Res, 2008. **49**(9): p. 1894-903.
475. Talukdar, S., et al., *Neutrophils mediate insulin resistance in mice fed a high-fat diet through secreted elastase.* Nat Med, 2012.
476. Pham, C.T., *Neutrophil serine proteases: specific regulators of inflammation.* Nat Rev Immunol, 2006. **6**(7): p. 541-50.
477. Houghton, A.M., et al., *Neutrophil elastase-mediated degradation of IRS-1 accelerates lung tumor growth.* Nat Med, 2010. **16**(2): p. 219-23.
478. Stehno-Bittel, L., *Intricacies of fat.* Phys Ther, 2008. **88**(11): p. 1265-78.
479. Donath, M.Y., et al., *Inflammatory mediators and islet beta-cell failure: a link between type 1 and type 2 diabetes.* J Mol Med (Berl), 2003. **81**(8): p. 455-70.
480. Jager, J., et al., *Interleukin-1beta-induced insulin resistance in adipocytes through down-regulation of insulin receptor substrate-1 expression.* Endocrinology, 2007. **148**(1): p. 241-51.

481. Wen, H., et al., *Fatty acid-induced NLRP3-ASC inflammasome activation interferes with insulin signaling.* Nat Immunol, 2011. **12**(5): p. 408-15.
482. McGillicuddy, F.C., et al., *Lack of interleukin-1 receptor I (IL-1RI) protects mice from high-fat diet-induced adipose tissue inflammation coincident with improved glucose homeostasis.* Diabetes, 2011. **60**(6): p. 1688-98.
483. Spranger, J., et al., *Inflammatory cytokines and the risk to develop type 2 diabetes: results of the prospective population-based European Prospective Investigation into Cancer and Nutrition (EPIC)-Potsdam Study.* Diabetes, 2003. **52**(3): p. 812-7.
484. Larsen, C.M., et al., *Interleukin-1-receptor antagonist in type 2 diabetes mellitus.* N Engl J Med, 2007. **356**(15): p. 1517-26.
485. Stienstra, R., et al., *The inflammasome-mediated caspase-1 activation controls adipocyte differentiation and insulin sensitivity.* Cell Metab, 2010. **12**(6): p. 593-605.
486. Vandanmagsar, B., et al., *The NLRP3 inflammasome instigates obesity-induced inflammation and insulin resistance.* Nat Med, 2011. **17**(2): p. 179-88.
487. Stienstra, R., et al., *Inflammasome is a central player in the induction of obesity and insulin resistance.* Proc Natl Acad Sci U S A, 2011. **108**(37): p. 15324-9.
488. Lee, J.Y., et al., *Saturated fatty acids, but not unsaturated fatty acids, induce the expression of cyclooxygenase-2 mediated through Toll-like receptor 4.* J Biol Chem, 2001. **276**(20): p. 16683-9.
489. Shi, H., et al., *TLR4 links innate immunity and fatty acid-induced insulin resistance.* J Clin Invest, 2006. **116**(11): p. 3015-25.
490. Haversen, L., et al., *Induction of proinflammatory cytokines by long-chain saturated fatty acids in human macrophages.* Atherosclerosis, 2009. **202**(2): p. 382-93.
491. Shanmugam, N., et al., *High glucose-induced expression of proinflammatory cytokine and chemokine genes in monocytic cells.* Diabetes, 2003. **52**(5): p. 1256-64.
492. Parikh, H., et al., *TXNIP regulates peripheral glucose metabolism in humans.* PLoS Med, 2007. **4**(5): p. e158.
493. Stoltzman, C.A., et al., *Glucose sensing by MondoA:Mlx complexes: a role for hexokinases and direct regulation of thioredoxin-interacting protein expression.* Proc Natl Acad Sci U S A, 2008. **105**(19): p. 6912-7.
494. Nakagawa, T., et al., *A causal role for uric acid in fructose-induced metabolic syndrome.* Am J Physiol Renal Physiol, 2006. **290**(3): p. F625-31.
495. Yuan, M., et al., *Reversal of obesity- and diet-induced insulin resistance with salicylates or targeted disruption of Ikkbeta.* Science, 2001. **293**(5535): p. 1673-7.
496. Hirosumi, J., et al., *A central role for JNK in obesity and insulin resistance.* Nature, 2002. **420**(6913): p. 333-6.
497. Aguirre, V., et al., *Phosphorylation of Ser307 in insulin receptor substrate-1 blocks interactions with the insulin receptor and inhibits insulin action.* J Biol Chem, 2002. **277**(2): p. 1531-7.
498. Shoelson, S.E., J. Lee, and A.B. Goldfine, *Inflammation and insulin resistance.* J Clin Invest, 2006. **116**(7): p. 1793-801.
499. Arkan, M.C., et al., *IKK-beta links inflammation to obesity-induced insulin resistance.* Nat Med, 2005. **11**(2): p. 191-8.
500. Sartipy, P. and D.J. Loskutoff, *Monocyte chemoattractant protein 1 in obesity and insulin resistance.* Proc Natl Acad Sci U S A, 2003. **100**(12): p. 7265-70.
501. Christiansen, T., B. Richelsen, and J.M. Bruun, *Monocyte chemoattractant protein-1 is produced in isolated adipocytes, associated with adiposity and reduced after weight loss in morbid obese subjects.* Int J Obes (Lond), 2005. **29**(1): p. 146-50.
502. Kanda, H., et al., *MCP-1 contributes to macrophage infiltration into adipose tissue, insulin resistance, and hepatic steatosis in obesity.* J Clin Invest, 2006. **116**(6): p. 1494-505.
503. Gregor, M.G. and G.S. Hotamisligil, *Adipocyte stress: The endoplasmic reticulum and metabolic disease.* J Lipid Res, 2007.

504. Martin, S. and R.G. Parton, *Caveolin, cholesterol, and lipid bodies.* Semin Cell Dev Biol, 2005. **16**(2): p. 163-74.
505. Marciniak, S.J. and D. Ron, *Endoplasmic reticulum stress signaling in disease.* Physiol Rev, 2006. **86**(4): p. 1133-49.
506. Wei, Y., et al., *Saturated fatty acids induce endoplasmic reticulum stress and apoptosis independently of ceramide in liver cells.* Am J Physiol Endocrinol Metab, 2006. **291**(2): p. E275-81.
507. Borradaile, N.M., et al., *Disruption of endoplasmic reticulum structure and integrity in lipotoxic cell death.* J Lipid Res, 2006. **47**(12): p. 2726-37.
508. Borradaile, N.M., et al., *A critical role for eukaryotic elongation factor 1A-1 in lipotoxic cell death.* Mol Biol Cell, 2006. **17**(2): p. 770-8.
509. Kharroubi, I., et al., *Free fatty acids and cytokines induce pancreatic beta-cell apoptosis by different mechanisms: role of nuclear factor-kappaB and endoplasmic reticulum stress.* Endocrinology, 2004. **145**(11): p. 5087-96.
510. Yacoub Wasef, S.Z., et al., *Glucose, dexamethasone, and the unfolded protein response regulate TRB3 mRNA expression in 3T3-L1 adipocytes and L6 myotubes.* Am J Physiol Endocrinol Metab, 2006. **291**(6): p. E1274-80.
511. Hosogai, N., et al., *Adipose tissue hypoxia in obesity and its impact on adipocytokine dysregulation.* Diabetes, 2007. **56**(4): p. 901-11.
512. Xue, X., et al., *Tumor necrosis factor alpha (TNFalpha) induces the unfolded protein response (UPR) in a reactive oxygen species (ROS)-dependent fashion, and the UPR counteracts ROS accumulation by TNFalpha.* J Biol Chem, 2005. **280**(40): p. 33917-25.
513. Cinti, S., et al., *Adipocyte death defines macrophage localization and function in adipose tissue of obese mice and humans.* J Lipid Res, 2005. **46**(11): p. 2347-55.
514. Vonakis, B.M., et al., *Inhibition of cytokine gene transcription by the human recombinant histamine-releasing factor in human T lymphocytes.* J Immunol, 2003. **171**(7): p. 3742-50.
515. Galanos, C., et al., *Synthetic and natural Escherichia coli free lipid A express identical endotoxic activities.* Eur J Biochem, 1985. **148**(1): p. 1-5.
516. Raetz, C.R. and C. Whitfield, *Lipopolysaccharide endotoxins.* Annu Rev Biochem, 2002. **71**: p. 635-700.
517. Rock, K.L. and H. Kono, *The inflammatory response to cell death.* Annu Rev Pathol, 2008. **3**: p. 99-126.
518. Asea, A., et al., *Novel signal transduction pathway utilized by extracellular HSP70: role of toll-like receptor (TLR) 2 and TLR4.* The Journal of biological chemistry, 2002. **277**(17): p. 15028-34.
519. Dybdahl, B., et al., *Inflammatory response after open heart surgery: release of heat-shock protein 70 and signaling through toll-like receptor-4.* Circulation, 2002. **105**(6): p. 685-90.
520. Majde, J.A., *Microbial cell-wall contaminants in peptides: A potential source of physiological artifacts.* Peptides, 1993. **14**(3): p. 629-632.
521. Lavelle, E.C., et al., *Cholera toxin promotes the induction of regulatory T cells specific for bystander antigens by modulating dendritic cell activation.* J Immunol, 2003. **171**(5): p. 2384-92.
522. McNeela, E.A., et al., *Pneumolysin activates the NLRP3 inflammasome and promotes proinflammatory cytokines independently of TLR4.* PLoS Pathog, 2010. **6**(11): p. e1001191.
523. Schuler, G. and R.M. Steinman, *Murine epidermal Langerhans cells mature into potent immunostimulatory dendritic cells in vitro.* J Exp Med, 1985. **161**(3): p. 526-46.
524. Romani, N., et al., *Presentation of exogenous protein antigens by dendritic cells to T cell clones. Intact protein is presented best by immature, epidermal Langerhans cells.* J Exp Med, 1989. **169**(3): p. 1169-78.
525. Moore, R.A., N.C. Bates, and R.E. Hancock, *Interaction of polycationic antibiotics with Pseudomonas aeruginosa lipopolysaccharide and lipid A studied by using dansyl-polymyxin.* Antimicrob Agents Chemother, 1986. **29**(3): p. 496-500.

526. Okamura, Y., et al., *The extra domain A of fibronectin activates Toll-like receptor 4.* J Biol Chem, 2001. **276**(13): p. 10229-33.
527. Jiang, D., et al., *Regulation of lung injury and repair by Toll-like receptors and hyaluronan.* Nat Med, 2005. **11**(11): p. 1173-9.
528. Suganami, T., et al., *Role of the Toll-like receptor 4/NF-kappaB pathway in saturated fatty acid-induced inflammatory changes in the interaction between adipocytes and macrophages.* Arterioscler Thromb Vasc Biol, 2007. **27**(1): p. 84-91.
529. Lieberman, J., *The ABCs of granule-mediated cytotoxicity: new weapons in the arsenal.* Nat Rev Immunol, 2003. **3**(5): p. 361-70.
530. MacDonald, S.M., et al., *Molecular identification of an IgE-dependent histamine-releasing factor.* Science, 1995. **269**(5224): p. 688-90.
531. Schroeder, J.T., L.M. Lichtenstein, and S.M. MacDonald, *An immunoglobulin E-dependent recombinant histamine-releasing factor induces interleukin-4 secretion from human basophils.* J Exp Med, 1996. **183**(3): p. 1265-70.
532. Bheekha-Escura, R., et al., *Human recombinant histamine-releasing factor activates human eosinophils and the eosinophilic cell line, AML14-3D10.* Blood, 2000. **96**(6): p. 2191-8.
533. Kang, H.S., et al., *Molecular identification of IgE-dependent histamine-releasing factor as a B cell growth factor.* J Immunol, 2001. **166**(11): p. 6545-54.
534. Chen, G.Y. and G. Nunez, *Sterile inflammation: sensing and reacting to damage.* Nat Rev Immunol, 2010. **10**(12): p. 826-37.
535. Sutton, C., et al., *A crucial role for interleukin (IL)-1 in the induction of IL-17-producing T cells that mediate autoimmune encephalomyelitis.* J Exp Med, 2006. **203**(7): p. 1685-91.
536. Hazuda, D.J., et al., *Structure-function mapping of interleukin 1 precursors. Cleavage leads to a conformational change in the mature protein.* J Biol Chem, 1991. **266**(11): p. 7081-6.
537. Matzinger, P., *Friendly and dangerous signals: is the tissue in control?* Nat Immunol, 2007. **8**(1): p. 11-3.
538. Taxman, D.J., et al., *The NLR adaptor ASC/PYCARD regulates DUSP10, mitogen-activated protein kinase (MAPK), and chemokine induction independent of the inflammasome.* J Biol Chem, 2011. **286**(22): p. 19605-16.
539. Ippagunta, S.K., et al., *The inflammasome adaptor ASC regulates the function of adaptive immune cells by controlling Dock2-mediated Rac activation and actin polymerization.* Nat Immunol, 2011. **12**(10): p. 1010-6.
540. Kolly, L., et al., *Inflammatory role of ASC in antigen-induced arthritis is independent of caspase-1, NALP-3, and IPAF.* J Immunol, 2009. **183**(6): p. 4003-12.
541. Shaw, P.J., et al., *Cutting edge: critical role for PYCARD/ASC in the development of experimental autoimmune encephalomyelitis.* J Immunol, 2010. **184**(9): p. 4610-4.
542. Li, H., et al., *Cutting edge: inflammasome activation by alum and alum's adjuvant effect are mediated by NLRP3.* J Immunol, 2008. **181**(1): p. 17-21.
543. Duewell, P., et al., *NLRP3 inflammasomes are required for atherogenesis and activated by cholesterol crystals.* Nature, 2010. **464**(7293): p. 1357-61.
544. Gavin, A.L., et al., *Adjuvant-enhanced antibody responses in the absence of toll-like receptor signaling.* Science, 2006. **314**(5807): p. 1936-8.
545. Winer, S., et al., *Normalization of obesity-associated insulin resistance through immunotherapy.* Nat Med, 2009. **15**(8): p. 921-9.
546. Nishimura, S., et al., *CD8+ effector T cells contribute to macrophage recruitment and adipose tissue inflammation in obesity.* Nat Med, 2009. **15**(8): p. 914-20.
547. Jordan, M.B., et al., *Promotion of B cell immune responses via an alum-induced myeloid cell population.* Science, 2004. **304**(5678): p. 1808-10.
548. Ghosn, E.E., et al., *Two physically, functionally, and developmentally distinct peritoneal macrophage subsets.* Proc Natl Acad Sci U S A, 2010. **107**(6): p. 2568-73.

549. Spence, S., et al., *Suppressors of Cytokine Signaling 2 and 3 Diametrically Control Macrophage Polarization.* Immunity, 2012.
550. Wu, D., et al., *Eosinophils sustain adipose alternatively activated macrophages associated with glucose homeostasis.* Science, 2011. **332**(6026): p. 243-7.
551. Liu, J., et al., *Genetic deficiency and pharmacological stabilization of mast cells reduce diet-induced obesity and diabetes in mice.* Nat Med, 2009. **15**(8): p. 940-5.
552. Wegner, M., et al., *IL-12 serum levels in patients with type 2 diabetes treated with sulphonylureas.* Cytokine, 2008. **42**(3): p. 312-6.
553. Surendar, J., et al., *Increased levels of both Th1 and Th2 cytokines in subjects with metabolic syndrome (CURES-103).* Diabetes Technol Ther, 2011. **13**(4): p. 477-82.
554. Wen, Y., et al., *Elevated glucose and diabetes promote interleukin-12 cytokine gene expression in mouse macrophages.* Endocrinology, 2006. **147**(5): p. 2518-25.
555. Rider, P., et al., *IL-1alpha and IL-1beta recruit different myeloid cells and promote different stages of sterile inflammation.* J Immunol, 2011. **187**(9): p. 4835-43.
556. Fujimoto, T., et al., *Lipid droplets: a classic organelle with new outfits.* Histochem Cell Biol, 2008. **130**(2): p. 263-79.
557. Murano, I., et al., *Dead adipocytes, detected as crown-like structures, are prevalent in visceral fat depots of genetically obese mice.* J Lipid Res, 2008. **49**(7): p. 1562-8.
558. Harman-Boehm, I., et al., *Macrophage infiltration into omental versus subcutaneous fat across different populations: effect of regional adiposity and the comorbidities of obesity.* J Clin Endocrinol Metab, 2007. **92**(6): p. 2240-7.
559. O'Connell, J., et al., *The relationship of omental and subcutaneous adipocyte size to metabolic disease in severe obesity.* PLoS One, 2010. **5**(4): p. e9997.
560. Pulendran, B., *Immune activation: death, danger and dendritic cells.* Curr Biol, 2004. **14**(1): p. R30-2.
561. Sancho, D., et al., *Tumor therapy in mice via antigen targeting to a novel, DC-restricted C-type lectin.* J Clin Invest, 2008. **118**(6): p. 2098-110.

Appendix